

**ASSESSMENT OF GROUNDWATER  
QUALITY AND RECHARGE POTENTIAL  
IN KABUL, AFGHANISTAN**

**A Thesis Submitted  
In Partial Fulfilment of the Requirements  
for the Degree of**

**DOCTOR OF PHILOSOPHY  
in**

**Environmental Engineering**

**by**

**Ali Reza Noori**

**(Roll No. 2K19/PHDEN/07)**

**Under the Supervision of**

**Prof. S.K. Singh**

**Professor, Department of Environmental Engineering,**

**Delhi Technological University**



**To the**

**Department of Environmental Engineering**

**DELHI TECHNOLOGICAL UNIVERSITY**

**(Formerly Delhi College of Engineering)**

**Shahbad Daultpur, Main Bawana Road, Delhi-110042,**

**India**

**December, 2024**

## ACKNOWLEDGMENTS

Reflecting on the intricate path of my Ph.D. journey, I am humbled by the profound impact of numerous individuals whose unwavering support has been indispensable in realizing this significant achievement. In this moment of reflection, I extend my deepest appreciation to all those who have played a pivotal role in facilitating my progress towards this momentous milestone.

At the forefront of this acknowledgement stands my esteemed research mentor, Prof. S.K. Singh, whose sage guidance and unwavering encouragement have been the guiding lights illuminating my path throughout the arduous terrain of Ph.D. research. Prof. Singh's profound insights, astute counsel, and unyielding patience instilled within me a deep sense of confidence and direction, empowering me to navigate the complexities of academic inquiry with clarity and purpose. His steadfast support has been instrumental in shaping not only my scholarly endeavours but also my personal growth, for which I am immensely grateful.

Equally deserving of recognition is Prof. A.K. Haritash, the distinguished head of the Environmental Engineering Department at Delhi Technological University, whose invaluable mentorship and unwavering cooperation have left an indelible imprint on my academic trajectory. Prof. Haritash's wealth of expertise, visionary leadership, and steadfast commitment to excellence have served as beacons of inspiration, propelling me towards greater heights of academic achievement.

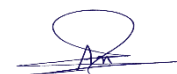
Furthermore, I'm grateful to the committed staff of the Environmental Engineering Department and the lab personnel. Their tireless efforts and expertise have fostered an environment for academic growth, laying the foundation for my pursuits.

I would be remiss not to express my heartfelt appreciation to my esteemed colleagues and fellow researchers, including Deepali Goyal, Riki Sarma, and Kulvendra Patel, whose collaborative spirit, camaraderie, and exchange of ideas have been instrumental in shaping my scholarly journey. Together, we have navigated the challenges, celebrated the victories, and forged bonds of camaraderie that have enriched my academic experience immeasurably.

I also thank the National Water Regulatory Authority of Afghanistan (NAWARA) (now the Ministry of Energy and Water), and colleagues from Kabul Polytechnic University for their valuable support and contributions to my research efforts, including providing data, support during fieldwork, and assistance with sample collections. Their cooperation has increased the quality and depth of my research and increased its impact and importance in the academic community.

I am profoundly grateful to the Indian Council for Cultural Relations (ICCR) for their generous scholarship support throughout my academic journey, alleviating the financial burdens associated with Ph.D. studies and enabling me to pursue my scholarly aspirations with unwavering focus and dedication.

Last but certainly not least, I want to express my profound gratitude to my father, family and friends for their consistent support and belief in me. Their encouragement and love have been the foundation of my academic success, and I am forever thankful.



Ali Reza Noori



## DELHI TECHNOLOGICAL UNIVERSITY

(Formerly Delhi College of Engineering)

Shahbad Daultpur, Main Bawana Road, Delhi-42

### CANDIDATE'S DECLARATION

I, **Ali Reza Noori**, hereby certify that the work which is being presented in the thesis entitled **Assessment of groundwater quality and recharge potential in Kabul Afghanistan** in partial fulfilment of the requirements for the award of the Degree of Doctor of Philosophy, submitted in the Department of **Environmental Engineering**, Delhi Technological University is an authentic record of my own work carried out during the period from **2019** to **2024** under the supervision of **Environmental Engineering**.

The matter presented in the thesis has not been submitted by me for the award of any other degree of this or any other institute.

**Candidate's Signature**

This is to certify that the student has incorporated all the corrections suggested by the examiners in the thesis and that the statement made by the candidate is correct to the best of our knowledge.

**Signature of Supervisor (s)**

**Signature of External Examiner**



## DELHI TECHNOLOGICAL UNIVERSITY

(Formerly Delhi College of Engineering)

Shahbad Daultapur, Main Bawana Road, Delhi-42

### CERTIFICATE BY THE SUPERVISOR

Certified that **Ali Reza Noori** (Roll No. 2K19/PHDEN/07) has carried out his research work presented in this thesis entitled **Assessment of groundwater quality and recharge potential in Kabul Afghanistan** for the award of **Doctor of Philosophy** from Department of Environmental Engineering, Delhi Technological University, Delhi, under my supervision. The thesis embodies the results of the original work, and the student himself carries out studies. The content of the thesis does not form the basis for the award of any other degree to the candidate or anybody else from this or any other University.

Signature

Prof. S.K. Singh

Professor

Department of Environmental Engineering,  
Delhi Technological University, Delhi, India

Vice Chancellor

RTU Kota

Rajasthan India

Date:

## ABSTRACT

Groundwater is an integral part of water resources. It has a vital role in water use in Kabul, Afghanistan. It is the only available source of water supply in the city. Since groundwater is the only accessible source for water supply purposes, studying the quantity and quality of underground water is of particular importance. The present study aimed to evaluate groundwater quality and its recharge potential in Kabul, Afghanistan. This study comprehensively analysed 35 groundwater samples and determined their hydrogeochemical characteristics, quality, water types, and suitability for drinking purposes. Various parameters were measured using different instruments and methods, including total dissolved solids (TDS), pH, electrical conductivity (EC), hardness, chloride, bicarbonate, sodium, calcium, magnesium, potassium, fluoride, sulphate, and nitrate. The distribution pattern of these parameters and the Water Quality Index (WQI) was spatially modelled using the ArcGIS tool. The results indicate that the main anions and cations follow an ascending order of Iron < Nitrate < Sulphate < Chloride < Bicarbonate and Potassium < Calcium < Sodium < Magnesium, respectively. Bicarbonate, chloride, nitrate, magnesium, sodium, calcium, and potassium exceeded the World Health Organization (WHO) permissible limits in drinking water samples. The Piper diagram analysis shows that the major water type is Mg-HCO<sub>3</sub> (about 83%). The rest is Na (11.4%), Ca-Na-HCO<sub>3</sub> (5.7%), and Ca-Mg-Cl (5.7%). According to Gibbs' plot results, all water samples are of rock dominance and precipitation dominance. According to the WQI, approximately 88.57% of the study area has excellent to good water quality, while 11.43% has poor to very poor water quality.

The Artificial Neural Network (ANN) model was developed in MATLAB to predict groundwater quality. The results of the ANN model for simulating sodium concentration in groundwater based on input data (EC, TDS, Salinity) have an average variance of 11.53%. The average variance for chloride and sulfate is 3.83% and -3.41%, respectively. However, the average variance for potassium and total hardness is 259.6% and 45.25%, respectively. These different mean percentages of variances show the models' accuracy and suitability. Based on these percentages, one can conclude that the model is very suitable for simulating the concentrations of sodium, chloride, and sulfate in groundwater with the suggested inputs (EC, TDS, and Salinity). Therefore, the model is unsuitable for predicting potassium and total hardness in groundwater with the same inputs.

Data on groundwater quality from 54 monitoring wells were collected by the National Water Affairs Regulation Authority of Afghanistan, including data from both dry and wet seasons. The analysis focused on specific water quality measures such as EC, TDS, hardness, nitrate, chloride, fluoride, sulfate, sodium, and some heavy metals such as iron and manganese. Spatial distribution maps and temporal variations were created to examine trends in groundwater quality and seasonal fluctuations. Statistical analysis revealed significant seasonal changes in magnesium, sodium, chloride, fluoride, iron, and manganese concentrations. Out of the 20 water quality assessments conducted, 14 during the dry season and 15 during the wet season showed concentrations exceeding the WHO recommendations. The variations in water quality metrics were influenced by factors such as recharge volume, hydraulic conductivity,

and the geological formation of the region. Notably, the levels of qualitative parameters were higher during the wet season, particularly in wells located near river routes or in agricultural areas.

The study also analyzed groundwater level trends and assessed drought dynamics in Kabul city. Cluster analysis was used to classify observation wells based on long-term trends in groundwater level data. The Mann-Kendall statistical test was employed to determine seasonal and annual variations in groundwater depth. The Standardized Groundwater Level Index (SGI) was used to measure groundwater drought. The trend analysis revealed that water levels in 82% of the observation wells were significantly decreasing. From 2014 to 2020, the study area experienced increasingly severe and persistent drought, according to the SGI results. The analysis of land use and land cover (LULC) indicated that the built-up area in the study area increased from approximately 15% in 2005 to 32% in 2020, while bare land decreased from about 67% in 2005 to 52% in 2020. The significant decline in groundwater level can be attributed to changes in LULC, excessive groundwater exploitation, and declining annual precipitation.

The study employed an integrated application of the analytical hierarchy process (AHP) and ArcGIS to identify potential groundwater zones in the study area. Ten different thematic variables were analyzed in the Arc GIS environment with various numerical weightage values in the basin. These variables included geology, geomorphology, land-use land cover, lineament density, drainage density, soil, slope, rainfall, elevation, and water depth. Static groundwater level records have been utilized to acquire precision and reliability for discovering groundwater potential zones. According to the final output of the results, most parts of the study area are covered by a reasonable and very good capacity of groundwater potential zones. Based on the results, four categories of the GWPZs were eventually recognized. According to the statistics, the area is divided into zones with very poor potential (16%), poor (18%), good (35%), and very good (31%).

Cities in arid and semi-arid regions face challenges in managing urban floods and water shortages. Kabul City in Afghanistan is particularly vulnerable to groundwater decline and urban floods. This study explores using rainwater harvesting (RWH) to manage floods and recharge groundwater in Kabul City. The research analyses rainfall patterns, including variability, rainy days, seasonality, probability, and maximum daily precipitation. The findings show rainfall greater than 30mm occurs approximately every 3-4 years. Rainfall in Kabul is seasonal, with a coefficient of variation of 127% in October and 46% in February. The study also investigates the potential of RWH in Kabul City for stormwater management and groundwater recharge. Based on LULC, implementing an RWH and recharge system could increase mean annual infiltration from 4.86 million cubic meters (MCM) to 11.33 MCM. A weighted curve number (CN) of 90.5% indicates the dominance of impervious surfaces. The study identifies a rainfall threshold of 5.3 mm for runoff generation. Two approaches to rainwater collection for groundwater recharge were explored: RWH for a residential house (yielding about 88m<sup>3</sup>/year) and RWH for a street sidewalk (collecting water from streets and sidewalks). These findings highlight the potential of RWH for effective management of urban floods and artificial groundwater recharge.

GIS software utilized remote sensing, geographic information, and a multi-influencing factor method to determine areas suitable for groundwater recharge structures. Geology, geomorphology, lineament density, drainage density, rainfall, soil type, LULC, and slope were considered. The results indicate that geology, geomorphology, lineament density, and slope are the main factors influencing groundwater recharge in the region. The projected recharge potential zones were categorized into four groups: very good, good, moderate, and least recharge potential areas. The very good and good recharge zones cover more than half of the basin, making them suitable for various groundwater-recharging techniques. Based on the diverse geo-environmental factors in the study area, several artificial groundwater recharge methods, including check dams, contour trenches, recharge wells, and rooftop rainwater harvesting with recharge wells, were recommended.

The findings of this study will contribute to the sustainable development of groundwater management strategies in the region. The following recommendations are suggested for future research: As cancer rates in the country continue to grow, assess water quality across the country, particularly arsenic and heavy metal levels, and their potential association with increased cancer rates. Using isotopic analysis to determine the age of groundwater in use. Examining and proposing suitable recharge methods such as contour trenches, check dams and recharge wells from a structural point of view. Modelling the quality and quantity of groundwater in current conditions and with artificial recharge applications. Finally, consider wastewater recycling as a viable option for groundwater recharge.

## TABLE OF CONTENTS

Title	Page No.
<b>CERTIFICATE BY THE SUPERVISOR</b>	<b>iv</b>
<b>ABSTRACT</b>	<b>v</b>
<b>List of Abbreviations</b>	<b>xii</b>
<b>List of tables</b>	<b>xiv</b>
<b>List of figures</b>	<b>xvi</b>
<b>CHAPTER 1 : INTRODUCTION</b>	<b>1-5</b>
<b>1.1 General</b>	<b>1</b>
<b>1.2 The importance of groundwater</b>	<b>1</b>
<b>1.3 The quality of groundwater</b>	<b>2</b>
<b>1.4 Research importance</b>	<b>2</b>
<b>1.5 Objectives of this research</b>	<b>3</b>
<b>1.6 Scope of the present study</b>	<b>3</b>
<b>1.7 Organization of thesis</b>	<b>3</b>
<b>CHAPTER 2 : REVIEW OF LITERATURE</b>	<b>5-25</b>
<b>2.1 General</b>	<b>5</b>
<b>2.2 Groundwater conditions in Kabul, Afghanistan</b>	<b>8</b>
2.1.1 Methodology	8
2.1.2 Groundwater distribution	10
2.1.3 Groundwater quality	12
2.1.4 The consumption of groundwater resources in Kabul	15
2.1.5 Alternatives to drinking water in Kabul	17
2.1.6 Conclusion	19
<b>2.3 Water Quality Index</b>	<b>20</b>
<b>2.2 Groundwater drought index</b>	<b>20</b>
<b>2.3 Application of RS and Arc GIS</b>	<b>21</b>
<b>2.4 AHP</b>	<b>22</b>
<b>2.5 MIF</b>	<b>22</b>
<b>2.6 Water harvesting</b>	<b>23</b>
<b>2.7 Artificial Neural Networks modeling</b>	<b>23</b>
<b>CHAPTER 3 : MATERIAL AND METHODS</b>	<b>25-58</b>
<b>3.1 Study area</b>	<b>25</b>
3.1.1 General	25
3.1.2 Drainage System	25
3.1.3 Geology	27
3.1.4 Hydrogeology	28
<b>3.2 Water sampling and water quality analysis</b>	<b>29</b>
3.2.1 Water sample collections and Lab works and Analysis of samples	29
<b>3.3 Water quality analysis</b>	<b>30</b>
3.3.1 Analysis of water	30
3.3.2 Water quality index	35
3.3.3 Geographic information system analysis	35
<b>3.4 Artificial neural networks</b>	<b>36</b>
3.4.1 General	36



3.4.2 Biological Neurons and ANN	37
3.4.3 Need for ANN model.	39
<b>3.5 Seasonal variation of groundwater quality</b>	<b>39</b>
3.5.1 The process of data acquisition and selection from (NWARA)	39
3.5.2 Development of geospatial distribution maps of groundwater quality data	40
3.5.3 Statistical evaluations	40
<b>3.6 Groundwater level analysis</b>	<b>41</b>
3.6.1 Static water level data	41
3.6.2 Data imputation	43
3.6.3 Hierarchical Cluster Analysis	44
3.6.4 Groundwater Levels and Groundwater Drought: A Nonparametric Trend Test	44
<b>3.7 Delineation of groundwater potential zones</b>	<b>45</b>
3.7.1 Thematic maps	45
3.7.2 Analytical hierarchy process (AHP)	46
<b>3.8 Artificial recharge potential of groundwater in urban area</b>	<b>48</b>
3.8.1 Data acquisition	48
3.8.2 LULC development	48
3.8.3 Rainfall Analysis	49
3.8.4 Rainwater harvesting potential based on LULC.	51
3.8.5 Groundwater recharge	51
3.8.6 Surface runoff	52
3.8.7 Models for rainwater harvesting and groundwater recharge.	54
<b>3.9 Delineation of groundwater recharge potential zones</b>	<b>54</b>
3.9.1 Enlarging the study area	54
3.9.2 Identifying influential factors	55
<b>CHAPTER 4 : RESULT AND DISCUSSION</b>	<b>58-146</b>
<b>4.1 Water quality analysis</b>	<b>58</b>
4.1.2 Physicochemical parameters	59
4.1.3 Hydrochemical facies	65
4.1.4 Gibbs diagram	68
4.1.5 Single factor pollution index	71
4.1.6 Nemerow pollution index method	72
4.1.7 Water quality index of groundwater	74
<b>4.2 Development of ANN model</b>	<b>76</b>
4.2.1 Network Architecture	78
4.2.2 Performance of ANN model	78
4.2.3 Inputs	78
4.2.4 Targeted outputs	79
4.2.5 Neural Network Tool	79
4.2.6 Network specifications	79
4.2.7 Train network	80
4.2.8 Validation of ANN models	84
4.2.9 Summary and applications of ANN	86
<b>4.3 Seasonal water quality analysis</b>	<b>89</b>
4.3.1 Generic evaluation of the quality of groundwater	89
4.3.2 Seasonal variations in the groundwater quality	91

4.3.3 Spatio-seasonal evaluation of groundwater quality criteria	97
<b>4.4 Groundwater level</b>	<b>103</b>
4.4.1 Cluster analysis of the wells	103
4.4.2 Trends of Groundwater Table on an Annual and Seasonal Basis	106
4.4.3 Extent and Severity of Groundwater Drought Conditions	109
4.4.4 Rainfall conditions and groundwater levels	111
4.4.5 Influence of land use/land cover on groundwater recharge	112
<b>4.5 Groundwater potential zone</b>	<b>115</b>
4.5.1 AHP Weights and Ranks	115
4.5.2 Geology	116
4.5.3 Drainage density	116
4.5.4 Land-use and land-cover	118
4.5.5 Slope	119
4.5.6 Geomorphology	119
4.5.7 Soil	119
4.5.8 Lineament density	120
4.5.9 Rainfall	120
4.5.10 Elevation	120
4.5.11 Groundwater levels	122
4.5.12 Groundwater potential zone mapping	122
4.5.13 Validation of results	123
<b>4.6 Artificial recharge potential of groundwater in urban area</b>	<b>124</b>
4.6.1 Rainfall conditions	124
4.6.2 RWHRs vs non-RWHRs conditions	128
4.6.3 Surface runoff estimation	129
4.6.4 Rooftop and street surface rainwater harvesting for groundwater recharge.	130
<b>4.7 Delineation of groundwater recharge potential zones</b>	<b>134</b>
4.7.1 Influential factors	134
4.7.2 Relative Importance of the Factors	141
4.7.3 Delineation of groundwater recharge potential zones	141
4.7.4 Discovering Appropriate Recharge Approaches for Groundwater	143
<b>CHAPTER 5 : CONCLUSION, FUTURE SCOP AND SOCIAL IMPACT</b>	<b>146</b>
<b>5.1 Conclusion</b>	<b>146</b>
5.1.1 Water quality analysis	146
5.1.2 ANN Model	146
5.1.3 Seasonal water quality analysis	147
5.1.4 Groundwater level analysis	147
5.1.5 GWPZs	148
5.1.6 Artificial recharge of groundwater in an urban area	148
5.1.7 GWRPZs	149
<b>5.2 Recommendations</b>	<b>150</b>
<b>5.3 Scope of future work</b>	<b>150</b>
<b>REFERENCES</b>	<b>151</b>
<b>Appendix-I</b>	<b>169</b>
<b>List of Publications</b>	<b>169</b>
<b>Plagiarism Verification</b>	<b>171</b>

**CURRICULUM VITA**

**172**

## List of Abbreviations

ADB	Asian Development Bank
AGS	Afghan Geological Survey
AHP	Analytical Hierarchy Process
AIMS	Afghanistan Information Management System
ANN	Artificial Neural Network
ANSA	Afghanistan National Standards Authority
APHA	American Public Health Association
BGR	Bundesanstalt Für Geowissenschaften and Rohstoffe
BOD	Biochemical Oxygen Demand
BP	Back-Propagation
CI	Contribution Index
CIA	Central Intelligence Agency
CN	Curve Number
COD	Chemical Oxygen Demand
CoV	Covariance
DACAAR	Danish Committee for Aid to Afghan Refugees
DEM	Digital Elevation Model
DS	Dissolved Solids
DTU	Delhi Technological University
E.Coli	Escherichia Coli
EDTA	Ethylenediaminetetraacetic Acid
GIS	Geographic Information System
GW	Groundwater
GWPZ	Groundwater Potential Zone
GWRPZ	Groundwater Recharge Potential Zone
HDPE	High Density Polyethylene
HSG	Hydrologic Soil Group
IDW	Inverse Distance Weighted
JICA	Japan International Cooperation Agency
KfW	Kreditanstalt Für Wiederaufbau
KMARP	Kabul Managed Aquifer Recharge Program
K-S	Kolmogorov–Smirnov
LULC	Land Use and Land Cover
MCDA	Multi-Criteria Decision Analysis
MCM	Million Cubic Meters
MIF	Multi Influential Factor
MK	Mann–Kendall
MSE	Mean Square Error
MWL	Monitoring Well Location
NDVI	Normalized Difference Vegetation Index
NDWQS	National Drinking Water Quality Standard
NNT	Neural Network Tool

NRCS	Natural Resources Conservation Services
NSIA	National Statistics and Information Authority
NWARA	National Water Affairs Regulation Authority
PCI	Precipitation Concentration Index
RS	Remote Sensing
RWH	Rainwater Harvesting
RWHRS	Rainwater Harvesting and Recharge System
SCS	Soil Conservation Service
SD	Standard Deviation
SGI	Standardized Groundwater Level Index
SI	Seasonal Index
SPI	Standardized Precipitation Index
SRTM	Shuttle Radar Topography Mission
SWL	Static Water Level
TDS	Total Dissolved Solids
TH	Total Hardness
TS	Total Solids
TSS	Total Suspended Solids
UNESCO	United Nations Educational, Scientific and Cultural Organization
UNHCR	United Nations High Commissioner for Refugees
USDA	United States Department of Agriculture
USGS	United States Geological Survey
UV VIS	Ultraviolet–Visible
WHO	World Health Organization
WQI	Water Quality Index

## List of tables

<b>Table No.</b>	<b>Pages No.</b>
Table 2. 1 Contaminant concentration in Kabul, Afghanistan. Source: (Hayat & Baba, 2017)	13
Table 3. 1 Relative weights ( $w_i$ ) for different water quality parameters.	36
Table 3. 2 Satellite data acquisition details	42
Table 3. 3 Pairwise comparison matrix of thematic layers.	46
Table 3. 4 Standardized matrix of AHP weights for each respective criterion.	47
Table 3. 5 Calculated matrices for CI and CR values.	47
Table 3. 6 Saaty's RI values for matrices based on variable size.	47
Table 3. 7 Infiltration coefficient of different surfaces (Nachshon et al., 2016).	52
Table 4. 1 Descriptive statistics and permissible limits of groundwater quality parameters concerning the (WHO, 2011)	58
Table 4. 2 Classification of groundwater according to electrical conductivity	59
Table 4. 3 Groundwater classification based on total dissolved solids	60
Table 4. 4 Groundwater classification based on TDS content	60
Table 4. 5 Classification of groundwater as per total hardness	61
Table 4. 6 calculated anions and cations for the Piper plot	66
Table 4. 7 The calculation process for the Gibbs plot	69
Table 4. 8 Water quality level determination based on the single factor pollution index method.	71
Table 4. 9 Nemerow pollution index technique for determining water quality level.	72
Table 4. 10 Water quality index-based groundwater classifications	74
Table 4. 11 Illustrate the summary of each network specification.	80
Table 4. 12 Validation of ANN output results with lab test results	87
Table 4. 13 Validation of ANN model simulation results with lab test results	88
Table 4. 14 Results of sample investigations statistically summarized and compared to drinking water quality requirements for Aug & Sep 2017 (Dry season)	90
Table 4. 15 Results of sample investigations statistically summarized and compared to drinking water quality requirements for Mar-May 2018 (Wet season)	92
Table 4. 16 Result of the "Kolmogorov-Smirnov test" for normal distribution of seasonal changes (n=53)	93
Table 4. 17 Summary of paired sample "t-test" for Ca and NO <sub>3</sub>	94
Table 4. 18 Summary of Wilcoxon signed-rank test	95
Table 4. 19 Annual and seasonal trend analysis results based on the MK statistics and Sen's slope values	107
Table 4. 20 Areal specification of LULC class	113
Table 4. 21 AHP ranking and weighting with classes of parameters	117
Table 4. 22 Uncertainty matrix of groundwater recharge potential zones	124
Table 4. 23 Calculated spatial proportion of LULC and their influence on $I_c(\text{eff})$ and groundwater recharge in the Kabul basin.	128
Table 4. 24 Curve Number values based on LULC.	129

Table 4. 25 Weightage of numerous thematic layers utilizing the MIF approach (Achu, Reghunath, et al., 2020; Kolanuvada, 2019; Magesh et al., 2012; Thapa et al., 2017c; Zghibi et al., 2020).	138
Table 4. 26 Weights of themes and their influences	140
Table 4. 27 Quantitative assessment of rechargeable categories	142

## List of figures

Figure No.	Pages
Figure 2. 1 The Kabul basin with groundwater sub-basins (Mack et al., 2010)	6
Figure 2. 2 The methodological flowchart of the review of literature for groundwater condition in Kabul, Afghanistan	9
Figure 2. 3 Spatial distribution of aquifer in Kabul city (Landell Mills Ltd., 2018)	12
Figure 2. 4 Total water balance of Kabul basin (recent ten years average) source: (JICA, 2011).	16
Figure 2. 5 Estimating water requirement as a component of water utilization and populace reproduced from (Houben, Niard, et al., 2009)	17
Figure 2. 6 Location of potential water resources reproduces from (Zaryab et al., 2017)	19
Figure 3. 1 Geographical location of the study area	26
Figure 3. 2 Elevation and stream map of the basin	27
Figure 3. 3 Surficial geology of the basin	28
Figure 3. 4 Sample collection and field water quality testing.	29
Figure 3. 5 Water Quality Testing and Analysis in DTU Laboratory	30
Figure 3. 6 Structure of a typical neuron (Suresh et al., 2020)	37
Figure 3. 7 Artificial representation of biological neuron (Samson S, 2010)	38
Figure 3. 8 Observational wells	42
Figure 3. 9 Well 16 observational data illustration pre and post imputation	43
Figure 3. 10 Location of meteorological station in the study area	48
Figure 3. 11 LULC map of the study area	49
Figure 3. 12 Location map of the study area	55
Figure 3. 13 mythological flow chart of the study	57
Figure 4. 1 Spatial distribution of observed parameters showing minimum to maximum ranges	62
Figure 4. 2 Pie chart illustrating percentage distribution of all measured parameters	65
Figure 4. 3 Piper diagram illustrating various hydrochemical facies of groundwater	67
Figure 4. 4 Percentage of different water types based on the Piper diagram	68
Figure 4. 5 Demonstration of principal influencing groundwater chemistry in Gibbs plot	70
Figure 4. 6 Results of water quality assessment by single factor pollution index method.	71
Figure 4. 7 Spatial distribution map of Nemerow pollution index	73
Figure 4. 8 Percentage of samples analyzed based on Nemerow pollution index	73
Figure 4. 9 Scatter plot showing water quality index (WQI) distribution in samples	75
Figure 4. 10 Geospatial model of water quality index (WQI) in Kabul Basin	75
Figure 4. 11 Correlation matrix of water quality data	77
Figure 4. 12 Typical structure of ANN model	78
Figure 4. 13 Performance plot of the network for modeling of Na.	81
Figure 4. 14 Training status of the network for modelling of Na	81



Figure 4. 15 Regression plot of the training network for modelling of Na	82
Figure 4. 16 Comparative illustrations of output figures from ANN model and target data (exact water quality data)	83
Figure 4. 17 Comparative illustrations of simulated figures by ANN model and actual data from lab	85
Figure 4. 18 Spatial distribution maps a. Ca and EC dry season, b. Ca and EC wet season, c. change in EC, d. Change in Ca, e. TDS and Mg dry season, f. TDS and Mg wet season, g. Change in TDS, h. Change in Mg	96
Figure 4. 19 Spatial distribution maps a. TH and K dry season, b. TH and K wet season, c. change in TH, d. Change in K, e. Na and Mn dry season, f. Na and Mn wet season	99
Figure 4. 20 Spatial distribution maps a. Fe and F dry season, b. Fe and F wet season, c. change in Fe, d. Change in F, e. NO <sub>3</sub> and Cl dry season, f. NO <sub>3</sub> and Cl wet season, g. Change in NO <sub>3</sub> , h. Change in Cl	101
Figure 4. 21 Dendrogram of hierarchical cluster analysis	103
Figure 4. 22 Elbow method for hierarchical cluster analysis	104
Figure 4. 23 Spatial distribution of wells classified based on cluster analysis	105
Figure 4. 24 Variability of groundwater levels in various clusters	105
Figure 4. 25 Annual groundwater level trends	109
Figure 4. 26 SGI time series for representative wells	110
Figure 4. 27 Rainfall and groundwater level time series	112
Figure 4. 28 LULC maps of the study area	114
Figure 4. 29 changes in built-up and bare land area	114
Figure 4. 30 Spatial distribution of variance in groundwater level from 2007 to 2019	115
Figure 4. 31 Geology, Drainage Density, LULC, and Slope maps of the basin	118
Figure 4. 32 Geomorphology, Soil, Lineament density, Rainfall, Elevation and Groundwater depth maps of the study area	121
Figure 4. 33 Groundwater recharge potential zones map using AHP	123
Figure 4. 34 Variability of precipitation during regular times as determined by the coefficient of variation	125
Figure 4. 35 The seasonality and concentration of precipitation (a) precipitation concentration index, (b) seasonality index, and (c) average per cent contribution to annual rainfall.	125
Figure 4. 35 Continue.	126
Figure 4. 36 Time series of annual precipitation, daily maximum precipitation, and yearly rainy days.	126
Figure 4. 37 daily precipitation probability curve from Jan 2009 to Dec 2019	127
Figure 4. 38 Maximum daily rainfall probability curve (2009–2019).	128
Figure 4. 39 Potential runoff time series.	130
Figure 4. 40 The proposed RWHRs structure for residential houses.	131
Figure 4. 41 Cross-section of the recharge system	132
Figure 4. 42 The proposed RWHRs structure for roads and streets (plan)	133
Figure 4. 43 The proposed RWHRs structure for roads and streets.	134
Figure 4. 44 a Geology, b Geomorphology, c Land use and Land cover types, and d Soil types of the basin	136

Figure 4. 45 a Lineament density, b Drainage density, c Rainfall, and d Slope of the basin	137
Figure 4. 46 Potential groundwater recharge zones	141
Figure 4. 47 Proposed locations for implementing different groundwater recharging structures in the basin	144
Figure 4. 48 Continued	145

## **CHAPTER 1**

### **INTRODUCTION**

#### **1.1 General**

Water is one of the vital resources on Earth, and all living things depend on water. It is a chemical substance available in three states: liquid, solid, and gas. These three water states are immensely beneficial to humans using them as per their convenience in amenities proportionally. It is a vital renewable resource on the earth, and can be replenished by the hydrologic cycle's annual rainfall. Water is also known as the universal solvent. It is also a substrate for most chemical, biochemical, and biological reactions. It is also known as the "elixir of life."

Human activities such as industrialization, urban development, population growth, agricultural activities, and deforestation have caused severe damage to the natural hydrological cycle. This profound impact causes ecological imbalances, causing climate change resulting in unnatural rainfall, global warming, drought and floods. This has left the current world facing the challenges of water resource scarcity on the one hand and rising water demand on the other. Water resource pollution is also growing as a result of development and modernization. As a result, a danger to the quantity and quality of this vital resource is rapidly arising.

#### **1.2 The importance of groundwater**

Groundwater is a safe and reliable source of freshwater for the world. Groundwater provides around a quarter of the world's water demands (Hao et al., 2018). According to a 2004 UNESCO estimate, groundwater serves 70 percent of the world's population, with 51 percent of countries obtaining more than 100 cubic meters per capita per year (Mengistu et al., 2019). Because groundwater is less susceptible to pollution and physicochemical and biological abnormalities, it may be used directly in most areas without treatment. Groundwater is readily available in every location, particularly in regions with scarce surface water resources. It is the only water source for any consumption in arid and semiarid areas. In most places, short-term droughts also have little effect on it. Therefore, due to its unique characteristics, groundwater is a superior source of water supply. Because groundwater is an important and essential natural resource, it must be fundamentally protected and maintained to survive and meet future sustainable development goals.

### **1.3 The quality of groundwater**

Water quality, in general, refers to the properties of provided water whose acceptability is established for specific uses, i.e., how well the quality fits the user's demands. A simple judgment of desirability may involve an individual choice, such as taste. Consumers may desire one source over the other if two drinking water of equivalent quality is available; the better-tasting water becomes the favoured supply (S, 2010).

Water quality is a fundamental and vital factor for humans because it is directly related to human health. A variety of natural and artificial influences influence the quality of groundwater. Groundwater pollution may happen during the various processes of the hydrological cycle. These processes include evaporation, transpiration, plant absorption oxidation and reduction, cation exchange, dissociation of minerals, secondary mineral precipitation, mixing of fluids, fertilizers, manure, and pollution (S, 2010).

Some minerals, such as calcium, sodium, iron, and others, may be helpful to human health when present in modest concentrations in groundwater because the human body requires a specific quantity of these nutrients. However, if these and other materials are dissolved excessively, the water may become unsafe to drink. Toxic or harmful chemicals such as arsenic, cadmium, and other metals may be present in the water, and even in tiny amounts, these substances in the water are harmful to human health.

When measuring the quality of water for industrial and agricultural purposes, it is also taken into account. In particular applications, other considerations are taken into account. Specific applications have varied quality requirements, and one water source is regarded as superior to another if it gives better outcomes and creates fewer difficulties. The nature of the relevant industry and the criteria for the quality of water utilized determine the quality of water used for industrial purposes. The water quality must meet the requirements or standards established for the intended application.

### **1.4 Research importance**

Groundwater is the only available source of water for Kabul city at the moment. It has declined significantly due to population growth and overuse, but its statistical significance and magnitude have not been analyzed yet. On the other hand, its quality is also deteriorating. However, previous studies in this area have not addressed whether seasonal changes also cause changes in groundwater quality. Another critical issue we do not yet know is the qualitative groundwater modeling in Kabul. This can help better manage and create sensitive and protected areas.

The literature review illustrates that the tentative project runs on a groundwater recharge named the Kabul Managed Aquifer Recharge Program (KMARP). Potential sites for artificial recharge systems that have been identified are still unclear. Researching and identifying such potential sites will lead to more success

in the artificial recharge of groundwater. On the other hand, the potential of harvested rainwater on the urban scale is unclear yet. As the reviewed literature illustrates, the groundwater has declined severely in the city for several reasons. Therefore, identifying the potential of harvesting rainwater for groundwater recharge is crucial in sustainable groundwater management in the study area.

## 1.5 Objectives of this research

Because groundwater in Kabul is the only source of drinking water, the overall goal of this study is to assess and evaluate the quality of groundwater and its recharge potential in Kabul.

The specific objectives are:

1. To study the status of groundwater quality in Kabul City, Afghanistan.
2. To analyse the seasonal variation in groundwater quality in the study area.
3. Modelling of groundwater quality using Water Quality Index and ArcGIS.
4. Trend analysis of groundwater table and its fluctuation in Kabul city.
5. Assessment of water harvesting (recharge) potential in the study area.

## 1.6 Scope of the present study

Groundwater quality in the research region will be evaluated seasonally as part of the current investigation. It gives the groundwater quality parameters as spatial models in the study area. The present study provides details on groundwater degradation in the research region. The current work offers a design approach for enhancing groundwater resources using artificial recharge. Additionally, it gives information on the research region's recharging potential zones and procedures. Furthermore, it provides more knowledge on the water that could be available for artificial groundwater recharge. The authorities can estimate the concentration of main cations and anions in the groundwater at any given site.

## 1.7 Organization of thesis

This thesis has been arranged in five chapters. A brief description of each chapter is given below.

**Chapter 1** provides information on the importance of groundwater and its quality. The significance of this research work and objectives of the current study. The scope of the present work is also discussed in this chapter.

**Chapter 2** gives clear and detailed information on the review of the literature. It includes a comprehensive literature review on groundwater quality and quantity in Kabul, Afghanistan. It provides sufficient evidence on the spatial

distribution of groundwater in the study area. Consumption of groundwater in Kabul and alternative sources, including remote sources and artificial groundwater recharge, have been discussed. Moreover, the literature on water quality index, groundwater drought index, application of RS and GIS in groundwater studies, AHP and MIF approaches, water harvesting, and ANN have been reviewed.

**Chapter 3** covers the materials and methodologies used in this contribution. It explains the characteristics of the study area, sample collection and analysis methods, and water quality analysis approaches, including WQI, geographic information system analysis, application of ANN, and seasonal variation of groundwater quality. It also explains the techniques used for groundwater level analysis and groundwater drought. Delineation of groundwater potential zones, rainfall assessment, artificial groundwater recharge in urban areas, and delineation of groundwater recharge potential zones are also discussed.

**Chapter 4** illustrates the results and findings of the study. Significant findings of the study, such as the quality of groundwater, comparison of water quality parameters with WHO/ANSA standards, WQI, Seasonal changes in groundwater quality, and ANN, have been discussed in detail. Groundwater level and trend analysis, including clustering of the monitoring wells, have been demonstrated in this chapter. Identified groundwater potential zones and the respected output map have been illustrated. Moreover, the potential for artificial groundwater recharge in the urban area has been discussed. The suitable sites for groundwater recharge and their mechanisms are analyzed in this chapter.

**Chapter 5** furnishes the conclusion of this research work based on the water quality analysis and suitability of groundwater for drinking purposes, seasonal changes in groundwater quality, modelling of groundwater quality using ANN, decline in groundwater level, delineation of potential zones of groundwater, the potential of artificial recharge in the urban area, and delineation of recharge potential zones with suitable mechanisms. This chapter also includes some recommendations and scope for future studies.

## CHAPTER 2

### REVIEW OF LITERATURE

#### 2.1 General

Water availability is a primary constraint on achieving sustainable development, mainly when both quantitative limitations, linked to population growth, and qualitative limitations, associated with threats like overuse, inefficient water utilization, and inadequate management of effluents, are considered. Approximately a quarter of the global water requirements rely on groundwater (Hao et al., 2018). As per a 2004 UNESCO report, roughly 70 per cent of the world's population relies on groundwater, with 51 per cent of nations reportedly extracting more than 100 cubic meters per capita annually (Mengistu et al., 2019). In numerous arid and semiarid regions, groundwater plays a pivotal role in meeting nearly all water requirements. Freshwater, constituting only 3% of the Earth's total water sources, finds approximately 30% of its availability in groundwater. This source is crucial for various aspects such as human health, ecosystems, power generation, and other water-dependent activities (Kalhor et al., 2019). In recent decades, there has been a notable increase in the rates of declining water levels in aquifers, destruction of wetlands, intrusion of seawater, and overall degradation of water quality (Niu et al., 2014). Simultaneously, there has been a substantial increase in groundwater research, encompassing a diverse array of topics, including the assessment of groundwater quality (Kalhor et al., 2019; Sadat-Noori et al., 2014; Saraswat et al., 2019; Selvakumar, Ramkumar, et al., 2017; Singaraja, 2017; Varol & Davraz, 2015; Verma et al., 2020), hydrogeochemical evaluation (Chidambaram et al., 2018; Haritash et al., 2017; Karami et al., 2018; Krishna Kumar et al., 2015; Srinivas et al., 2017), vulnerability assessments (Abdeslam et al., 2017; Awawdeh et al., 2015; Naik et al., 2008; Oroji, 2019), purification of groundwater

(Ahmad et al., 2018; Dinh et al., 2020; Khan et al., 2020; Nguyen et al., 2020; Uhl & Tahiri, 2003) Groundwater quantity assessment and modelling, the relationship between groundwater, urbanization, and land use (Hall et al., 2020; Hou et al., 2020; G. Huang et al., 2020; Kalhor & Emaminejad, 2019; Malik et al., 2010; H. Zhang et al., 2019) and groundwater recharge (Abijith et al., 2020; Achu, Thomas, et al., 2020; Adhikari et al., 2020; Arefin, 2020; Lentswe & Molwalefhe, 2020; Patel et al., 2020; Prabhu & Venkateswaran, 2015; Senanayake et al., 2016; Yeh et al., 2016) are the most focused topics globally.

The Kabul basin, a component of the Kabul River (Indus) basin, represents a geological valley encompassing Afghanistan's capital city. Geographically oriented from north to south, the Pghman Mountains border to the west and the Saffi Mountains to the east (Figure 2.1) (R. Bohannon, 2010). The basin was subdivided into six distinct sub-basins, namely Central Kabul, encompassing Kabul, Paghman, Upper Kabul, Logar, Deh Sabz, Shomali, and Panjsher (Mack et al., 2009). This study explicitly targets the basin's southern region, with a particular emphasis on the Central Kabul, Paghman, Upper Kabul, and Logar sub-basins that encompass the city of Kabul. These areas are deemed of special significance, as illustrated in Figure 2.1.

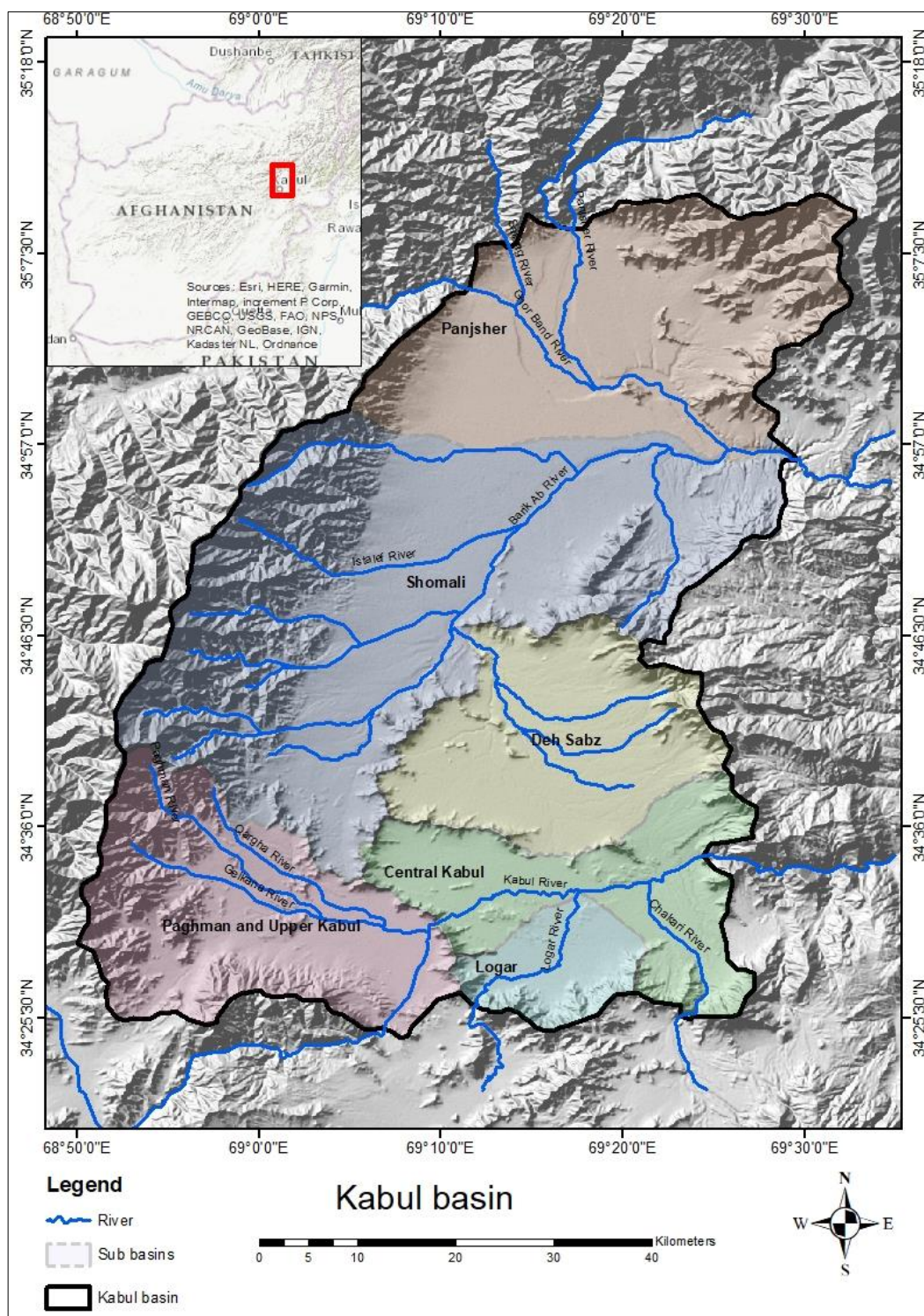


**Figure 2. 1** The Kabul basin with groundwater sub-basins (Mack et al., 2010)

The geological composition of the Kabul basin includes sand, gravel conglomerates, and loess loams endowed with sufficient filtration capacity. However, rapid population growth has led to extensive, unplanned urban expansion, creating impervious surfaces that hinder natural groundwater infiltration. Notably, the Kabul



metropolis lacks a comprehensive wastewater collection and treatment system. Pollution sources such as drainage pit latrines, roadside ditches, sewerage, septic tank leakage, the Kabul River, and irrigation channels have significantly contributed to environmental contamination.

Furthermore, additional pollution sources impacting groundwater quality in the Kabul basin include cesspits, domestic waste, unregulated disposal of generated garbage, over-exploitation, the absence of a robust water supply system, and limited public awareness of water quality issues. Agricultural practices, such as fertilizer usage and landfill sites in highly permeable areas, contaminate groundwater. The relatively low precipitation and slow groundwater recharge and depletion result in an imbalance between extractions and regeneration. This implies that the cumulative exploitation of groundwater is unsustainable, and the diminishing groundwater reserves struggle to dilute the increasing groundwater contamination.

Kabul is one of those urban centres where nearly all water requirements are met through groundwater extraction. With a population of approximately five million, the city heavily relies on groundwater to fulfil its water needs. In the current context, groundwater serves as the predominant accessible source of potable water and caters to all residential uses for the city's inhabitants. Earlier feasibility studies aimed at expanding the water supply infrastructure projected a population of 4,089,000 in 2015, with corresponding water requirements estimated at around 123.4 million cubic meters per year (Zaryab et al., 2017). Nevertheless, the anticipated groundwater supply for Kabul city is approximately 44 million cubic meters per year. The city faces challenges as it is a community with constrained water resources and relatively underdeveloped water supply and sanitation infrastructure. Merely 1% of its residents have access to the sewerage network.

Additionally, only 29% are connected to the public water supply system, with water provision primarily managed by over 70 private companies serving the residents. On a broader scale, the national distribution of access to safe drinking water is at 27%, with approximately 20% of the rural population having access to clean drinking water. This highlights the need for improved water infrastructure and accessibility in urban and rural settings (Arezoo TV, 2020; Paiman & Noori, 2019; Saffi & Kohistani, 2013).

A critical literature review component involves examining existing works on groundwater quality, quantity, status, and trends within the Kabul basin. This evaluation encompasses a diverse range of reports, articles, and published materials sourced from various outlets. Over the past two decades, numerous national and international organizations and institutions, in addition to academic research, have actively contributed to the understanding of groundwater resources in the Kabul basin across different scales.

Given the breadth of this body of work, it is essential to conduct a comprehensive review and succinctly present its summary. The upcoming sections of this chapter aim to provide detailed insights into the groundwater status, enriching factual and intellectual knowledge. Analyzing the historical state of groundwater is

crucial for anticipating future consequences. A grasp of the current scenario will facilitate the enhancement of future research topics and aid in avoiding redundant and repetitive observations. Furthermore, summarizing the findings of prior studies is integral to fostering improved groundwater management strategies and exploring alternative water resources.

## **2.2 Groundwater conditions in Kabul, Afghanistan**

### **2.1.1 Methodology**

The review process employed data from diverse sources, with Google Scholar as the primary tool to explore the various available data types. Additionally, Scopus, the United States Geological Survey (USGS) library, Springer Link, and Science Direct were consulted to identify relevant and similar works. Printed reports and valuable information from various sources were also included in the review. Initial searches were conducted using general terms in online databases to compile a comprehensive list of research data. The process commenced with a basic search of groundwater in Afghanistan. Subsequently, strategies were devised to refine and optimize search phrases, drawing insights from the initial Google Scholar data. This iterative approach allowed for identifying more specific and pertinent information related to the groundwater scenario in the Kabul basin.

The current review employed carefully selected search terms to gather relevant information. These terms include *Groundwater, Afghanistan, Kabul basin, Kabul city, groundwater quality, groundwater quantity, hydrogeology, condition, status, review on groundwater, aquifer, recharge, assessment, analysis, and study*. To ensure the retrieval of the most precise and pertinent documents, these phrases were combined using the directives "AND" and "IN." Most search phrases were formulated by the outcomes of an initial search conducted on platforms such as Google Scholar and other databases. The Snowball approach was also utilized to identify additional papers and reports beyond the initial database search. Each chosen keyword is integral to the review's intent, contributing to the overall suitability and significance of the review article.

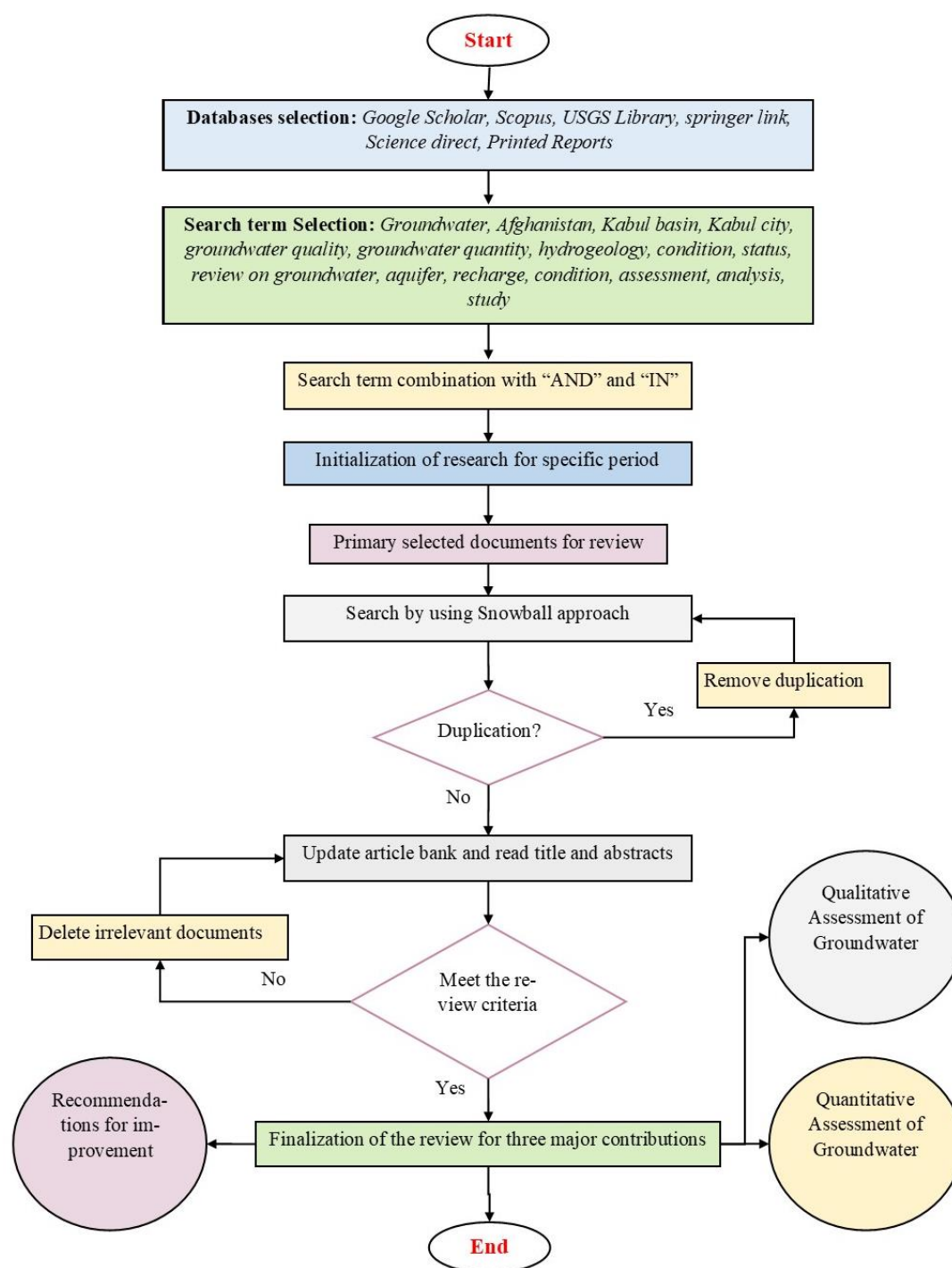


**Figure 2. 2** The methodological flowchart of the review of literature for groundwater condition in Kabul, Afghanistan

In this study, paramount importance is given to the validity and reliability of all information. Several measures were employed to assess the resources' credibility: a) Data's Timeliness: The data currency was scrutinized to ensure its relevance to the current context. b) Relevance to Study Objectives: The alignment of

the source with the study's objectives was assessed to confirm its appropriateness. c) Author's Qualifications: The qualifications and expertise of the author were considered to ascertain the source's reliability. The majority of the cited references in this study are from the last two decades, reflecting a focus on recent and relevant information. Emphasis was placed on publications where correct analysis protocols were indicated, ensuring the robustness of the observations. Specifically, for the qualitative status of groundwater, attention was directed toward samples with qualitative evaluations, highlighting and addressing qualitative issues pertinent to the area under investigation. This meticulous approach ensures the credibility and accuracy of the information included in the study.

Conversely, the collected data underwent thorough scrutiny for quantitative aspects and groundwater tables to identify research specifically addressing groundwater levels. Subsequently, the gathered information was meticulously summarized and synthesized in the assessment of both qualitative and quantitative data. This synthesis aimed to validate the groundwater status in the Kabul basin, Afghanistan. The methodological flowchart illustrating the steps followed in this comprehensive review of groundwater status in Kabul is presented in Figure 2.2, offering a visual representation of the review procedure.

### **2.1.2 Groundwater distribution**

In the Kabul basin, the predominant flow of groundwater originates from saturated alluvium and other ground-fill deposits. Across most of the basin, the water table surface mirrors the topography, leading to a general groundwater flow in the direction of surface-water discharge (Broshears et al., 2005). The study area illustration reveals the presence of four major interconnected Quaternary aquifers, as depicted in Figure 2.3. The lower Kabul, encompassing the sub-basins of Kabul-Logar, consists of two aquifers situated along the course of the Logar River and the lower section of the Kabul River. Similarly, the Upper Kabul, which includes the sub-basins of Darulaman-Paghman, comprises two aquifers situated along the Paghman River and the Kabul River (Pell Frischmann, 2012; Uhl & Tahiri, 2003; Zaryab et al., 2017). The Logar aquifer, aptly named after its location beneath and along the sides of the Logar River, extends approximately 10 km in length and boasts a width of about 3 km. It exhibits an average thickness ranging from thirty to forty meters, with a maximum depth of seventy meters. Pump test results indicate that the hydraulic conductivity of this aquifer is generally high, albeit subject to some heterogeneity, ranging from 12 to 112 m/day.

On the other hand, the Kabul aquifer is situated in a coarse-grained deposit adjacent to the Kabul River, spanning a length of approximately 9 km and a width of around 2.5 km. The aquifer's thickness varies between 40 and 80 meters, and its permeability ranges from 4.32 to 64.8 m/day. The gravel bed alongside the Paghman River, which is around 10 km long and 4 km wide, has an average thickness of 45 meters, with local thicknesses reaching 70 meters. Comprised predominantly of sand and gravel, this aquifer is recognized as the primary aquifer within the basin. Sandstones and aggregates are present in limited quantities at specific locations. The conductivity of this aquifer ranges from 1.73 to 25.92 m/day, indicating its high

permeability, which remains relatively uniform throughout the aquifer (Houben, Tünnermeier, et al., 2009).

As noted by the Bundesanstalt für Geowissenschaften und Rohstoffe (BGR), groundwater recharge occurs during the snowmelt process through direct infiltration from waterways and subsurface penetration at the basin's edges (Niard, 2005). Kabul's conventional continental climate, characterized by low precipitation and high evaporation levels, hinders groundwater replenishment primarily from rainfall. According to observations by the USGS and the Afghan Geological Survey spanning from 2004 to 2013, water levels beneath the land surface range from less than 1.5 to 73.34 meters, while static water levels varied from 1.5 to 40 meters. Seasonal fluctuations in water levels ranged from under 1 to 8 meters between September 2005 and May 2006 (Houben, Niard et al., 2009; JICA, 2011; Niard, 2005; Taher et al., 2013).

The decline in groundwater levels in Kabul has a longstanding history attributed to various factors, including overexploitation, population growth, and diminishing recharge zones. This phenomenon has been documented in numerous reports over the years (Banks, 2002; DACAAR, 2011; Houben, Niard, et al., 2009; JICA, 2011; Pell Frischmann, 2012; Qureshi, 2002; Saffi, 2007; Taher et al., 2013; Tünnermeier & Houben, 2005; Uhl & Tahiri, 2003). According to (Mack et al., 2013), The rate of decline in the city's groundwater levels has shown an acceleration, particularly in recent years. The period from 2008 to 2012 witnessed a higher decline rate, with a mean of 1.5 meters per year, compared to the earlier period from 2004 to 2008, where the mean decline ranged from 0 to 0.7 meters per year. Notably, the most recent years have recorded an excessive decrease in groundwater levels. According to an evaluation by Zaryab et al. (2017), significant declines in water levels have been observed, with reductions exceeding 10 meters in the foothills and ranging from 5 to 6 meters in the Kabul city area. In the upper Kabul basin regions, water levels have decreased by more than 15 meters between 2003 and 2016. The period from 1982 to 2003 saw a mean groundwater level decrease of 6 meters, averaging 0.28 meters per year. However, from 2003 to 2016, the mean reduction in groundwater levels was 15 meters, averaging 1.15 meters per year. The average annual decrease in groundwater levels between 2008 and 2016 further accelerated to 1.7 meters. Notably, approximately 33% of supply wells are non-operational due to declining water levels. The principal factors contributing to the decreased groundwater levels are population growth, which has doubled since the 1990s, and overexploitation of groundwater resources.

As indicated by (JICA, 2011), the aquifer structure of the Kabul basin comprises three layers: the shallow aquifer (alluvial aquifer), deep confiners (upper Neogene Aquifer), and deep aquifer (lower Neogene Aquifer). Water quality examinations conducted on samples from all test wells indicate that the water within the deep aquifer should be classified as "Fossil Water," distinct from the regular water circulation. Isotopic analysis at the deep and upper deep test wells suggests that the groundwater age in these layers corresponds to the glacial epoch. Chemical and isotopic studies of surface water and groundwater samples conducted by (Mack et al., 2010) reveal that shallow groundwater (within 100 meters below the surface) is

typically 20 to 30 years old, while in deeper aquifers, groundwater is likely to be thousands of years old. This differentiation in age provides insights into the complex hydrogeological dynamics and distinct characteristics of various aquifer layers within the Kabul basin.

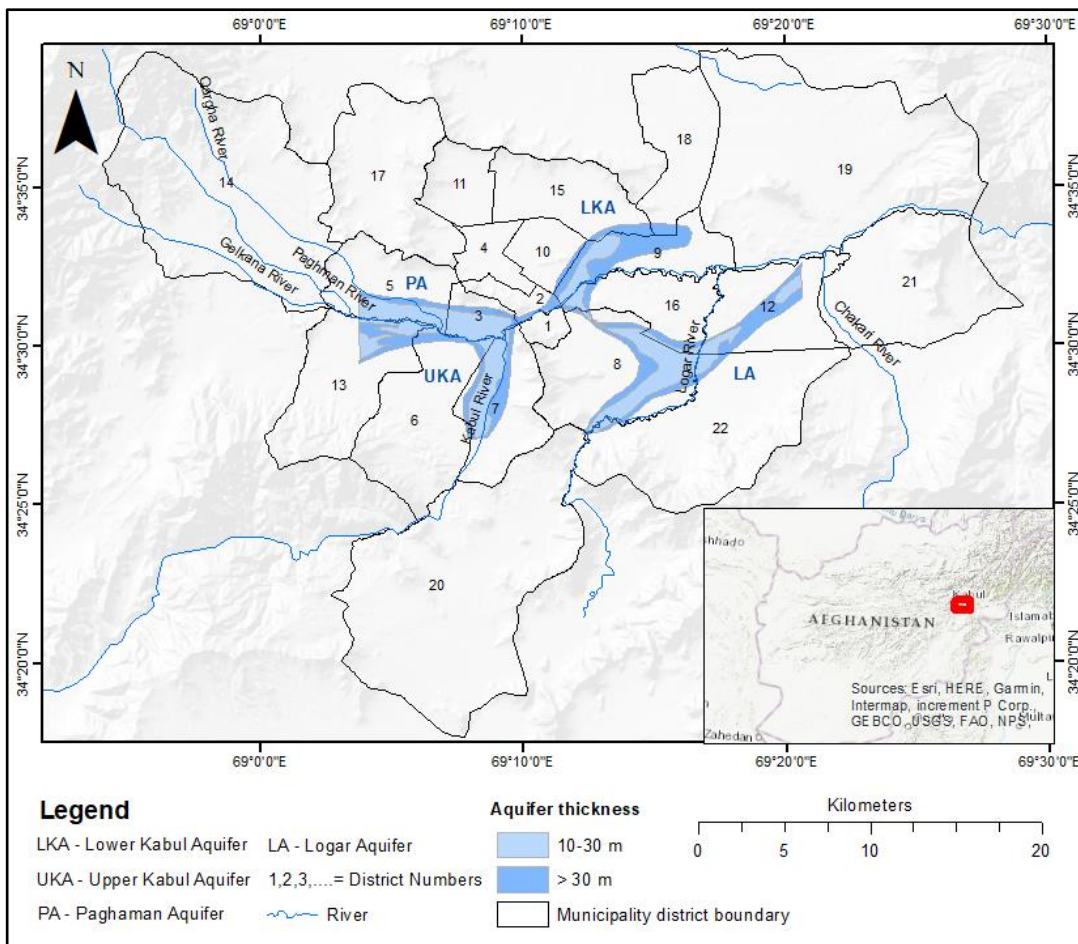


**Figure 2. 3** Spatial distribution of aquifer in Kabul city (Landell Mills Ltd., 2018)

### 2.1.3 Groundwater quality

The water quality examinations reveal a concerning pattern, indicating a continuous acceleration of groundwater contamination. This underscores the urgent need for comprehensive measures to address and mitigate the factors contributing to the deterioration of groundwater quality in the Kabul basin. Results from the National Groundwater Monitoring Network of wells covering roughly 80 per cent of Afghanistan's river basins for data management, evaluation, and mapping demonstrate that groundwater capacity in Afghanistan has been consistently declining, and water quality is progressively worried due to over-exploitation, low recharge, high evaporation and mismanagement (DACAAR, 2011). The water quality examinations highlight various groundwater quality issues, particularly in urban environments. Kabul's primary qualitative groundwater concerns include nitrate, salinity, boron,

hardness, and coliform microorganisms. Addressing and managing these issues are crucial for ensuring safe and sustainable groundwater resources in the city. Bacterial examinations indicate excessive and increasing degrees of fecal (coliform) bacteria in around 58-70% of the groundwater in Kabul's urban vicinity (Saffi, 2011). Given that the primary sources of drinking water in Kabul are shallow groundwater, pollution-related diseases pose a significant threat to the population. Contaminated water sources can lead to the spread of waterborne diseases, emphasizing the critical importance of addressing and mitigating pollution to safeguard public health in the region. The observed intensity exceeds recommendations for drinking water by the World Health Organization (WHO) and National Drinking Water Quality Standard (NDWQS) (ANSA, 2013)<sup>1</sup>.

For nitrates, the evaluations show that one-third of the groundwater has a concentration of more than or equal to 45 mg/L, while the WHO has limited the concentration of nitrates for drinking water to 50 mg/L. An analysis from Danish Committee for Aid to Afghan Refugees (DACAAR, 2019) for the entire province of Kabul indicates that the central part of the province, which mostly covers the city has nitrate contamination greater than WHO requirements (Brati et al., 2019; WHO, 2017). In reports, several levels of heavy metals showed comparatively high concentrations than WHO and NDWQS standard values. According to Barati et al. (2019), Mn, Ni, Zn are the elements exceeding the WHO standard level of drinking water. The elements of Cu, Fe, Me, NO<sub>2</sub>, PO<sub>4</sub>, COD, and TN are under the range of standard.

**Table 2. 1 Contaminant concentration in Kabul, Afghanistan. Source: (Hayat & Baba, 2017)**

Contaminant	Statistics					# Of sample	Acceptable Limits	
	Minimum	Maximum	Mean	SD	CoV		WHO	NDWQS
<b>Arsenic</b>	No detectable	0.690	0.003	0.044	14.136	241	0.01	0.05
<b>Fluoride</b>	No detectable	5.200	0.663	0.578	0.871	276	1.5	1.5
<b>Boron</b>	No detectable	4.000	0.784	0.660	0.882	276	2.4	2.4
<b>Sulfate</b>	18.0	1360.0	120.9	150.4	1.2	276	250	250
<b>Nitrate</b>	0.10	96.0	24.06	24.80	1.03	276	50	50
<b>Fecal coliform</b>	No detectable	820	112.32	64.69	5.25	276	0	0
<b>E. Coli</b>	No detectable	>200				108	0	0

Note: The measuring unit for Arsenic, Flouride, Boron, Sulfate, and Nitrate is mg/L, while for Fecal coliform and E. Coli is (Col/100 ml)

According to the analysis conducted by Gesim & Okazaki, (2018) on the physical and chemical characteristics, including metallic elements, the findings reveal a range in the Water Quality Index (WQI) from 36.21 to 716.29. The results indicate

<sup>1</sup> Afghanistan National Standards Authority (ANSA)

that only 0.2% of the groundwater in the studied area exhibits outstanding quality, 19.69% is deemed appropriate, 62.21% falls under poor quality, 13.65% is categorized as very poor quality, and 4.25% is considered unsuitable for drinking. Elevated concentrations of chemical elements such as Arsenic, Fluoride, Boron, Sulfate, Nitrate, and bacteriological contaminants like Fecal coliform and *E. coli* exceed the limits set by the World Health Organization (WHO) and the National Drinking Water Quality Standards (NDWQS) in Kabul and the Kabul Basin (Hayat & Baba, 2017). A summary of the statistical data is presented in Table 1.

An assessment conducted by (Frahmand, 2011) underscores that the groundwater in Kabul City and its surrounding areas is characterized by poor quality. Elevated concentrations of chemical elements, including lead and arsenic, align with the presence of Coliform and *E. coli* bacteria. Physical parameters such as specific conductivity, alkalinity, and bicarbonates also exhibit higher values near the city. As one moves away from the city center, the concentration levels of essential constituents decrease, suggesting a decay phenomenon. Thus, a notable correlation exists between the concentration of significant constituents in groundwater and the population density in the city region.

In-depth investigations conducted by the United States Geological Survey (USGS) suggest that the essential ion chemistry of groundwater primarily falls into the bicarbonate of calcium-magnesium type. The concentrations of various elements in assessments gathered from the central Kabul sub-basins were consistently higher than those from other sub-basins. The collected samples frequently exhibited indications of anthropogenic contaminants.

The conditions in the aquifers appeared to be Oxidic with varying oxygen levels. Among the chemical elements, the highest nitrate concentration, at 40.2 mg/lit, was reported in central Kabul. Reports indicate that lead and uranium exceeded WHO guidelines in three percent of the samples, while arsenic and selenium surpassed guidelines in one percent of the tested samples. Electrical conductivity was also reported at elevated levels. Coliform organisms were present in almost all groundwater samples, with concentrations exceeding 100 colonies per 100 mL identified in six sub-basins. *E. coli* was identified in 97 percent of groundwater quality assessments, but its concentration was scattered randomly throughout the basin.

Based on the specific CFC proportions analyzed, the average age of the young groundwater component in the study region is approximately 21 years. The majority of tested water is reported to be classified as young water. The average ages for groundwater in the sub-basin varied slightly depending on the CFC assessment method used. Still, they were around twenty years in the upper Kabul and Paghman sub-basin, 28 years in the central Kabul and Deh Sabz sub-basin, and 15-19 years in the Shomali sub-basin. CFC records suggest that the age of groundwater increases with depth. Recharge rates for the entire basin have been estimated to be between 0.4 to 0.8 m/yr for 30 percent expected porosity and 0.35 to 0.7 m/yr for 25 percent expected porosity based on the interpretation of CFC ages and the depth at which samples were collected (Mack et al., 2009).



The water assessment conducted by BGR in 2004 encompassed various water quality parameters. Among physical characteristics, electrical conductivity exceeded WHO limits, and most tested samples were classified as "hard" and "very hard" water. Elevated concentrations of magnesium, sodium, and chloride were also noted. From the standpoint of Redox potential, the samples fell within the weakly oxidizing zone. However, this report highlighted nitrate and sulfate contaminations exceeding WHO limits. Notably, only a few samples from the Kabul basin were below the limit of 0.5 mg/l for boron or two mg/l for  $\text{BO}_2$ .

Bacteriological examinations revealed that most investigated wells had a significant bacterial content. A considerable number of all explored wells exhibited significant coliform bacteria contamination, surpassing the WHO limits of 0 CFU/100 ml (Houben, Niard, et al., 2009; Houben & Tünnermeier, 2005).

Nevertheless, an investigation conducted by DACAAR on drinking water wells selected by UNHCR in various parts of the country, regularly used by returnees, also indicates that the following parameters exceed WHO limits: physical parameters, including EC, Hardness, and Turbidity. Chemical variables such as Sulfate, Fluoride, Boron, Sodium, Arsenic, Chromium, and Fecal Coliform as bacteriological pollutants were reported to be higher than the WHO-recommended limits (Saffi & Jawid, 2013).

A quality assessment of a shallow aquifer, as presented in the "Piper Diagram" by (JICA, 2011), reveals that the water characteristics in most parts of the study area fall within the zone of type-II, known as "Bicarbonate Calcium type." However, approximately 30% were categorized in Type-I, labeled as "Non-Bicarbonate Calcium type," or between types II and I. The former represents the typical water quality of a common shallow aquifer fed by rainwater. On the other hand, the latter represents a somewhat unique water quality known as "Fossil Water" outside the natural hydraulic cycle. This suggests that many observation wells have reached the deep aquifer or contain a combination of groundwater from shallow and deep aquifers. Wells labeled as type II generally include freshwater, whereas those categorized as type I or intermediate between II and I are relatively saline water.

In summary, the analysis of existing literature on groundwater quality in Kabul highlights several critical qualitative issues. Kabul's key groundwater quality parameters include elevated levels of nitrate, boron, hardness, coliform microorganisms such as fecal coliform and *E. coli*, sulfate, fluoride, and heavy metals such as Mn, Ni, and Zn. Additionally, arsenic, selenium, uranium, and lead are reported, indicating excessive and increasing concentrations in the urban area of Kabul. These parameters consistently exceed the limits of the WHO and the NDWQS.

#### **2.1.4 The consumption of groundwater resources in Kabul**

The comprehensive water balance assessment for the shallow aquifer conducted by JICA in 2011 reveals that the primary sources of groundwater recharge are the surface system, accounting for 85.2%, followed by the subsurface influx at 14.7%. The calculated volume of groundwater extraction is approximately 25 million  $\text{m}^3/\text{yr}$ , constituting about 79.8%, with about 10.2% of groundwater lost as outflow.

The total storage quantity of groundwater is estimated to be 7869 million cubic meters (Figure 2.4). The overall water balance for groundwater resulted in a deficit of 2.7 million m<sup>3</sup>/yr. This deficit in the groundwater system was supplied from groundwater storage, leading to an overall drawdown of the groundwater level.

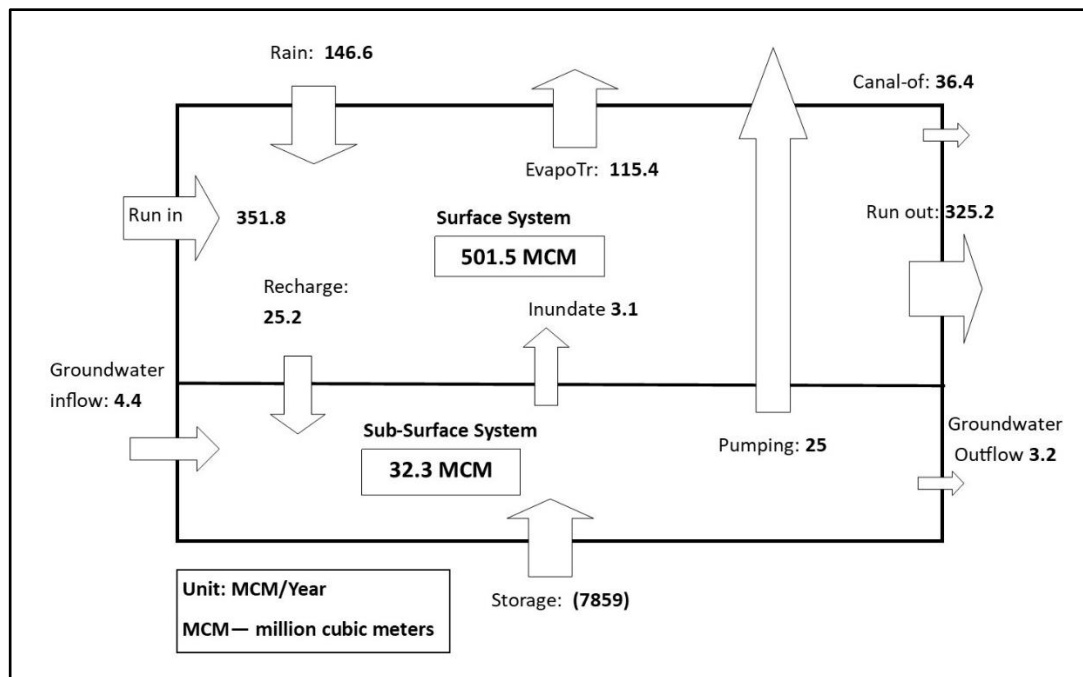


**Figure 2. 4** Total water balance of Kabul basin (recent ten years average) source: (JICA, 2011).

The water consumption in Kabul is closely tied to the population and per capita water demand. Previous studies indicate that the population of Kabul city was 320,000 in 1962, 590,000 in 1972, and 1.8 million in 2001. The exact current population is unclear, but estimates from sources such as the Central Intelligence Agency (CIA) and the National Statistics and Information Authority (NSIA) suggest that Kabul city's population is around 4.3 million people as of 2020 (CIA, 2020; NSIA, 2020). Notably, the city relies solely on groundwater sources for its water supply.

Water is sourced through four major suppliers: approximately 52% of households use their own wells, around 38% are supplied by commercial water companies, public water supply covers 13% of the population, and public wells serve 3% of the populace (Brati et al., 2019; Houben, Niard, et al., 2009; Zaryab et al., 2017). Additionally, 6% of households use public and private water supply companies. Unfortunately, precise data on groundwater extraction are not readily available, and uncertainties also exist regarding the exact population and per capita water consumption. Figure 2.5 illustrates the estimated annual water demand based on population growth and assumed per capita water rates.

The anticipated groundwater availability in Kabul is approximately  $44 \times 10^6 \text{ m}^3/\text{year}$ , according to the Kreditanstalt für Wiederaufbau (KfW) study. The Logar aquifer is reported to have the potential of about 24.64 million cubic meters annually, followed by the Allaudin and upper Kabul aquifers, with a combined capability of approximately 12.48 million cubic meters yearly. The Afshar and lower Kabul aquifers each have an estimated potential of about 3.65 million cubic meters per year. Another study by (Houben, Niard, et al., 2009) suggests that the entire groundwater recharge volume during the wet period through all mechanisms might range between  $15 \times 10^6$  to  $40 \times 10^6 \text{ m}^3/\text{yr}$ . In the maximum scenario, this study estimates the entire storage volume of groundwater to be about  $2405 \times 10^6 \text{ m}^3$  with a depth of 50 m and effective porosity of 0.13.

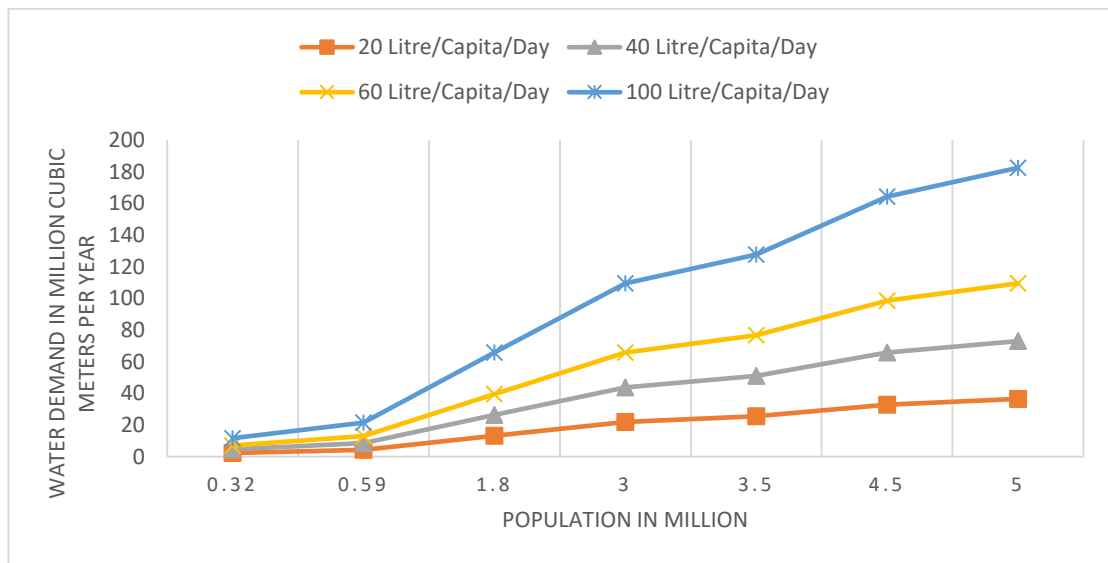


**Figure 2. 5** Estimating water requirement as a component of water utilization and populace reproduced from (Houben, Niard, et al., 2009)

## 2.1.5 Alternatives to drinking water in Kabul

### 2.1.5.1 Artificial groundwater recharge

To address water scarcity and counteract excessive groundwater abstraction, there is an urgent need for artificial recharge of the Kabul Basin groundwater and the implementation of rainwater harvesting as a viable water source for Kabul City (Masoom, 2018; K. M. A. Noori & Nasimi, 2019). A pilot project on groundwater recharge, known as the Kabul Managed Aquifer Recharge Project (KMARP), is currently being implemented at up to four specific sites. This ongoing experimental project aims to assess the feasibility of managing groundwater recharge, offering a potential solution to water scarcity in Kabul.

KMARP involves hydrogeological studies, groundwater recharge experiments, and comparisons with other alternatives. If the experiments prove successful, the outcomes could pave the way for a comprehensive project to elevate Kabul's groundwater levels and enhance water resources (KMARP, 2017). Financial support for the project comes from the Asian Development Bank (ADB) and the government of Afghanistan. The project commenced on February 10, 2017, and is expected to conclude on April 30, 2020.

#### **2.1.5.2 Remote sources**

Fortunately for Kabul city, there are several potentially proximate surface water resources (Figure 2.6). Feasibility studies for most dams above these water resources have already been conducted. However, the construction of each of these reservoirs requires substantial financial support from the government. The feasibility study for the Shatoot dam was completed in 2010, estimating an average available water amount of  $87.2 \times 10^6 \text{ m}^3/\text{yr}$  upon constructing this reservoir. Another reservoir in the planning stages is the Gulbahar dam, which is intended to be built on the Panjsher River in the northern part of Kabul city. Completing this multipurpose dam is anticipated to solve the ongoing water shortage in the Kabul region. The required feasibility study, conducted by JICA, was completed in December 2012. The Gulbahar dam is designed as an arch-type concrete dam, with a proposed height of 140 m and a storage capacity of  $240 \times 10^6 \text{ m}^3$ .

Furthermore, a feasibility study for the Salang dam was conducted by JICA and concluded in December 2012. This dam is categorized as a rockfill dam based on its construction material. The proposed height is 110 m, with a capacity limit of  $40 \times 10^6 \text{ m}^3$ . The Salang Dam is envisioned to provide water for household and industrial purposes in the new city, ensuring water availability for ecological and agricultural utilization.

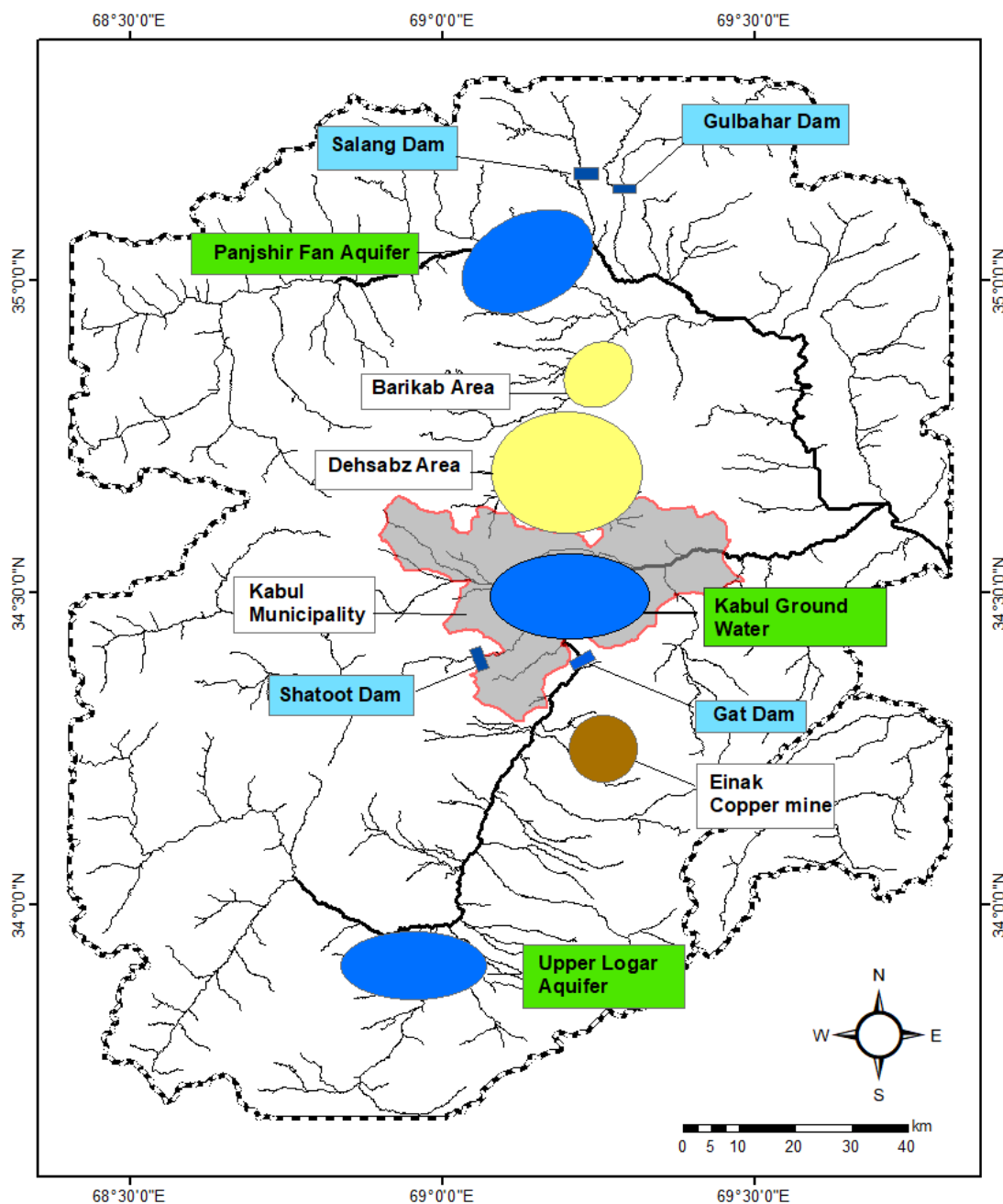


**Figure 2. 6** Location of potential water resources reproduces from (Zaryab et al., 2017)

### 2.1.6 Conclusion

The exclusive source of domestic water supply in Kabul city is groundwater. This study aims to critically review the existing literature on groundwater quality, quantity, status, and trends in the Kabul basin. The findings indicate an average annual decrease in groundwater levels of 1.7 meters between 2008 and 2016. Primary factors contributing to this decline include overexploitation, population growth, urban development, land cover changes, and diminishing recharge

zones. The annual groundwater extraction volume is estimated at approximately 25 million m<sup>3</sup>. In the most optimistic scenario, studies suggest that the entire storage volume of groundwater in Kabul could be around  $2405 \times 10^6$  m<sup>3</sup>. The total water demand for Kabul is projected to range between 73-183 million cubic meters. The aquifer structure of the Kabul basin comprises three layers: The Alluvial Aquifer, Upper Neogene Aquifer, and Lower Neogene Aquifer. Water within the deep aquifer is characterized as "Fossil Water," isolated from the regular water circulation.

The physicochemical and bacteriological composition of groundwater in Kabul exceeds the limits set by the World Health Organization (WHO) and the National Drinking Water Quality Standards (NDWQS). The findings reveal that only 0.2% of groundwater within the research area is of outstanding quality, 19.69% is of appropriate quality, 62.21% is of poor quality, 13.65% is of very poor quality, and 4.25% is unsuitable for drinking. Water is sourced through four leading suppliers: private wells (52% of households), private suppliers (38%), public water supply (13%), and public wells (3%). Two prominent solutions have been explored to address water scarcity in Kabul. The widespread adoption of artificial groundwater recharge is contingent upon the success of the pilot project "Managed Aquifer Recharge." Additionally, the utilization of surface water resources near Kabul City has been proposed as an alternative source of water supply.

**Note:** *The content of the above literature review is reproduced from the review paper titled "Status of groundwater resource potential and its quality at Kabul, Afghanistan: a review" (A. R. Noori & Singh, 2021b) With permission from Springer Nature.*

## 2.3 Water Quality Index

The Water Quality Index (WQI) is widely acknowledged as a comprehensive method for evaluating water quality. (Rabeiy, 2018) utilized the WQI to assess groundwater quality and ensure suitability. The study examined 812 water samples in the central region of Upper Egypt (Sohag Governorate) to evaluate groundwater quality for both drinking and irrigation purposes. The study results indicate that 20% of groundwater samples are classified as excellent, 75% are deemed suitable for drinking, and 7% are categorized as very poor water quality, with only 1% considered unsuitable for drinking. Numerous studies have employed the WQI to assess the quality and suitability of various water sources (Adimalla, 2021; Aenab et al., 2012; Akter et al., 2016; Alum et al., 2021; Boyacioglu, 2007; Chakraborty et al., 2021; Haritash et al., 2017; Karunanidhi et al., 2021; Liou et al., 2004; Mahmud et al., 2020; Oukil et al., 2021; Rabeiy, 2018; Radouane et al., 2021; Ram et al., 2021; Ramakrishnaiah et al., 2009; River et al., 2018; Shan et al., 2021; Tunc Dede et al., 2013; Uddin et al., 2021; Vaiphei et al., 2020; Vasanthavigar et al., 2010; Yisa & Jimoh, 2010; D. Zhang et al., 2018).

## 2.2 Groundwater drought index

The Standardized Groundwater Level Index (SGI) is an innovative tool for normalizing groundwater level time series and identifying periods of groundwater

shortages. Building on the Standardized Precipitation Index (SPI) concept, the SGI considers variations in both groundwater level and precipitation time series' structure and properties (Bloomfield & Marchant, 2013). (Halder et al., 2020) applied the SGI to analyze years of groundwater scarcity in the West Bengal region of India. In a study by (Pathak & Dodamani, 2019), SGI was employed to assess groundwater drought in the Ghataprabha River Basin, India. Over 61% of the wells in the studied area exhibited significant declining trends, with an average decrease of 0.21 meters. The study's SGI findings indicated that wells in clusters 1 and 2 frequently experienced droughts, which were attributed to declining rainfall and overuse of groundwater resources. SGI has been utilized in various studies to examine groundwater drought in different regions (Hsin-Fu Yeh & Chang, 2019; Jeongju et al., 2018; Sishodia et al., 2016).

### **2.3 Application of RS and Arc GIS**

Remote sensing (RS) and Geographic Information Systems (GIS) hybrid applications provide a potent method for identifying potential groundwater zones and minimizing time consumption and human resources. By incorporating various influential factors such as geology, lineament and drainage density, slope, geomorphology, precipitation, land-use land-cover, soils, elevation, and water depth, this approach ensures precision and reduces the likelihood of human errors. Integrating primary and secondary datasets is feasible in RS and GIS applications (Etikala et al., 2019).

Recently, several researchers have utilized RS and GIS to delineate groundwater potential zones employing different methodologies, including the Analytical Hierarchy Process (AHP) (Abijith et al., 2020; Achu, Reghunath, et al., 2020; Luo et al., 2020; Muralitharan & Palanivel, 2015), the Influence Factor (IF) technique (Etikala et al., 2019; Selvam et al., 2016; Siddi Raju et al., 2019), the linear equation approach, and others (Al-Abadi et al., 2016; Arnous, 2016), Probabilistic approach (Dadgar et al., 2017; Manap et al., 2014), geophysical technique (Abuzied & Alrefaee, 2017; Kolandhavel & Ramamoorthy, 2019; Mpofu et al., 2020), and Multi-criteria decision analysis (MCDA) (Akinlalu et al., 2017; Chowdhury et al., 2010; JHARIYA et al., 2016).

ArcGIS facilitates the analytical extrapolation of diverse experimental results to generate thematic maps and geospatial representations, reducing the unknowns in water characteristics. It employs a statistical approach to depict groundwater quality across the research area visually. Commonly used methods for creating spatial distribution maps include inverse distance weighting (IDW), kriging, and co-kriging. IDW interpolation estimates missing parameters based on proximity, giving greater weight to the nearest points and decreasing with increasing distance. Researchers like (Tiwari et al., 2018) have utilized this method to produce geographic distribution maps of various characteristics. Interpolation maps provide a generalized overview of hydrogeochemical processes and the drainage system in the studied region, aiding individuals and decision-makers in understanding groundwater quality. This information can be crucial for water management, pollution prevention, identifying pollution sources, and future groundwater conservation modelling.

## 2.4 AHP

The Analytical Hierarchy Process (AHP), proposed by Thomas L. Saaty, is a systematic multi-criteria approach used to assess and interpret complex decisions. This method analyzes dynamic decision-making problems through analysis, comparative decisions, and priority synthesis (Achu, Thomas, et al., 2020). AHP is designed to handle intricate decision scenarios by breaking them down into a hierarchical structure, facilitating a structured evaluation of criteria and alternatives to arrive at informed decisions.

In recent studies, researchers have applied the Analytical Hierarchy Process (AHP) integrated with Remote Sensing (RS) and Geographic Information Systems (GIS) to identify groundwater potential zones (Abijith et al., 2020; Achu, Reghunath, et al., 2020; Luo et al., 2020; Muralitharan & Palanivel, 2015). For example, (Muralitharan & Palanivel, 2015) presented a methodology for delineating groundwater potential zones using integrated RS, GIS, and AHP methods. The study focused on the Karur area in Tamil Nadu, Southern India, considering seven thematic maps: lithology, lineament density, geomorphology, slope, post-monsoon water level, drainage density, and land use/land cover. The attributes of these thematic layers were assigned weights based on their relevance to groundwater occurrence using Saaty's scale. After normalization using AHP, a groundwater targeting map was generated through a weighted linear combination approach in GIS. The resulting map classified the research area into five groundwater potential zones: "very good," "good," "moderate," "poor," and "very poor." The accuracy of the map was verified using well discharge data, yielding satisfactory results and highlighting advantageous groundwater potential zones in the study area.

## 2.5 MIF

The multi-influencing factor (MIF) method is a valuable technique for assessing groundwater potential zones and recharge potential zones. In a study by (Mandal et al., 2021), the MIF method delineated groundwater potential zones in Port Blair and its surrounding areas in the south Andaman District of the Andaman & Nicobar Islands. Various variables, including geology, geomorphology, slope, soil, drainage density, lineament density, rainfall, NDVI, and land use/land cover (LULC), were considered for defining groundwater potential zones (GWPZ). Thematic layers for each component were created using ground and remotely sensed data, and weights were assigned based on their impact on groundwater, as identified in previous research and literature.

Following integrating all thematic layers, a map of Port Blair's GWPZ and its surroundings was generated using overlay analysis. The resulting map identified high, medium, and low groundwater potential zones. This approach, combining GIS and the MIF method with various input factors, has been applied in several studies to identify groundwater potential zones and optimal locations for recharging (Anbarasu et al., 2020; Etikala et al., 2019; Fagbohun, 2018; Magesh et al., 2013; Mandal et al., 2021; Sidiqi & Shrestha, 2021).



## 2.6 Water harvesting

Rainwater harvesting is a traditional method employed in arid and semi-arid regions to address water shortages, and it has historical roots in many ancient civilizations for drinking and agriculture (Mahmoud et al., 2014). In modern contexts, rainwater harvesting serves as a sustainable adaptation strategy in urban areas to combat water scarcity and mitigate flooding issues (Gado & El-Agha, 2020; Krishna kumar et al., 2015; Ranaee et al., 2021; Zabidi et al., 2020). Urban hydrological challenges arise from surface runoff and river flow distribution alterations, reduced infiltration, groundwater recharge, and the prevalence of impermeable surfaces (Nachshon et al., 2016).

Traditional rainwater harvesting involves collecting and storing rainwater for various purposes, such as drinking and agriculture. A recent approach gaining attention involves collecting rainwater to replenish underground aquifers. This innovative method addresses urban water challenges and contributes to sustainable water management (Ghazavi et al., 2018; Z. Huang et al., 2021; Hussain et al., 2019; Qi et al., 2019). Floods are a widespread phenomenon, with their increasing frequency often linked to changes in climatic factors. Urban floods can have severe consequences, disrupting daily life, causing damage to both public and private infrastructure, eroding riverbanks, contaminating water resources, and even leading to fatalities. Beyond substantial economic and environmental impacts, urban floods disrupt traffic systems, water supply, electricity supply, telephone lines, and socio-cultural disturbances.

In Kabul city, urban flooding is a significant challenge. A study by (Manawi et al., 2020) reveals that from 1964 to 2009, there have been substantial changes in land use and land cover patterns in Kabul. The study indicates a 15% reduction in green areas, a 27% decrease in bare soil, and a 51% increase in impervious surfaces. The primary contributors to urban floods in Kabul are unsustainable urbanization, a deficient drainage system, and substantial changes in land cover.

Hence, in watershed systems, metropolitan areas, and regions facing uneven water resource distribution, implementing a rainwater harvesting (RWH) strategy can prove beneficial by reducing runoff loss and augmenting water resource potential. The inevitable increase in population and subsequent urban development leads to increased impermeability of land surfaces, resulting in urban floods even with minimal rainfall. Therefore, rainwater through RWH is a supplementary water source to address water shortages in arid and semi-arid urban areas. Recent research has recognized rainwater as a dependable source and RWH as an effective method for replenishing underground water resources (Alataway & El Alfy, 2019; Nachson et al., 2022; Rajasekhar et al., 2020; Stiefel et al., 2009).

## 2.7 Artificial Neural Networks modeling

Artificial neurons were initially developed in 1943, and the introduction of the back-propagation training (BP) technique for feedforward Artificial Neural Networks (ANNs) marked the inception of their applications in various research fields

in 1986 (Palani et al., 2008). An artificial neural network is an information processing system designed to simulate the functionality and connections of biological neurons, approximating the behaviour of the human brain. In ANNs, various parameters are adjusted or trained to optimize their output and make it more comparable to the measured output on a known dataset. ANNs can represent complex, non-linear functions, requiring substantial historical data for training. Once trained, ANNs can generate output for previously unseen inputs.

(Samson S, 2010) employed Artificial Neural Networks (ANN) to predict the Total Dissolved Solids (TDS) of groundwater. This study considered TDS as the output variable, and various input variables were processed to achieve the prediction. The input or independent variables included Conductivity of topsoil, Depth of topsoil, Geomorphologic type, Depth of each substratum layer, Conductivity of each substratum, Land cover, Rainfall, and Water level. The accuracy evaluation of the ANN model suggests that its output is suitable for estimating TDS from hydrogeological data at any location during both the pre-monsoon and post-monsoon seasons.

(Dadhich et al., 2021) conducted a study using eight years of groundwater data (2012-2019) for 171 Phagi tehsil, Jaipur district villages. The research focused on analyzing water level and quality patterns and projecting future trends. The study utilized three different time series forecasting models (Simple Exponential Smoothing, Holt's Trend Method, ARIMA) and artificial neural network (ANN) algorithms to achieve accurate forecasts for groundwater level and quality characteristics.

The results indicated that the ANN model outperformed time series forecasting techniques in accurately characterizing groundwater level and quality characteristics. While the ANN findings for 2023–2024 projected no significant rise in water level (>4.0 m), there had been notable changes in groundwater level, with over a 4.0 m rise observed in 81 villages during 2012–2013. However, the anticipated findings for 2024 suggested that the water level would decrease by more than 6.0 m in 16 Phagi villages. Furthermore, the water quality index indicated that groundwater in 74% of the villages would be unfit for human consumption in 2024.

(Najwa Mohd Rizal et al., 2022) utilized artificial neural networks (ANN) to predict six distinct water quality metrics in Langat, Malaysia. The study involved the prediction of biochemical oxygen demand (BOD5), total suspended solids (TSS), dissolved solids (DS), total solids (TS), nitrate, and phosphate. The researchers employed 25 water quality factors and six hydrological parameters as inputs for the ANN models. Additionally, they developed an application (app) based on the ANN models they created.

The study's findings suggest that ANNs can effectively forecast various water quality metrics by incorporating diverse inputs. Artificial neural networks have come increasingly common as a valuable tool in water quality modelling (Ghobadi et al., 2022; Gholami et al., 2022; Kuo et al., 2004; Sunayana et al., 2020).

## **CHAPTER 3**

### **MATERIALS AND METHOD**

#### **3.1 Study area**

##### **3.1.1 General**

The research region is the Kabul Basin (JICA, 2011), which includes most parts of Kabul City, the centre of Afghanistan. The research area is located in the country's central-east region, between 34°36'30" N and 34°24'40" N latitude and 69°01'25" E and 69°22'30" E longitude (Figure 3.1). The basin has a total size of 496 sq. km. The climate condition of the study area is arid to semiarid. Rainfall in Kabul is seasonal and usually snows and rains during winter (December, January, February) and early spring (March, April). The study area's annual average precipitation was around 330 mm yearly (Source: Afghanistan Meteorological Department, data recorded 2008-2018). Kabul is the country's most populated city, with a population of more than four million (CIA, 2020; NSIA, 2020). The basin's highest and lowest average temperature ranges were 32°C in July and -7°C in January (Zaryab et al., 2017). The most common land use typology in the research region is built-up. It is the country's leading national commercial base, and many refugees returned to their homeland after 2001, mostly settling in Kabul city. Also, many people from other provinces came to Kabul to find a career. Low but quite steep mountain ranges enclose the basin. The basin's elevation ranges from 1763m to 2823m (Figure 3.2). Generally, the southern and southwestern mountains have a higher elevation than the others.

##### **3.1.2 Drainage System**

Three waterways have entered the city of Kabul. Paghman stream spills out from east to west. The Maidan River (Kabul River) arrives at the study area from the south and flows 21 kilometres before joining the Paghman River.

The Logar River, an enormous tributary of the Kabul River, flows south-north and joins the Kabul River around 17 km downstream of the mouth of the Paghman waterways (Figure 3.2). In recent years, the Kabul and Paghman rivers have some discharge only in late winter due to rainfall and the spring period due to snow melting and rain. The river beds have seemed to be the primary medium of groundwater recharge in Kabul. Groundwater recharge from precipitation through infiltrating accounts for a small percentage for many reasons, such as low precipitation, high evapotranspiration, covering the recharge zones by built-up areas, and clay layers (Tünnermeier & Houben, 2005).

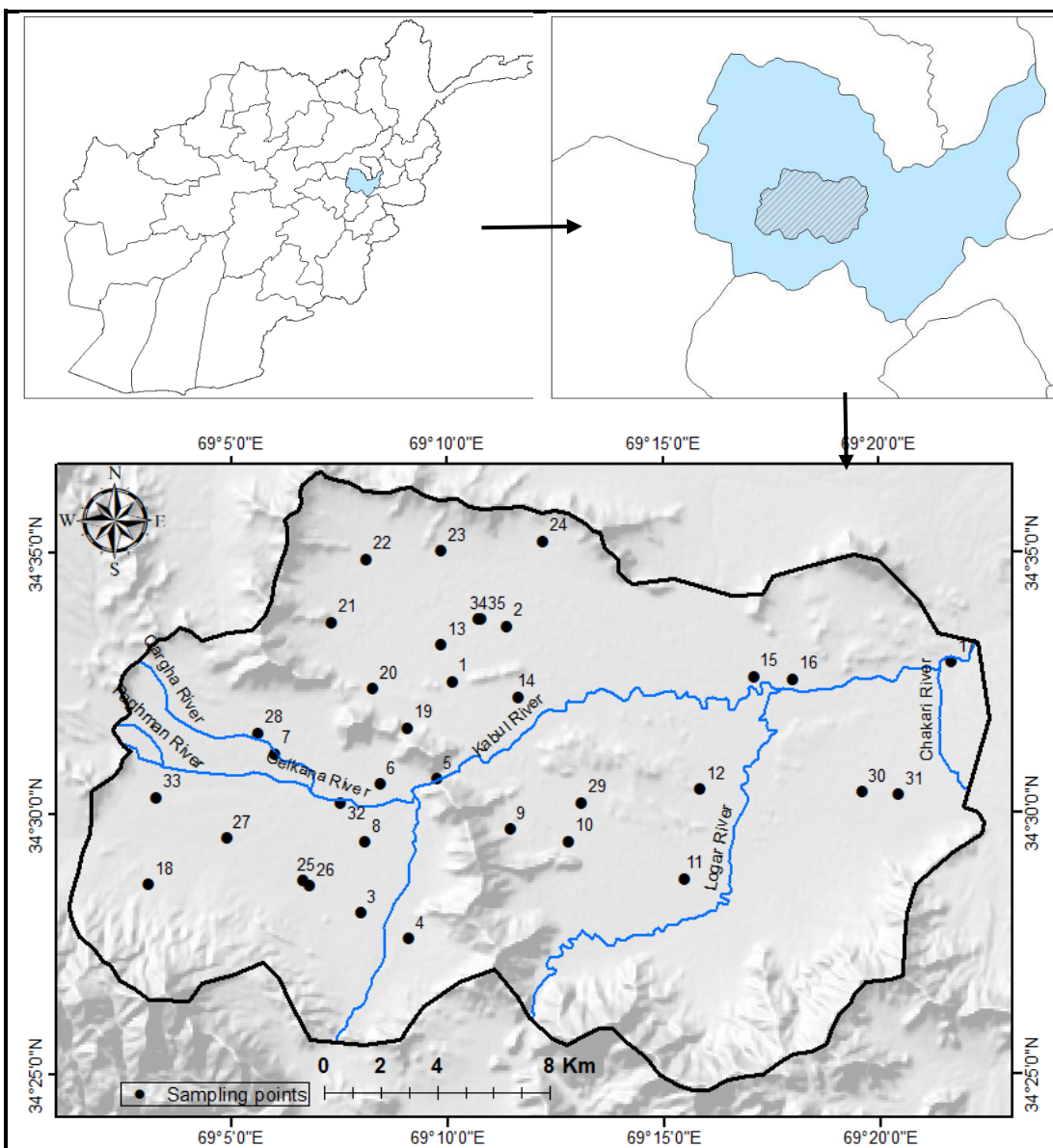


**Figure 3. 1 Geographical location of the study area**

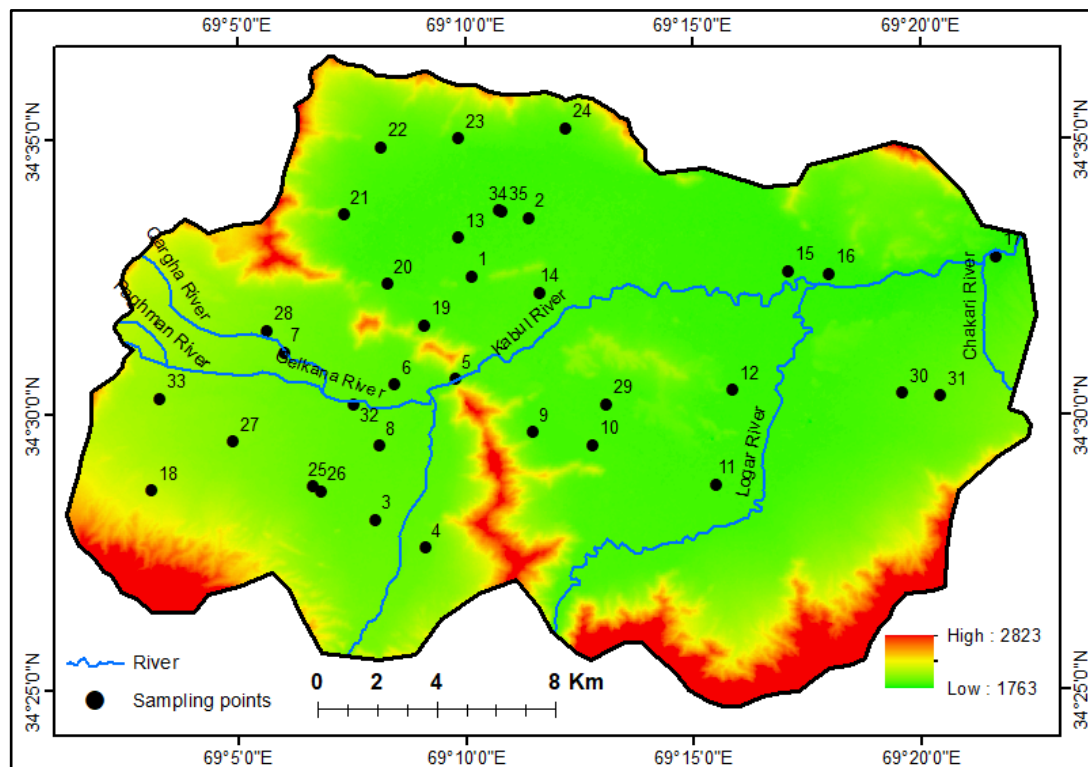


**Figure 3. 2 Elevation and stream map of the basin**

### 3.1.3 Geology

The research region is a part of the flat Kabul Basin. Metamorphic rocks comprise most of the mountain range surrounding and underpin the study region. The basin's structure developed due to plate movements during the Late Paleocene. Plate movements shaped the Kabul Basin's structure during the early Tertiary (Late Paleocene). The rocks, which are part of the Kabul block, are intersected by the Herat-Bamyan-Panjsher major fault in the west and northwest, the Sorobi fault in the east, and the Chaman fault system in the southeast. The common surficial geological forms (Figure 3.3) confirmed in the Kabul basin are conglomerate and sandstone, loess, metamorphic rocks, limestone, fan alluvium and colluvium, gneiss, limestone and dolomite, sandstone and siltstone, ultramafic intrusions and river channel alluvium. The Kabul Basin is filled with an aggregation of terrestrial and lacustrine deposits, mostly uncemented and semi-consolidated lacustrine, fluvial, and aeolian sedimentary rocks such as sand, gravel, and silt from the Quaternary and Neogene periods (Mack et al., 2009; Tünnermeier & Houben, 2005; Zaryab et al., 2017).

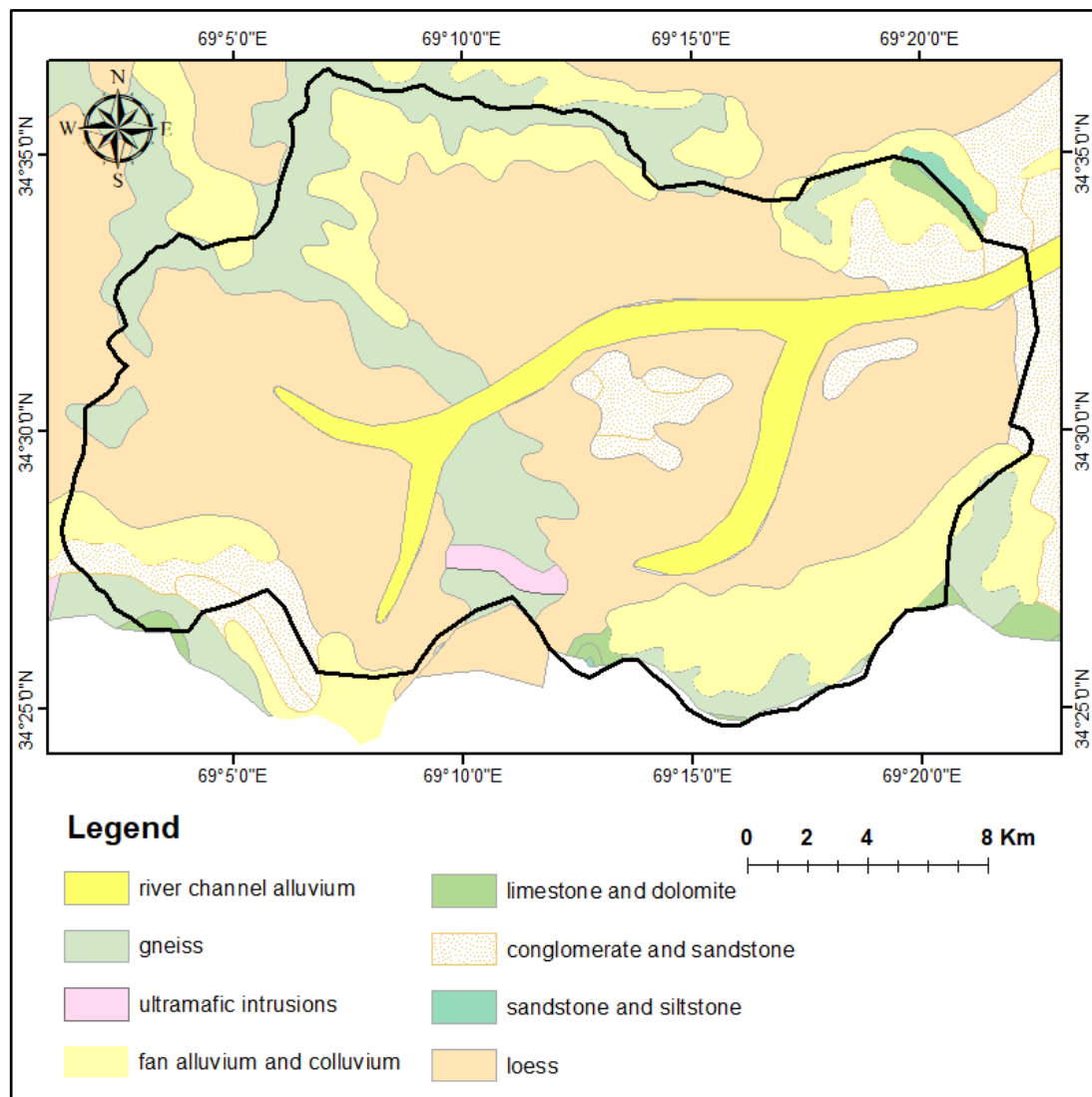


**Figure 3. 3 Surficial geology of the basin**

### 3.1.4 Hydrogeology

The hydrogeological condition of the Kabul basin is mainly formed of four interconnected Quaternary aquifers. The western region of the city, along the banks of the Paghman River and the upper stream of the Kabul River, has two aquifers. Along the Logar River path and the lower portion of the Kabul River course, two interconnected aquifers spanned the southeast, east, and northeast (lower Kabul sub-basin). The Quaternary and Tertiary upper aquifers are primarily extracted to supply the city's water. The most commonly stated processes for groundwater recharge in Kabul City include recharge from riverbeds, snowmelts in the foothills, drainage channels, and direct recharge from precipitation surplus (Zaryab et al., 2017). Recharge from the water distribution network, wastewater filtration, septic system leaks, and toilet facilities are all possibilities. The high flow in the river is

usually accompanied by the melting of snow and spring rains (April and May), which will most likely be the same period of high groundwater recharge.

## 3.2 Water sampling and water quality analysis

### 3.2.1 Water sample collections and Lab works and Analysis of samples

Thirty-five samples were acquired from different parts of Kabul city, with each municipality district receiving 2-3 samples to enable optimal spatial distribution and coverage of the whole research region. The sampling was done from October to December 2020. Figure 3.4 shows the sample collection in the field. Before sampling water from the hand pump and submersible wells, the water was pumped out for ten minutes. For sample collection, one-liter prewashed HDPE bottles were utilized. The bottles have been washed with sample water 2-3 times. A portable digital multiparameter equipment (LABMAN Scientific instrument) was used to measure the temperature, pH, TDS, and EC on-site. The fluoride test was done using a portable digital multiparameter kit.

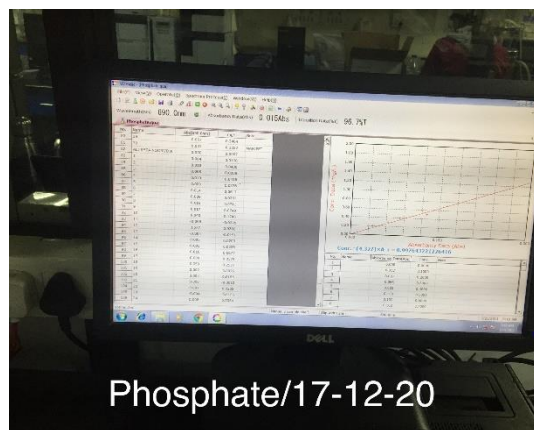


**Figure 3. 4 Sample collection and field water quality testing.**

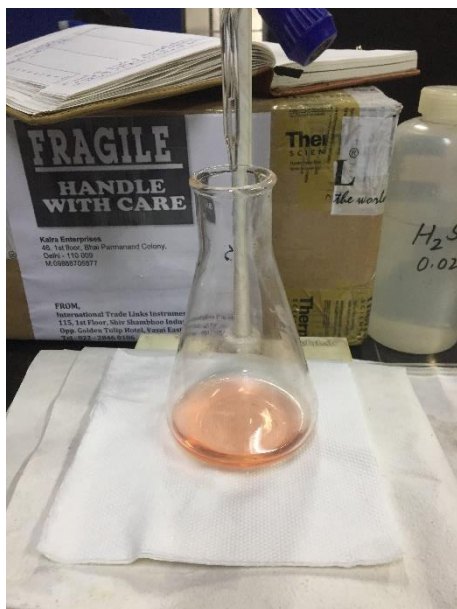
Collected samples were moved to the water lab of Delhi Technological University's Department of Environmental Engineering and were promptly analyzed. Total hardness, chloride, and bicarbonate were evaluated utilizing the titrimetric technique (APHA, 2005). Sodium, calcium, magnesium, and potassium contents were measured using a flame photometer. Fluoride was determined using a portable digital multiparameter. The concentration of Sulfate and Nitrate was determined using UV-VIS spectrophotometers (UV 3092 & LT-290). Figure 3.5



A. Work with spectrophotometer



B. Results of Phosphate analysis



C. Titration method



D. Tabletop digital multiparameter

**Figure 3. 5 Water Quality Testing and Analysis in DTU Laboratory**

### 3.3 Water quality analysis

#### 3.3.1 Analysis of water

Different laboratory methodologies and instruments have been utilized to determine the physicochemical parameters and characteristics of the water sample. Each is discussed below.



## 1- Utilizing a multimeter equipped with an electrode

### Electrical Conductivity (EC)

The electric conductivity was calculated using a multiparameter developed by the LABMAN scientific instrument. The EC electrode was first calibrated with a standard KCl solution (1413  $\mu\text{S}/\text{cm}$ ) before analyzing water samples. The multimeter's readings were recorded and represented in  $\mu\text{S}/\text{cm}$ .

### Total Dissolved Solids (TDS) and Salinity

Using a multimeter of the LABMAN scientific instrument, the total dissolved solids and salinity in each sample were calculated and recorded in mg/l.

### Hydrogen potential (pH)

A digital pH meter (HANNA) was used to determine the pH of water samples. Buffer solutions with pH strengths of 4.0, 7.0, and 9.2 were used to calibrate the pH meter before analyzing all samples.

### Flouride (F)

This test was done using a portable digital multiparameter kit. First, the device is calibrated with 0.1mg/l, 1mg/l, and 10mg/l fluoride concentrations. Then, the test was performed with one ml of cyclohexane diamine tetraacetic acid (CDTA) in a 10 ml sample.

## 2- Conventional titration method

### Chloride (Cl<sup>-</sup>)

The Mohr titration method, which uses silver nitrate as a titrant, was used to quantify the amount of chloride in water samples. After adding a couple of drops of indicator (potassium chromate) to a 10 ml sample volume in a conical flask, samples were titrated against a standard  $\text{AgNO}_3$  solution to produce an endpoint with a brick-red color. Using the following formula, the chloride concentration was calculated:

$$\text{Chloride in } \left(\frac{\text{mg}}{\text{l}}\right) = \frac{N \times V \times 35.5 \times 1000}{V_s} \dots\dots\dots (3. 1)$$

Where V is the amount of titrant ( $\text{AgNO}_3$ ) used (ml), N denotes the normality of  $\text{AgNO}_3$  (0.01 N),  $V_s$  is the volume of the sample (10 ml).

### Bicarbonates ( $\text{HCO}_3^-$ )

By titrating a 10 ml sample volume with standard solution  $\text{H}_2\text{SO}_4$  using the following formula, bicarbonate ( $\text{HCO}_3^-$ ) in a water sample was determined:

$$\text{HCO}_3 \left( \frac{\text{mg}}{\text{l}} \right) = \frac{B \times N \times \text{Eq. Wt. of HCO}_3 \times 1000}{V_s} \dots\dots\dots (3. 2)$$

Where B is the amount of titrant ingested; N is the titrant's normality ( $\text{H}_2\text{SO}_4$ );  $V_s$  is the sample volume (10 ml); and the equivalent weight of  $\text{HCO}_3$  is equal to 61

### Total Hardness (TH)

The total hardness of water samples as  $\text{CaCO}_3$  was assessed using the conventional EDTA titration technique. Eriochrome Black T (EBT) indicator (in the powdered form) and 1 ml of ammonium buffer were added to a conical flask containing 20 ml of sample volume. Samples were then titrated against a standard EDTA solution (0.01 M) to obtain an endpoint with a blue color. The following formula is used to calculate total hardness:

$$\text{Total hardness (as CaCO}_3) \text{ (mg/l)} = \frac{M \times V \times M.W \times 1000}{V_s} \dots\dots\dots (3. 3)$$

Where M stands for the molarity of the EDTA solution (0.01M), V is the volume of EDTA utilized, M.W. stands for the molecular weight of  $\text{CaCO}_3$  (100), and  $V_s$  is the sample volume (20 ml).

### Calcium Hardness (CaH)

Titration of water samples ascertained the water's calcium hardness against a Standardized EDTA solution. In a conical flask, 20 ml of sample volume and 1 ml of sodium hydroxide (NaOH) solution were combined. A small amount of peroxide indicator (in powder form) was also added to the sample solution to get an endpoint with a purple color. The following formula is used to calculate the calcium hardness:

$$\text{Ca hardness (mg/l)} = \frac{M \times V \times M.W \times 1000}{V_s} \dots\dots\dots (3. 4)$$

Where M stands for the EDTA solution's molarity (0.01M), V is the amount of EDTA utilized, M.W. stands for calcium's molecular weight (40), and  $V_s$  stands for the sample volume (20 ml).

### 3- Spectrophotometer

UV-VIS spectrophotometers determined the sulfate, phosphate, nitrate, and silica concentrations.

#### **Sulfate ( $\text{SO}_4^{2-}$ )**

The amount of sulfate in the samples obtained was calculated using the turbidimetric (Barium Chloride) method. Standard solutions of  $\text{Na}_2\text{SO}_4$  at the following concentrations were created using the stock solution: 10, 20, 30, 40, 50, 60, 70, 80, 90, and 100 ppm. 10 ml of each sample are mixed with 1 ml of a conditioning agent to create a turbid solution, then mixed continuously with 1 ml of HCl. Use a UV-VIS Spectrophotometer to measure the absorbance at 420 nm after adding that turbid solution to a glass cuvette cell.

#### **Phosphate ( $\text{PO}_4^{3-}$ )**

Stannous chloride was used to calculate the total phosphate in water samples. Using salt and potassium dihydrogen phosphate, a stock solution of 100 ppm was created ( $\text{KH}_2\text{PO}_4$ ). The stock solution was used to develop standard solutions with concentrations of 0.5, 1.0, 1.5, 2.0, 2.5, 3.0, 3.5, 4.0, 4.5, and 5 ppm. Add 1 ml of the acid solution (1 ml  $\text{H}_2\text{SO}_4$  + 3 ml  $\text{HNO}_3$ ) to 10 ml of the sample in the conical flask and heat the mixture until it boils to transform the bound state phosphate into a free form or the organic phosphate into the inorganic form. Then, after cooling the solution, add one drop of the phenolphthalein indicator and continue adding 6N NaOH until the solution becomes pink rather than colorless. Right now, note the increased volume and determine the dilution factor. Now divide the sample volume equally among the test tubes (10 ml), add 0.4 ml of ammonium molybdate to the solution, and the pink hue vanishes. A UV-VIS Spectrophotometer was used to detect the intensity of the generated blue hue at 690 nm after adding one drop of stannous chloride and mixing it thoroughly.

#### **Nitrate**

A UV-VIS Spectrophotometer and Brucine Sulphanilic Acid measured nitrate in water samples. Standard 5, 10, 15, 20, 25, 30, 35, 40, 45, and 50 ppm solutions were created using a 100 ppm  $\text{KNO}_3$  stock solution. One milliliter of brucine sulphanilic acid was added to each 50-millilitre test tube containing 10 millilitres of material from each site. Then, each test tube received 10 ml of nitrate acid (60 ml  $\text{H}_2\text{SO}_4$  plus 40 ml distilled water), and the test tubes were left in the dark for 25 minutes. Each test tube received 10 ml of distilled water, added after 25 minutes, and correctly mixed with the solution. A yellow hue emerged. The additional solution was put into a glass cuvette, and the UV-VIS Spectrophotometer assessed the colour intensity at 410 nm.

## Silica

To test silica with the Molybdenum blue photometry method, a UV-VIS spectrophotometer uses a wavelength of 410 nm. In the first step, 0.2 ml of HCl solution with a volume of 10 ml is added to the sample. Then add 0.4 ml of ammonium ortho-molybdate ((NH<sub>4</sub>)<sub>2</sub>MoO<sub>4</sub>) solution and wait two minutes. After that, add 0.4 ml of oxalic acid (C<sub>2</sub>HcO<sub>4</sub>) and perform the test.

## 4- Flame photometer

### Cations (Sodium, Na<sup>+</sup>; Potassium, K<sup>+</sup>; Calcium, Ca<sup>2+</sup> and Magnesium, Mg<sup>2+</sup>)

A Flame photometer was used to determine the presence of the cation's sodium (Na<sup>+</sup>), potassium (K<sup>+</sup>), and calcium (Ca<sup>2+</sup>). The stock solution created standard solutions at 10, 20, 40, 60, 80, and 100 ppm. The standard graph was created by adhering to standards using these standard solutions (APHA, 2005).

Using the volume of titrant (EDTA) used to estimate calcium and total hardness, the content of magnesium in water samples was determined using the following formula:

$$\text{Mg}^{2+} \text{ (mg/l)} = \frac{(V_1 - V_2) \times 400.8}{V_s \times 1.645} \dots\dots\dots (3. 5)$$

V1 is EDTA used to determine total hardness (Ca + Mg), V2 is used to determine CaH, and Vs is the sample volume (10 ml).

### Single factor pollution index

The single-factor index approach was used to determine the level of contamination of one pollutant in a water sample (Dey et al., 2021). This approach was employed in the current study to evaluate the level of pollution caused by one contaminant in the groundwater samples. This technique might identify the pollutants that significantly impact the pollution levels at each sample location. A single pollution index was calculated using the following criteria:

$$P_i = \frac{C_i}{S_i} \dots\dots\dots (3. 6)$$

P<sub>i</sub> is the single factor pollution index; C<sub>i</sub> indicates the measured value of the pollutant content of the i parameter (mg/l), and S<sub>i</sub> shows the allowable limit of the i parameter (mg/l).

### Nemerow pollution index method

An environmental quality index that weighs many factors and considers extreme or exceptional maximum values is called the Nemerow index (Su et al., 2022). The Nemerow pollution index is calculated using the following formula:

$$P_N = \sqrt{\frac{(P_1)^2 + (P_{imax})^2}{2}} \dots\dots\dots (3. 7)$$

In the equation, PN stands for the sample point's overall pollution index,  $P_{imax}$  indicates the maximum value of the single factor pollution index, and  $P_1 = \frac{1}{n} \sum_{i=1}^n P_i$  is the mean value of the single factor pollution index.

### 3.3.2 Water quality index

The WQI assesses groundwater quality in the current investigation according to 13 variables evaluated at each location. The weight value ( $w_i$ ) for each metric varies from 1 to 5 depending on the degree of contamination's influence on human health Table 3.1. At the first step of WQI computation, the relative weight of each parameter is calculated, as indicated in Equation (3.8)

$$W_i = w_i / \sum_{i=1}^n w_i \dots\dots\dots (3. 8)$$

Where,  $W_i$  stands for relative weight,  $w_i$  for variable weight, and  $n$  for the number of variables. Each parameter's quality rating scale ( $q_i$ ) will be calculated in the second step utilizing Equation (3.9).

$$q_i = \frac{C_i}{S_i} \times 100 \dots\dots\dots (3. 9)$$

Where  $q_i$  is quality rating,  $C_i$  is a measured concentration for each parameter of samples in mg/l.  $S_i$  is the standard limit for each parameter according to WHO in mg/l.

Sub-indices are calculated by multiplying Equations (3.8) and (3.9).

$$SI_i = W_i \times q_i \dots\dots\dots (3. 10)$$

Ultimately, WQI (Equation 3.11) is calculated by summing all SI values for a particular sample, yielding a composite score based on ranges and water classes.

$$WQI = \sum SI_i \dots\dots\dots (3. 11)$$

### 3.3.3 Geographic information system analysis

ArcGIS aids the analytical extrapolation of various experimental results to create theme maps and geospatial representations. It reduces the number of unknown water characteristics. It enables a statistical approach to characterize groundwater quality in the research area graphically. The most commonly used and recommended methods for generating spatial distribution maps are inverse distance weighting, kriging, and co-kriging. As a result, for 35 samples of the research region in this study, spatial distribution models of all variables for groundwater quality were developed using the Inverse Distance Weighted (IDW) interpolation method in ArcGIS-10.7 software. The IDW interpolation technique estimates missing parameters concerning

an interval, with the nearest point receiving more significant weightage and decreasing as the distance increases.

Furthermore, several researchers utilize this approach to create geographic distribution maps of various characteristics. Interpolation maps assist individuals and decision-makers in understanding groundwater quality by providing a generalized picture of hydrogeochemical processes and the drainage system of the studied region. This can aid subsequent water management, prevention, source of pollution, and groundwater modelling for future groundwater conservation.

**Table 3. 1 Relative weights ( $w_i$ ) for different water quality parameters.**

Chemical parameters	WHO Limits mg/lit	Weights $W_i$	Relative weights $W_i = w_i / \sum w_i$
1 TDS	1500	5	0.116
2 $\text{NO}_3^-$	45	5	0.116
3 $\text{F}^-$	1.5	5	0.116
4 pH	8.5	4	0.093
5 EC	1000	4	0.093
6 $\text{SO}_4^{2-}$	250	4	0.093
7 $\text{HCO}_3^-$	600	3	0.070
8 $\text{Cl}^-$	250	3	0.070
9 TH	500	3	0.070
10 $\text{Na}^+$	200	2	0.047
11 $\text{K}^+$	12	2	0.047
12 $\text{Ca}^+$	75	2	0.047
13 $\text{Mg}^+$	30	1	0.023
Total		43	1

### 3.4 Artificial neural networks

#### 3.4.1 General

Modern systems and computer techniques for machine learning, knowledge visualization, and eventually using the acquired information to forecast the output reactions of complex systems are known as Artificial Neural Networks (ANN) or neural networks. The fundamental principle underlying these networks draws some inspiration from how the biological nervous system functions in processing data and information necessary for learning and knowledge creation. Despite this apparent surface similarity, artificial neural networks exhibit a surprising number of brain-like characteristics. For instance, they draw important traits from inputs, including irrelevant data, and learn from experience, generalizing from previous examples to new ones. Each neuron gathers inputs from several sources and then generates an output after processing the weighted aggregate inputs by an activation function. The output for a given set of input values may be predicted using a network once trained.

Neural networks effectively spot internal connections, patterns, and trends. Figure 3.6 depicts the typical biological neuron.

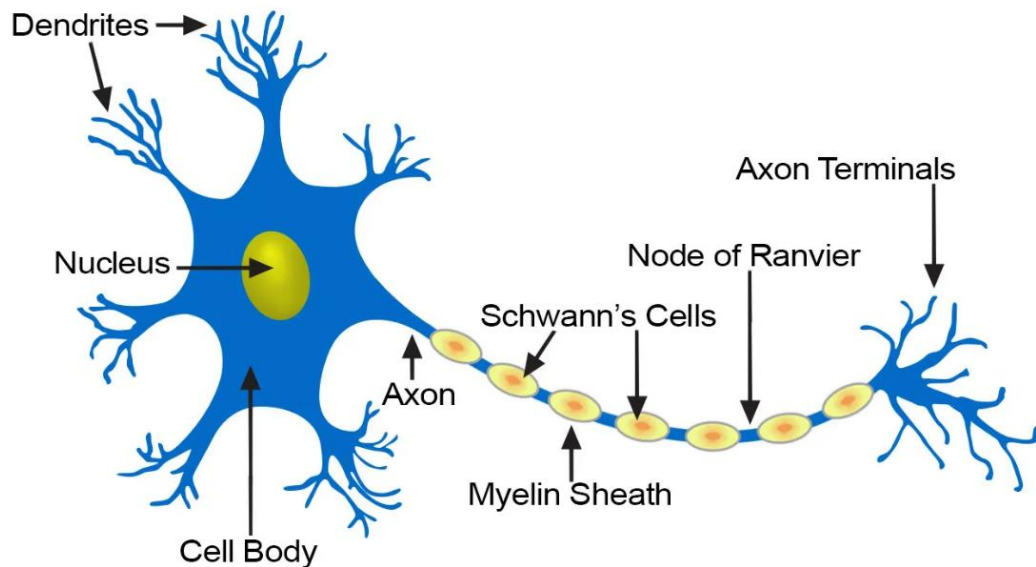


**Figure 3. 6 Structure of a typical neuron** (Suresh et al., 2020)

As seen in Figure 3.6, the neuron comprises three main parts.

1. The dendrites (constituting a vastly multi-branching tree-like structure that collects inputs from other cells).
2. The cell body (the processing part, called the soma).
3. The axon (which carries electrical pulses to other cells).

### 3.4.2 Biological Neurons and ANN

The following points may be used to describe the ideas of biological neurons and the human brain system, and they can also be expressed schematically, as seen in Figure 3.7.

1. The inputs are the process of gathering information from the necessary sources.
2. The weights regulate how inputs affect a neuron. In other words, each connection in an ANN is given weight, and information is saved over it. These weights are continuously changed while attempting to optimize the relationship between input and output.

3. Net input readings from the processing components are calculated using the summation function.
4. The transfer (activation) function takes the net input from the summation function and uses it to calculate the neuron's output. The choice of transfer and summation functions depends on the problem's nature.

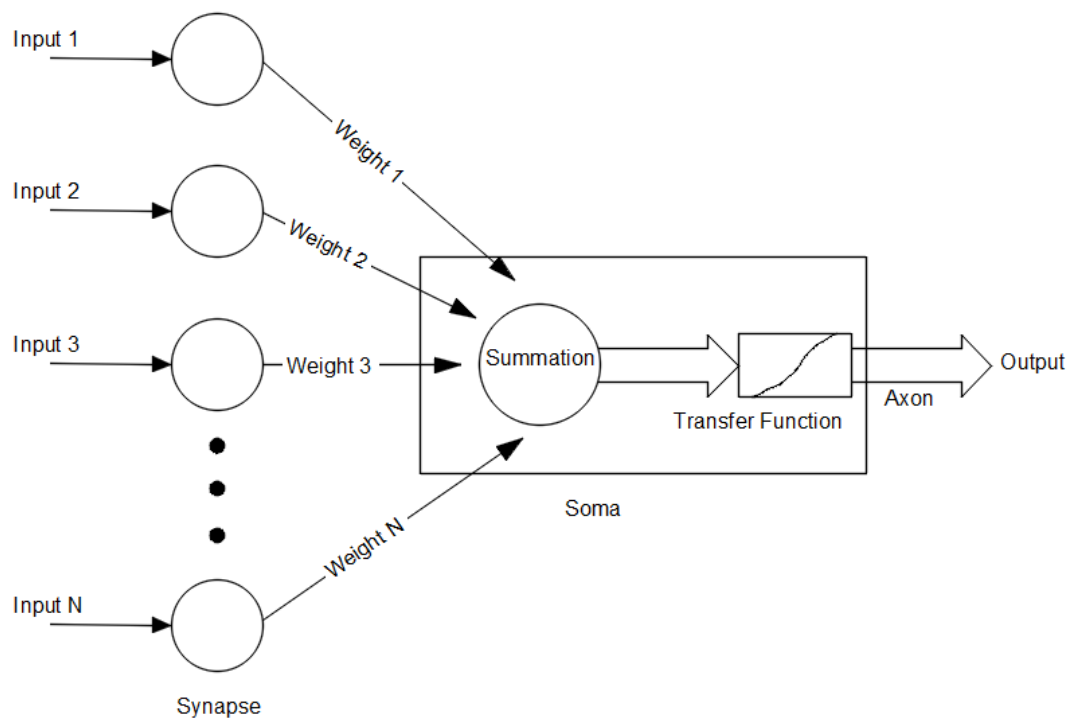


**Figure 3. 7 Artificial representation of biological neuron** (Samson S, 2010)

Transfer function generally consists of algebraic equations of linear or nonlinear form. Given its self-limitation and straightforward derivative, the sigmoid function is frequently utilized. The outputs consider the transfer function's findings and present them to the appropriate processing element. The summation function, transfer function, structure, and learning algorithm that are all part of an ANN may be considered a directed graph. To construct a layer of networks, the processing parts must have connections between them. There are three layers of a neural network. They are the output layer, the concealed layer, and the input layer.



### **3.4.3 Need for ANN model.**

For forecasting groundwater's chemical and physical properties, ANN models have been widely employed in groundwater quality prediction. The composition and solubility of the rock materials in the soil or aquifer, water temperature, partial pressure of CO<sub>2</sub>, acid-base reactions, oxidation-reduction reactions, loss or gain of constituents as water percolates through clay layers, and mixing of groundwater from adjacent strata can all have an impact on the quality of groundwater. Each effect's impact will vary in size according to how long the water stays in each setting. The solubility of rocks and the amount of time water has been present in the subsurface affect groundwater quality in general. In addition, the kind of rock and the amount of percolating water affect how easily rocks may be dissolved. In addition, surface impacts impair the quality of the groundwater.

However, the groundwater's interaction with the rocks is the primary factor influencing the groundwater quality in the studied region. By using the artificial neural network model and having some water quality parameters easily determined by portable devices, many water quality parameters can be estimated without conducting laboratory tests. Estimating water quality parameters without lab tests is essential to reduce laboratory materials' time, cost, and consumption. On the other hand, the result of this model is vitally crucial for areas where water and chemical materials laboratories are inaccessible.

Employing high-level software based on artificial intelligence may be an appropriate method because constructing mathematical relations between various water quality metrics is non-linear and highly laborious. The tool ANN is considered and implemented in this study to forecast multiple water quality parameters from other parameters.

## **3.5 Seasonal variation of groundwater quality**

### **3.5.1 The process of data acquisition and selection from (NWARA)**

The required groundwater quality data from the General Directorate of Water Resources of Afghanistan's National Water Affairs Regulation Authority (NWARA) has been obtained. The NWARA has some monitoring wells that cover most parts of Kabul city. The hydrogeological authority of Kabul city has executed the monitoring of groundwater. They collected water samples and analyzed them from 14 August to 27 September 2017 (dry season) and 27 March to 9 May 2018 (wet season). The groundwater quality data includes the seasonal water quality data for 54 monitoring wells. Out of 54 monitoring wells, only one does not have data in the dry season. This well was excluded from the study, and all 53 other wells were included in the current Analysis. Groundwater quality figures obtained from the NWARA include the following data: static water level (SWL), Temperature (T), Electrical Conductivity (EC), pH, Dissolved Oxygen (DO), Total Dissolved Solids (TDS), Salinity, Colour, Turbidity, Total Hardness (TH), Calcium (Ca), Magnesium (Mg), Sodium (Na), Total Alkalinity, Phenolphthalein Alkalinity, Carbonate (CO<sub>3</sub>), Bicarbonate (HCO<sub>3</sub>), Chloride (Cl), Fluoride (F), Sulphate (SO<sub>4</sub>), Phosphate (PO<sub>4</sub>),

Potassium (K), Nitrite (NO<sub>2</sub>), Nitrate (NO<sub>3</sub>), Ammonia (NH<sub>3</sub>), Iron (Fe), Manganins (Mn), Copper (Cu), Aluminium (Al), Arsenic (As) and Cyanide (CN). The following data from the collected dataset have been selected for the current Analysis: EC, pH, TDS, TH, Mg, Na, HCO<sub>3</sub>, Cl, F, SO<sub>4</sub>, PO<sub>4</sub>, K, Fe, Mn, Cu, Al, and CN. The analyzed parameters have been selected from the presented figures based on the following three fundamental factors. The parameters exceeded the permissible limits of the World Health Organization (WHO) and Afghanistan National Standard Authority (ANSA). The parameters that show the most seasonal variations in visual observation. Quality parameters are essential in drinking water quality.

### 3.5.2 Development of geospatial distribution maps of groundwater quality data

Data on the quality of groundwater collected from the NWARA were aggregated and reviewed for irregularities and inconsistencies. To visualize and investigate the geospatial distribution of EC, TDS, TH, Ca, Mg, K, Mn, Na, Cl, F, Fe, and NO<sub>3</sub>, the dataset was entered into a database created within an ArcGIS 10.7.1 environment. The principal method for deriving regional distributions of groundwater quality metrics in the following research was interpolation using the Inverse Distance Weighting (IDW) methodology. Interpolation was utilized to convert point data, such as concentration levels at each observational point, into a total averaged number. For this investigation, an IDW with a power coefficient of 2 was used, assuming that contents at any sample point should be closer to the recorded quantity at the measurement point.

Geospatial distribution maps depicting changes for each selected criterion were also created to measure seasonal changes in groundwater quality. The positive values indicate an increase in concentration, and the negative values show a decrease. The following equation was used to compute the change in concentration.:

$$\text{Seasonal variation of concentration (mg/l)} = C_{\text{wet period}} - C_{\text{dry period}} \dots\dots\dots (3. 12)$$

As a result, these geospatial maps depicted the regional distribution of variation in concentration of each groundwater quality indicator from fall (dry season data) to spring (wet season data).

### 3.5.3 Statistical evaluations

The "one-sample Kolmogorov–Smirnov (K–S)" test was used to assess the normalcy of seasonal changes in the quality of groundwater samples (Elçi & Polat, 2011) before the testing to see if the seasonal variation in its quality was significant. In the normal distribution of seasonal variations, "the paired sample t-test" was employed. With the help of this parametric statistical test from a statistical standpoint, it will be established if the means of the two populations differ. Only when the distribution of accessible data sets meets normal distribution criteria can the "t-test" be used (Elçi & Polat, 2011). Another prerequisite for this statistical test is that each group's sample size should be more than 30. When employing paired sample "t-tests," the computed p-value of two-tailed significance was compared to  $\alpha$  (the significance level), set at 0.05 in this study. The hypotheses have been proposed as follows:

$H_0$ : The water quality data will not have any seasonal difference from the dry to wet period.

$H_s$ : The water quality data will have seasonal differences from the dry to wet period.

Suppose the p-value is estimated at less than  $\alpha$ . In that case, the null hypothesis will be rejected, which indicates no seasonal changes in groundwater quality. The alternative hypothesis is accepted, suggesting the seasonal water quality difference. An alternative statistical test must be employed in case of an abnormal distribution of seasonal variation. The alternate options for parametric statistical tests are nonparametric tests that do not have to follow any specific assumptions for data distribution.

Furthermore, the data ranks, a crucial feature of these techniques, are used rather than the data values. The alternative to the "t-test" is the "Wilcoxon signed-rank test" (Elçi & Polat, 2011), which is employed in this investigation to find out whether there is any significant variation in the concentrations of groundwater quality with differences of abnormal distribution. The "one-sample Kolmogorov–Smirnov test," the "paired-samples t-test," and the "Wilcoxon signed-rank test" were all performed using the statistical program SPSS statistics v25 to make statistical studies easier.

### **3.6 Groundwater level analysis**

#### **3.6.1 Static water level data**

The National Water Affairs Regulation Authority (NWARA) of Afghanistan provided monthly groundwater-level data for 128 wells in the research region used in this study. Observations and records of groundwater levels are available from November 2006 to May 2009. No figures were available from June 2009 to October 2013. Observational data is again available from November 2013 to April 2020. In order to compensate for this shortcoming and eliminate the data gaps, the process of data imputation has been done. During the observations, some wells, for various reasons such as drying, destruction, and collapse, have been replaced by alternative wells in their vicinity, which is mentioned in the available figures. The obtained data were checked for the maximum length of observations with continuous records. Many wells have been excluded from the present study for the following reasons: a) wells with observations for a period of less than 45 months were removed; b) wells with unknown geographical coordinates; c) wells without measurements before 2013; and d) wells with incomplete data after the data imputation step. Finally, after the exclusion and the data imputation process, the observations of 66 wells (Figure 3.8) for 15 years have been considered for the Analysis.

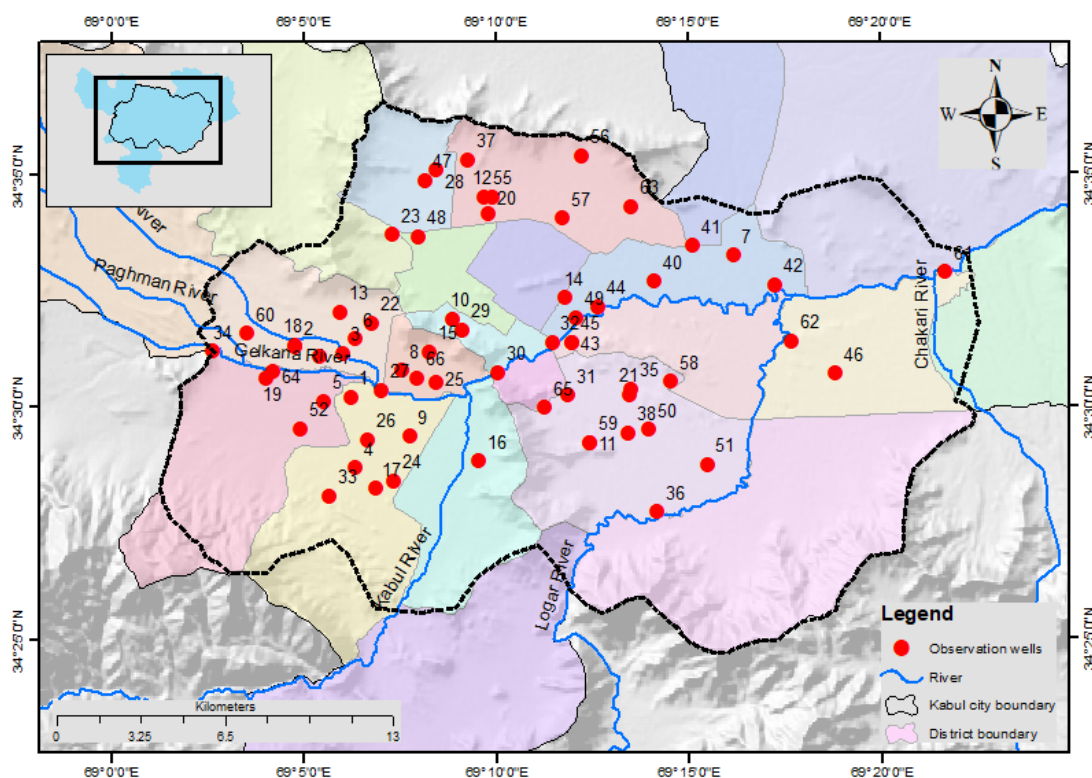


**Figure 3. 8 Observational wells**

Precipitation data for six stations in Kabul province were also collected from NWARA. Collected data were in the form of daily records from 2008 to 2020, converted into monthly and annual total figures for Analysis. Out of six stations, only two stations (Payin-i-Qargha and Tang-i-Sayedan) are located within the study area. The data for 2008 and 2020 are not complete. Therefore, it was intended to analyze the records from 2009 to 2019. Landsat imagery was downloaded to create LULC identity maps for four different years: 2005, 2010, 2015, and 2020. The required satellite data was obtained from the USGS Portal (<https://earthexplorer.usgs.gov/>) using the address "path 153 and rows 36." (Table 3.2). Gap filling was done by ENVI 5.3 by downloading the Landsat Gap-fill IDL model for data downloaded from the Landsat 7 satellite. "Supervised classification approach with maximum likelihood algorithm" in ENVI 5.3. the environment was applied to create LULCs in the study area.

**Table 3. 2 Satellite data acquisition details**

Acquisition date	Address (Path & Row)	Spacecraft ID
<b>01/06/2005</b>	153/36	"L7 ETM"
<b>23/06/2010</b>	153/36	"L5 TM"
<b>05/06/2015</b>	153/36	"LANDSAT 8"
<b>18/06/2020</b>	153/36	"LANDSAT 8"

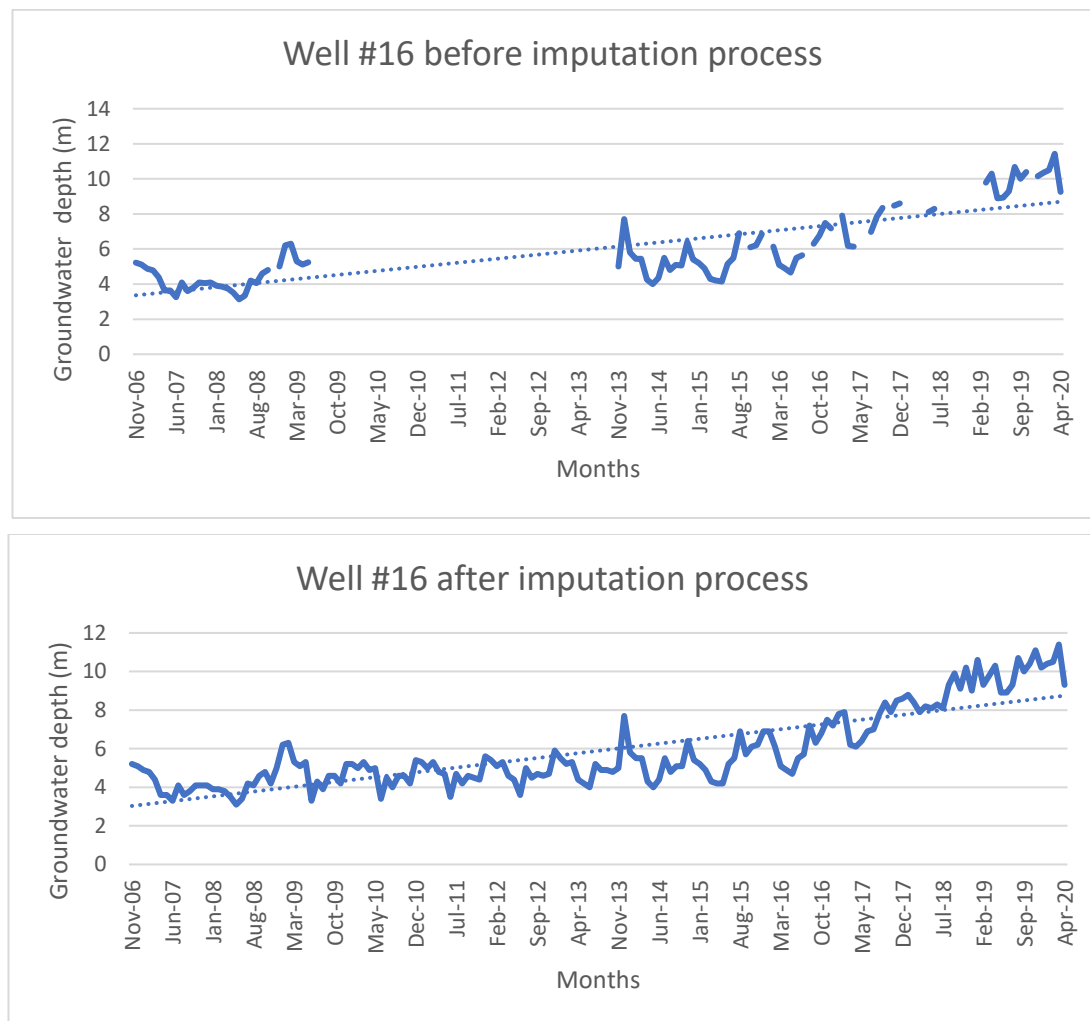


**Figure 3. 9 Well 16 observational data illustration pre and post imputation**

### 3.6.2 Data imputation

The lack of consistent evidence or a gap between observations is a common problem in statistical Analysis. As a consequence, imputation is necessary to provide sufficient measurements. The data imputation approach is widely used to fill the observational gap between monitoring figures with substituted values (Efron, 1994; Evans et al., 2020; Manago et al., 2019; Z. Zhang et al., 2017). A univariate time series imputation approach was utilized in this study to impute missing values aided by the "imputeTS" package in the "R Studio" environment (M. S. Moritz, 2021; S. Moritz et al., 2015; S. Moritz & Bartz-Beielstein, 2017). The function "na\_seasplit" with the algorithm of "Kalman" was used to consider both seasonality and trends in the imputation process. The primary status of observed records on well #16 and imputed figures results are depicted in (Figure 3.9).

### 3.6.3 Hierarchical Cluster Analysis

Groundwater levels used in trend analysis differ dramatically across the wells. Clustering is classifying observations based on their similar observed variables (Sinharay S, 2010). The observational wells in the present study were classified based on their water table characteristics. Monthly groundwater observation over a long (15 years) was used as a clustering variable. Hierarchical clustering is a fundamental groundwater study method used among the various clustering methods (El-Hames et al., 2013; Halder et al., 2020; Pathak & Dodamani, 2019; Rahbar et al., 2020). The "Ward's linkage method" of hierarchical clustering was utilized to locate homogeneous wells using static water tables in this Analysis (Vijaya et al., 2019; Yidana et al., 2010). The square "*Euclidean Distance*" measure was applied to assess the degree of correlation across the observational water level data. The distance matrix based on the groundwater table is determined first in a hierarchical cluster analysis, and each well is assigned to a separate category. The "Ward's linkage mechanism" is then used to merge each group with the groups nearest to it. Cluster analysis has been conducted using the "hclust" package in the "RStudio" statistical framework.

### 3.6.4 Groundwater Levels and Groundwater Drought: A Nonparametric Trend Test

The "Mann–Kendall (MK)" test is mainly utilized to determine whether there is a significant upward or downward trend in a group of time-series data (P. Kumar et al., 2018; Ribeiro et al., 2015; Venegas-Quiñones et al., 2019). Mann first suggested the MK test as a nonparametric trend detection test, which Kendall later adopted as a test statistic. Statistically, the null hypothesis ( $H_0$ ) indicates that the variable has no trends, while the alternative hypothesis ( $H_1$ ) means trends. The value of  $Z$  suggests the state of the statistic test in the MK test. Positive trends are shown by  $Z > 0$ , negative trends are demonstrated by  $Z < 0$ , and  $Z = 0$  signals no trend. The lag one autocorrelation of data at a 95% confidence interval level should be checked before utilizing the MK test. The annual and seasonal groundwater levels in Kabul city have been studied in this Analysis using the nonparametric MK statistical test. All observational wells were subjected to a trend test with a 95% confidence interval, and Sen's slope (Sen, 1968) approach was utilized to evaluate the amplitude of the trend.

This study used the SGI to quantify the degree and significance of groundwater drought indicated by water level data. The SGI was suggested (Bloomfield & Marchant, 2013) to evaluate groundwater droughts utilizing groundwater depths. The SGI is a nonparametric approach in which typical monthly groundwater information values are converted with a reciprocal ordinary cumulative distribution function, and scores are organized simultaneously per month to provide an SGI time series. The identification through SGI was performed similarly to the "Standardized Precipitation Index" given by (Rahman et al., 2017). This was done considering a given threshold (-1 throughout this research) for SGI to describe groundwater drought features, including frequency, period, and strength. When the SGI value is less than zero, it indicates groundwater drought, but a value lower than the threshold indicates a moderate drought.

## 3.7 Delineation of groundwater potential zones

### 3.7.1 Thematic maps

Arc GIS.10.6 was utilized to digitize and pre-process multiple thematic maps needed for this study. Various data sources were employed. To delineate the groundwater potential zone using AHP, ten different influential parameters were selected and produced in the form of raster data, including geology, drainage density, land-use and land-cover, slope, geomorphology, soil types, lineament density, rainfall, elevation, and water depth. These variables are relevant and influential in evaluating the potential groundwater recharge zone.

The geological map was digitized and georeferenced from the "geologic map of quadrangle 3468, Chak Wardak-Syahgerd (509), and Kabul (510) quadrangles, Afghanistan" (R. G. Bohannon & Turner, 2005). The geomorphological thematic map was digitized and extracted from the country geomorphological map prepared by the Afghanistan Information Management System (AIMS) at a scale of 1: 6,000,000. The soil map was interpolated based on soil data sources from the Afghanistan Soil Catalogue (Ahmadzai & Omuto, 2019). Landsat-8 OLI satellite data was utilized to configure the study area's land use and land cover map. Using the address, the required Landsat data was obtained from USGS Portal (<https://earthexplorer.usgs.gov/>). In the Arc GIS 10.6 environment, a "supervised classification strategy" was created by training samples for each LULC category. A post-classification smoothing step was conducted using the majority filter tool in the Arc GIS environment to reduce and merge the tiny pixel distribution of LULC classes in the research area.

Shuttle Radar Topography Mission (SRTM) Version, 3.0. Global 1 arc sec data was downloaded and applied to create the slope thematic layer. Landsat-8 OLI data (Landsat Scene Identifier: LC08\_L1TP\_153036\_20200704\_20200708\_01\_T1; Date of acquisition: 02-08-2020) was downloaded to provide the lineament thematic layer with the integration PCI Geomatica Banff and Arc GIS 10.6 software. The rainfall map was created based on meteorological data (2008-2018) from NWARA Afghanistan. An Inverse Distance Weighting (IDW) interpolation technique has been employed to determine its spatial dissemination in the Arc GIS environment. As well as the elevation map was developed using SRTM- Digital Elevation Model (DEM)-30 m data in an Arc GIS environment. A part of nine years (2004-2013) of groundwater level data, recorded by AGS with support of the USGS, was used to create the groundwater level thematic layer. The study area's watershed map was generated in Arc GIS 10.6 environment employing DEM.

The weights for each factor were assigned based on the priority scale using AHP. Different influential presentive variables had been integrated into the Arc GIS environment to discover the GWPZs. The consolidated method's findings were characterized in five categories: very good, good, moderate, poor, and very poor zones. The accuracy and effectiveness of the adopted methodology for delineating groundwater recharge potential zones were obtained utilizing groundwater level data. The overall and kappa accuracy assessment methods validated the groundwater potential zones map.

### 3.7.2 Analytical hierarchy process (AHP)

Using AHP, each variable's ranking is assigned between one and five for equal and extreme importance. All of the attributes are evaluated based on the paired comparison. The current investigation will determine the relevance of the variables affecting groundwater potential. Weights obtained from this process are assigned to the prepared thematic maps in the Arc GIS environment using an overlay analysis approach. A pairwise comparison matrix operates to judge interaction across each thematic layer. The maximum eigenvalue is extracted and normalized from the pairwise matrix to evaluate each variable's relative significance. Accordingly, a weight comparison between the parameters in terms of their impact on groundwater occurrence was carried out based on professional judgment and Analysis of the relevant publications. Eventually, the following equations will provide the consistency ratio and index of consistency accordingly (Abijith et al., 2020; Muniraj et al., 2020).

$$CR = \frac{CI}{RI} \dots\dots\dots (3. 13)$$

CI – displays the consistency index, CR – indicates the consistency ratio, and RI - represents the random index,

$$CI = \frac{\lambda_{\max} - n}{n - 1} \dots\dots\dots (3. 14)$$

Where  $\lambda_{\max}$  illustrates the matrix's maximum eigenvalue while n is the square matrix order, the RI depends on the number of components. It should be noted that the weights provided through this matrix are only reliable when CR is less than 10%.

Table 3.3 shows how the criteria were rated against each other. Looking at the top row, geology scored a "3" above geomorphology and a "2" above land cover, slope, soil, and lineament density rainfall. In contrast, drainage density scored a "3" above soil, and elevation scored a "2" above soil.

**Table 3. 3 Pairwise comparison matrix of thematic layers.**

Item Description	Geology	Drainage Density	Land cover	Slope	Geomorphology	Soil	Lineament Density	Rain	Elevation	Water table
Geology	1	1	2	2	3	2	2	2	1	1
Drainage Density	1	1	1	2	1	3	1	2	2	1
Land cover	1/2	1	1	1	2	2	2	1	1	2
Slope	1/2	1/2	1	1	1	2	2	2	1	1
Geomorphology	1/3	1	1/2	1	1	2	1	1	1	1
Soil	1	1/3	1/2	1/2	1/2	1	3	2	1/2	1/2
Lineament Density	1/2	1	1/2	1/2	1	1/3	1	1/2	1/3	1/2
Rain	1	1/2	1	1/2	1	1/2	2	1	1/4	1/4
Elevation	1	1/2	1	1	1	2	3	4	1	3
Water table	2	1	1/2	1	1	2	2	4	1/3	1
Sum	8.83	7.83	9.00	10.50	12.50	16.83	19.00	19.50	8.42	11.25

To calculate the standardized matrix of AHP, the rated criteria in the Table 3.3 will be divided by the total value. Table 3.4 illustrates the standardized matrix of AHP. The weights for each criterion will then be found by averaging the standardized matrix.



**Table 3. 4 Standardized matrix of AHP weights for each respective criterion.**

Item Description	Geology	Drainage Density	Land cover	Slope	Geomorphology	Soil	Lineament Density	Rain	Elevation	Water table	Weight
Geology	0.1132	0.1277	0.2222	0.1905	0.2400	0.1188	0.1053	0.1026	0.1188	0.0889	0.1428
Drainage Density	0.1132	0.1277	0.1111	0.1905	0.0800	0.1782	0.0526	0.1026	0.2376	0.0889	0.1282
Land cover	0.0566	0.1277	0.1111	0.0952	0.1600	0.1188	0.1053	0.0513	0.1188	0.1778	0.1123
Slope	0.0566	0.0638	0.1111	0.0952	0.0800	0.1188	0.1053	0.1026	0.1188	0.0889	0.0941
Geomorphology	0.0377	0.1277	0.0556	0.0952	0.0800	0.1188	0.0526	0.0513	0.1188	0.0889	0.0827
Soil	0.1132	0.0426	0.0556	0.0476	0.0400	0.0594	0.1579	0.1026	0.0594	0.0444	0.0723
Lineament Density	0.0566	0.1277	0.0556	0.0476	0.0800	0.0198	0.0526	0.0256	0.0396	0.0444	0.0550
Rain	0.1132	0.0638	0.1111	0.0476	0.0800	0.0297	0.1053	0.0513	0.0297	0.0222	0.0654
Elevation	0.1132	0.0638	0.1111	0.0952	0.0800	0.1188	0.1579	0.2051	0.1188	0.2667	0.1331
Water table	0.2264	0.1277	0.0556	0.0952	0.0800	0.1188	0.1053	0.2051	0.0396	0.0889	0.1143

The equations (3.6) and (3.7) will be applied to find out the CI and CR values. Table 3.5 shows the matrix for calculating CI and CR values. The column values of each criterion will be calculated by multiplying the values from pairwise comparison to the weights from Tables 3.3 and 3.4. The value of ( $\lambda$  max = 11.216) would be the average of sum/weight. The CR can be measured by calculating the CI value of 0.135. Based on the matrix size, the RI can be obtained from Saaty's RI values (Table 3.6). According to the size of the variables, which is equal to 10, the RI value is 1.49. Based on the obtained values, the CR value was calculated as 0.09.

**Table 3. 5 Calculated matrices for CI and CR values.**

Item description	Geology	Drainage Density	Land cover	Slope	Geomorphology	Soil	Lineament Density	Rain	Elevation	Water table	SUM	SUM/Weight
Geology	0.1428	0.1282	0.2245	0.1882	0.2480	0.1445	0.1099	0.1308	0.1331	0.1143	1.5643	10.9553
Drainage Density	0.1428	0.1282	0.1123	0.1882	0.0827	0.2168	0.0550	0.1308	0.2661	0.1143	1.4371	11.2066
Land cover	0.0714	0.1282	0.1123	0.0941	0.1653	0.1445	0.1099	0.0654	0.1331	0.2285	1.2527	11.1597
Slope	0.0714	0.0641	0.1123	0.0941	0.0827	0.1445	0.1099	0.1308	0.1331	0.1143	1.0571	11.2323
Geomorphology	0.0476	0.1282	0.0561	0.0941	0.0827	0.1445	0.0550	0.0654	0.1331	0.1143	0.9209	11.1411
Soil	0.1428	0.0427	0.0561	0.0471	0.0413	0.0723	0.1649	0.1308	0.0665	0.0571	0.8216	11.3698
Lineament Density	0.0714	0.1282	0.0561	0.0471	0.0827	0.0241	0.0550	0.0327	0.0444	0.0571	0.5987	10.8942
Rain	0.1428	0.0641	0.1123	0.0471	0.0827	0.0361	0.1099	0.0654	0.0333	0.0286	0.7222	11.0431
Elevation	0.1428	0.0641	0.1123	0.0941	0.0827	0.1445	0.1649	0.2616	0.1331	0.3428	1.5428	11.5935
Water table	0.2856	0.1282	0.0561	0.0941	0.0827	0.1445	0.1099	0.2616	0.0444	0.1143	1.3214	11.5648

**Table 3. 6 Saaty's RI values for matrices based on variable size.**

Size of Matrix	Random Consistency (CIr)
1	0
2	0
3	0.58
4	0.90
5	1.12
6	1.24
7	1.32
8	1.41
9	1.45
10	1.49

## 3.8 Artificial recharge potential of groundwater in urban area

### 3.8.1 Data acquisition

Precipitation data from six meteorological stations in Kabul province were obtained from the Department of Meteorology, General Directorate of Water Resources, NAWARA Afghanistan, for the 2008–2020 period. The gathered data were in the form of daily logs from 2008 to 2020, which were then transformed into monthly and yearly totals for study. Only one meteorological station (Payin-i-Qargha), located within the research region, is considered out of the six stations for the current study (Figure 3.11). Since the data for 2008 and 2020 were not complete, they were omitted from the analysis, and the intention was to consider the records from 2009 to 2019 only. Landsat imagery was downloaded to create land use and land cover (LULC) identity maps for 2020. The required satellite data were obtained from the USGS Portal (<https://earthexplorer.usgs.gov/>) using the address "path 153 and rows 36."

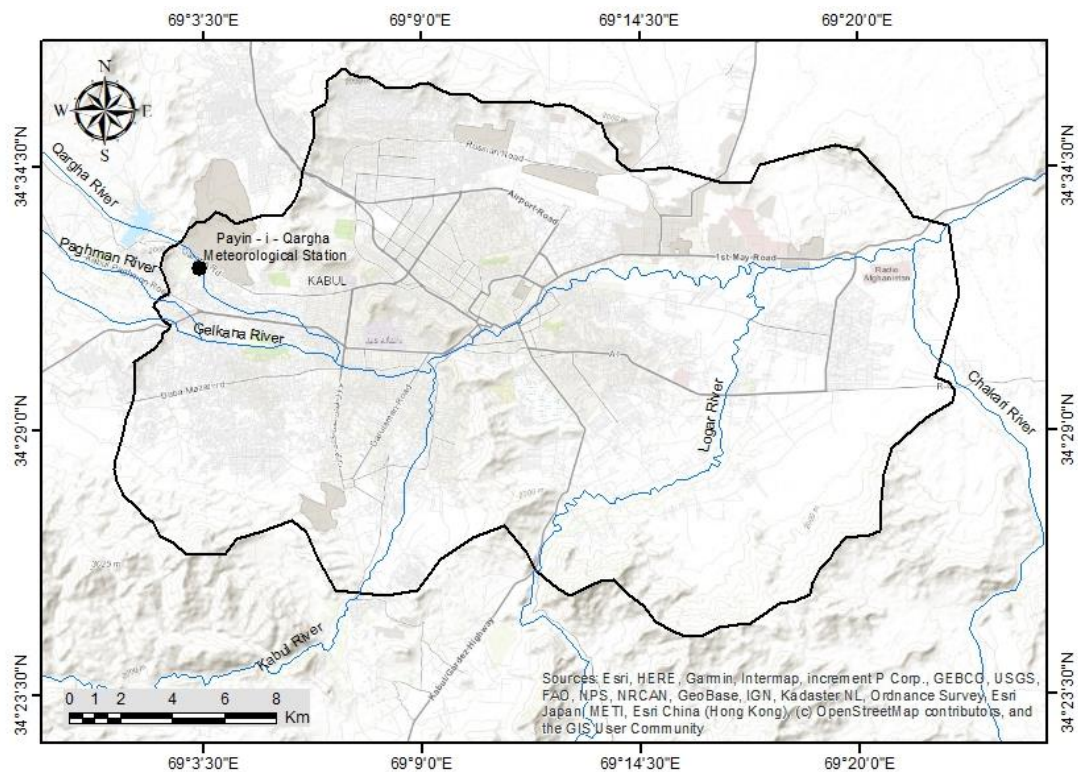


**Figure 3. 10 Location of meteorological station in the study area**

### 3.8.2 LULC development

The availability and sustainability of groundwater are impacted by many variables, including land use and land cover (Machiwal et al., 2011; Martin et al., 2017). Expanding impermeable land surfaces, such as asphalt, concrete roads, streets, and waterproof roof materials, would hinder groundwater recharge. To create the LULC map of the study area, remotely sensed Landsat-8 satellite data was analyzed.

"Supervised classification approach with maximum likelihood algorithm" in ENVI 5.3 environment was applied to create LULC of the study area (Figure 3.12). The research area has bare land and rock, cropland and vegetation, settlements (built-up area), water bodies, and marshland. Built-up areas reduce the effect of groundwater recharge, whereas vegetation-covered regions provide better prospects for groundwater recharges.

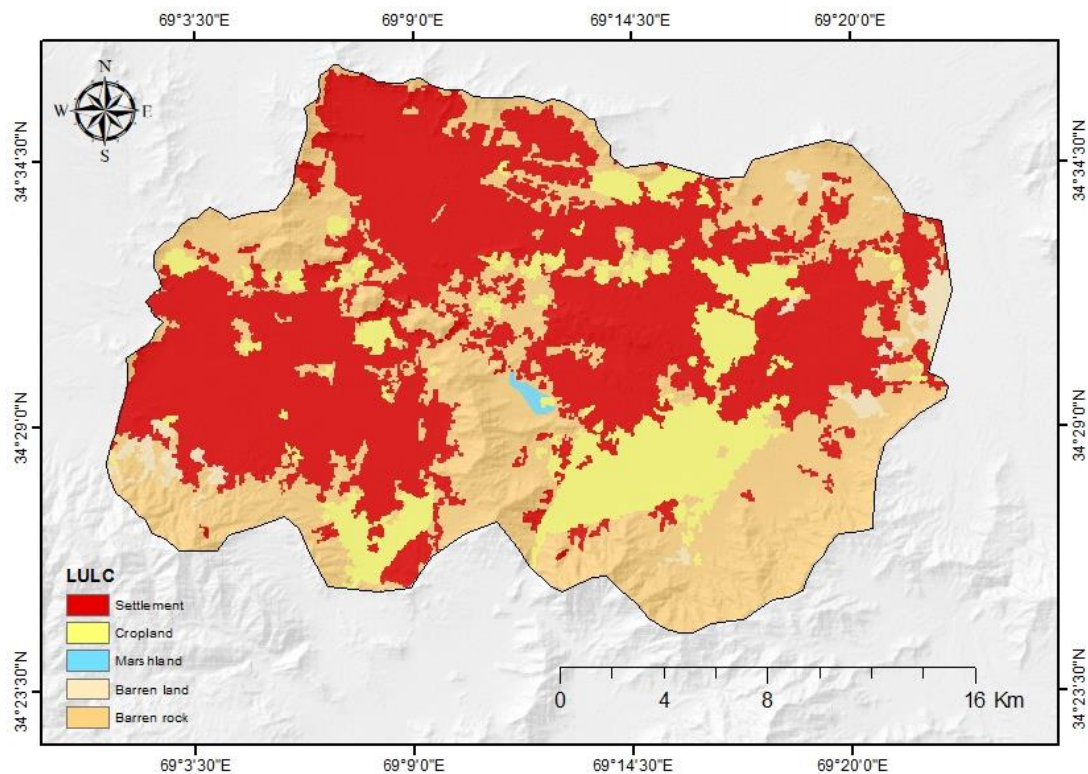


**Figure 3. 11 LULC map of the study area**

### 3.8.3 Rainfall Analysis

This study examined many precipitation characteristics: variability, the number of rainy days, their distribution across the season, the likelihood of daily precipitation, and the highest amount of rainfall ever recorded in a day.

The precipitation concentration index (PCI) and seasonal index (SI) were introduced by (Oliver, 1980; Walsh & Lawler, 1981), and the contribution index (CI) (Mahmoud et al., 2014) was utilized to identify the irregularity and seasonal distribution of precipitation over the year. Equation (3.15) was used to calculate the PCI using RStudio, while equation (3.16) was used to get the SI.

$$PCI = 100 \times \sum_{n=1}^{12} \left( \frac{X_n^2}{R^2} \right) \dots\dots\dots (3. 15)$$

$$SI = \frac{1}{R} \sum_{n=1}^{12} \left| \frac{X_n - R}{12} \right| \dots\dots\dots (3. 16)$$

Where R displays the yearly precipitation, and X<sub>n</sub> indicates the precipitation in month n. The daily, monthly, or seasonal precipitation is calculated as a percentage of the annual total rainfall for the contribution index. By employing the Weibull method (Mansell, 2003), daily precipitation data collected from the Payin-i-Qargha meteorological station from 2009 to 2019 were statistically evaluated:

$$P = \frac{m}{N+1} \times 100 \dots\dots\dots (3. 17)$$

Where P shows the probability of the precipitation (%), N is the data size, and m is the rank given to the data when sorted in descending order.

The probability of maximum daily precipitation and its return period were analyzed employing the Gumbel distribution approach. The method is the limiting form of a large number of uniformly sized samples with an exponential starting distribution. The cumulative distribution is used to calculate the likelihood (percent) that a rainfall depth X (mm) will be greater than a specified rainfall depth x<sub>0</sub> (mm) (Mahmoud et al., 2014):

$$P(X \geq x_0) = 1 - e^{-e^{-y}} \dots\dots\dots (3. 18)$$

Where y is a dimensionless variable and calculated as follows:

$$y = \frac{1.286(x-\bar{x})}{\sigma_x} + 0.577 \text{ where } x \text{ is variate} = \frac{\sigma_x(y_T - 0.577)}{1.2825} + \bar{x} \dots\dots\dots (3. 19)$$

$\bar{x}$  is the mean value, and  $\sigma_x$  is the standard deviation of variate x, as well as y<sub>T</sub> is the reduced variate for a given T

$$y_T = - \left[ \ln . \ln \frac{T}{T-1} \right] \dots\dots\dots (3. 20)$$

By determining the reduced mean y<sub>n</sub> and reduced standard deviation S<sub>n</sub> using tables based on the sample size, the frequency factor K can be calculated as follows:

$$K = \frac{(y_t - \bar{y}_n)}{S_n} \dots\dots\dots (3. 21)$$

The following relation may be used to compute X<sub>t</sub> by providing the value of K.

$$x_t = \bar{x} + K\sigma_{n-1} \dots\dots\dots (3. 22)$$

### **3.8.4 Rainwater harvesting potential based on LULC.**

Land use is a fundamental factor determining the likelihood of surface runoff, which directly affects how quickly rain and other precipitation permeates the ground. More permeable surfaces become impenetrable as cities expand. Different sources have reported the permeability coefficients of various materials. Nachshon et al., (2016), quoted from (Pauleit & Duhme, 2000a), illustrated the infiltration coefficients for the built-up and asphalt areas at 5%, pavement areas at 20%, woody and vegetation areas at 25%, meadow, and pastures at 35%, arable land 40%, and bare soil 50%. Also, according to the argument by (Nachshon et al., 2016), the permeability coefficient for the built-up areas with rainwater harvesting and recharge system (RWHRs) increases up to 80%, and the remaining 20% they consider as the reason for evapotranspiration. As aforementioned, contrary to conventional rainwater harvesting (RWH) systems, which store the water on the land for individual use by the property owners, some researchers recently addressed the potential of rainwater for recharging the nearby aquifers through infiltration wells.

The site's hydrological, climatic, and surface area characteristics must be considered while building the infiltration well structure tools for the rainfall. Considering the hydraulic conductivity of the medium at the specific site of infiltration, it is necessary to create a deep enough infiltration well with a long filter length to allow sufficient water flow from the well into the ground to ensure the effective infiltration of collected rainwater into the aquifer without flooding the infiltration well system.

### **3.8.5 Groundwater recharge**

Estimating the rainwater infiltrating the underground water and the vadose zone depends on the target area's infiltration coefficients. The infiltration coefficient is related to soil hydraulic characteristics, topography, land surface coverage, etc. For the different types of substrates mentioned in Table 3.7, Nachshon et al., (2016) used an illustration from (Pauleit & Duhme, 2000b) to show the infiltration coefficients ( $I_c$ ) values in percent, which indicates the portion of yearly rainfall that is infiltrated underground.

Here, it is projected that 80% of the water is seeping into groundwater for RWHRs that route the gathered water from the collecting sites straight into the subsurface, either into the vadose zone or the aquifer. In other words, instead of the 5 percent shown in Table 1 for non-RWHRs situations, the  $I_c$  of constructed areas where RWHRs is applied is 80 percent. This cautious estimate permits a 20% water loss due to evaporation and retention along the RWHRs system. This percentage is most likely significantly lower than 20%.

**Table 3. 7 Infiltration coefficient of different surfaces** (Nachshon et al., 2016).

<b>Land cover</b>	<b>Ic (%)</b>
<b>Built up (without RWHRS)</b>	5
<b>Asphalt</b>	2
<b>Pavement</b>	20
<b>Woody Vegetation</b>	25
<b>Meadow and pastures</b>	35
<b>Arable lands</b>	40
<b>Bare soil</b>	50
<b>Built up (with RWHRS)</b>	80

By using the weighted arithmetic mean of various infiltration coefficients from regions with different land cover qualities ( $I_c(i)$ ) and taking into account the associated surface areas ( $A(i)$ ) of each LULC (e.g., built-up, bare soil, cropland, etc.), the effective infiltration coefficient ( $I_c(\text{eff})$ ) can be calculated.

$$I_c(\text{eff}) = \frac{\sum(A_i \times I_{c(i)})}{\sum A_i} \dots\dots\dots (3. 23)$$

The exact amount of infiltrated water into groundwater  $I$  ( $\text{m}^3$ ) is determined as follows:

$$I = A \cdot R \cdot I_c(\text{eff}) \dots\dots\dots (3. 24)$$

Where  $A$  is the surface area ( $\text{m}^2$ ) through which infiltration is occurring, and  $R$  is the yearly rainfall ( $\text{m}$ ). By assumption of three leading land cover components in urban contexts (i.e., built-up, bare soil, and arable land), it is straightforward to estimate  $I_c(\text{eff})$  for any given area with any combination of the three components by knowing the  $I_c$  values for each of these constituents. According to Table 3.7, the infiltration coefficients ( $I_c$ ) of built-up areas without RWHRS are equivalent to 5% and 80% for regions developed with RWHRS, 50% for bare soil, and 40% for arable land.

### **3.8.6 Surface runoff**

Due to drainage systems failing during intense rain events, extreme flooding events are occurring more frequently in urban contexts due to the combined effects of global climate change and the impenetrable nature of modern cities. Flooding threatens structures, additional public and private infrastructure, and people's lives. Surface runoff must be decreased in urban settings to lessen the risk of flooding and the cost of drainage systems (Nachshon et al., 2016). RWHRS may be beneficial since it increases the quantity of water that permeates the subsurface instead of flowing as surface runoff.

A variety of circumstances influence runoff and rainfall relationships. Some refer to meteorological properties such as precipitation intensity, duration, and evapotranspiration. In contrast, others relate to physical factors of the surfaces receiving the precipitations, like their impermeabilities and slopes. These elements function in how much of the rainfall depth is absorbed by the atmosphere, the surface of the earth, or both. Runoff coefficients were established to calculate the potential runoff from a given rainfall depth. These coefficients show how much of the depth of the rainfall should be subtracted and accounted for as a loss to runoff.

The "Natural Resources Conservation Services (NRCS)" equation for rainfall-runoff has been employed to determine the possible runoff from a rainstorm. The equation, formerly known as the "Soil Conservation Service (SCS)" approach for estimating direct runoff from rainstorms, was created by the "United States Department of Agriculture (USDA) in 1972"(Mahmoud et al., 2014). It is seen as either a probabilistic or deterministic model.

Since the only relevant rainfall data for this study were daily rainfall time series, applying this approach is ideal for the study region because it eliminates rainfall intensity and removes time as a component. The correlation between the land cover, the "Hydrologic Soil Group (HSG)," and the "Curve Number (CN)" is included in the model. A soil class with high CN values is impermeable and will have more runoff than infiltration:

$$Q = \frac{(P-I_a)^2}{P-I_a+S} = \frac{(P-0.2S)^2}{P+0.8S} \dots\dots\dots (3. 25)$$

Q represents the amount of daily runoff in mm, P represents the amount of daily precipitation in mm, S represents the region's potential maximum storage (mm), and Ia represents the initial abstraction (usually taken as 0.2S) in mm. The following equation indicates how much rainfall is directed to surface runoff by using CN, the runoff curve number of a hydrologic soil group and land cover combinations:

$$S = \frac{25400}{CN} - 254 \dots\dots\dots (3. 26)$$

According to (USDA, 2009), the average CN values for impervious surfaces (built-up area) are about 98. For cropland, it is taken around 76; for bare land, it is assumed to be about 86. The following equation gives the weighted calculated curve number (CN<sub>w</sub>) considering different land-use classifications of the study area.

$$CN_w = \frac{\sum CN_{wi}}{100} \dots\dots\dots (3. 27)$$

Where CN<sub>wi</sub> stands for the weighted curve number of the specific land cover.

### **3.8.7 Models for rainwater harvesting and groundwater recharge.**

Two models have been designed to use precipitation to replenish groundwater, avoid waste in terms of surface flows, and stop urban floods. The first model is used to collect and direct rainwater from residential houses to feed underground water, and the second model is employed to manage and control rainwater from the surfaces of roads and streets for groundwater recharge. The first case considers a typical residential home, where rainfall is collected and channeled to the groundwater recharge (absorbing well) from the roof and the yard. The rainwater collecting channels collect the water from the roof and the yard and send it to the grease and oil trap basin.

Grease and oil traps allow water accumulation to be separated from grease and oil residues. It is constructed from a tank with a baffle wall in the middle. Water enters the basin from one side; solid particles sink to the bottom, while grease and oil float to the top. The clear water enters the basin's other side from under the baffle wall and exits to the sand filter.

Sand filters refine the water by passing it through fine sand to eliminate the tiniest contaminants. It comprises a basin with a fine-sand layer and a gravel layer. The water enters the basin from above and passes through both of these layers to be purified. To prevent pore clogging, this filter also has to be backwashed sometimes. For backwash water that can have its overflow linked to municipal rainfall channels, a backwash water drying basin is also considered. The filtered water enters the recharge well, typically equipped with a casing, screen, gravel pack, and gravel bed.

Similarly, the second model is considered for collecting rainwater from roads and streets to direct it to groundwater recharge wells. The system of groundwater recharge wells can be constructed at a distance on the sides of the streets (pedestrian area). The rainwater from the road surface and sidewalk is collected through the closed channel on the side of the road, which is equipped with screens and enters the sedimentation basin through specific chambers. The settling tank is separated into two separate parts by a buffer wall. The first part is the grease and oil separator, and the second is the settling tank. The settling tank is connected to a recharge well similar to recharge wells of residential houses based on construction. The settling tanks can be cleaned out regularly during the year.

## **3.9 Delineation of groundwater recharge potential zones**

### **3.9.1 Enlarging the study area**

Groundwater supply is not only directly affected by the area where rainfall occurs, but it can also be affected by distant areas. Therefore, the recharge zones can be searched inside and around the study area. The movement of underground water follows the surface slope and topography. This encourages the search for more applicable methods of artificial recharge in the upper streams of the basin. Therefore, it can be said that the groundwater recharge areas can contain large parts of the higher points of the basin. Based on the hydrological characteristics (drainage basin) of the



studied area, it has been enlarged so that it can be used to identify more groundwater recharge areas and explore more and more applicable artificial recharge methods.

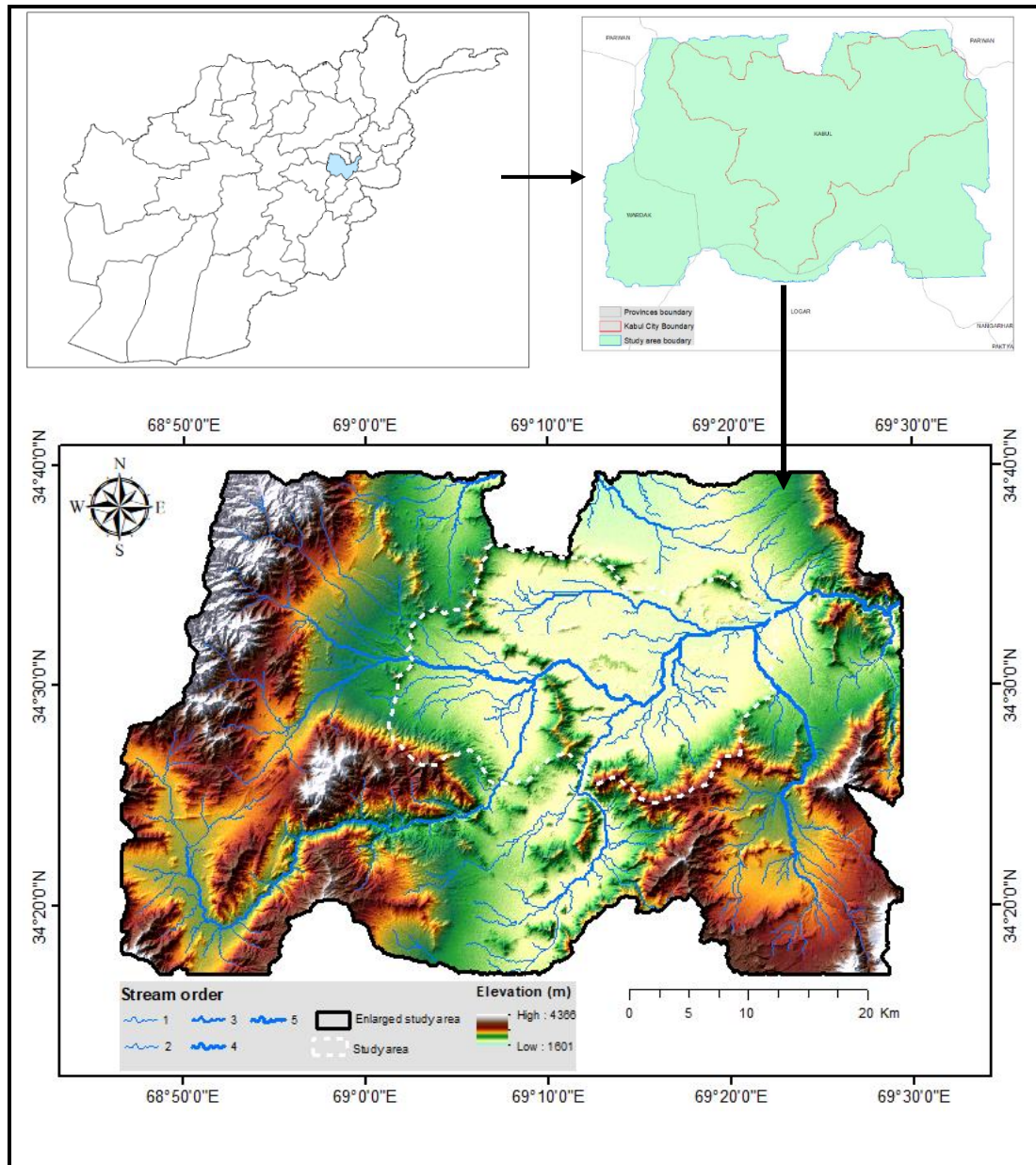


**Figure 3. 12** Location map of the study area

### 3.9.2 Identifying influential factors

The characteristics that broadly impact groundwater potential recharge zones were identified in the first stage. Each relevant factor's thematic layers were created and pre-processed in Arc GIS 10.7 using the UTM Zone 42 Geographic coordinate system and a pixel size of 30 meters. Using the MIF approach, each theme layer was assigned a defined weight. All thematic layers were exposed to a weighted overlay approach in Arc GIS to determine the optimal zones for groundwater recharge.

A "rule-based" method has been employed to locate and recognize the artificial recharge mechanisms.

The following influential indicators have been employed to discover the potential sites for groundwater recharge in the Kabul Basin: "geology, geomorphology, lineament density, drainage density, rainfall, soil, land use and the land cover type, and slope."

The MIF technique examined how distinct geoenvironmental factors influence groundwater recharge capacity. A major influence was assigned a numerical value of 1, while a minor impact was rated 0.5 (Table 3.7). The recommended weight of each element was then calculated by adding together all of the major and minor impacts using the following equation (Equation 3.28):

$$\text{Proposed weight} = \left[ \frac{(A+B)}{\sum(A+B)} \right] \times 100 \dots\dots\dots (3. 28)$$

Where A represents the factor's significant impacts, and B signifies the factor's lesser effects. The weighting and interrelationships between each variable were determined using recently published literature (Achu, Reghunath, et al., 2020; Kolandhavel & Ramamoorthy, 2019; Magesh et al., 2012; Thapa et al., 2017; Zghibi et al., 2020). Finally, the groundwater recharge potential zones for the study region were determined using the weighted overlay method with the thematic layers in an Arc GIS environment and the following equation (Equation 3.29).

$$\text{GWRPZ} = \sum_{i=1}^n F_i \times W_i \dots\dots\dots (3. 29)$$

Whereby  $F_i$  represents the influential variables used for groundwater recharge potential zones, and  $W_i$  denotes the associated weights. Additionally, a "rule-based" identification procedure was used to determine the optimal areas in the basin for artificial recharge techniques such as check dams, contour trenches, recharge wells, and rooftop rainwater harvesting combined with recharge wells.

The summary of overall methodological approaches is illustrated in Figure 3.13.

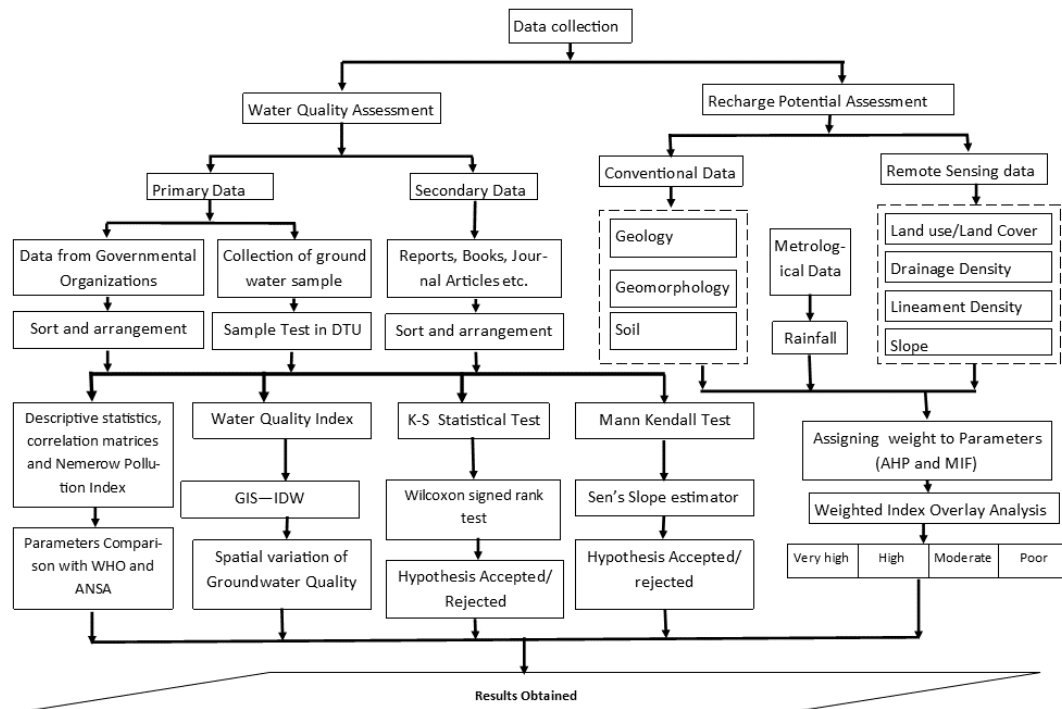


**Figure 3. 13** mythological flow chart of the study

**Note:** Major parts of the contents of the above methodologies are reproduced from the following research papers with permission from Springer Nature.

- Groundwater quality assessment and modelling utilizing water quality index and GIS in Kabul Basin, Afghanistan (Singh & Noori, 2022b)
- Assessment of seasonal groundwater quality variation employing GIS and statistical approaches in Kabul basin, Afghanistan(A. R. Noori & Singh, 2023a)
- Spatial and temporal trend analysis of groundwater levels and regional groundwater drought assessment of Kabul, Afghanistan(A. R. Noori & Singh, 2021a)
- Delineation of groundwater recharge potential zones for its sustainable development utilizing GIS approach in Kabul basin, Afghanistan (Singh & Noori, 2022a)
- Rainfall Assessment and Water Harvesting Potential in an Urban Area for Artificial Groundwater Recharge with Land Use and Land Cover Approach (A. R. Noori & Singh, 2023b)
- Delineation of optimal locations for artificial groundwater recharge utilizing MIF and GIS in a semi-arid area (A. R. Noori & Singh, 2024)

## CHAPTER 4

### RESULTS AND DISCUSSION

#### 4.1 Water quality analysis

The results of water quality parameters are summarized in Table 4.1. All physicochemical parameters of main anions and cations levels are provided in mg/l except pH and electrical conductivity. The table indicates the descriptive statistics of the data. It also displays the number of samples that exceeded the allowed limit and the percentages of observations that exceeded the allowable limit in line with WHO criteria. The following are the details of the groundwater quality metrics investigated for drinking purposes.

**Table 4. 1 Descriptive statistics and permissible limits of groundwater quality parameters concerning the (WHO, 2011)**

Parameter	Min	Max	Mean	Median	STD	WHO Limit	Samples exceeding permissible limit WHO	
							# Of samples	% Of samples
EC	541	15060	2280.00	1199	3050.52	1500	12	34.29
pH	6.6	7.7	7.19	7.2	0.19	6.5-8.5	Nil	Nil
TDS	270	7450	1135.20	598	1515.61	1000	5	14.29
Salinity	0.19	8.55	1.04	0.535	1.63	-	-	-
T_Hardness	160	790	318.00	290	147.05	500	4	11.43
Ca_Hardness	22.0275	420.525	88.45	74.0925	73.23	-	-	-
Mg_Hardness	109.9375	587.8725	229.55	195.945	113.25	-	-	-
Calcium	8.811	168.21	35.38	29.637	29.29	75	3	8.57
Magnesium	26.7148	142.853	55.78	47.6146	27.52	30	34	97.14
Sodium	23.6	1132.7	152.55	64.74	239.57	200	6	17.14
HCO <sub>3</sub>	353.8	2013	800.84	774.7	333.89	600	25	71.43
Alkalinity	290	1650	656.43	635	273.68	-	-	-
Chloride	35	2865	315.86	100	557.36	250	8	22.86
Sulphate	22.872	264.76	114.07	102.79	74.61	250	3	8.57
Phosphate	0	2.9302	0.13	0.0404	0.49	-	-	-
Fluoride	0.13	0.87	0.34	0.29	0.17	1.5	Nil	Nil
Silica	40.34	104.5	62.40	60.96	13.82	-	-	-
Potassium	2.41	80.5	9.15	5.5	13.19	12	6	17.14
Nitrate	0.233	59.7	8.71	6.047	10.82	45	1	2.86

## 4.1.2 Physicochemical parameters

### 4.1.2.1 Electrical conductivity (EC)

This characteristic determines the quantity of current that an aqueous medium can convey. Based on the WHO standard, the highest permitted level for electrical conductivity is 1500  $\mu\text{S}/\text{cm}$ . The detected EC ranges from 541 to 15060  $\mu\text{S}/\text{cm}$ . Based on (Todd, 1980), there are five primary EC groundwater quality classifications, as illustrated in Table 4.2. No sample in the study region had an excellent water type with an EC of less than 250  $\mu\text{S}/\text{cm}$ . As shown in Figure 4.1a, 17.14 percent of observations have a good water type (EC, 250–750  $\mu\text{S}/\text{cm}$ ), 62.86 percent have a permissible water type (EC, 750 – 2000  $\mu\text{S}/\text{cm}$ ), 5.71 percent have a doubtful water type (EC, 2000 – 3000  $\mu\text{S}/\text{cm}$ ), and 14.29 percent have an unsuitable water type (EC > 3000  $\mu\text{S}/\text{cm}$ ). As a result of this research, it is apparent that 20 percent of groundwater is inadvisable for residential usage.

**Table 4. 2 Classification of groundwater according to electrical conductivity**

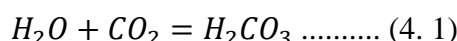
EC	Classification	Samples exceeded permissible levels	% Of the sample that exceeds permissible levels
< 250	Excellent	Nil	Nil
250 - 750	Good	6	17.14
750 - 2000	Permissible	22	62.86
2000 - 3000	Doubtful	2	5.71
> 3000	Unsuitable	5	14.29
	Total	35	100.00

### 4.1.2.2 Hydrogen ion concentration (pH)

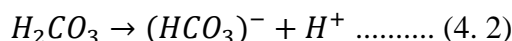
The pH values of water are the most significant and deciding component for its level of corrosivity, and this is due to water reacting with  $\text{CO}_2$  underground to create carbonic acid. The interaction of  $\text{CO}_2$ ,  $\text{CO}_3$ , and  $\text{HCO}_3$ , and their balance, determines the pH content of natural water. The pH measurements found in this study ranged between 6.6 and 7.7, within the acceptable limits of the ANSA standard. Based on the findings, the pH value in the research location is not acidic.

The following equations illustrate the natural changes of pH in groundwater before reaching the aquifer system:

1. Carbonic acid is formed when rainwater reacts with the atmosphere.



2. Carbonic acid dissociates into bicarbonate, releasing hydrogen ions, which make it acidic.



#### 4.1.2.1 Total Dissolved Solids (TDS)

Total dissolved solids (TDS) refer to the inorganic salts and trace amounts of organic compounds in aqueous solutions. Natural rock formation controls TDS primarily through weathering (transport), porosity, and permeability. Sewage disposal and fertilizer runoff are examples of anthropogenic sources. TDS readings with a highest and lowest range of 270 – 7450 mg/l were discovered, with an allowed limit of 2000 mg/l suggested by the ANSA standard. Figure 4.1b represents the geographical distribution layout of TDS in the research area. As indicated in Table 4.3, according to (Davis & DeWiest, 1966) classification, 40% of the samples are desirable for drinking with TDS less than 500 mg/l, 37.14% are permissible for drinking, having TDS 500–1000 mg/l, followed by 11.43 % useful for irrigation and 11.43% are unfit for drinking and irrigation. According to (Freeze & Cherry, 1979), 77.14 percent of observations are freshwater, 22.86 percent are brackish water, and no samples are saline or brine water, as indicated in Table 4.4.

**Table 4. 3 Groundwater classification based on total dissolved solids**

TDS	Classification	The samples exceed permissible levels	% Of samples that exceed permissible levels
<500	Desirable for drinking	14	40.00
500-1000	Permissible for drinking	13	37.14
1000-3000	Useful for irrigation	4	11.43
>3000	Unfit for drinking and irrigation	4	11.43
	Total	35	100.00

**Table 4. 4 Groundwater classification based on TDS content**

TDS	Classification	Samples exceeded permissible levels	% Of samples that exceed permissible levels
<1000	Fresh water type	27	77.14
1000-10000	Brackish water type	8	22.86
10000-100000	Saline water type	Nil	Nil
>100000	Brine water type	Nil	Nil
	Total	35	100.00

#### 4.1.2.2 Total Hardness (TH)

Total hardness is an essential factor in determining the properties of drinking water quality. It reflects the concentration of Ca and Mg ions in water. In the current study, TH concentrations vary from 160 to 790 mg/l. The total hardness

maximum threshold has been limited to 500 mg/l by WHO guidelines. Water is divided into four categories based on its hardness (i.e., soft, moderate, hard, and very hard). No sample has fallen in the soft and moderate water categories with TH less than 75 mg/l and (TH; 75–150 mg/l). As illustrated in Table 4.5 and the geographical distribution map (Figure 4.1c), 57.14 percent of observations are in the hard group (TH = 150-300 mg/l), and 42.86 percent are in the very hard classification (TH > 300 mg/l).

**Table 4. 5 Classification of groundwater as per total hardness**

TH as CaCO <sub>3</sub>	Classification	Samples exceed permissible levels	% Of samples that exceed permissible levels
<75	Soft	Nil	Nil
75-150	Moderately hard	Nil	Nil
150-300	Hard	20	57.14
>300	Very hard	15	42.86
	Total	35	100.00

#### 4.1.2.3 Major ions chemistry

Anions concentrations were discovered in this investigation in the ascending order: F < NO<sub>3</sub> < SO<sub>4</sub> < Cl < HCO<sub>3</sub> with percentages of 0.03% < 0.70% < 9.20% < 25.48% < 64.59% respectively. Bicarbonate (HCO<sub>3</sub><sup>-</sup>) is water's most common and stable ion. Temperature, pH, dissolved CO<sub>2</sub>, cations, and other salts all play a role in bicarbonate concentration in water. As shown in Table 4.1, about 71 percent of the samples are over the WHO standards, whereas 28.6 percent are below the permitted level. Bicarbonate levels in the Kabul basin range from 354 to 2013 mg/l (Figure 4.1d). Chloride is the second most prevalent ingredient. Chloride in groundwater is due to weathering, sediment, soil leaching, and urbanization (Karanth, 1987). Cl<sup>-</sup> ion concentrations in the examined water samples ranged between 35 and 2862 mg/l (Figure 4.1e), except for five samples below the WHO-permitted limit (Table 4.1). Sulfate has a mean content of 114 mg/l and a variation of 22.87 to 265 mg/l, within the acceptable ranges (Figure 4.1f). Sulfate is commonly found in groundwater due to the oxidation of sulfite minerals such as pyrite (FeS<sub>2</sub>) (Yadav et al., 2012). The nitrate concentration in the basin is within the acceptable limit (Figure 4.1g), except for one sample that surpassed the WHO guidelines (greater than 45 mg/l).

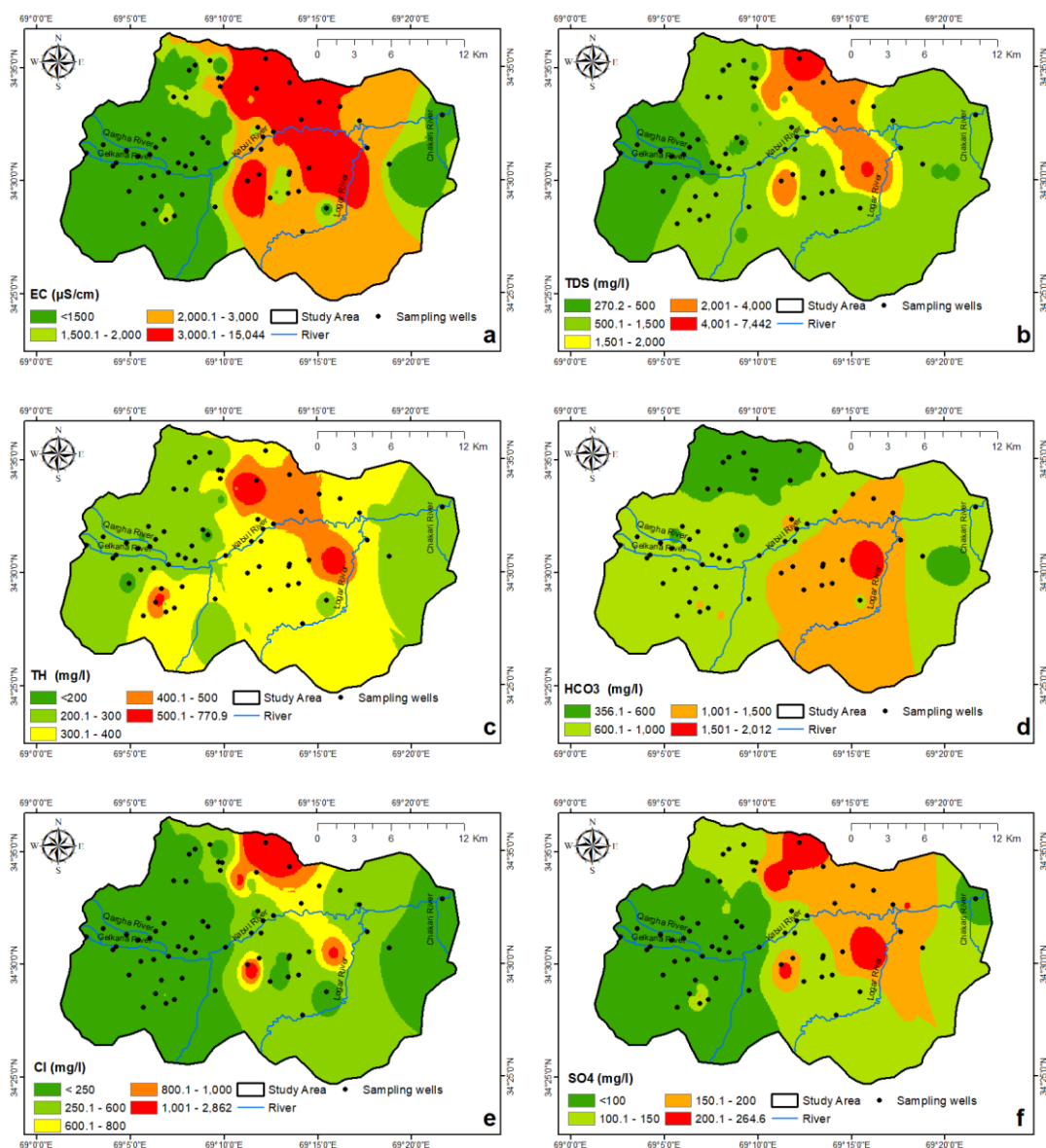


**Figure 4. 1** Spatial distribution of observed parameters showing minimum to maximum ranges



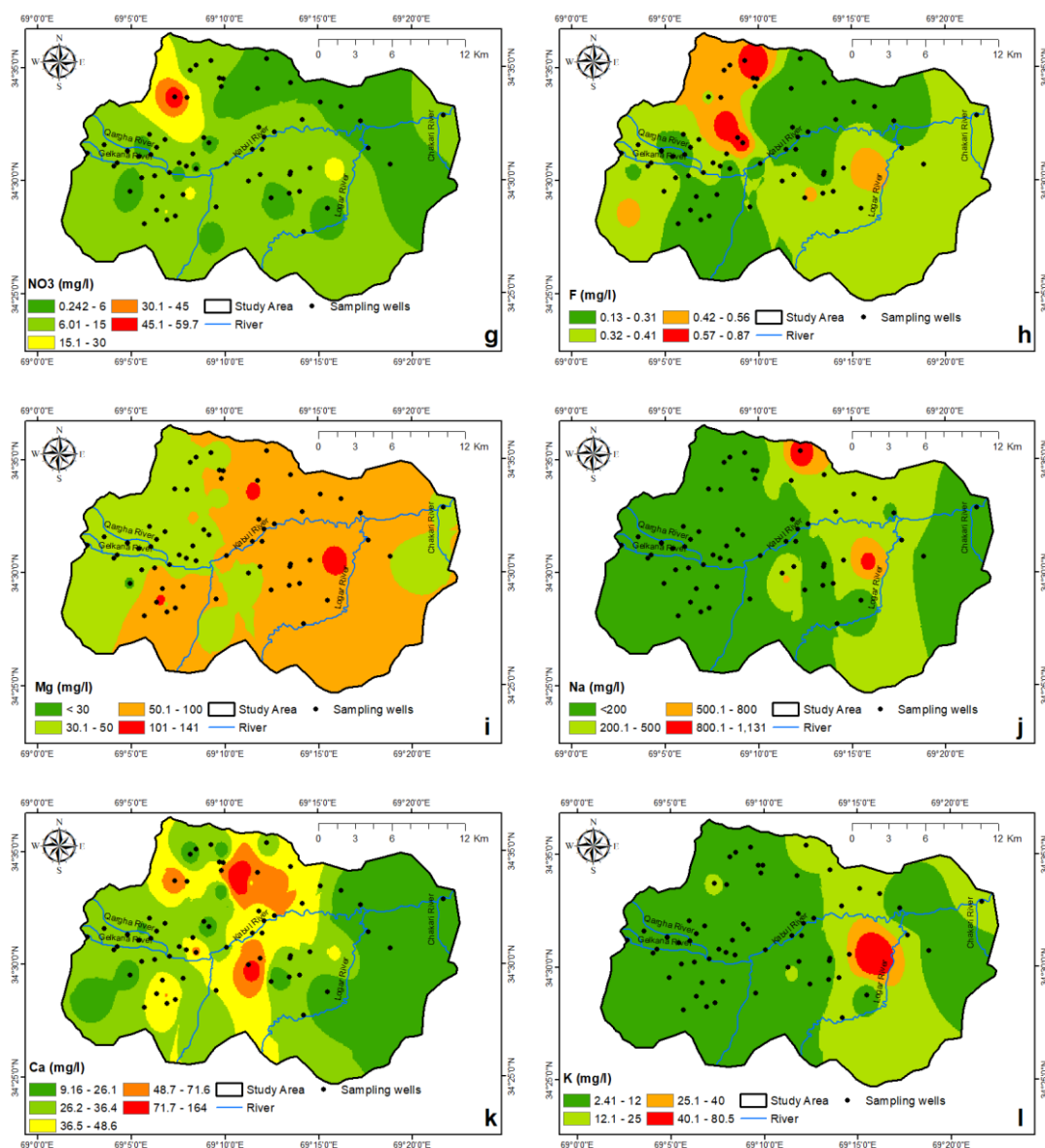


**Figure 4.1 (continued)**

The region's average fluoride content is 0.34 mg/l, with minimum and maximum values ranging from 0.13 to 0.87 mg/l (Figure 4.1h), all within WHO's allowed thresholds. Fluoride sources in groundwater are mainly of orogenic processes due to the weathering of granitic rocks having  $F^-$ -rich minerals as an accessory like amphiboles, apatite, fluorite, and mica (Reddy et al., 2010). Fluorosis of the teeth and skeleton is caused by high fluoride levels in water (beyond the permitted limit).

The quantity of cations is shown in ascending order:  $K^+ < Mg^{+2} < Ca^{+2} < Na^+$  contributing 3.28% < 20% < 22% < 55% respectively. Sodium has the greatest proportion, with 152.55 mg/l on average (Figure 4.1j). The highest amount of sodium is 1132.7 mg/l, and the lowest observation is 23.6 mg/l. Compared with WHO recommendations, 82.85% of the samples are within allowed ranges, whereas 17.14

percent of the detected samples exceed the permissible sodium limits.  $\text{Na}^+$  is found in groundwater from silicate minerals. Rainwater, the dissolution of evaporated minerals, sewage, and industrial outlets (Handa, 1975) are the other sources of sodium. With an average concentration of 61 mg/l, calcium is the second most prevalent element in the sample. It constitutes about 22% of the cation concentration. The highest calcium content is 453 mg/l, while the least is nine mg/l (Figure 4.1k). Only six of the 35 tested samples exceeded the WHO's acceptable threshold. The primary sources of calcium in groundwater are igneous and sedimentary rocks. Calcium and magnesium concentration relate to the hardness of water and are freely available on both surface and subsurface water as carbonates and sources are from rocks like limestone, gypsum, and dolomite (Domenico & Schwartz, 1998).

Magnesium has the third proportion, with 55.77 mg/l on average (Figure 4.1i). The highest amount of magnesium is 142.85 mg/l, and the lowest observation is 26.7 mg/l. Only 20 percent of the observed wells have a concentration above the allowable limit. The remaining 80 percent of the wells are within the WHO guidelines. Magnesium is found to have its source from all three types of rocks, such as igneous (basalt, dunites, pyroxenites), metamorphic (amphibolite, talc, tremolite-schists), and sedimentary (dolomite, gypsum) (Karanth, 1987). Potassium has the lowest concentration, with a mean of 9.14 mg/l and a variation of 2.41 to 80.5 mg/l (Figure 4.1l). The concentration of 17.14 percent of the samples in the basin exceeds the WHO recommendations, while the other samples are within limits. The distribution of different parameter concentration percentages in groundwater samples is depicted in Figure 4.2. EC is first with 43.36 percent, TDS is second with 21.59 percent,  $\text{HCO}_3^-$  is third with 15.24 percent, TH is fourth with 6.05 percent, and chloride is fifth with 6.01 percent. Sodium concentration comprises about 3 percent of the overall groundwater quality, while sulfate makes up only about 2% of the concentrations. The remaining elements, Ca, Mg, K, F, and  $\text{NO}_3^-$ , comprise only 2.7% of the concentration.

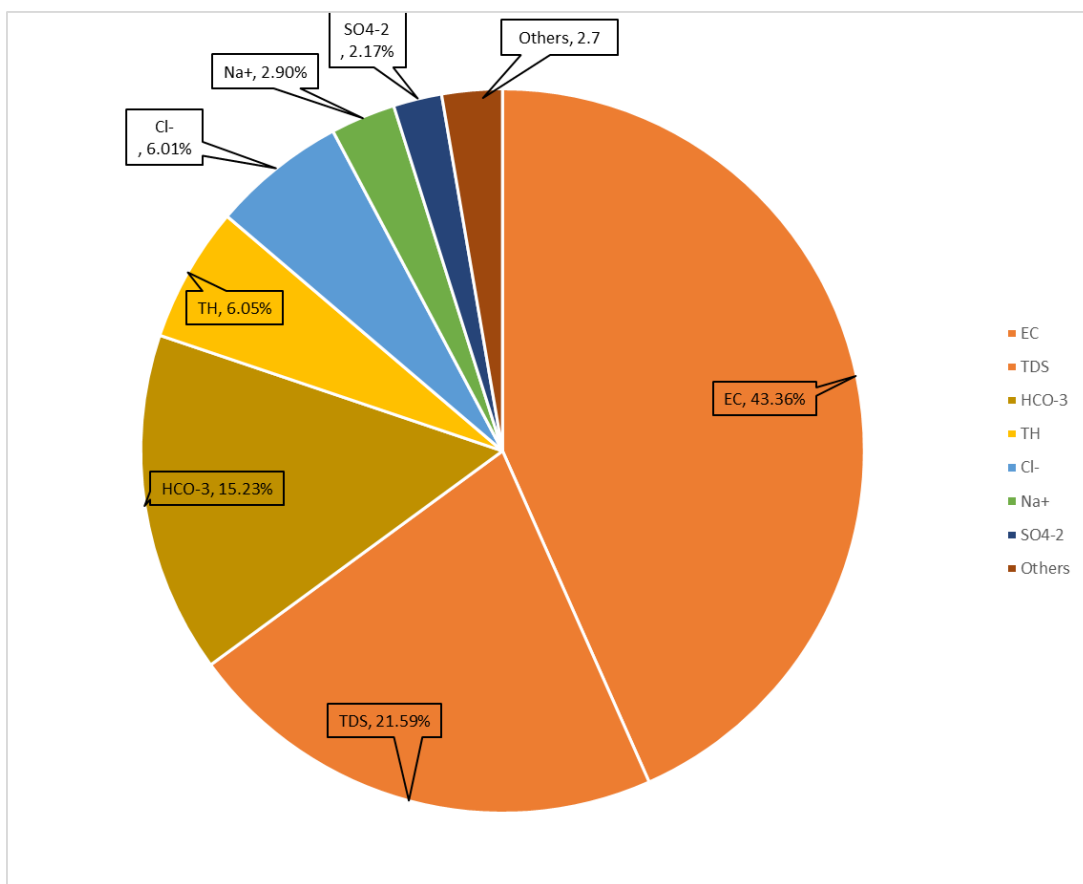


**Figure 4. 2 Pie chart illustrating percentage distribution of all measured parameters**

#### 4.1.3 Hydrochemical facies

The interaction between major anions and cations, as well as their behaviors, is addressed by the hydrochemical facies of groundwater. Hydrochemical facies aid in the identification and classification of various water types (Piper, 1944; Venugopal et al., 2009). As a result, the hydrogeochemical facies of groundwater were estimated by plotting the concentrations of main anions ( $\text{Cl}^-$ ,  $\text{SO}_4^{2-}$ , and  $\text{HCO}_3^-$ ) and cations ( $\text{Ca}^{2+}$ ,  $\text{Mg}^{2+}$ ,  $\text{Na}^+$ , and  $\text{K}^+$ ) in meq/L in a Piper diagram (Figure 4.3). There are six main water types in the geochemical evolution process. Six distinct forms of water categorization are depicted in Figure 4.3. Grapher 13 was utilized to plot the Piper diagram. The following is the percentage distribution of samples of each kind of water: about 77% Mg- $\text{HCO}_3$  type, 11% Na-Cl type, and about 7% each of Mixed Ca- Na- $\text{HCO}_3$  and mixed Ca-Mg-Cl type. Bicarbonate leads the proportion in the anion's triangle with 83%, followed by chloride with 11 percent, and 6 percent of samples had no dominance. For cations, no dominance is the most prominent ion with 48.5 percent dominance, magnesium with 34 percent, and 17 percent of samples with sodium type (Figure 4.4).

**Table 4. 6 calculated anions and cations for the Piper plot**

<b>No.</b>	<b>Ca</b>	<b>Mg</b>	<b>Na + K</b>	<b>Cl</b>	<b>SO<sub>4</sub></b>	<b>HCO<sub>3</sub></b>
<b>1</b>	14.04	62.76	7.33	16.16	4.94	78.90
<b>2</b>	12.60	59.13	9.33	47.93	14.63	37.44
<b>3</b>	18.18	49.45	11.51	11.28	5.76	82.96
<b>4</b>	20.81	52.64	8.99	11.17	4.75	84.08
<b>5</b>	19.48	51.24	10.14	14.26	7.41	78.33
<b>6</b>	33.15	40.77	9.43	13.74	8.38	77.89
<b>7</b>	24.16	59.80	4.97	8.54	4.49	86.97
<b>8</b>	16.75	52.36	10.72	14.21	7.21	78.58
<b>9</b>	14.49	10.40	48.72	58.32	8.13	33.55
<b>10</b>	6.19	49.34	16.91	13.59	10.10	76.31
<b>11</b>	9.74	48.50	15.72	15.15	10.62	74.23
<b>12</b>	3.52	18.55	47.79	43.68	7.90	48.42
<b>13</b>	8.51	55.33	12.68	12.58	6.35	81.07
<b>14</b>	17.76	46.58	13.12	23.29	8.03	68.67
<b>15</b>	4.31	39.54	24.45	24.07	12.55	63.37
<b>16</b>	2.82	31.82	32.15	34.94	13.87	51.19
<b>17</b>	14.29	42.00	17.33	17.05	6.41	76.54
<b>18</b>	13.22	42.30	17.68	7.89	3.33	88.78
<b>19</b>	10.63	42.51	18.87	17.32	15.18	67.51
<b>20</b>	16.56	42.58	15.87	14.65	10.70	74.65
<b>21</b>	36.29	29.98	13.61	29.37	12.74	57.89
<b>22</b>	11.96	53.28	12.25	24.26	24.16	51.58
<b>23</b>	12.71	47.95	14.65	19.53	22.32	58.15
<b>24</b>	2.39	9.91	65.21	86.13	5.88	7.99
<b>25</b>	11.42	65.83	7.06	14.95	8.22	76.83
<b>26</b>	24.69	27.06	21.80	26.43	12.06	61.51
<b>27</b>	19.11	42.04	14.96	9.41	8.05	82.54
<b>28</b>	23.65	51.24	8.51	9.32	5.70	84.98
<b>29</b>	16.07	44.70	14.90	21.94	9.93	68.13
<b>30</b>	12.39	49.56	13.94	15.89	21.80	62.31
<b>31</b>	11.80	51.43	13.23	16.27	22.22	61.51
<b>32</b>	23.70	46.74	10.51	11.52	6.15	82.33
<b>33</b>	25.39	50.77	8.05	12.43	6.79	80.78
<b>34</b>	21.59	20.00	30.00	66.61	14.74	18.65
<b>35</b>	28.38	24.97	21.17	77.36	10.99	11.65

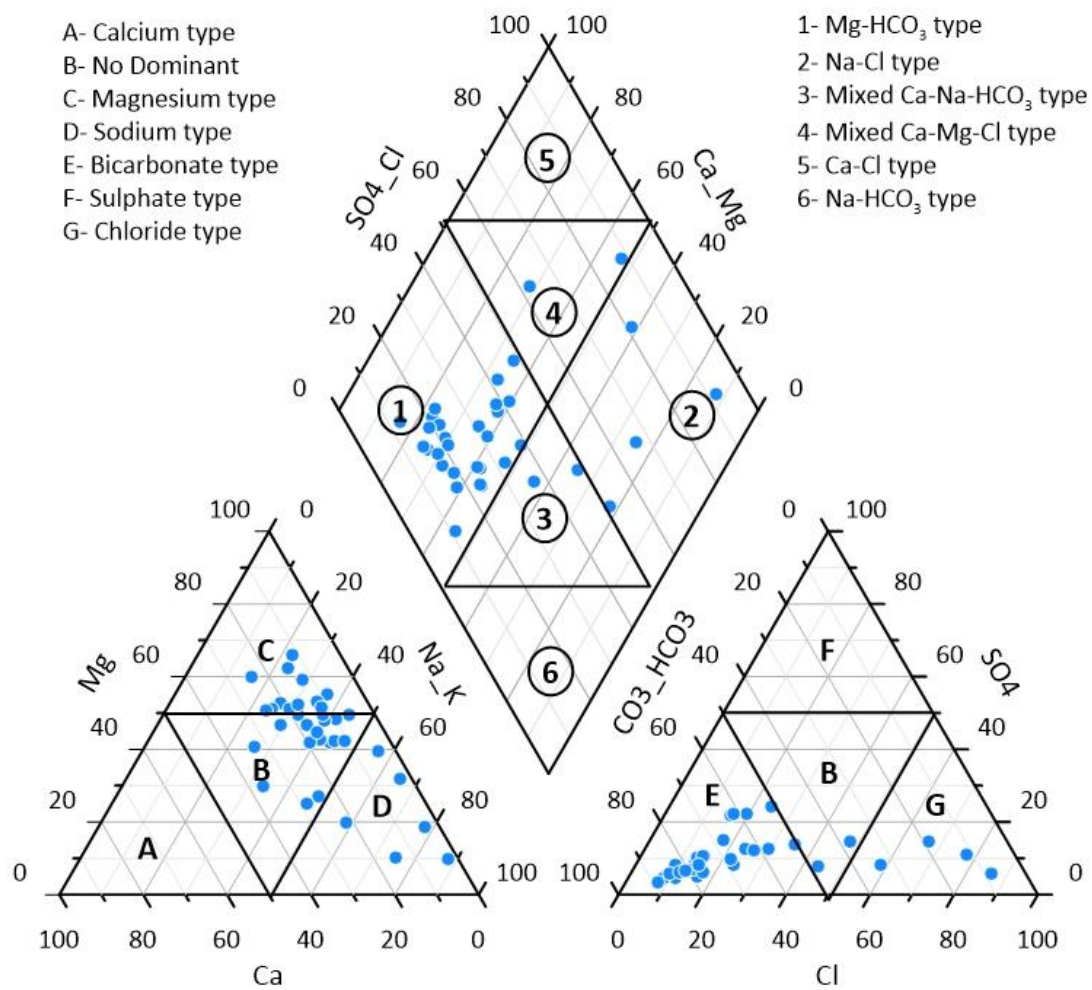
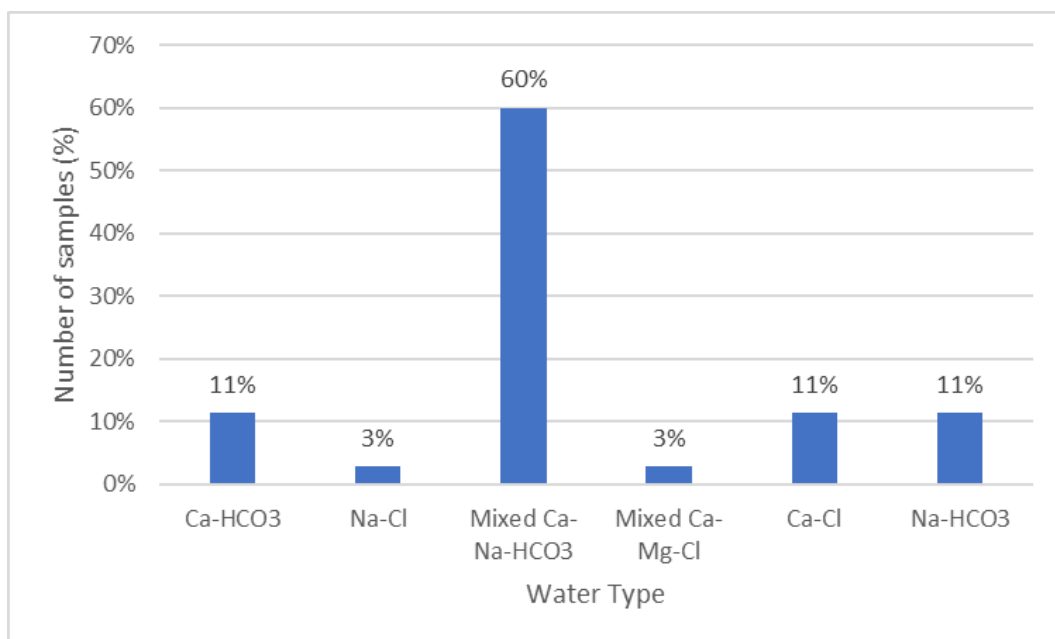
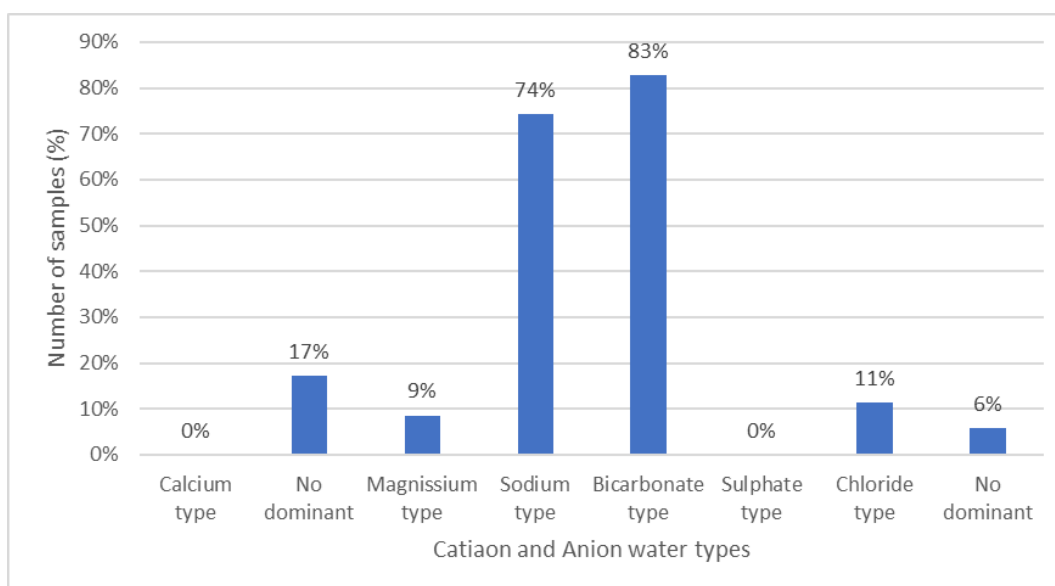


**Figure 4. 3 Piper diagram illustrating various hydrochemical facies of groundwater**



a. Water type percentage



b. Water type based on Anion and Cation

**Figure 4. 4 Percentage of different water types based on the Piper diagram****4.1.4 Gibbs diagram**

Gibbs plot illustrates the chemical specifications of water and the method of their interaction with various subsurface rock lithologies. The classification is of three types: type-I evaporation dominant (due to the rate of surface/ subsurface evaporation), type-II rock dominance (due to chemical rock weathering by water), and type-III precipitation dominance (surface/subsurface precipitation).

**Table 4. 7 The calculation process for the Gibbs plot**

No	Ca	Mg	Na	K	HCO <sub>3</sub>	Cl	SO <sub>4</sub>	TD S	Cl/(Cl+HCO <sub>3</sub> )	(Na+K)/(Na+K+C a)
1	26	69	46	5.14	756	90	37	472	0.106332703	0.664247727
2	46	132	115	7.07	659	490	203	1285	0.426532033	0.724950861
3	33	54	63	6.28	1013	80	55	581	0.073219843	0.679603126
4	27	42	38	3.94	842	65	37	443	0.071680635	0.603603866
5	34	54	55	4.64	946	100	70	598	0.095648015	0.640469371
6	52	39	45	3.34	976	100	83	580	0.092936803	0.481656628
7	33	49	24	2.41	702	40	29	364	0.053944707	0.441963603
8	32	61	65	5.16	952	100	69	638	0.095093191	0.685697469
9	90	39	526	13.2	1183	1195	226	3430	0.502438614	0.857262868
10	14	66	107	9.22	1208	125	126	729	0.093787515	0.894992944
11	18	56	88	5.29	970	115	109	642	0.106000553	0.834344906
12	38	120	910	80.5	2013	1055	259	4390	0.343872229	0.963387202
13	9	35	40	4.85	610	55	38	291	0.082706767	0.836107959
14	39	62	87	5.5	1116	220	103	879	0.16463369	0.702408844
15	12	67	175	7.5	1110	245	173	985	0.180785124	0.938262724
16	10	66	253	5.8	946	375	202	1218	0.28398334	0.964122548
17	26	47	83	16.81	811	105	53	573	0.114591291	0.790418877
18	20	39	76	2.72	775	40	23	381	0.049097827	0.796607587
19	13	31	59	10.11	403	60	71	304	0.129701686	0.843394105
20	34	52	89	9.84	921	105	104	680	0.102329208	0.746885157
21	62	31	58	14.69	543	160	94	782	0.227628397	0.537741014
22	18	48	57	3.67	366	100	135	474	0.214592275	0.773821748
23	18	40	59	5.86	384	75	116	371	0.163291966	0.786715403
24	27	69	1133	23.1	458	2865	265	7450	0.862302483	0.976979529
25	41	143	91	3.82	885	100	75	602	0.101574403	0.699295552
26	50	33	109	3.84	1061	265	164	1000	0.199788902	0.694560618
27	20	27	42	8.46	604	40	46	309	0.062121447	0.714763906
28	24	32	27	3.37	549	35	29	270	0.059931507	0.560534016
29	33	55	88	7.25	1122	210	129	799	0.157610327	0.742969844
30	18	43	60	3.53	506	75	139	450	0.129021159	0.782878687
31	17	44	58	3.64	488	75	139	452	0.13321492	0.785558573

Continued to the next page

Table 4.7 (Continued)

No	Ca	Mg	Na	K	HCO <sub>3</sub>	Cl	SO <sub>4</sub>	TD S	Cl/(Cl+HCO <sub>3</sub> )	(Na+K)/(Na+K+Ca)
32	30	35	40	4.69	738	60	43	405	0.075178549	0.59942963
33	32	39	32	5	671	60	44	405	0.082079343	0.533148769
34	77	43	234	7.8	390	810	243	2080	0.674775075	0.758792457
35	168	90	310	12.2	354	1365	263	4420	0.794158715	0.657071212

The Gibbs diagram was created by visualizing the main ions data from groundwater samples using the following two equations for anions and cations:

$$\text{Gibbs ratio I for anions } \left(\frac{\text{meq}}{L}\right) = \frac{\text{Cl}^-}{(\text{Cl}^- + \text{HCO}_3^-)} \dots\dots\dots (4.3)$$

$$\text{Gibbs ratio II for cations } \left(\frac{\text{meq}}{L}\right) = \frac{\text{Na}^+ + \text{K}^+}{(\text{Na}^+ + \text{K}^+ + \text{Ca}^{2+})} \dots\dots\dots (4.4)$$

As illustrated in Figure 4.5, except for some samples that are dominated by evaporation, the rock category dominates the bulk of the samples. The evaporation process is rare in surface and subsurface water, but the hot and dry conditions of the region's climate can cause some of the samples to fall into it (Selvakumar, Chandrasekar, et al., 2017). Nonetheless, maximal observations in rock domination show that silicate rocks are chemically degraded with groundwater at appropriate pressure and temperature.

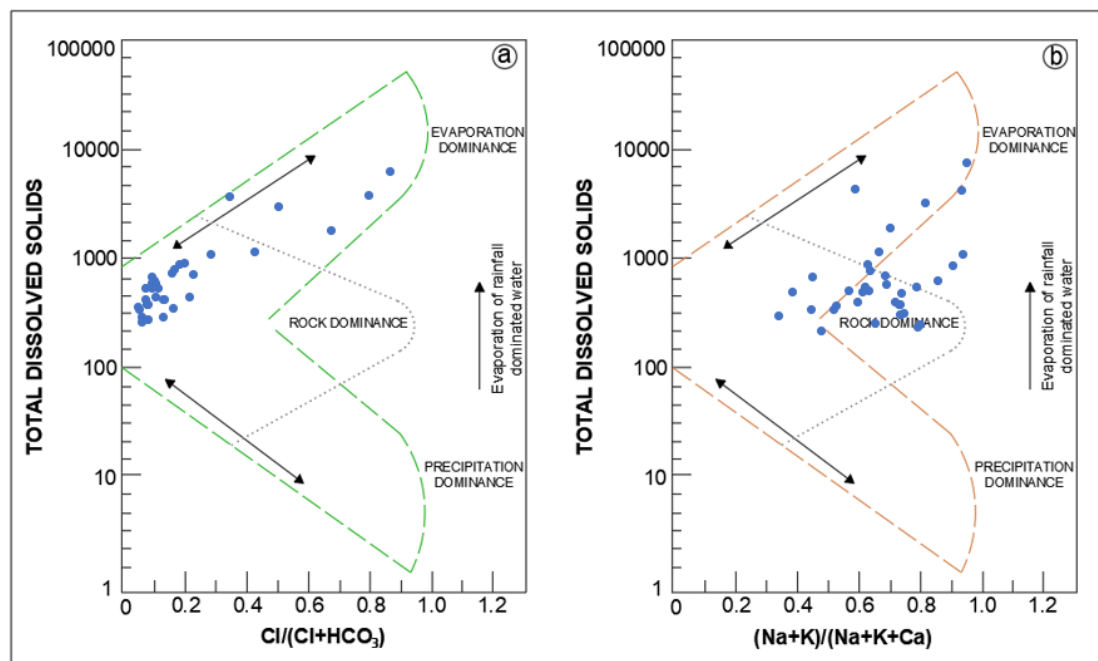


Figure 4.5 Demonstration of principal influencing groundwater chemistry in Gibbs plot



#### 4.1.5 Single factor pollution index

Table 4.8 displays the single-factor pollution index technique's environmental quality standard assessment grading. Based on Figure 4.6 EC, 66% of groundwater samples illustrated no pollution, 20% are slightly polluted, 3% are lightly and moderately polluted, but 9% are seriously polluted. pH in all samples is safe. TDS has no pollution marks in 77% of the samples. Total hardness in 89% of samples has no pollution. From the TH perspective, only 11% of the samples have slight pollution conditions. Ca also has shown no pollution in 91% of samples and 6 and 3 percent slightly to moderately polluted, respectively. Mg only has pollution in samples that are different. Only 3% of samples are safe, 66% are slightly polluted, 23% are lightly polluted, and 9% are moderately polluted. Na in 83% of samples are not safe. Bicarbonate in 29% of samples is safe, while in 66% of samples slightly polluted. Cl in 77% of samples, Sulphate in 91%, fluoride in 100%, potassium in 86%, and nitrate in 97 percent of analyzed samples are safe. To sum up, EC, Mg, and  $\text{HCO}_3$  are the parameters that illustrate most pollution conditions in groundwater.

**Table 4. 8 Water quality level determination based on the single factor pollution index method.**

Water quality level	$P_i$	Pollution assessment
1	$\leq 1$	No pollution
2	1-2	Slightly pollution
3	2-3	Lightly pollution
4	3-5	Moderately polluted
5	$> 5$	Seriously polluted

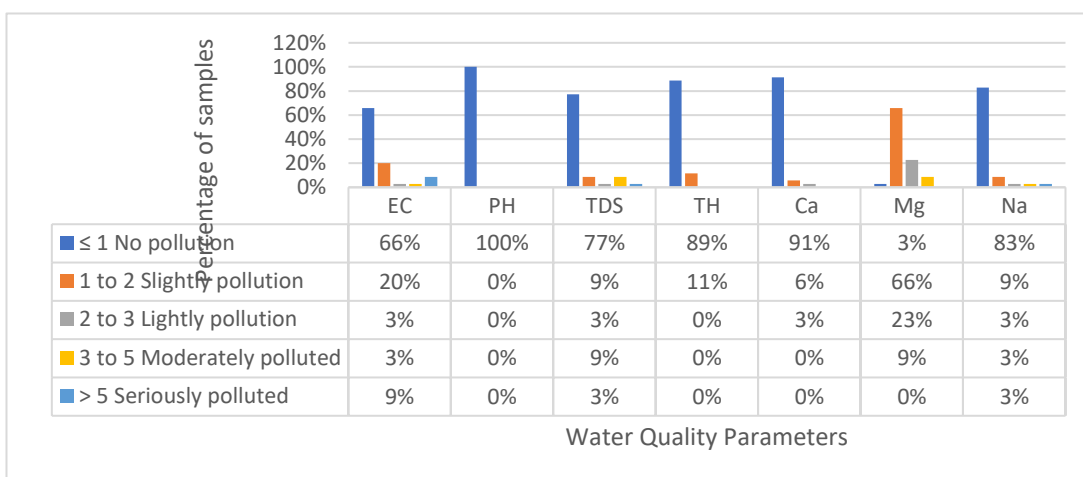


**Figure 4. 6 Results of water quality assessment by single factor pollution index method.**

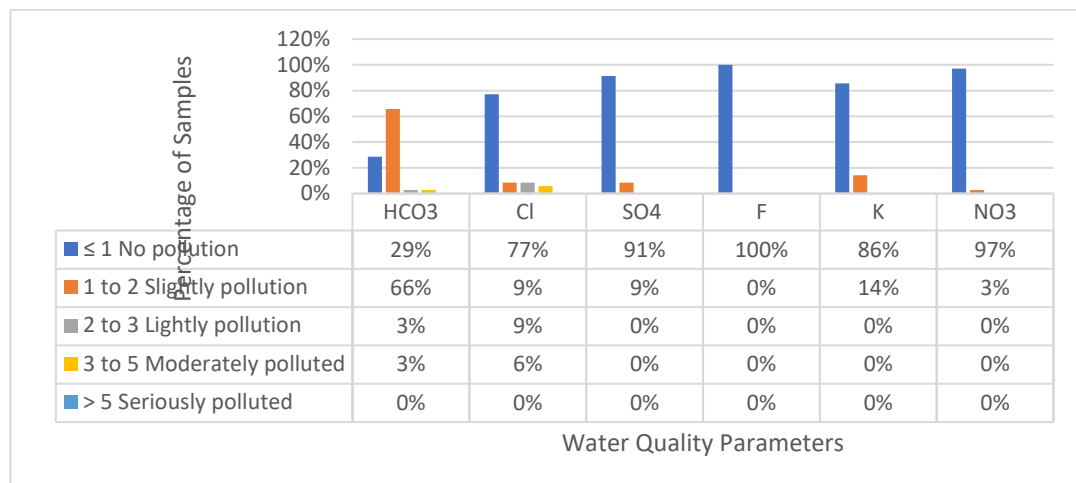


**Figure 4.6 Continued.**

#### 4.1.6 Nemerow pollution index method

Table 4.9 displays the grading scale for the Nemerow pollution index method of evaluating environmental quality. The spatial distribution map of the Nemerow pollution index has been created using the IDW technique in the ArcGIS environment. As illustrated in Figure 4.7, based on the Nemerow pollution index, most of the area has low pollution conditions. Some central-northern parts of the area have moderately polluted conditions, and only one monitoring well in the north shows high pollution. Some monitoring wells in the western part of the study area illustrated clear water conditions. Based on Figure 4.8, 20% of the samples are clear water, 63% are low pollution, 14% are moderate pollution, and only 3% are highly polluted.

**Table 4. 9 Nemerow pollution index technique for determining water quality level.**

Water quality level	PN	Pollution assessment
1	$PN \leq 1$	Clearwater
2	$1 < PN \leq 2.5$	Low Pollution
3	$2.5 < PN \leq 7$	Moderate Pollution
4	$PN > 7$	High Pollution

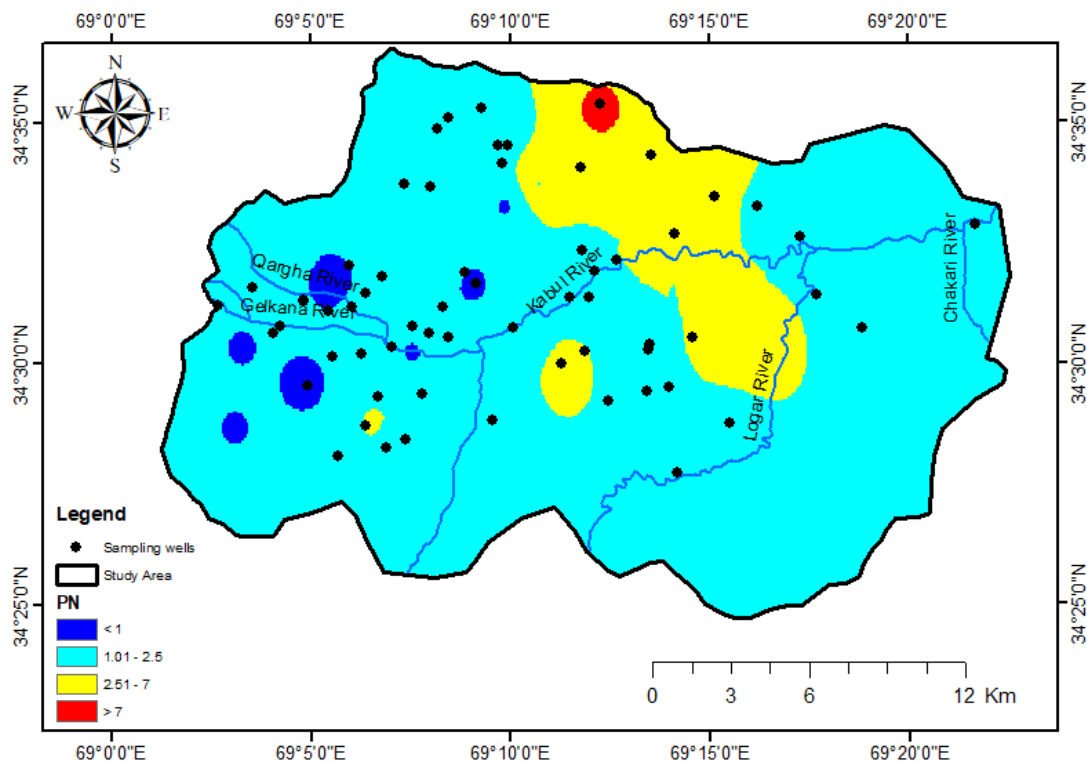


**Figure 4. 7 Spatial distribution map of Nemerow pollution index**

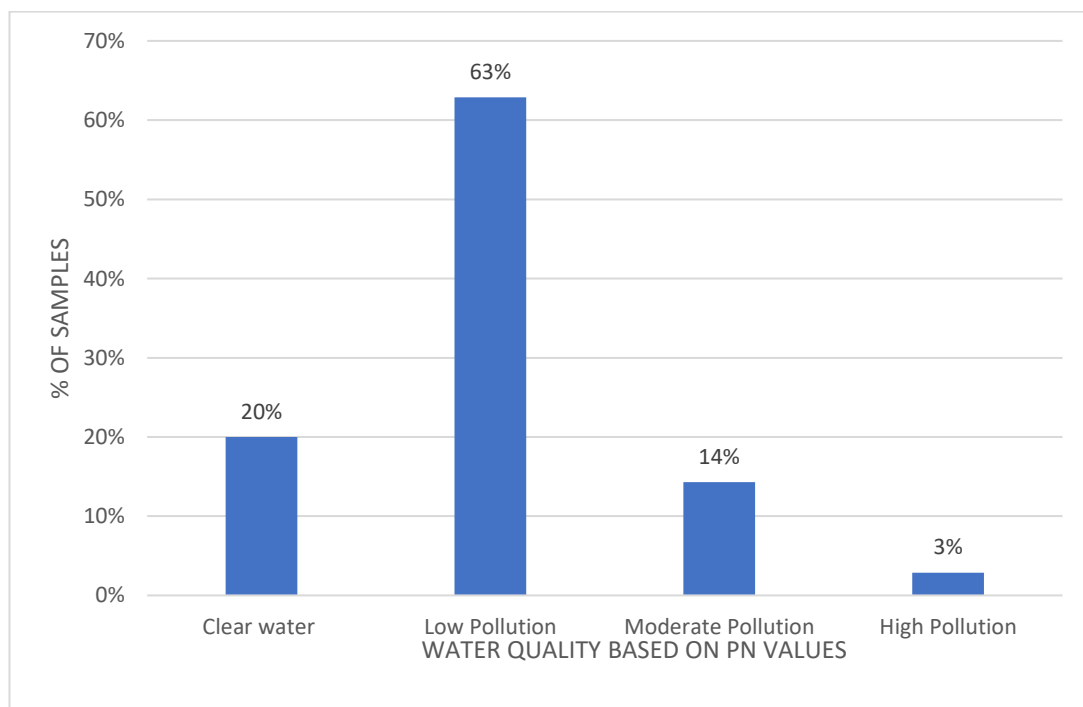


**Figure 4. 8 Percentage of samples analyzed based on Nemerow pollution index**

#### 4.1.7 Water quality index of groundwater

WQI is a concise, consistent, and dependable index for analyzing groundwater quality and determining its safety for drinking. Water has been categorized into five classes based on WQI values, including excellent water type (WQI less than 50), good water type (WQI 50-100), poor water type (WQI 100-200), very poor water type (WQI 200-300), and unsafe for drinking (WQI greater than 300). Most of the samples assessed in the Kabul basin were deemed good water. As shown in the scatter plot (Figure 4.6), based on WQI results, 42.85% of observed samples are excellent water. Also, 45.71% of tested water is good water for drinking. The poor and very poor classes of water types each have 5.71%, respectively. Table 4.10 indicates no samples of the unfit-for-drinking water type have been identified. Figure 4.9 illustrates the WQI geospatial distribution map. The high value of WQI is seen in the central (wells 9 and 12) and northern parts (wells 24,34 and 35) of the basin.

**Table 4. 10 Water quality index-based groundwater classifications**

WQI level	Water type	Samples	Percentage
< 50	Excellent water	15	42.86%
50.00 - 100	Good water	16	45.71%
100.01 - 200	Poor water	2	5.71%
200.01 - 300	Very poor water	2	5.71%
> 300	Unfit for drinking proposes	Nil	Nil
	<b>Total</b>	<b>35</b>	<b>100.00%</b>

Higher content of EC, chloride, sodium, and calcium, accompanied by sulfate and bicarbonate, indicate that the investigated location's rock–water interaction mechanism is the primary source of water quality decline. Agricultural activities may also have an impact on the sample wells in the center region of the basin. In the center regions of the Kabul basin, there are several agricultural fields around the mentioned wells. The high WQI values in this area might be attributed to the widespread usage of fertilizers combined with a lack of appropriate waste disposal facilities.

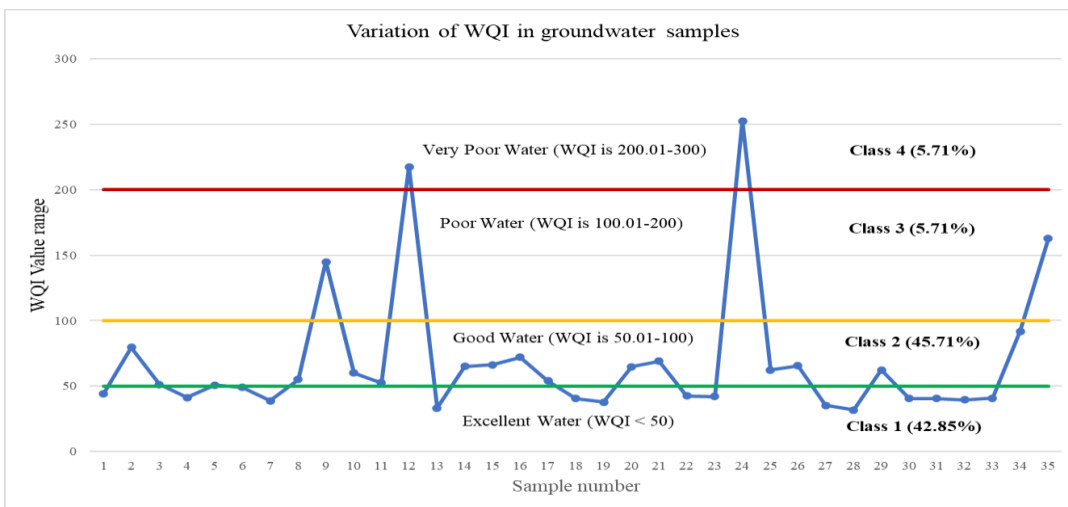


Figure 4. 9 Scatter plot showing water quality index (WQI) distribution in samples

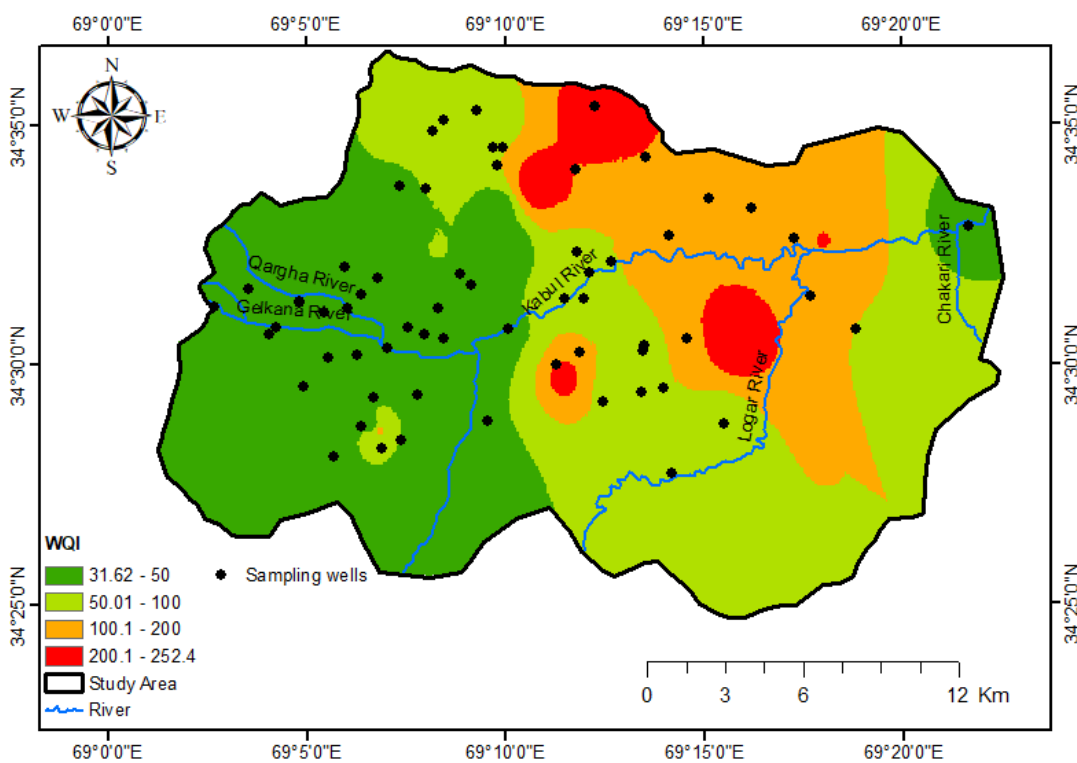


Figure 4. 10 Geospatial model of water quality index (WQI) in Kabul Basin

## 4.2 Development of ANN model

The correlation of groundwater quality data has been studied and evaluated to develop the ANN model. The water quality from the previous section obtained from laboratory test results at DTU was utilized to produce a model for water quality prediction by the ANN method. First, there is a need to know the highest correlation between different water quality parameters. Figure 4.10 shows the correlation matrix of water quality figures. The correlation matrix indicates a strong positive correlation between EC, TDS, Salinity, Sodium, and Chloride. A moderate correlation exists between EC, TDS, Salinity, Sodium, Chloride, Total Hardness, and potassium. As well as Total Hardness has a strong correlation with magnesium hardness and magnesium. Since the determination of EC, TDS, and salinity is simple and done in situ, these parameters have been selected as input for developing the ANN model. The output parameters are Sodium, Chloride, Sulphate, and potassium.

	EC	pH	TDS	Salinity	T_Hardness	Ca_Hardness	Mg_Hardness	Calcium	Magnesium	Sodium	HCO3	T-Alkalinity	Chloride	Sulphate	Phosphate	Flouride	Silica	Potassium	Nitrate
EC	1.0000																		
pH	-0.1500	1.0000																	
TDS	1.0000	-0.1511	1.0000																
Salinity	0.9997	-0.1450	0.9996	1.0000															
T_Hardness	0.5017	-0.2288	0.5057	0.4900	1.0000														
Ca_Hardness	0.4645	-0.4428	0.4694	0.4490	0.6575	1.0000													
Mg_Hardness	0.3510	-0.0108	0.3531	0.3458	0.8733	0.2071	1.0000												
Calcium	0.4645	-0.4428	0.4694	0.4490	0.6575	1.0000	0.2071	1.0000											
Magnesium	0.3510	-0.0108	0.3531	0.3458	0.8733	0.2071	1.0000	0.2071	1.0000										
Sodium	0.9452	-0.0609	0.9440	0.9474	0.3833	0.2198	0.3556	0.2198	0.3556	1.0000									
HCO3	0.1171	-0.0326	0.1175	0.1111	0.2257	-0.0835	0.3471	-0.0835	0.3471	0.2934	1.0000								
T-Alkalinity	0.1171	-0.0326	0.1175	0.1111	0.2257	-0.0835	0.3471	-0.0835	0.3471	0.2934	1.0000	1.0000							
Chloride	0.9845	-0.1539	0.9838	0.9859	0.4407	0.4337	0.2918	0.4337	0.2918	0.9128	0.0003	0.0003	1.0000						
Sulphate	0.7717	-0.0924	0.7731	0.7622	0.5518	0.4712	0.4118	0.4712	0.4118	0.7213	0.1395	0.1395	0.7531	1.0000					
Phosphate	0.3728	0.0168	0.3740	0.3688	0.3172	0.0164	0.4013	0.0164	0.4013	0.5503	0.6458	0.6458	0.2308	0.3320	1.0000				
Flouride	-0.1540	0.3053	-0.1551	-0.1501	-0.3543	-0.3280	-0.2480	-0.3280	-0.2480	-0.0228	-0.0370	-0.0370	-0.1872	-0.1045	0.1853	1.0000			
Silica	0.0111	0.1171	0.0099	0.0103	-0.0483	-0.2594	0.1051	-0.2594	0.1051	0.1080	0.4224	0.4224	-0.0216	0.1760	0.1116	0.3947	1.0000		
Potassium	0.5769	-0.0085	0.5776	0.5743	0.3638	0.1100	0.4012	0.1100	0.4012	0.7217	0.5623	0.5623	0.4531	0.4663	0.9339	0.2057	0.1158	1.0000	
Nitrate	-0.0481	-0.2927	-0.0480	-0.0499	0.0448	0.1564	-0.0429	0.1564	-0.0429	-0.0350	0.1497	0.1497	-0.0968	-0.0698	0.1309	0.2029	0.0812	0.2207	1.0000

Figure 4. 11 Correlation matrix of water quality data

### 4.2.1 Network Architecture

In the ANN model, Neural Network/Data Manager (nntool) was selected based on its excellent accuracy in similar function approximation, which contains many input data sets. Neural networks are made of three different layers: the input layer, the hidden layer, and the output layer. Their water quality parameter (i.e., EC, TDS, and Salinity), which can be measured easily in situ using portable water quality test devices, has been used as an input layer. The model has been developed separately for each output target (i.e., Na, Cl, SO<sub>4</sub>, K). Out of 35 water samples, 25 were used for training and testing the model, and ten were used for prediction purposes and accuracy assessment. The model used in this research will be trained using ten hidden neurons. After observing the regression terms and mean square error (MSE) terms, the final network structure (3-10-1) was selected. Figure 4.12 shows a typical structure of the ANN model for the current study.

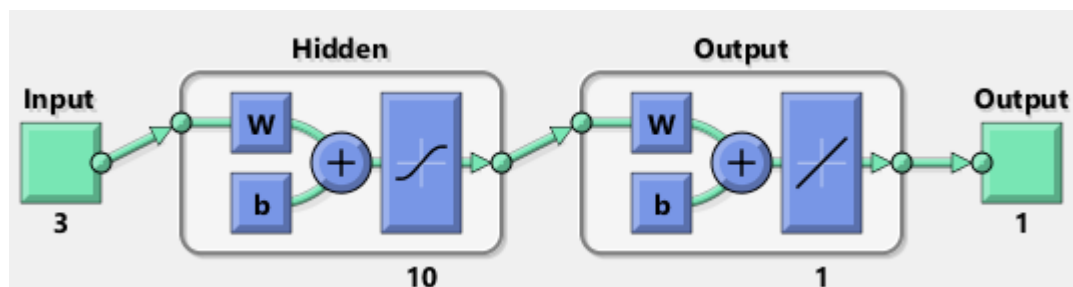


Figure 4. 12 Typical structure of ANN model

### 4.2.2 Performance of ANN model

Here is an illustration of the numerous phases taken in constructing the model. An ANN model is created using the MATLAB R2016a program, version 9.0.0.341360. The program is simple to use and has a wide range of uses.

### 4.2.3 Inputs

Salinity, TDS, and EC are chosen as the input data. A 3 x 25 matrix makes up the complete input data set. It has three parameters drawn from 25 sample sites. The input data is copied from the Excel sheet database. A new variable was created in the MATLAB workspace and renamed "input." The copied data from the Excel sheet is pasted into a variable (input) in MATLAB. The pasted data has been transposed in the MATLAB environment for further processing. Each input matrix row represents a water quality indicator of the study area.

To justify the model's validity, a new variable has been created in the MATLAB workspace named "sample." The remaining data from the database (10 remaining samples out of 35 samples) of groundwater quality data has been copied from the Excel sheet and pasted into this new variable (sample) in the MATLAB environment. After training the model, the sample data was inputted for the proposed



simulation. The values of the simulation and the precise values of the lab report's data should be equal, or their differences should be tiny.

#### 4.2.4 Targeted outputs

The Sodium, Chloride, sulfate, and potassium values of 25 locations, which are found from water quality analysis, are copied from Excel sheet data and pasted in newly created variables in MATLAB workspace named “Na\_Target, Cl\_Target, Sulfate\_Target, and Potassium\_Target.” Each newly focused variable is represented as a 1 x 25 matrix. The ANN model must be trained to produce this new variable, which is the desired outcome.

#### 4.2.5 Neural Network Tool

Neural Network Tool (NNT) provides tools, functions, and applications for building, practicing, simulating, and visualizing neural networks. It can carry out time-series prediction, dimensionality reduction, clustering, regression, classification, and dynamic system modeling and control. An input-output network with two layers and several types of networks is solved using NNT. The neural network maps between the numerical input dataset and numerical targets in fitting problems. Mean square error and regression analysis are used by NNT to assess the performance of neural networks. After adding input, target, and sample data in the workspace, by writing *nntool* command in the command window, the Neural network/data manager (nntool) page will appear. By selecting the import option, the input, sample, and target data will be imported into the Neural Network page by selecting their correct path. A new network can be created on the Neural Network page. The new network can be renamed based on desired outputs (i.e., Na, Cl, Sulfate, Potassium, TH).

#### 4.2.6 Network specifications

By renaming the network, the process will proceed with selecting the network type. All network types are selected for this modeling based on the “*Feed-Forward Backup*” type. After selecting input and output data, the training function will be selected. Mainly, the “*TRAINLM*” function is used. The adoption learning function which is mainly used is “*LEARNGDM*.” The adopted performance function is *Mean Square Error* “*MSE*.” The number of layers is typically 2, and properties were selected for *layer 1*. The number of neurons and transfer functions varies based on the desired output variable, illustrated in Table 4.11.

**Table 4. 11 Illustrate the summary of each network specification.**

<b>target variable</b>	<b>Network type</b>	<b>No. of neuron</b>	<b>Transfer Function</b>	<b>R</b>
<b>Sodium</b>	Feed-forward backup	10	LOGSIG	0.996
<b>Chloride</b>	Feed-forward backup	10	LOGSIG	0.999
<b>Sulphate</b>	Feed-forward backup	10	PURELIN	0.927
<b>Potassium</b>	Feed-forward backup	10	LOGSIG	0.955
<b>Total Hardness</b>	Feed-forward backup	20	TANSIG	0.92

#### 4.2.7 Train network

The network is trained to match the input and targets. Except for “*max fail = 1000*”, the network has been trained using the default training parameter settings. When generalization reaches a plateau, training is automatically terminated. Mean Squared Error is the average squared difference between input and targets. The MSE should be lower. Zero denotes the absence of inaccuracy. R values measure the correlation between production and objectives. An R-value of 1 indicates that the NNT output and the desired values are most closely related. About 70% of the samples were used in the training process. The MSE and R values are  $827.04665e-0$  and  $9.966e-1$ , respectively. With a low MSE and R-value close to 1, training has demonstrated the best results. Numerous training trials have been conducted while modifying the transfer function and number of neurons. The best result for each parameter was found in the last trials. With 1000 epochs, the training was generalized. This allows for determining the number of iterations, time required for convergence, performance status, validation checks, gradients, etc. The performance plot and training status for Na modeling are presented in Figures 4.13 and 4.14.

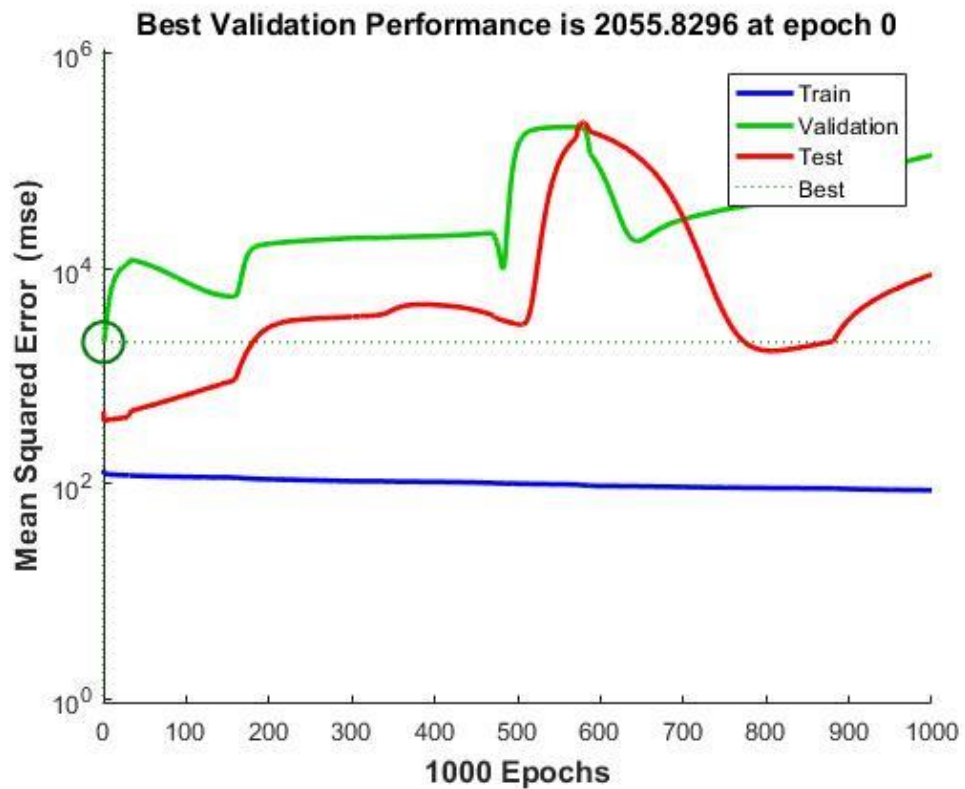


Figure 4. 13 Performance plot of the network for modeling of Na.

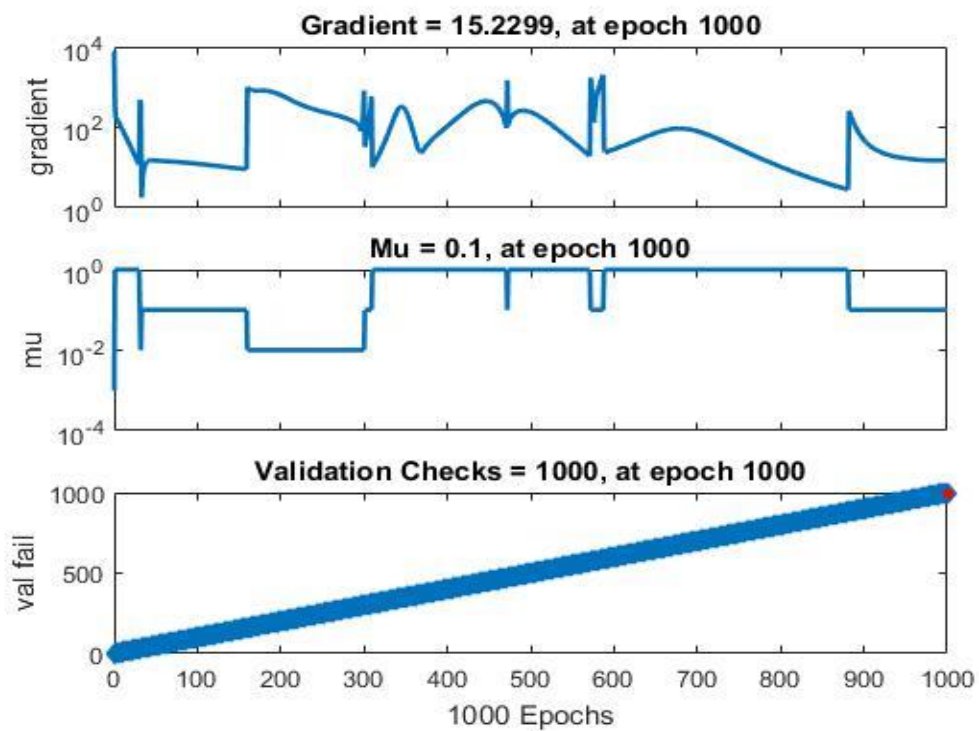


Figure 4. 14 Training status of the network for modelling of Na

The regression value R gives a measure of relationship between training output and targeted output. The R-value was 0.70 in early iterations, then reached 0.80 and 0.996. At the end of 1000 epochs, the R-value has a maximum of closer to 1. This shows the presence of a high correlation between output and targeted values. The various R values are illustrated in Figure 4.15.

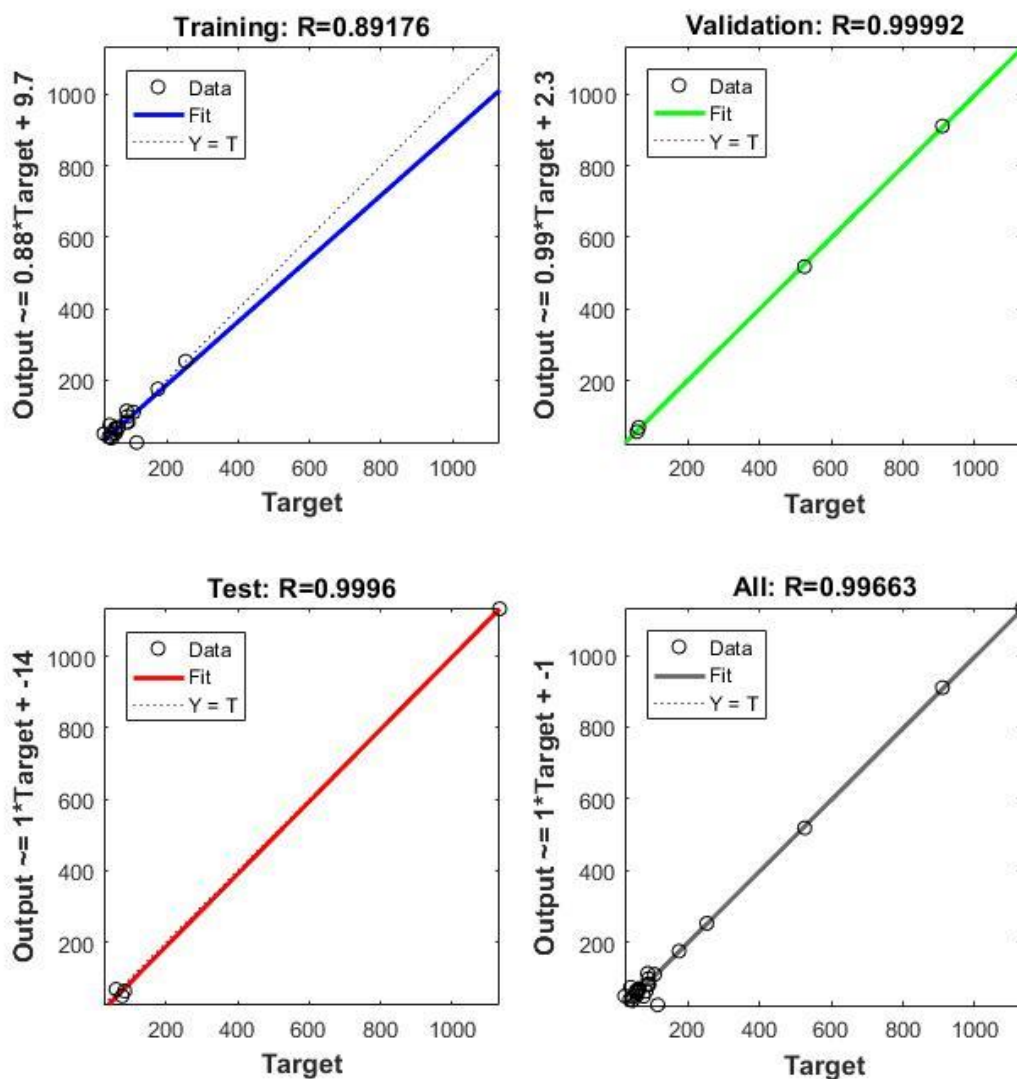
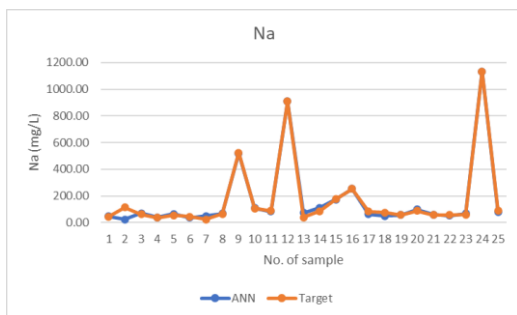
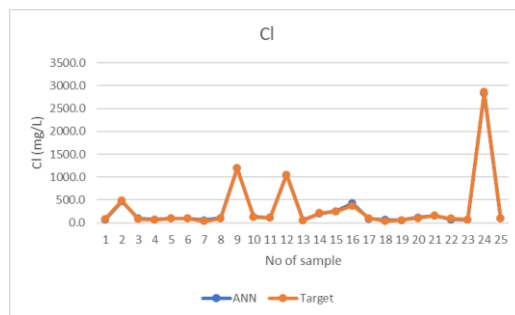


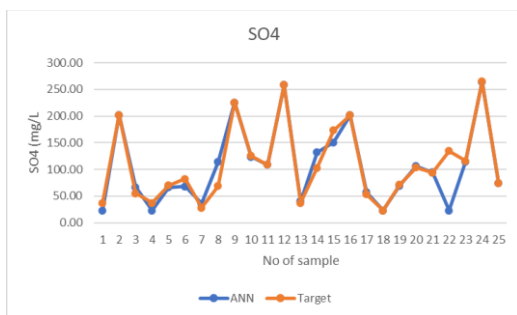
Figure 4. 15 Regression plot of the training network for modelling of Na



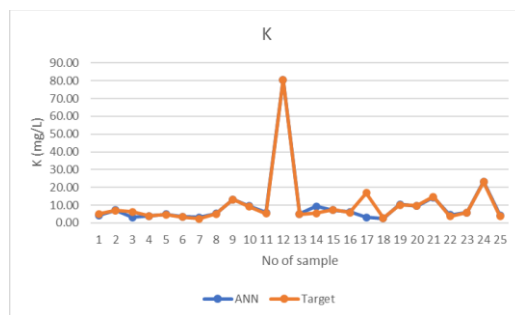
a. Sodium



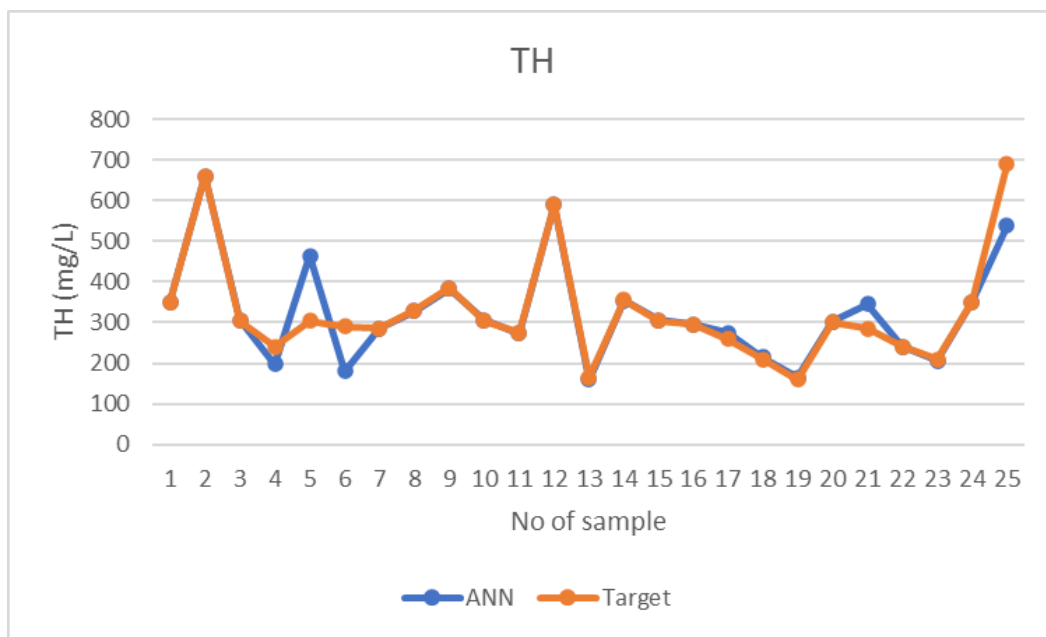
b. Chloride



c. Sulfate



d. Potassium



e. Total Hardness

**Figure 4. 16 Comparative illustrations of output figures from ANN model and target data (exact water quality data)**

The results of the training of neural networks are satisfactory, and the results are saved. Simulink diagrams are formed to give different inputs and get respective outputs to apply the trained network to meet its purpose. The display option is preferred to display the Na value as output. The Simulink library browser option of the network is chosen to formulate the required Simulink diagram. The Simulink is saved as mdl file of MATLAB. The various inputs are given in the constant value box of the source block parameter window. The input values are saved, and the program is run. The output value is shown in the display box of the Simulink window. Figure 4.16 illustrates the exact water quality values used as target data and the ANN output values for all parameters that have been modelled.

#### **4.2.8 Validation of ANN models**

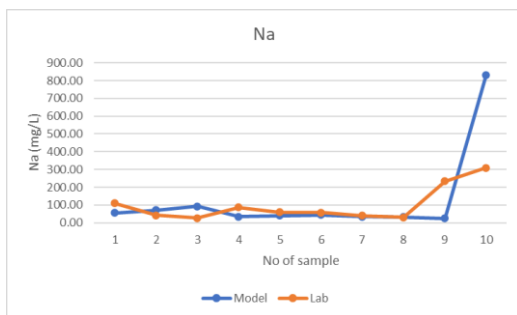
The model's validity is checked with the groundwater quality test results, which have been tested in the DTU Department of Environmental Engineering. Out of 35 tested groundwater samples, only 25 were used to train the models, and ten remaining samples were randomly used to validate the model. The inputs are named as sample and fed into the ANN model. Na content of the sampling points are determined from ANN model. Comparisons are made between the output from the ANN model and the Na content of the observations from the DTU lab results. It mentions the variance's proportion. For a few other factors, this process is performed as well. The DTU lab findings for water quality and the ANN output are used to assess the model's validity.

The results of water samples collected from ten different places and analysed in a water lab for water quality parameters were compared to ANN findings to investigate the model's practical applicability. A comparison of water quality from the lab test results and simulation from the ANN model is illustrated in Figure 4.17.

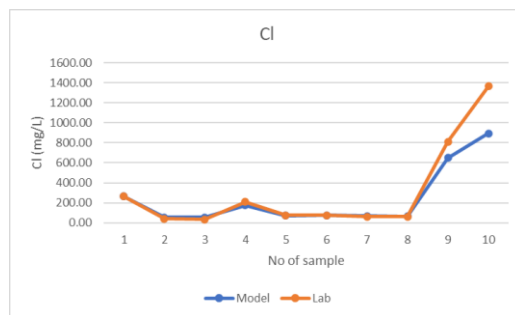
Groundwater quality test data from DTU water lab reports are used to verify the model's accuracy. Ten water samples were chosen randomly, and the results were utilized to simulate the water quality characteristics.

The validation using lab findings is shown here for the ANN model created for the autumn season. By utilizing an ANN model, it is possible to determine the presence of water quality characteristics at the sample locations. Comparing ANN findings with the water quality content in the groundwater at certain sample places. Table 4.12 offers an overview of the validation outcomes.

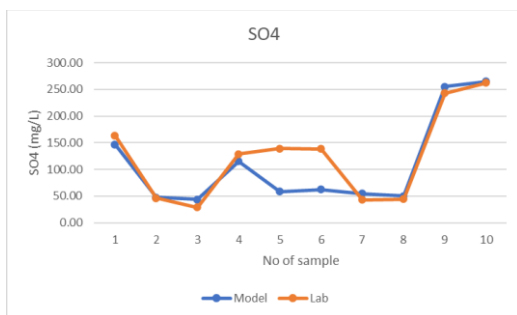
The findings of the feasibility test are used to determine if the ANN model application is practically feasible. Since the samples for the feasibility test were gathered in the autumn, the ANN model created for that time of year was utilized to validate the findings. Table 4.13 provides a summary of the validation outcomes.



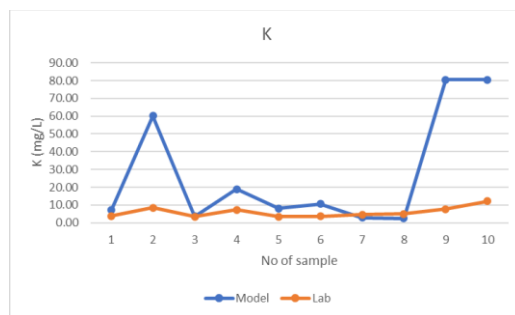
a. Sodium



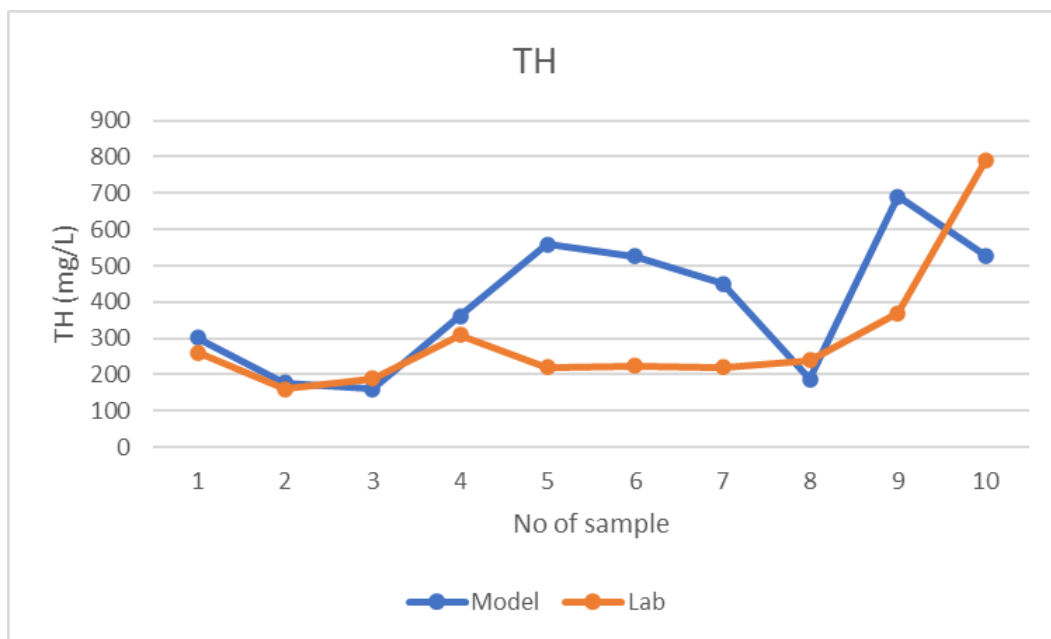
b. Chloride



c. Sulfate



d. Potassium



e. Total Hardness

**Figure 4. 17 Comparative illustrations of simulated figures by ANN model and actual data from lab**

The results of the ANN model for simulating sodium concentration in groundwater based on input data (EC, TDS, Salinity) have an average variance of 11.53%. The average variance for chloride and sulfate is 3.83% and -3.41%, respectively. However, the average variance for potassium and total hardness is 259.6% and 45.25%, respectively. These differences in mean percentage of variances show the models' accuracy and suitability. Based on these percentages, one can conclude that the model is very suitable for simulating the concentrations of sodium, chloride, and sulfate in groundwater with the suggested inputs (EC, TDS, and Salinity). However, looking at Figure 4.18 d and e, it can be seen that the output result of potassium quality parameters and total hardness after several trainings of the model seem to be excellent. But, looking at Table 4.10, it can be seen that the model's output does not match the real values from the water laboratory. Therefore, the model is unsuitable for predicting potassium and total hardness in groundwater with the same inputs. It can be said that the parameters of potassium and total hardness might need more correlated inputs for better results.

#### **4.2.9 Summary and applications of ANN**

A new location's groundwater quality often requires extensive research, which takes time and money. However, creating an expression to determine the value of water quality parameters before analyzing the water in a water lab is pretty challenging. Due to the significant nonlinearity of the pertinent parameters, it is quite tricky. Therefore, a method using artificial intelligence is presented in this study to derive the values of water quality parameters from these nonlinear and naturally drastic regulating factors. An artificial neural network is deemed suitable for this based on its underlying concepts.

The following is the procedure for utilizing the ANN software. A well is chosen from the research area's base map. Groundwater quality metrics such as EC, TDS, and salinity are in-situ measured using portable instruments. As a result, the generated ANN model is fed the input's arriving values. The result is a single number representing the target parameters' value in mg/L.



Table 4. 12 Validation of ANN output results with lab test results

No. of sample	Coordinate				Input parameters										Target and model outputs											
	Lat	Long	Date	EC	TDS	Salinity	Sodium			Chloride			Sulphate			Potassium			Total Hardness							
							ANN	Target	% of Variance	ANN	Target	% of Variance	ANN	Target	% of Variance	ANN	Target	% of Variance	ANN	Target	% of Variance					
1	34.54224	69.16893	16/11/2020	946	472	0.41	48.434	45.570	6.284	74.768	90.000	-16.924	22.874	37.296	-38.670	4.249	5.140	-17.339	349.823	350.000	-0.051					
2	34.55993	69.19006	16/11/2020	2560	1285	1.28	100.000	115.380	-13.330	471.166	490.000	-3.844	202.436	202.590	-0.076	7.146	7.070	1.072	660.049	660.000	0.007					
3	34.46848	69.13362	17/11/2020	1169	581	0.53	70.513	63.380	11.254	93.759	80.000	17.199	66.808	55.321	20.764	3.143	6.280	-49.958	306.223	305.000	0.401					
4	34.4601	69.15203	17/11/2020	888	443	0.38	39.765	37.530	5.956	70.832	65.000	8.973	22.872	37.427	-38.889	3.971	3.940	0.797	198.103	240.000	-17.457					
5	34.51113	69.16297	17/11/2020	1199	598	0.54	64.329	55.290	16.348	97.945	100.000	-2.055	66.169	70.374	-5.975	4.918	4.640	5.986	463.696	305.000	52.031					
6	34.50964	69.1409	17/11/2020	1174	580	0.52	37.258	45.040	-17.277	95.703	100.000	-4.297	68.181	82.616	-17.473	3.585	3.340	7.328	179.499	290.000	-38.104					
7	34.51932	69.10053	17/11/2020	730	364	0.29	30.000	23.600	27.119	62.595	40.000	56.486	35.858	28.527	25.700	3.072	2.410	27.489	284.440	285.000	-0.197					
8	34.49096	69.13519	17/11/2020	1281	638	0.59	68.452	64.740	5.734	106.629	100.000	6.629	114.275	68.707	66.322	5.217	5.160	1.110	328.260	330.000	-0.527					
9	34.49509	69.19124	18/11/2020	6890	3430	3.69	518.643	525.600	-1.324	1194.936	1195.000	-0.005	225.679	225.680	0.000	13.232	13.200	0.244	383.270	385.000	-0.449					
10	34.49109	69.21333	18/11/2020	1473	729	0.69	109.974	106.840	2.933	134.635	125.000	7.708	123.944	125.780	-1.460	9.546	9.220	3.532	305.280	305.000	0.092					
11	34.47908	69.25838	18/11/2020	1293	642	0.59	83.168	87.500	-4.951	109.006	115.000	-5.212	108.968	109.210	-0.222	5.914	5.290	11.799	273.752	275.000	-0.454					
12	34.50778	69.26444	18/11/2020	8810	4390	4.82	910.236	910.100	0.015	1054.974	1055.000	-0.003	258.585	258.580	0.002	80.500	80.500	0.000	590.002	590.000	0.000					
13	34.55389	69.16439	23/11/2020	588	291	0.22	50.000	40.100	24.688	56.502	55.000	2.732	40.864	37.620	8.622	5.058	4.850	4.294	160.551	165.000	-2.697					
14	34.53721	69.19416	24/11/2020	1779	879	0.85	113.117	87.140	29.811	198.810	220.000	-9.632	131.845	102.790	28.267	9.319	5.500	69.430	354.682	355.000	-0.090					
15	34.54361	69.285	24/11/2020	1980	985	0.96	175.018	175.100	-0.047	254.846	245.000	4.019	150.950	173.110	-12.801	7.193	7.500	-4.099	305.176	305.000	0.058					
16	34.54279	69.30001	24/11/2020	2450	1218	1.21	252.487	252.500	-0.005	428.359	375.000	14.229	201.738	201.590	0.073	6.250	5.800	7.762	295.017	295.000	0.006					
17	34.54806	69.36139	24/11/2020	1154	573	0.52	62.537	82.880	-24.545	92.436	105.000	-11.966	57.002	53.491	6.564	3.112	16.810	-81.489	274.440	260.000	5.554					
18	34.4775	69.05173	25/11/2020	766	381	0.31	48.886	75.710	-35.429	64.260	40.000	60.649	23.291	22.872	1.834	2.658	2.720	-2.264	214.375	210.000	2.083					
19	34.5275	69.15167	25/11/2020	610	304	0.23	58.474	58.910	-0.740	57.411	60.000	-4.316	69.336	71.245	-2.679	10.441	10.110	3.274	164.200	160.000	2.625					
20	34.54	69.13806	25/11/2020	1368	680	0.63	97.846	89.430	9.410	119.351	105.000	13.668	106.505	103.900	2.507	9.508	9.840	-3.372	302.196	300.000	0.732					
21	34.56109	69.12213	25/11/2020	1572	782	0.74	60.440	57.990	4.224	153.651	160.000	-3.968	94.476	94.044	0.460	14.381	14.690	-2.101	345.936	285.000	21.381					
22	34.58139	69.13582	25/11/2020	953	474	0.41	51.475	56.620	-9.086	75.518	100.000	-24.482	22.878	134.930	-83.044	4.606	3.670	25.497	239.870	240.000	-0.054					
23	34.58401	69.16439	25/11/2020	750	371	0.3	67.116	59.140	13.487	63.487	75.000	-15.350	114.789	116.130	-1.155	5.853	5.860	-0.116	206.497	210.000	-1.668					
24	34.58699	69.20369	25/11/2020	15060	7450	8.55	1132.482	1132.700	-0.019	2836.868	2865.000	-0.982	264.601	264.760	-0.060	23.209	23.100	0.472	350.001	350.000	0.000					
25	34.47873	69.11102	26/11/2020	1204	602	0.55	81.417	91.180	-10.707	97.598	100.000	-2.402	74.186	74.526	-0.457	4.299	3.820	12.546	537.631	690.000	-22.082					
							avg		1.592		avg	3.474		avg	-1.674		avg	0.876		avg	0.046					

**Table 4. 13 Validation of ANN model simulation results with lab test results**

No. of sample	Coordinates				Sample for input				Predicted values and lab results												
	Lat	Long	Date	EC	TDS	Salinity	Sodium			Chloride			Sulphate			Potassium			Total Hardness		
							Model	Lab	% of Variance	Model	Lab	% of Variance	Model	Lab	% of Variance	Model	Lab	% of Variance	Model	Lab	% of Variance
26	34.47714	69.11356	26/11/2020	1995	1000	0.97	54.920	109.090	-49.656	265.961	265.000	0.363	147.279	163.850	-10.114	7.373	3.840	92.013	301.522	260.000	15.970
27	34.49222	69.08167	26/11/2020	619	309	0.23	71.316	41.720	70.940	56.207	40.000	40.517	47.720	46.334	2.990	60.103	8.460	610.439	178.005	160.000	11.253
28	34.52585	69.09383	28/11/2020	541	270	0.19	92.266	27.280	238.218	52.842	35.000	50.976	44.001	28.963	51.923	3.577	3.370	6.151	160.033	190.000	-15.772
29	34.50352	69.2185	28/11/2020	1594	799	0.75	34.058	87.680	-61.157	175.518	210.000	-16.420	115.354	128.760	-10.412	19.017	7.250	162.301	361.201	310.000	16.516
30	34.50679	69.32663	29/11/2020	897	450	0.38	40.118	60.010	-33.148	73.467	75.000	-2.044	58.879	139.450	-57.778	8.146	3.530	130.769	558.873	220.000	154.033
31	34.50583	69.34092	29/11/2020	903	452	0.38	44.730	57.980	-22.853	74.524	75.000	-0.635	62.188	138.770	-55.187	10.634	3.640	192.141	526.120	225.000	133.831
32	34.50361	69.12556	26/11/2020	805	405	0.33	35.327	39.660	-10.926	67.388	60.000	12.314	54.635	43.390	25.916	2.935	4.690	-37.424	451.380	220.000	105.173
33	34.5052	69.05463	01/12/2020	809	405	0.34	32.336	31.590	2.360	64.695	60.000	7.825	49.928	44.393	12.468	2.455	5.000	-50.903	187.688	240.000	-21.797
34	34.56214	69.17902	09/10/2020	4200	2080	2.18	24.169	234.100	-89.676	648.132	810.000	-19.984	255.572	242.780	5.269	80.421	7.800	931.043	690.000	370.000	86.486
35	34.56207	69.18013	09/10/2020	8790	4420	4.73	531.000	310.100	71.235	893.128	1365.000	-34.569	264.692	262.600	0.797	80.500	12.200	559.836	528.188	790.000	-33.141
							avg	avg	11.534	avg	avg	3.834	avg	avg	-3.413	avg	avg	259.637	avg	avg	45.255

### 4.3 Seasonal water quality analysis

The findings of the groundwater quality data subsequent processing and assessment are illustrated here. In the first stage, groundwater quality in the study region was evaluated using descriptive statistics and compared with drinking water quality regulations. Additionally, statistical studies such as the "*paired-samples t-test*" and "*Wilcoxon signed-rank test*" are available to evaluate the significance of seasonal variations in groundwater quality in the research region. Lastly, geospatial maps illustrating the regional distribution of groundwater quality characteristics with concentrations more than WHO/ANSA drinking water guidelines exhibit statistically significant seasonal changes. One parameter has no concentration exceeding WHO/ANSA guidelines and does not exhibit substantial changes. Furthermore, change maps demonstrating seasonal changes in groundwater quality metrics are shown in a geographically dispersed format.

#### 4.3.1 Generic evaluation of the quality of groundwater

A summarized output of statistical evaluation added a comparison of water quality with drinking water quality regulations represented in Tables 4.14 and 4.15. According to the findings, the Kabul basin's groundwater temperature (T) varied from 12.2 to 23.1 degrees Celsius in August and September and from 12 to 27 degrees Celsius in March and May. The pH ranges for all samples were 6.96–8.21 in the dry period and 7.08–8.57 in the wet period, indicating neutral to mild alkaline waters within permitted drinking water standards. The high EC values for most samples and the comparatively significant standard deviations are evident. According to WHO and ANSA, the maximum permissible concentration of EC in drinking water is 1500  $\mu\text{S}/\text{cm}$  (ANSA, 2013; WHO, 2011). More than 40% of sampling points have EC higher than regulations limits in both seasons.

TDS and TH values were statistically similar to EC. The TDS in sampling points ranged between 241 to 6354 mg/l in the dry period and 353 to 5807 mg/l in the wet period. The mean content of TDS is 1240 and 1205 mg/l for dry and wet seasons, respectively. More than 20% of the samples in both seasons exceeded the required TDS limits (1500 mg/l suggested by ANSA) in drinking water. Total hardness in April-May varies from 28 to 2700 mg/l with a mean of 847 and a standard deviation of 567 mg/l. From August to September, it varies from 50 to 3580 with a mean value of 772 and a standard deviation of 745 mg/l. The maximum overall allowed total hardness suggested by WHO and ANSA is 500 mg/l. More than 50% of samples in the dry season and more than 70% in the wet season exceed the guidelines values.

**Table 4. 14 Results of sample investigations statistically summarized and compared to drinking water quality requirements for Aug & Sep 2017 (Dry season)**

Water quality parameters	Unit	Regulations for drinking water quality		Wells (n = 53)				Samples exceeding WHO or ANSA limits	
		WHO	ANSA	Min	Mean	Max	Standard Deviation	No. of Sample	% Of Sample
<b>T</b>	C	12 to 25	12 to 25	12.20	17.24	23.10	2.09	Nil	Nil
<b>pH</b>	-	6.5 - 8.5	6.5 - 8.5	6.96	7.54	8.21	0.27	Nil	Nil
<b>EC</b>	μS/cm	1500	1500	364.0	1888.11	9600.0	1940.49	22.00	41.51
<b>TDS</b>	mg/l	1000	1500	241.7	1240.0	6353.6	1316.31	22.00	41.51
<b>TH</b>	mg/l	500	500	50.00	771.74	3580.0	744.57	27.00	50.94
<b>Ca</b>	mg/l	75	75	16.00	117.56	505.00	99.77	31.00	58.49
<b>Mg</b>	mg/l	30	30	13.10	285.64	1977.9	360.72	48.00	90.57
<b>Na</b>	mg/l	200	200	0.00	123.62	1400.0	247.63	7.00	13.21
<b>HCO<sub>3</sub></b>	mg/l	600	600	150.0	388.68	1600.0	217.29	4.00	7.55
<b>F</b>	mg/l	1.5	1.5	0.00	0.49	1.21	0.40	0.00	0.00
<b>Cl</b>	mg/l	NA	250	0.000	0.011	0.050	0.014	0.000	0.00
<b>NO<sub>3</sub></b>	mg/l	50	50	0.00	2.42	7.50	1.86	0.00	0.00
<b>SO<sub>4</sub></b>	mg/l	250	250	5.00	105.51	1000.0	134.16	2.00	3.77
<b>PO<sub>4</sub></b>	mg/l	NA	6	0.00	0.25	2.12	0.32	0.00	0.00
<b>K</b>	mg/l	10	10	0.90	17.73	146.20	29.20	16.00	30.19
<b>Al</b>	mg/l	0.2	0.2	0.000	0.035	0.214	0.062	6.000	11.11
<b>Mn</b>	mg/l	NA	0.3	0.000	0.724	11.500	1.554	30.000	55.56
<b>Fe</b>	mg/l	0.3	0.3	0.000	0.057	0.610	0.112	3.000	5.56
<b>CN</b>	mg/l	NA	0.05	0.000	0.012	0.270	0.039	3.000	5.56
<b>Cu</b>	mg/l	2	2	0.000	0.311	6.710	0.990	1.000	1.85

The calcium concentration in the wet season varies from 8 to 721 mg/l, with 73% of samples greater than WHO and ANSA limitations (>75mg/l). The mean concentration of Ca in the wet season is 193, and its standard deviation is 170 mg/l. It ranges from 16 to 505 mg/l in the dry season, with 58% of samples greater than the

guideline value. In the autumn, the mean value of Ca is 118, and the standard deviation is 100 mg/l. In the wet season, magnesium concentrations range from 4.8 to 589 mg/l, with a mean of 118.2 and a standard deviation of 117. About 70% of samples exceed the guidelines for drinking water in the wet season. The minimum Mg concentration in the dry season is 13, and the maximum is 1977 mg/l, with a mean of 286 and a standard deviation of 360 mg/l. About 90% of samples exceeded WHO and ANSA standards for drinking water (> 30 mg/l). In the wet season, sodium concentrations vary from 25 to 1800 mg/l, with a mean of 173 mg/l. Meanwhile, in the dry season, it ranges from 0 to 1400 mg/l, with a mean of 123 mg/l. About 16% of samples in the spring and around 13% in the autumn exceed the drinking water guidelines requirements.

Manganese is the other ion concentration with a high concentration in both seasons. In the wet season, about 75% of samples and about 55% in the dry season exceed the guideline. Potassium concentration in both seasons has exceeded the guideline with more than 30% sampling points. Fluoride, chloride, nitrate, and phosphate are the parameters with concentrations less than the maximum limits of WHO and ANSA in the autumn. In the spring, fluoride and chloride concentrations exceed the guidelines in some low percentages. Bicarbonate, sulfate, aluminum, iron, cyanide, and copper are the parameters in which less than 10% of samples have a concentration higher than drinking water quality standards.

Eventually, the groundwater in the Kabul basin is of poor quality compared to existing guidelines. Most qualitative indicators, such as EC, TDS, TH, Ca, Mg, Na, Mn, and K, are the parameters that exceed the suggested ranges of guidelines for drinking water. On the other hand, from descriptive statistics, the concentration of most qualitative parameters in the spring is higher than in the autumn. This evaluation is discussed later in this study.

#### 4.3.2 Seasonal variations in the groundwater quality

At the inception stage, the "*K-S test*" was employed to investigate the statistical distribution of variances. For each quality metric across data sets, the difference in values between spring and fall was stated as follows:

$$d_i = x_{1i} - x_{2i} \dots\dots\dots (4. 5)$$

Where *i* indicates the groundwater quality indicator,

$x_{1i}$  shows metrics from the dry period (measurements of Aug - Sep 2017)

$x_{2i}$  illustrates metrics of the wet period (measurements of Mar-May 2018)

The null ( $H_0$ ) and alternative ( $H_s$ ) hypotheses are developed as follows to figure out if the changes are normally distributed:

$H_0$ : The observed data set has a normal distribution.

$H_s$ : The observed data set has no normal distribution.

**Table 4. 15 Results of sample investigations statistically summarized and compared to drinking water quality requirements for Mar-May 2018 (Wet season)**

Water quality parameters	Unit	Regulations for drinking water quality		Wells (n = 53)				Samples exceeding WHO or ANSA limits	
		WHO	National	Min	Mean	Max	Standard Deviation	No. of Sample	% Of Sample
<b>T</b>	C	12 to 25	12 to 25	12.00	17.68	27.00	2.55	Nil	Nil
<b>pH</b>	-	6.5 - 8.5	6.5 - 8.5	7.08	7.58	8.57	0.30	Nil	Nil
<b>EC</b>	μS/cm	1500	1500	380.	1817.	8710.0	1552.47	25.00	47.17
<b>TDS</b>	mg/l	1000	1500	253.	1205.6	5807.5	1042.71	11.00	20.75
<b>TH</b>	mg/l	500	500	28.80	847.34	2700.0	566.93	38.00	71.70
<b>Ca</b>	mg/l	75	75	8.02	192.82	721.40	170.62	39.00	73.58
<b>Mg</b>	mg/l	30	30	4.80	118.02	584.70	116.59	37.00	69.81
<b>Na</b>	mg/l	200	200	25.00	173.87	1800.0	272.14	9.00	16.98
<b>HCO<sub>3</sub></b>	mg/l	600	600	125.0	368.40	775.00	134.02	2.00	3.77
<b>F</b>	mg/l	1.5	1.5	0.020	0.751	4.010	0.727	3.00	5.66
<b>Cl</b>	mg/l	NA	250	-0.020	20.674	331.00	51.530	1.000	1.89
<b>NO<sub>3</sub></b>	mg/l	50	50	-2.60	2.69	8.70	2.22	0.00	0.00
<b>SO<sub>4</sub></b>	mg/l	250	250	7.00	165.64	1900.0	339.02	3.00	5.66
<b>PO<sub>4</sub></b>	mg/l	NA	6	0.05	0.32	4.05	0.56	0.00	0.00
<b>K</b>	mg/l	10	10	0.30	17.43	142.80	26.42	17.00	32.08
<b>Al</b>	mg/l	0.2	0.2	-0.020	0.026	0.152	0.045	0.000	0.00
<b>Mn</b>	mg/l	NA	0.3	-0.500	6.618	266.00	36.581	40.000	75.47
<b>Fe</b>	mg/l	0.3	0.3	0.000	0.114	1.160	0.221	5.000	9.43
<b>CN</b>	mg/l	NA	0.05	0.000	0.008	0.130	0.018	1.000	1.89
<b>Cu</b>	mg/l	2	2	0.00	0.31	4.26	0.79	3.000	5.66

The calculated p-values have been compared with the selected significance level ( $\alpha = 0.05$ ), and the output statistical test is concluded in Table 4.16. Since all groundwater quality variables except Calcium and Nitrate have an abnormal distribution (95% confidence interval) substantially, the nonparametric "*Wilcoxon rank test*" has been utilized to examine the significance of groundwater quality variation. For the Ca and NO<sub>3</sub> (seasonal differences of Ca and NO<sub>3</sub> concentration), the p values were larger than the  $\alpha$  values ( $p = 0.072 > 0.05$  and  $p = 0.2 > 0.05$  for Ca and NO<sub>3</sub>, respectively); consequently, the alternative hypothesis has been rejected, and the data of Ca and NO<sub>3</sub> might be regarded to have a normal distribution with a 95% confidence interval.

**Table 4. 16 Result of the "Kolmogorov-Smirnov test" for normal distribution of seasonal changes (n=53)**

Differences of Parameters	Mean	SD	K-S Statistic	p Value	Hypothesis
EC	70.717	831.694	0.311	0.000	Hs
pH	-0.039	0.232	0.152	0.004	Hs
TDS	34.368	543.813	0.320	0.000	Hs
TH	-75.600	741.260	0.160	0.002	Hs
Ca	-75.260	187.179	0.116	0.072	H <sub>0</sub>
Mg	167.619	341.657	0.189	0.000	Hs
Na	-46.962	193.054	0.177	0.000	Hs
HCO <sub>3</sub>	20.283	156.216	0.292	0.000	Hs
Cl	-20.663	51.532	0.344	0.000	Hs
F	-0.260	0.853	0.200	0.000	Hs
SO <sub>4</sub>	-60.136	349.471	0.420	0.000	Hs
PO <sub>4</sub>	-0.069	0.606	0.258	0.000	Hs
K	0.299	18.065	0.294	0.000	Hs
NO <sub>3</sub>	-0.271	2.187	0.093	0.200	H <sub>0</sub>
Fe	-0.057	0.218	0.287	0.000	Hs
Mn	-5.894	36.602	0.480	0.000	Hs
Cu	0.001	1.097	0.332	0.000	Hs
Al	0.009	0.085	0.229	0.000	Hs
CN	0.004	0.043	0.361	0.000	Hs

To statistically examine seasonal groundwater quality changes, the following null (H<sub>0</sub>) and alternative (H<sub>s</sub>) hypotheses were proposed:

H<sub>0</sub>: The change in seasonal concentration values between dry and wet seasons is insignificant.

H<sub>s</sub>: The change in seasonal concentration values between dry and wet seasons is significant.

The "*t-test*" can only be used for Ca and NO<sub>3</sub> variables based on the results of the statistical normality test because their seasonal fluctuation has a normal distribution. Ca's seasonal variation is statistically significant, as shown by the paired samples "*t-test*" analysis (Table 4.17). The alternative hypothesis was accepted because the p-value is smaller than the  $\alpha$  value ( $p = 0.005$  less than 0.05). It was established with a 95% confidence interval that calcium concentrations significantly vary from the dry to wet period. Although the mean Ca content increased from 117.56 to 192.82 mg/l over time (all sample sites), the statistical test findings significantly increased.

Furthermore, the "*t-test*" result for NO<sub>3</sub> shows that the seasonal change in its concentration is not statistically significant. The calculation results show that the p-value is larger than the  $\alpha$  value ( $p = 0.372 > 0.05$ ); eventually, the null hypothesis was accepted, and the alternative hypothesis was rejected with a 95% confidence interval. It was concluded that there is no significant variation in NO<sub>3</sub> levels from the dry to rainy periods. In addition, the average NO<sub>3</sub> level rose significantly from 2.42 to 2.69 mg/l over time. The increase was not significant according to the statistical test results.

**Table 4. 17 Summary of paired sample "*t-test*" for Ca and NO<sub>3</sub>**

Parameters	Mean	SD	95% Confidence Interval of the Differences		t	p	Hypothesis
			Lower	Upper			
Ca	-75.260	187.179	-126.853	-23.667	-2.927	0.005	Ha
NO <sub>3</sub>	-0.271	2.187	-0.874	0.332	-0.901	0.372	H <sub>0</sub>

The "*Wilcoxon signed-rank test*" was used to determine if seasonal variations in quantities of several groundwater quality measures, including EC, pH, TDS, TH, Mg, Na, HCO<sub>3</sub>, Cl, F, SO<sub>4</sub>, PO<sub>4</sub>, K, Fe, Mn, Cu, Al, and CN, were statistically significant.

The test results are shown in (Table 4.18) and revealed that most seasonal variations were statistically insignificant. On the other hand, the changes in Mg, Na, Cl, F, Fe, and Mn contents appeared significant. The table provided positive rankings to data pairs with the increasing conditions in their values from dry to wet season. Negative ranks have been employed in the opposite instance. The alternative hypothesis has been accepted for the data pairs of Mg, Na, Cl, F, Fe, and Mn since  $p < \alpha$ . From a statistical standpoint, the seasonal variation in concentrations constituted significant. It can be summarized that except for Mg, which decreased its concentration from the dry to the wet season, the concentration of all other parameters, i.e., Na, Cl, F, Fe, and Mn, increased in the spring. The null hypothesis has been accepted since  $p > \alpha$  for the rest of the water quality parameters.



**Table 4. 18 Summary of Wilcoxon signed-rank test**

Parameter s	Negative ranks			Positive ranks			Test statistics			Hypothesi s
	n	Mean rank	sum of ranks	n	Mean rank	sum of ranks	Ties	Z	p	
<b>EC</b>	2 5	25.92	648	2 8	27.96	783	0	- 0.598 <sup>b</sup>	0.55	H <sub>0</sub>
<b>pH</b>	2 3	24.57	565	2 9	28.03	813	1	- 1.129 <sup>b</sup>	0.259	H <sub>0</sub>
<b>TDS</b>	2 4	24.52	588.5	2 8	28.2	789.5	1	- 0.915 <sup>b</sup>	0.36	H <sub>0</sub>
<b>TH</b>	2 2	24.25	533.5	3 0	28.15	844.5	1	- 1.416 <sup>b</sup>	0.157	H <sub>0</sub>
<b>Mg</b>	4 1	28.46	1167	1 2	22	264	0	- 0.997 <sup>a</sup>	0.000	Ha
<b>Na</b>	1 6	23.44	375	3 3	25.76	850	3	- 2.363 <sup>b</sup>	0.018	Ha
<b>HCO<sub>3</sub></b>	2 8	21.46	601	1 8	26.67	480	7	- 0.666 <sup>a</sup>	0.505	H <sub>0</sub>
<b>Cl</b>	7	8.93	62.5	4 1	27.16	1113.5	5	-5.393 <sub>b</sub>	0.000	Ha
<b>F</b>	1 9	25.24	479.5	3 4	27.99	951.5	0	-2.089 <sub>b</sub>	0.037	Ha
<b>SO<sub>4</sub></b>	2 5	23.32	558	2 6	29.54	768	2	-0.985 <sub>b</sub>	0.325	H <sub>0</sub>
<b>PO<sub>4</sub></b>	2 1	24.4	512.5	2 9	26.29	762.5	3	-1.207 <sub>b</sub>	0.227	H <sub>0</sub>
<b>K</b>	2 0	29.28	585.5	3 3	25.62	845	0	-1.151 <sub>b</sub>	0.25	H <sub>0</sub>
<b>Fe</b>	1 1	28.55	314	3 7	23.3	862	5	-2.814 <sub>b</sub>	0.005	Ha
<b>Mn</b>	2 0	23.15	463	3 3	29.33	968	0	-2.236 <sub>b</sub>	0.025	Ha
<b>Cu</b>	2 2	28.59	629	3 0	24.97	749	1	-0.547 <sub>b</sub>	0.584	H <sub>0</sub>
<b>Al</b>	2 2	28.82	634	2 9	23.86	692	2	-0.272 <sub>b</sub>	0.786	H <sub>0</sub>
<b>CN</b>	1 8	22.08	397.5	2 6	22.79	592.5	9	-1.14 <sup>b</sup>	0.254	H <sub>0</sub>

a. according to negative rank

b. according to positive rank

Numerous factors, such as mineral dissolution, anthropogenic and urban influences, and evaporitic lacustrine deposits, are potential indicators that could impact groundwater quality. The critical determining element of groundwater quality in the Kabul basin, according to Zaryab et al. (2021), is evaporitic lacustrine deposits. The interaction of water with particular rocks and minerals, such as gypsum and limestone, is the cause of the presence of Calcium and magnesium in groundwater. The presence of sodium and chloride in groundwater can be attributed to several sources, "including the weathering of minerals in the soil, salt-bearing geological formations, deposition of salt spray, the use of salt for road de-icing, and in coastal areas, intrusion of salty ocean water into fresh groundwater sources." Fluoride is found in groundwater due to

weathering and leaching of fluoride-bearing minerals from sediments and rocks. The most frequent sources of iron and manganese in groundwater occur naturally, such as weathering rocks and minerals containing iron and manganese. Sewage, landfill leachate, industrial effluent, and acid-mine drainage can all add iron and manganese to the surrounding groundwater.

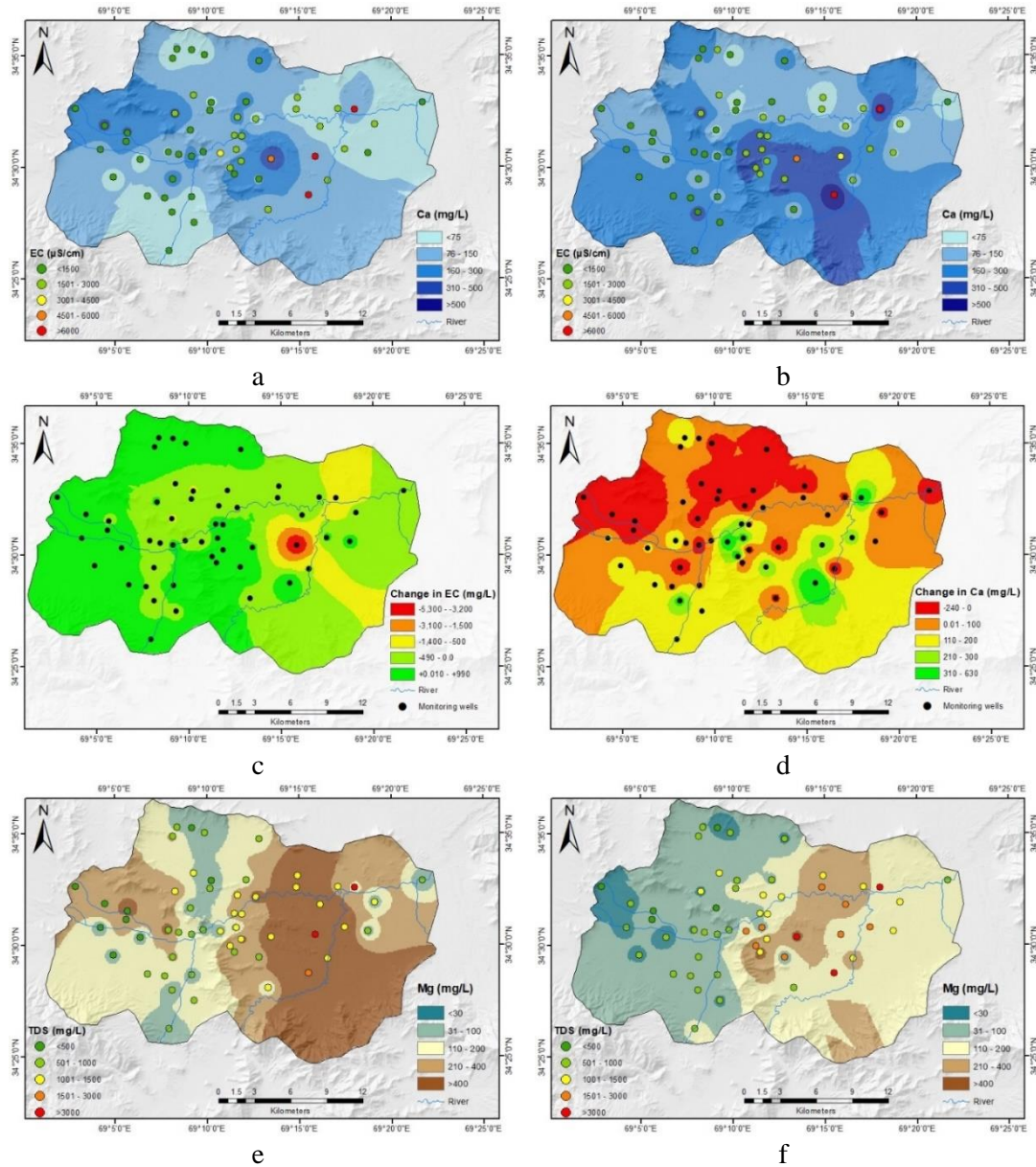


**Figure 4. 18 Spatial distribution maps a. Ca and EC dry season, b. Ca and EC wet season, c. change in EC, d. Change in Ca, e. TDS and Mg dry season, f. TDS and Mg wet season, g. Change in TDS, h. Change in Mg**

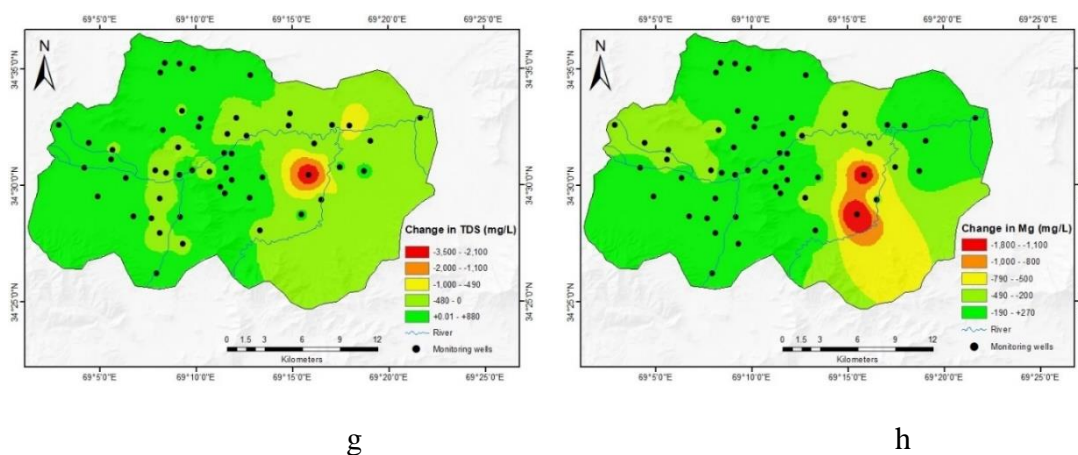


**Figure 4.18 (Continued)**

According to those above, the weathering of minerals and rocks is significant in determining most quality criteria in groundwater. Seasonal precipitations may infiltrate the soil beds along rivers and nearby lands, sometimes agricultural fields and hillsides. During infiltration, they come into contact with rocks and minerals containing magnesium, sodium, Calcium, fluoride, and chloride. This can be the main reason for increasing these parameters in groundwater in the wet season. The infiltration and weathering of minerals in the soil is also a case of iron and manganese. Another reason that may increase iron and manganese in groundwater is the infiltration of surface water contaminated with sewage through the river beds and municipality channels. The city of Kabul does not have a sewage collection and disposal system.

### 4.3.3 Spatio-seasonal evaluation of groundwater quality criteria

In order to spatially depict the quality of groundwater in the Kabul basin, spatial distribution maps of some qualitative indicators of groundwater were prepared for both dry and wet seasons. Qualitative variables like EC, TDS, TH, Ca, Mg, K, and Mn were chosen for geographic distribution maps since their values exceed WHO and ANSA drinking water recommendations. Parameters like Ca, Mg, Na, Cl, F, Fe, and Mn were considered for spatial distribution maps because they have significantly changed. One parameter ( $\text{NO}_3$ ) was chosen for the geographical distribution map from the other qualitative indicators that are not above WHO and ANSA criteria and have not been modified considerably. Furthermore, the spatial distribution maps of changes illustrating the degree of differences in measurement results were created to highlight how the regional distribution of several groundwater quality indicators altered as the seasons switched from dry to wet.

The spatial pattern of EC contents and Ca values for each measurement interval is presented in Figure 4.18 a and b. The concentration of electrical conductivity in the west and north parts of the basin is less than  $3,000 \mu\text{S}/\text{cm}$ . Only a few wells in the central-eastern part of the basin have an electrical conductivity higher than  $3,000 \mu\text{S}/\text{cm}$  for both seasons. Also, the concentration of Ca is lower in the marginal areas added in the western and northern parts of the basin but increases in the

central and southeastern parts of the basin and reaches more than 300 mg /l. Figure 4.18 c and d illustrate the change in EC and Ca in the study area from the dry to wet season. The concentration of EC has grown throughout the study's peripheral regions, particularly in the south, north, and west. The EC value decreased in other parts of the area by changing the season from dry to wet. The minus marks in the figure's legends illustrate the decrease in concentration, while the plus marks indicate increased concentrations. Ca concentrations in the study region declined in the north, west, and some eastern sections up to -240 mg/l but climbed to 630 mg/l in the middle and south.

Figure 4.18 e and f illustrate the spatial distribution maps of TDS and Mg concentrations. TDS values in most observation wells are less than 1000 mg/l in both seasons. Only three wells in the middle and central-eastern regions of the basin have values larger than 1500 mg/l during the dry season, whereas eleven wells have values greater than 1500 mg/l during the wet season. Mg concentration exceeds 400 mg/l in most of the basin during the dry period. In comparison, it has decreased in most parts of the basin in the wet period.

Based on Figure 4.18 g, the TDS concentration has increased in the western area of the basin up to +880 mg/l from dry to wet season. In contrast, the eastern part of the basin shows a negative trend, especially in the central-east, up to -3500 mg/l. The concentration of Mg (Figure 4.18 h) also has a similar distribution in the basin. It has increased to +270 mg/l and decreased to -1800 mg/l in the exact locations as TDS.

The spatial distribution map of TH and K is depicted in Figure 4.19 a and b. The concentration of TH has great values in the central parts of the study area. Eleven observational points have TH > 1000 mg/l in the autumn, increasing to 16 wells in the spring. The K content in the west part of the study area has fewer values (i.e., less than ten mg/l) in both seasons. In autumn and spring, concentration rises in the middle area of the study and continues to the southeast.

In the west section of the research region and north to southeast, there is a reduction in TH concentration. The decreasing value in TH is up to -3600 mg/l (Figure 4.19 c). Other parts of the study area have a light increase in TH concentration. A few wells in the central and east parts of the basin increased in concentrations up to 2200 mg/l. The concentration in K has conditions that are almost similar using spatial distribution. It dropped to -79 mg/l and rose to +67 mg/l in some particular wells in the basin's center and east (Figure 4.19 d).

The spatial distribution map of Mn and Na is depicted in Figure 4.19 e and f. During the dry season, the concentration of Mn in three wells in the middle section of the study region reaches high levels. However, its concentration increased in most wells across the study area during the wet season. The Na content is smooth in most parts of the basin during the dry season, while it has increased in the eastern region.

In the research area's middle to the northwest region, there is a reduction in Na concentration. It decreases to -720 mg/l from the dry to wet season (Figure 4.19 g). Other parts of the basin have increased up to +720 mg/l. The situation for Mn

content is different in the basin. Smaller areas in the north and south of the basin and certain south-easterly regions have decreasing levels of up to -10 mg/l (Figure 4.19 h). Other parts of the basin have a smooth increase, but only one well in the northern region has dramatically increased up to +260 mg/l.

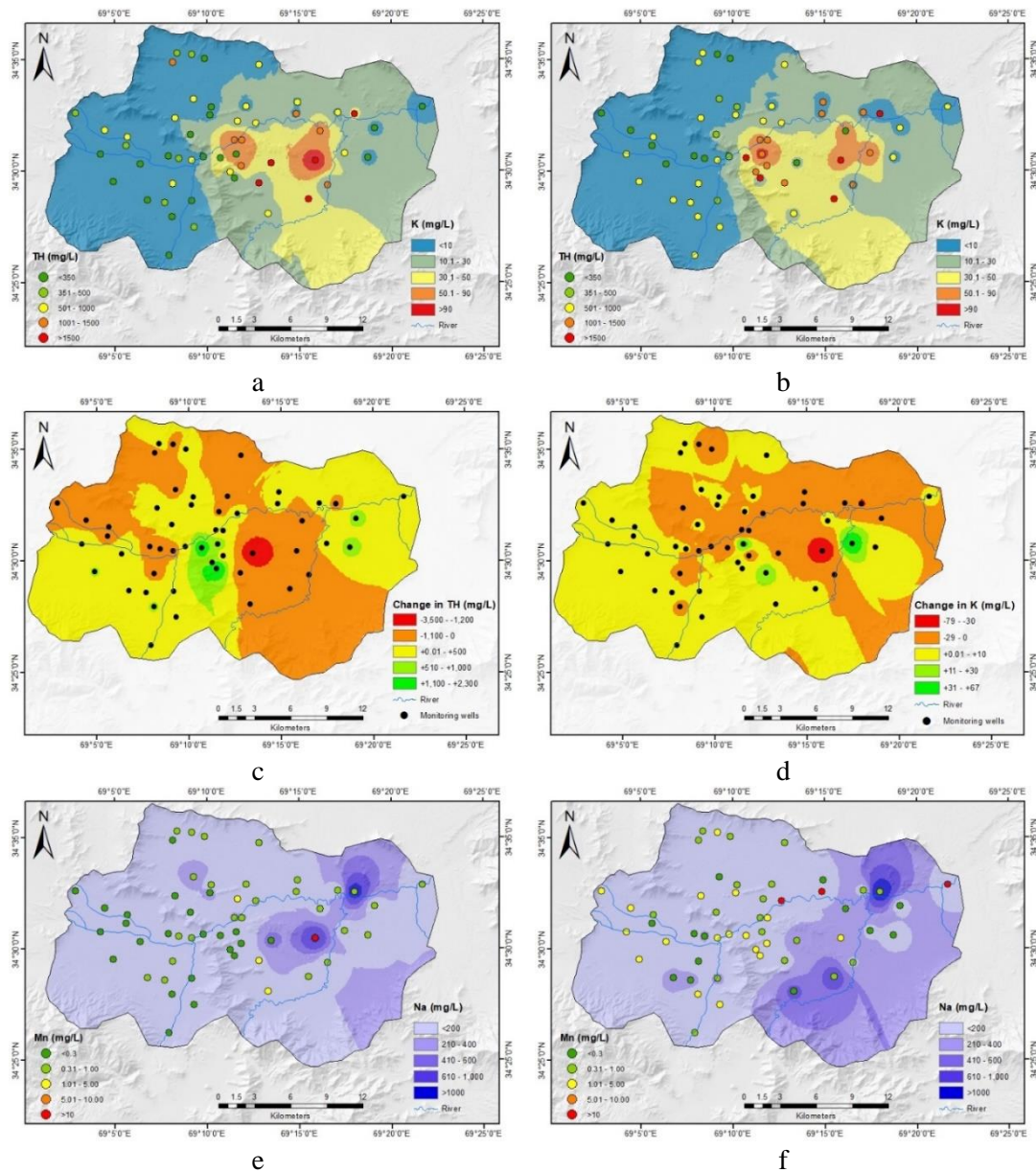


**Figure 4. 19 Spatial distribution maps a. TH and K dry season, b. TH and K wet season, c. change in TH, d. Change in K, e. Na and Mn dry season, f. Na and Mn wet season**

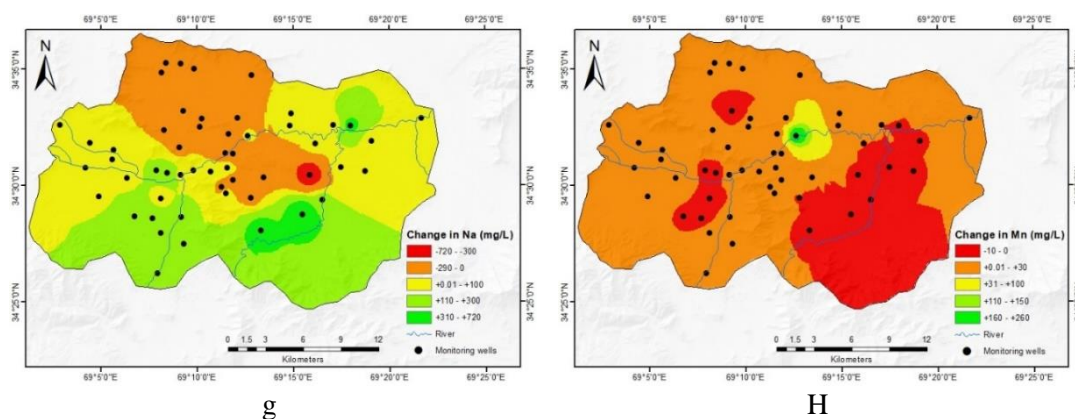


**Figure 4.19 (Continued)**

As illustrated in Figure 4.20 a and b, the spatial distribution of F and Fe is delineated for dry and wet climate conditions. The concentration of F is less than 0.5 mg/l in most of the study areas during the dry season. Some parts in the central western section, north to south, and a small part in the central-eastern portion of the basin has a concentration of greater than 0.5 mg/l. However, during the wet season, the concentration of F has increased in most of the research regions. Based on Figure 4.20 b, most of the basin has a concentration greater than 0.5 mg/l in the spring. Fe concentration in three sampling points has a value greater than 0.3 mg/l. Most other monitoring wells in the study area have concentrations less than 0.09 mg/l. The concentration of Fe during the wet period has increased in some wells, and the wells with a value greater than 0.3 mg/l are five wells. Some of the monitoring wells with low concentrations during the dry period have increased Fe concentrations during the wet period.

Spatially seasonal change in Fe concentration is illustrated in (Figure 4.20 c). The mainly northern part of the basin has decreased values up to -0.55 mg/l. Some wells around the central part of the basin have reduced values. However, most of the study areas have increased the change in Fe concentration up to +1 mg/l. The shift in F concentration looks similar to Fe in spatial distribution (Figure 4.20 d). It has mainly decreased in the north and south of the basin up to -0.94 mg/l. While other parts of the basin have an increasing change in F concentration up to +4 mg/l.

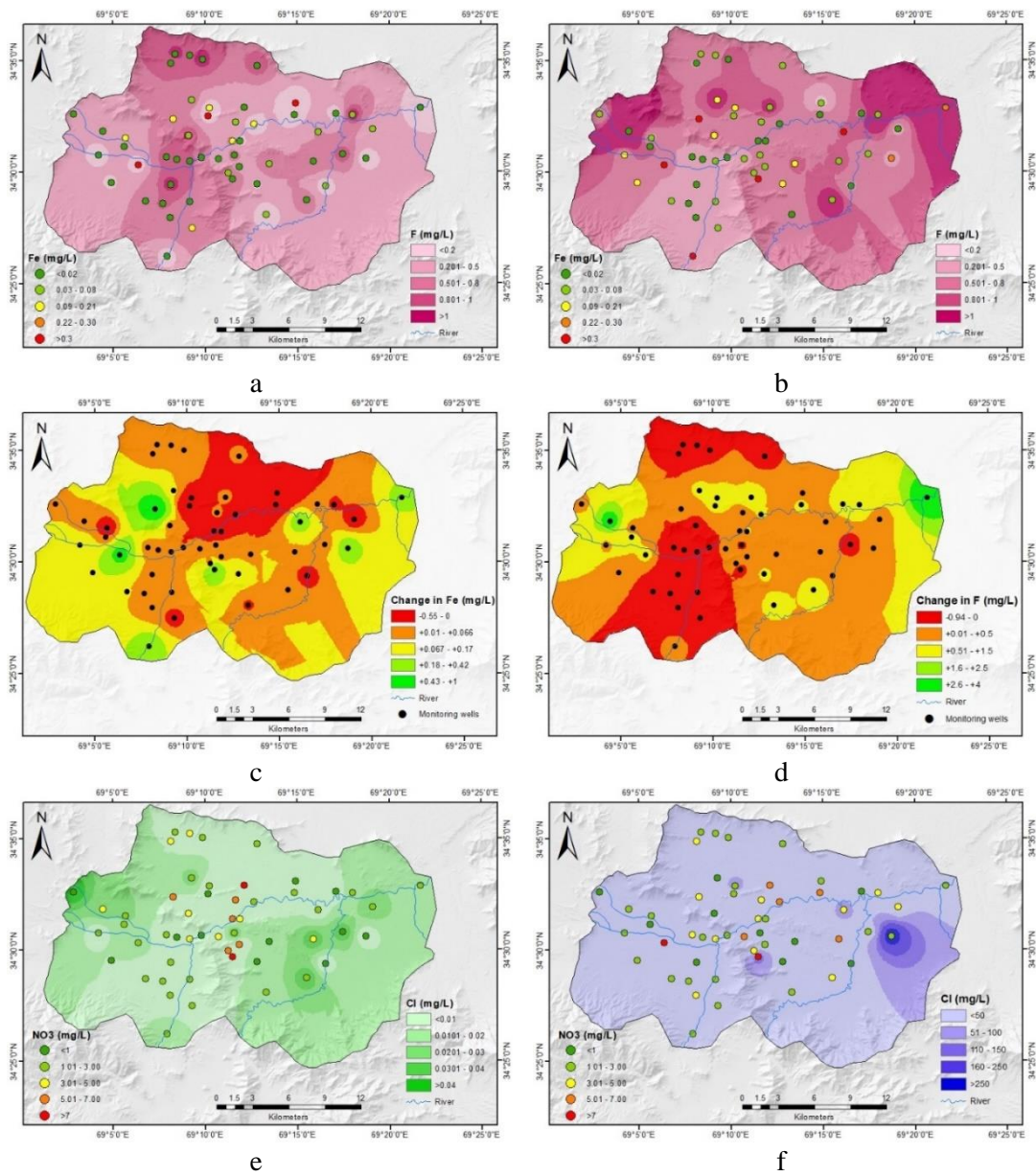


**Figure 4. 20 Spatial distribution maps a. Fe and F dry season, b. Fe and F wet season, c. change in Fe, d. Change in F, e. NO<sub>3</sub> and Cl dry season, f. NO<sub>3</sub> and Cl wet season, g. Change in NO<sub>3</sub>, h. Change in Cl**

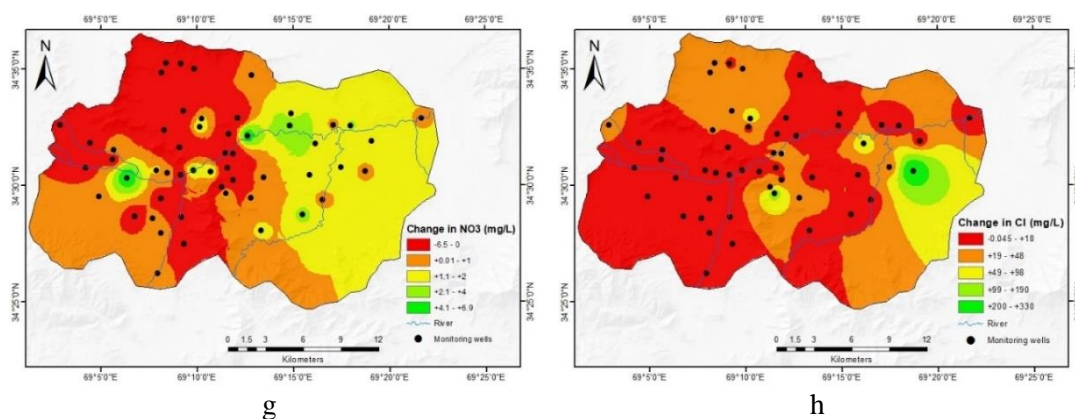


**Figure 4.20 (Continued)**

Figure 4.20 e and f delineate the spatial distribution of  $\text{NO}_3$  and Cl for both climate conditions. The content of  $\text{NO}_3$  is less than three mg/l in most of the observational points during the dry season. Only five wells in the central section of the basin have a concentration greater than five mg/l in the dry period. However, the concentration of  $\text{NO}_3$  during the wet period increased in some wells. The number of wells with rising  $\text{NO}_3$  concentrations has risen, particularly in the basin's center region. The chloride concentration is very low during the dry period in the whole season. But it has increased dramatically in all parts of the basin. The spatial distribution of chloride concentration is uniform in all parts of the basin in the wet season except for one well in the east of the basin with a high concentration.

Spatially seasonal change in  $\text{NO}_3$  concentration is illustrated in (Figure 4.20 g). Based on the change in  $\text{NO}_3$  concentration, the basin is divided into two blocks, west and east. The west part has decreased in  $\text{NO}_3$  concentration while the east part of the basin has increased values. The decrease rate of  $\text{NO}_3$  is about  $-6.5$  mg/l, and the increasing rate is about  $+5.9$  mg/l. Cl concentration (Figure 4.20 h) has increased in almost all of the basin, but the eastern section has increased concentration values up to 330 mg/l.

With the increase in urbanization, the recharge area of groundwater has decreased significantly. On the other hand, the study area's groundwater level has decreased drastically during the last two decades. Groundwater in Kabul is mainly recharged through river beds. Public water supply wells are also located next to river beds. Other recharge areas, such as hillsides and some open areas, can also have some role in groundwater recharge. Increasing and decreasing changes in water quality parameters are correlated to recharge volume, hydraulic conductivity, and the geological formation of the region. More groundwater recharge causes more contact and weathering of minerals and rocks, thus increasing the level of qualitative parameters in groundwater. This is the case for the wells that are located near the riverbeds. The level of qualitative parameters, such as calcium, sodium, iron, manganese, chloride, and fluoride, increases in the wet season, mainly in wells close to river beds or in agricultural areas. In some wells located next to riverbeds or agricultural fields, and the quality parameters have not increased, the feeding path will probably have different geological formations.



On the other hand, the concentration of most parameters has decreased in the northern and western areas of the study area. The north and western parts of the study area have witnessed more urban development in the last two decades, and groundwater levels have decreased significantly in these areas. These locations receive minimal recharge, and since the groundwater level is so much lower, the recharge water is probably unable to reach the groundwater in a single season due to its tiny volume and weak hydraulic conductivity. As a result, there is less of a concentration of quality factors in the groundwater in these areas.

## 4.4 Groundwater level

### 4.4.1 Cluster analysis of the wells

The observational wells were characterized using cluster analysis based on the similarity of their water level measurements. The dendrogram that resulted from hierarchical clustering with Ward's linkage approach is shown in Figure 4.21.

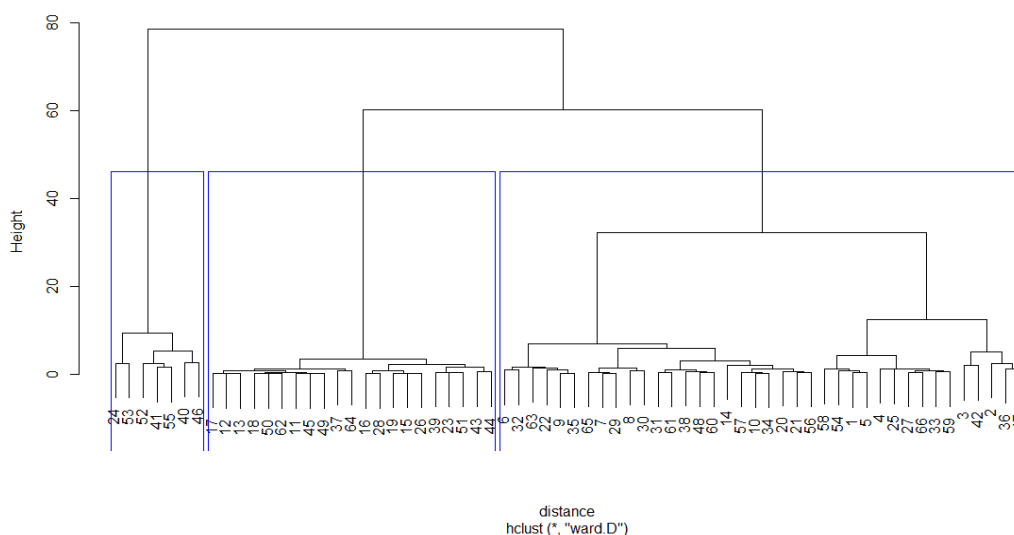


**Figure 4. 21 Dendrogram of hierarchical cluster analysis**

The dendrogram must be split at a certain amount of linkage gap called threshold to achieve various clusters. Threshold selection is a personal decision that differs from person to person. For example, a threshold of 40 results in three clusters, while a threshold of 20 results in four clusters.

A specific approach is required to prevent confusion when selecting a threshold. The optimal clustering algorithm was determined using the "*Elbow method*". The aim of cluster grouping techniques, or "total within-cluster sum of square (WSS)," is to find clusters with the least amount of intra-cluster variation. The "*Elbow method*" calculates the cumulative WSS as a function of cluster size: The cluster numbers should be chosen such that adding another cluster would not increase the total WSS significantly.

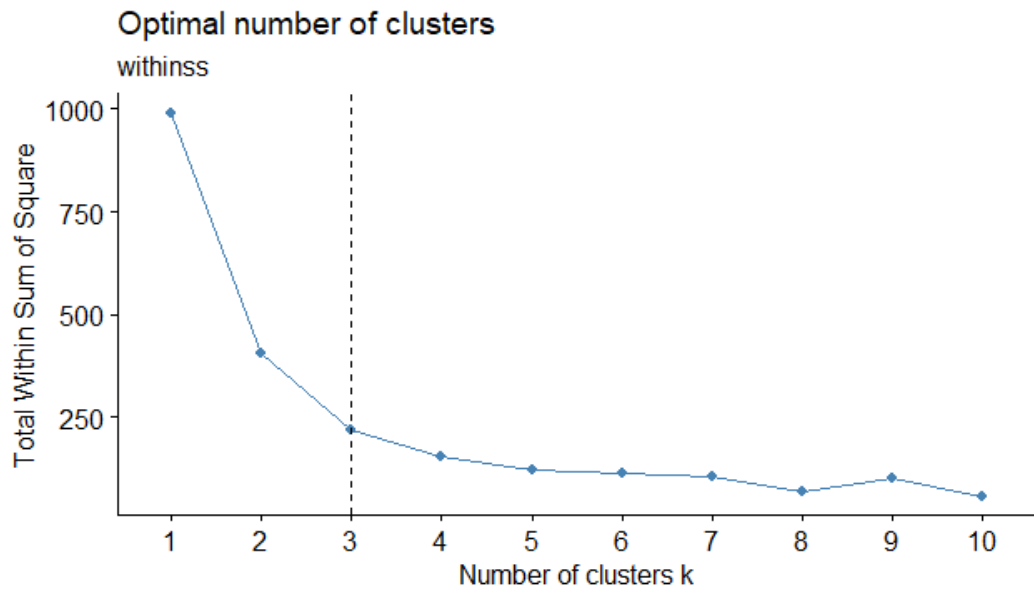


**Figure 4. 22 Elbow method for hierarchical cluster analysis**

A WSS plot is constructed based on the number of clusters " $k$ " (Figure 4.22). The position of a bend (knee) in the plot determines the number of clusters needed. From (Figure 4.22), it is seen that the hook is located at  $k=3$ , and it indicates that the optimal clustering algorithm throughout all wells is three. Based on the geographical heterogeneity in the various clusters (Figure 4.23), a group of seven wells in the study area's east, west, and north parts shaped cluster 3. Cluster 2 consists of 22 wells with the same geographic distribution of east, west, and north. Cluster 1 is made up of the remaining 37 wells that are scattered across the region.

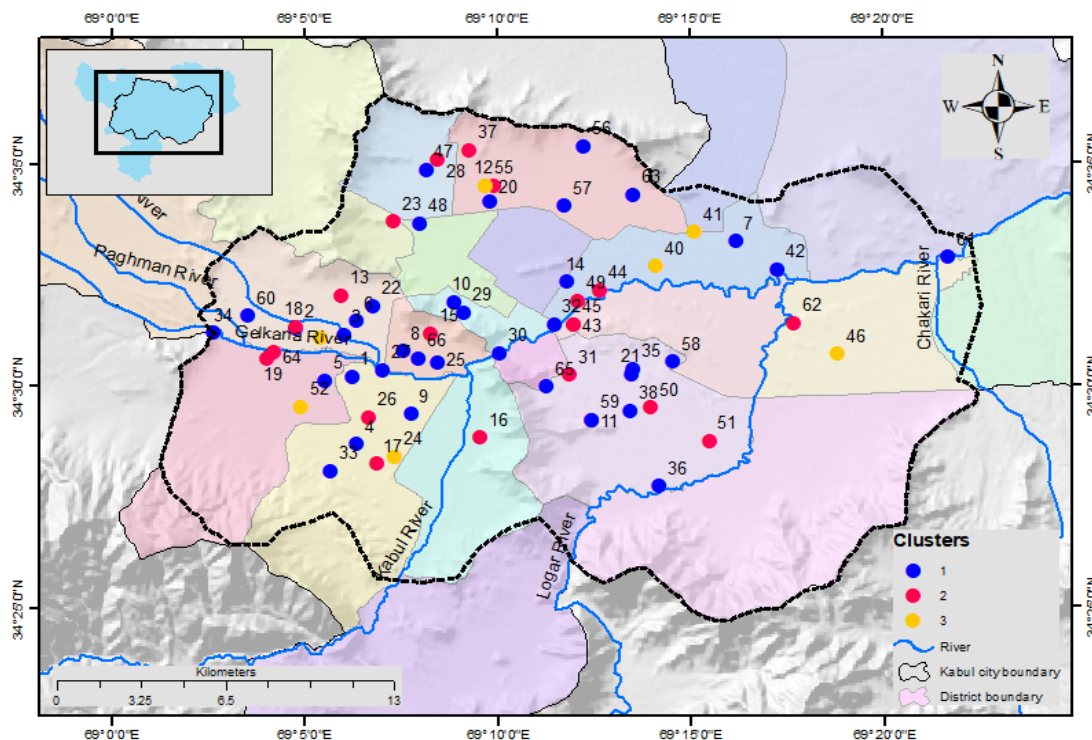


**Figure 4. 23 Spatial distribution of wells classified based on cluster analysis**

The average annual static water level in cluster 1 varies from 9 to 28 meters below ground level, with a median of 17 meters and a mean of 18 meters (Figure 4.24). Cluster 2 has a mean and median yearly averaged static water depth of 6 m below ground level, with a least of 5 m and utmost of 9 m. The static water level in cluster 3 is slightly different. It has a minimum (33 m) variation and maximum (56 m) yearly averaged static water table below ground level. The mean and median values in cluster 3 are 42 and 39 m, respectively.

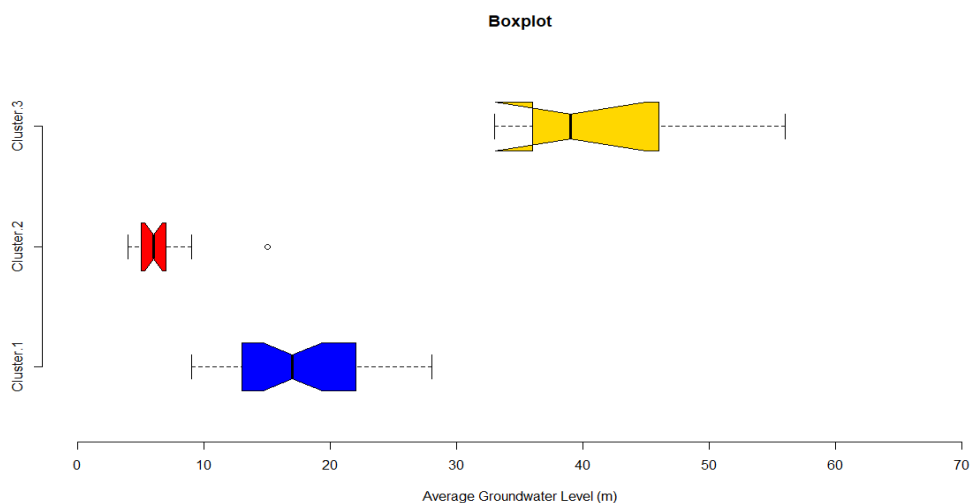


**Figure 4. 24 Variability of groundwater levels in various clusters**

#### 4.4.2 Trends of Groundwater Table on an Annual and Seasonal Basis

Seasonal spring (March-May), summer (June - August), fall (September - November), winter (December - February), and annual trends of groundwater- table for all observational points in the study area were evaluated using the nonparametric Mann-Kendall test with a significance level of 0.05. The seasonal and yearly groundwater level data were subjected to an autocorrelation test before being included in the Mann-Kendall trend test. Most wells had a significant lag 1 serial correlation with seasonal and annual groundwater levels. The "*Modified Mann-Kendall (MMK) test*" was utilized to integrate serial correlation effects on trend assessment of groundwater level variability. As there is no alter in variance and p-value of the test using "*mkttest*" and "*bcpw*" tests, therefore "*mkttest*" the trend analysis is run on the initial time series of the groundwater table for all stations in each cluster.

Table 4.19 displays the findings of groundwater level trends and their magnitudes based on Sen's slope procedure. Both annual and seasonal groundwater level measurements showed significant trends. According to the trend report, just six out of 66 observational wells with annual groundwater levels show increasing trends. In comparison, according to the trend report, the remaining 60 wells show decreasing trends, often with significant trends (Figure 4.25).

A total of 32 observational wells included in cluster 1 had a significant decrease with an average magnitude of 1.38 m yearly. Additionally, two other clusters (2&3) have 15 and 8 wells. Cluster 2 has a significant negative trend value of 0.31 m per year, while Cluster 3 has a significant negative trend value of 2.84 m per year. Conversely, four regional wells showed a significant increase in groundwater depth, with an annual average of 0.7 m. The trend assessment results indicate that most wells in both clusters are declining. The Clusters 1 and 3 wells have more significant trends than Cluster 2. With an average decline of 4.26 meters per year for all seasons, the well 53rd in cluster 3 recorded the greatest decrease in groundwater level among all observation points. Similarly, the highest increasing groundwater level is recorded in the 42nd cluster 1, with an average value of 1.68 m per year. The water level in 89 per cent of cluster 1 wells and 82 per cent of the overall wells in the research region significantly decreases annually and, in all seasons, based on a trend evaluation of groundwater depth in different clusters.

In general, the depth of groundwater in more than 90% of the monitoring wells is decreasing, with an average annual decline of 1.18 m, which may be attributed to a variety of factors, including heavy groundwater use, changes in LULC, low precipitation, and poor water resource management. The groundwater level depth in a few clusters 1 and 2 wells showed increasing conditions. Wells with positive groundwater levels are located near riverbeds in the Kabul area, most likely due to these features' vital role in providing groundwater recharge.

**Table 4. 19 Annual and seasonal trend analysis results based on the MK statistics and Sen's slope values**

Wells	Spring		Summer		Autumn		Winter		Yearly	
	Z	Sen's Slope	Z	Sen's Slope	Z	Sen's Slope	Z	Sen's Slope	Z	Sen's Slope
1	4.38	2.48	4.70	1.61	4.93	1.53	4.49	1.77	<b>4.65</b>	1.79
2	1.64	1.57	1.16	1.23	0.88	0.83	1.42	1.23	1.09	1.00
3	-3.61	-0.25	-3.11	-0.30	-2.52	-0.29	-3.18	-0.31	<b>-4.35</b>	-0.34
4	4.71	2.80	4.70	2.47	4.71	2.34	4.93	2.54	<b>5.05</b>	2.52
5	4.60	2.20	4.70	1.74	4.71	1.60	4.38	1.97	<b>4.45</b>	1.85
6	2.74	1.39	3.48	1.43	2.85	1.23	2.96	1.17	<b>3.27</b>	1.26
7	4.93	1.89	4.70	1.58	4.49	1.62	4.66	1.39	<b>4.75</b>	1.56
8	4.71	1.75	4.70	2.49	4.82	2.21	4.60	1.96	<b>4.85</b>	2.10
9	4.27	0.81	4.45	0.73	4.60	0.67	4.71	0.67	<b>4.75</b>	0.69
10	4.93	0.74	4.52	0.71	4.55	0.68	4.49	0.62	<b>4.95</b>	0.66
11	1.20	0.08	3.49	0.32	3.50	0.20	3.61	0.28	<b>3.46</b>	0.15
12	-1.42	-0.08	4.21	0.28	3.61	0.21	2.30	0.10	<b>2.67</b>	0.11
13	3.94	0.23	4.28	0.26	3.56	0.16	3.34	0.10	<b>3.17</b>	0.15
14	-2.74	-0.30	-1.96	-0.37	-2.41	-0.53	-2.63	-0.42	<b>-2.97</b>	-0.32
15	4.49	0.40	3.32	0.26	4.05	0.35	4.49	0.44	<b>4.45</b>	0.32
16	3.23	0.36	4.58	0.39	4.11	0.39	3.61	0.35	<b>4.06</b>	0.34
17	3.28	0.18	3.72	0.19	3.07	0.13	4.17	0.13	<b>2.87</b>	0.13
18	-1.04	-0.03	2.83	0.08	1.43	0.10	1.09	0.06	0.79	0.03
19	4.16	0.35	4.21	0.57	3.72	0.50	3.07	0.37	<b>4.16</b>	0.40
20	3.14	0.13	3.79	0.28	3.34	0.16	1.33	0.09	<b>3.27</b>	0.15
21	4.77	0.70	4.33	0.55	3.94	0.76	2.69	0.33	<b>4.16</b>	0.54
22	4.71	1.29	4.33	1.20	3.61	1.03	4.60	1.00	<b>4.65</b>	1.11
23	3.45	0.20	3.11	0.28	4.05	0.33	4.16	0.29	<b>3.56</b>	0.25
24	4.60	3.63	4.70	3.74	4.93	3.41	4.71	3.40	<b>5.05</b>	3.43
25	4.93	2.05	4.45	2.08	4.82	2.07	4.93	2.28	<b>4.95</b>	2.05
26	4.27	0.72	4.33	0.55	4.60	0.49	4.49	0.55	<b>4.55</b>	0.56
27	4.88	2.40	4.70	2.39	4.93	1.98	4.82	2.25	<b>4.95</b>	2.18
28	4.28	0.37	4.70	0.52	4.55	0.45	4.49	0.51	<b>4.75</b>	0.42
29	4.49	1.89	4.70	1.57	4.93	1.28	4.49	1.67	<b>4.85</b>	1.54
30	4.93	1.98	4.33	1.62	4.93	1.44	4.93	1.41	<b>5.05</b>	1.62
31	4.71	1.61	3.97	1.29	3.61	1.15	4.60	0.95	<b>4.55</b>	1.19
32	3.61	1.42	3.30	0.98	4.93	0.69	3.34	1.20	<b>4.26</b>	1.05
33	4.60	2.46	4.70	2.92	4.82	2.65	4.82	2.33	<b>5.05</b>	2.54
34	4.71	0.78	4.45	0.79	4.38	0.84	4.71	0.84	<b>4.65</b>	0.77
35	4.66	0.58	4.45	0.63	4.49	0.58	4.71	0.57	<b>4.85</b>	0.60
36	2.08	1.17	2.50	0.89	1.76	0.45	2.08	0.83	<b>1.98</b>	0.79

Continued to the next page

Table 4.1(9 Continued)

Wells	Spring		Summer		Autumn		Winter		Yearly	
	Z	Sen's Slope	Z	Sen's Slope	Z	Sen's Slope	Z	Sen's Slope	Z	Sen's Slope
<b>37</b>	3.83	0.31	3.60	0.41	3.50	0.42	4.38	0.29	<b>4.26</b>	0.35
<b>38</b>	2.19	0.75	2.50	0.96	1.64	0.67	1.86	0.61	<b>1.98</b>	0.68
<b>39</b>	3.07	0.19	2.26	0.41	0.11	0.04	-0.11	-0.01	0.89	0.06
<b>40</b>	4.38	1.77	4.58	2.02	4.38	1.84	4.05	2.05	<b>4.35</b>	1.86
<b>41</b>	4.05	4.04	4.58	2.85	4.27	3.48	3.94	3.67	<b>4.16</b>	3.29
<b>42</b>	-3.50	-1.80	-4.21	-1.81	-4.05	-1.75	-3.94	-1.53	<b>-4.45</b>	-1.68
<b>43</b>	0.66	0.08	0.24	0.02	-1.75	-0.19	-2.30	-0.36	-1.39	-0.15
<b>44</b>	-2.80	-0.33	-2.87	-0.54	-3.61	-0.55	-2.74	-0.42	<b>-2.77</b>	-0.48
<b>45</b>	2.36	0.11	3.55	0.12	1.04	0.05	2.97	0.06	<b>2.57</b>	0.09
<b>46</b>	4.16	1.73	3.60	1.54	3.39	1.29	3.61	1.48	<b>3.76</b>	1.33
<b>47</b>	4.38	1.51	4.58	2.05	1.97	2.73	1.70	1.31	<b>3.17</b>	1.63
<b>48</b>	3.18	1.11	3.42	0.70	2.63	0.69	4.05	1.13	<b>3.17</b>	0.91
<b>49</b>	1.53	0.17	3.97	0.21	1.87	0.09	2.58	0.17	<b>2.97</b>	0.15
<b>50</b>	-1.59	-0.11	2.75	0.19	0.00	0.00	2.36	0.06	-0.55	-0.01
<b>51</b>	-1.20	-0.14	-1.47	-0.22	2.08	0.28	-0.60	-0.07	0.20	0.02
<b>52</b>	4.82	3.52	4.45	3.92	4.82	3.32	4.27	2.96	<b>4.85</b>	3.29
<b>53</b>	4.82	3.80	4.58	4.51	4.93	4.61	4.82	4.28	<b>5.15</b>	4.26
<b>54</b>	4.44	1.00	3.97	2.87	4.38	2.00	4.71	2.30	<b>4.85</b>	2.03
<b>55</b>	4.71	2.49	4.58	2.23	4.93	2.75	4.93	2.43	<b>5.05</b>	2.42
<b>56</b>	3.23	0.76	4.21	0.50	3.50	0.76	2.19	0.73	<b>4.11</b>	0.62
<b>57</b>	4.82	0.67	4.58	0.52	4.38	0.53	4.77	0.49	<b>4.55</b>	0.55
<b>58</b>	3.67	1.61	3.97	1.64	3.89	1.62	4.11	1.93	<b>4.55</b>	1.59
<b>59</b>	4.60	2.06	4.58	2.41	4.38	2.38	4.49	2.68	<b>4.65</b>	2.35
<b>60</b>	2.25	1.16	1.77	0.96	1.31	0.87	1.65	1.07	1.68	0.95
<b>61</b>	2.69	1.57	4.58	1.54	3.83	1.51	2.30	1.19	<b>3.56</b>	1.28
<b>62</b>	3.15	0.07	1.65	0.09	3.72	0.15	1.98	0.03	1.93	0.06
<b>63</b>	4.93	1.15	3.18	1.02	4.16	1.13	4.11	0.98	<b>4.65</b>	0.91
<b>64</b>	-2.85	-0.21	1.83	0.17	4.77	0.45	2.96	0.12	<b>2.38</b>	0.11
<b>65</b>	3.18	2.08	4.70	1.69	4.82	1.87	4.82	1.51	<b>5.15</b>	1.88
<b>66</b>	4.05	2.43	4.45	2.23	4.82	2.34	4.88	2.42	<b>5.05</b>	2.30

\* Values that are bolded illustrate a significant trend at a 95% confidence interval

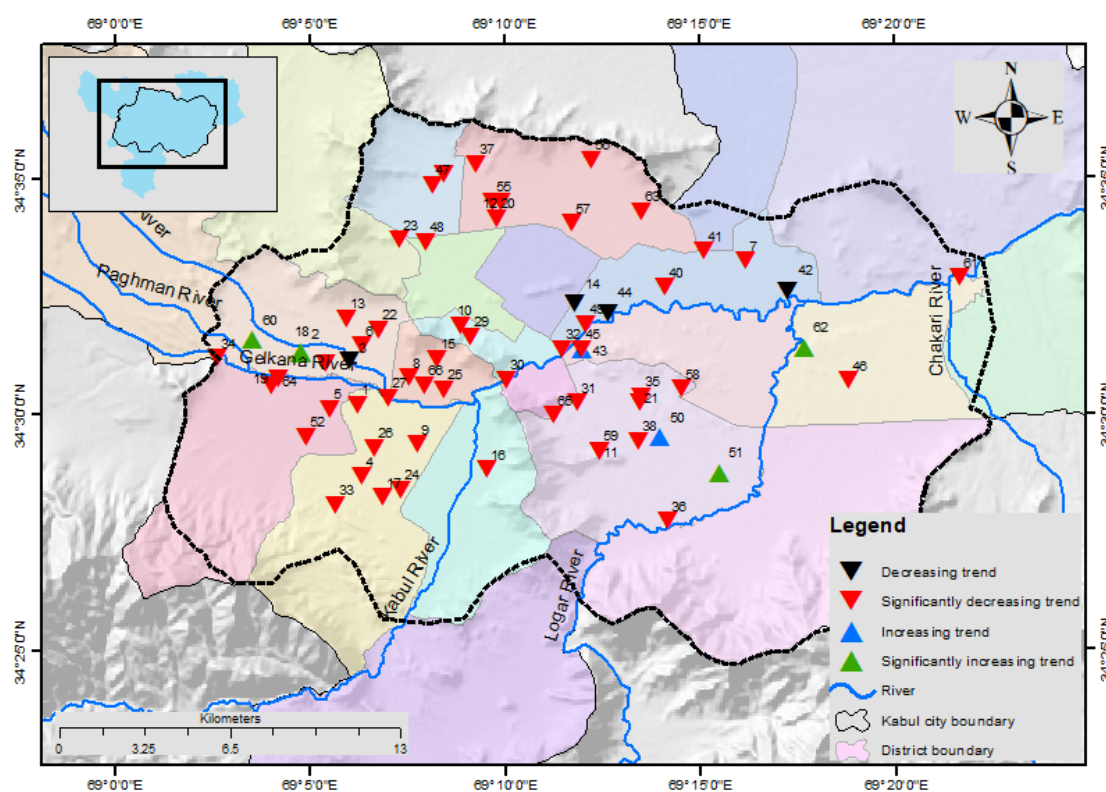


**Figure 4. 25 Annual groundwater level trends**

#### 4.4.3 Extent and Severity of Groundwater Drought Conditions

Groundwater drought index (SGI) values were calculated for all of the 66 observational points of the research area to determine the region's severity and spatial distribution of groundwater drought conditions. It is complicated and impossible to illustrate the groundwater drought results for all monitoring wells in this paper, so only key trends will be outlined here. According to Figure 4.25, all observational wells are divided into four main groups based on trend similarities, and a representative well within each category was chosen to reflect the groundwater drought outcomes. These are the wells identified as ID 1, which is typical of the group of wells that have significant decreasing trends; the wells identified as ID 60, which also has a significant decreasing trend; the wells ID 50 and ID 14, which have significant increasing trends. According to the SGI results, drought in groundwater has developed in the study area in recent years and is progressively worsening. Negative SGI values marked in red (Figure 4.26) indicate drought months, while values above zero indicate normal conditions, as shown in blue.

The drought conditions in Well 1 started in 2014 and continued until 2020. The SGI value increased gradually. During recent years (2019-2020), this well experienced extreme drought conditions. As represented in this well, the drought conditions in most wells started in 2014 and continued to deteriorate until 2020. This well illustrates the drought conditions in most of the wells of the study area. Extreme drought conditions in the well were recorded in 2019 with an SGI value of 2.2. The situation for well 60, which represents the wells with decreasing trends, is similar to

well 1. The drought conditions in this well commenced in 2016 and continued to intensify until 2020. During 2019-2020, this well experienced extreme drought conditions with an SGI value of 2.2. The condition for well 50 is different. It has undergone several months of drought conditions during its operation. The drought conditions appeared in this well alternatively from 2006 to 2011 and 2014 to 2020. A particularly high SGI value of 3 occurred in 2008 in this well.

The condition for well 14 is entirely different because it shows the positive trends in its group of wells. Drought in this well started in 2006 and ended in 2014. Again, it appeared in 2018 and continued to 2020 but generally with much lower SGI values than in the previous group of wells, although this well-experienced extreme had an SGI value of 2 in 2014. Only a limited number of wells in the study area show positive water level trends.

The SGI evaluation revealed that most of the wells in the city have been experiencing severe and ongoing drought since 2014. However, from a climate change perspective, rainfall in one of the meteorological stations shows a decreasing trend. It cannot be said that the decrease in groundwater level and drought in groundwater is due only to the reduction of rainfall. Consequently, analyses linking meteorological factors to groundwater drought are needed to understand the dynamic nature of groundwater drought by considering LULC changes and groundwater aquifer structures. This helps reduce the effects of groundwater drought vulnerability in a given area.

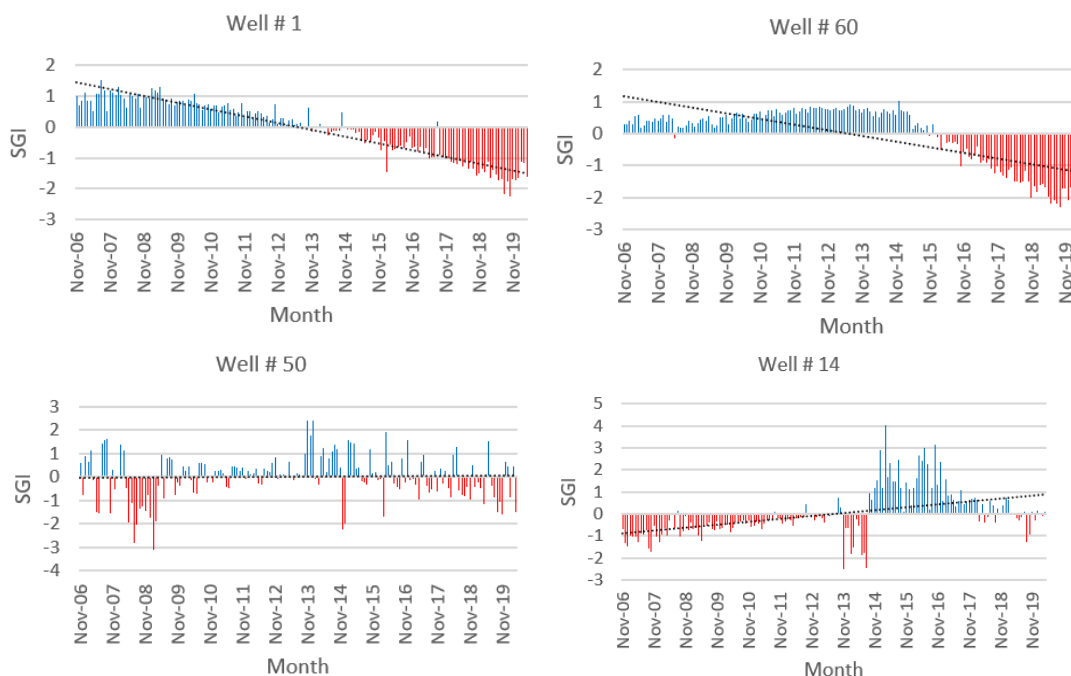


**Figure 4. 26 SGI time series for representative wells**



It can be inferred that the wells with IDs of 1 and 60, which have significantly declining water levels, have been experiencing severe and continuous drought since 2014 and 2016. The groundwater drought is similar to all other wells of these two groups. The condition in well 50 is different. This well belongs to a group of wells that showed an increasing water level trend. Therefore, the Well 50 experienced several short periods of drought conditions, which can be very intense. Well, 14, which belongs to a group of wells showing significantly increasing water levels, experienced continuous drought conditions before 2014. Subsequently, water levels in the well increased up to 2017. The signs of drought again appeared in 2018 and continued until 2020.

The persistent drought conditions observed in representative wells in each group are of concern for the ongoing management of groundwater resources in Kabul. The calculated SGI values in well numbers one and sixty, representing a large part of the study wells in the city, indicate the extent and severity of groundwater depletion in the region and indicate that management measures are urgently needed to address the situation.

#### **4.4.4 Rainfall conditions and groundwater levels**

Groundwater levels in the region are likely to be influenced by variations in the magnitude, duration, and intensity of rainfall events. Daily precipitation data from 2009 to 2019 have been collected from NWARA. Among six meteorological stations in the Kabul province, two stations (Payin-i-Qargha & Tangi-i-Sayedan) are located within the study area. The annual total precipitation and annual mean groundwater levels of all the wells have been plotted to visualize their relationships. As illustrated in (Figure 4.27), total yearly rainfall has been plotted with annual mean groundwater level separately for both meteorological stations where the continuous lines present the groundwater depth; bar charts indicate precipitation and dotted lines show linear trends.

Precipitation and groundwater depth have been graphically illustrated from 2009 to 2019. The chart displays the spatiotemporal distribution of two variables. From the chart, it can be seen that there is a correlation between precipitation and groundwater depth. The Payin-i-Qargha meteorological station shows a slightly increasing precipitation trend, but the Tang-i-Sayedan station indicates a decreasing trend in rainfall. On the other side, the mean depth of groundwater is going deeper and shows a gradual trend. The graph shows that the annual rise in rainfall does not positively impact groundwater levels. For instance, the total precipitation in 2012 and 2014 has risen, but the average depth to groundwater still shows the same linear trend. Even the slightly increasing trend in the western part of the city (Payin-i-Qargha station) does not positively affect groundwater depth. As already illustrated in the trend evaluation of groundwater, some wells in the study area show positive trends. Such temporal variance can include a rough estimate of groundwater recharge, although it will also be influenced by the LULC features, which can be measured concurrently.

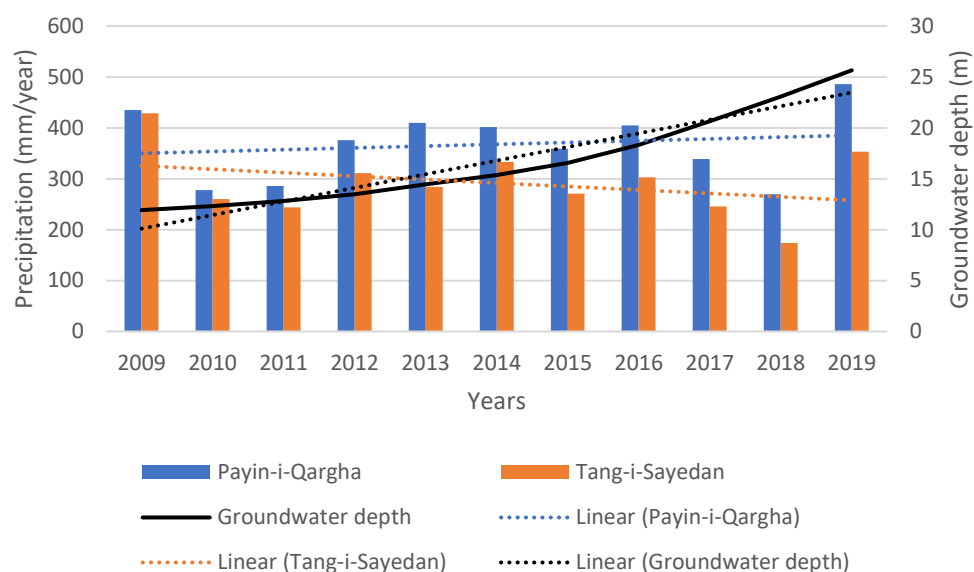


**Figure 4. 27 Rainfall and groundwater level time series**

#### 4.4.5 Influence of land use/land cover on groundwater recharge

The extent to which groundwater recharge can occur in a rainfall event may also be influenced by land use and land cover (LULC). Human interactions, such as the construction of roads and residential areas, can increase the area of impervious surfaces that may reduce groundwater recharge. Consequently, the process of urbanizing agricultural land may reduce groundwater recharge.

Due to these factors, LULC patterns in the Kabul area were examined in 2005, 2010, 2015, and 2020 (Figure 4.28). Six classes of LULC have been developed, and their accuracy has been measured using overall accuracy assessment and the Kappa index. The overall accuracy index for LULC classification in the study area for the years 2005, 2010, 2015, and 2020 was determined to be 94%, 90%, 90%, and 90%, while the Kappa accuracy index was 91%, 86%, 86%, and 86% respectively. The summary of LULC analysis of the study area is illustrated in (Table 4.20).

The urbanized area is a critical component of LULC, as it significantly negatively affects groundwater recharge. The proportion of the study area covered by urban development was determined to be about 15% in 2005, 20% in 2010, 27% in 2015, and 32% in 2020.

The agricultural area is a critical LULC component crucial in groundwater recharge. A decrease in agricultural areas can be due to increased urbanization or decreased rainfall and desertification of agricultural land (conversion of agricultural areas to bare land). However, from 2005 to 2020, the area of agricultural land in Kabul decreased by only about two percent. On the other hand, the bare land is more permeable than built-up areas. Water melted by snow can cause the gradual feeding of groundwater in the bare land area. The area covered by bare land in the study area has decreased from about 67 % in 2005 to 52 % in 2020. Figure 4.29 illustrates the

decrease in bare land and the increase in built-up. The percentage of water bodies (Qargha Lake) has not changed. The marshland area also has decreased.

The LULC analysis indicated that the number of trees in the study area has increased.

To sum up, the city's development and built-up area will cause the reduction of agricultural and bare land area. City development would result in increased region coverage by impervious surfaces and a decrease in groundwater recharge. Most monitoring wells are located in urban areas where artificial groundwater recharge measures would be required to increase groundwater availability.

**Table 4. 20 Areal specification of LULC class**

Classes	2005		2010		2015		2020	
	Area (km <sup>2</sup> )	Area (%)	Area (km <sup>2</sup> )	Area (%)	Area (km <sup>2</sup> )	Area (%)	Area (km <sup>2</sup> )	Area (%)
<b>Waterbody</b>	0.76	0.07	0.70	0.07	0.9621	0.09	0.70	0.07
<b>Marshland</b>	1.09	0.11	1.02	0.10	1.3833	0.13	0.79	0.08
<b>Built up</b>	157.90	15.33	209.79	20.36	275.0058	26.70	328.45	31.88
<b>Bare Land</b>	687.52	66.73	691.66	67.14	589.8357	57.26	538.17	52.24
<b>Agricultural Area</b>	175.73	17.06	117.09	11.37	160.4259	15.57	151.50	14.71
<b>Trees</b>	7.32	0.71	9.98	0.97	2.5479	0.25	10.51	1.02
<b>Total</b>	1030.32	100.00	1030.22	100.00	1030.16	100.00	1030.13	100.00

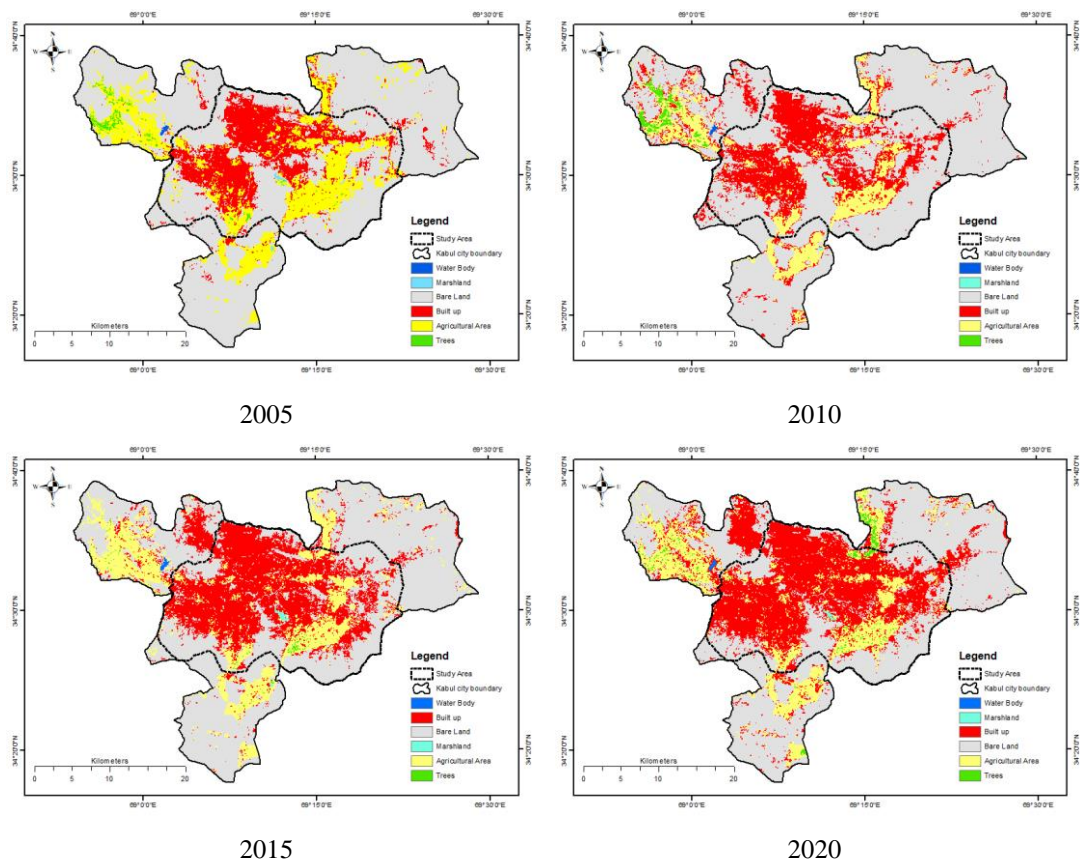


**Figure 4. 28 LULC maps of the study area**

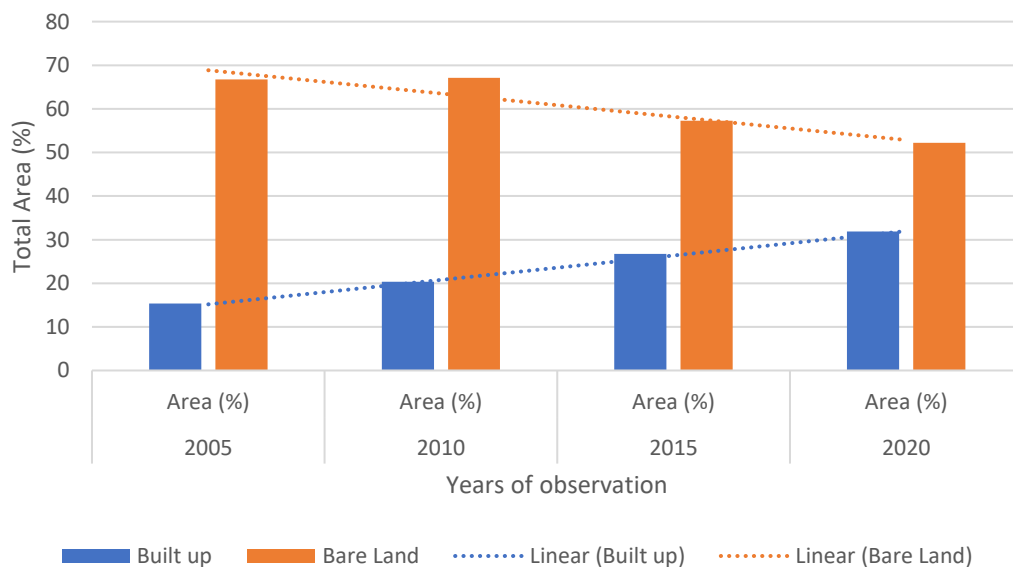


**Figure 4. 29 changes in built-up and bare land area**

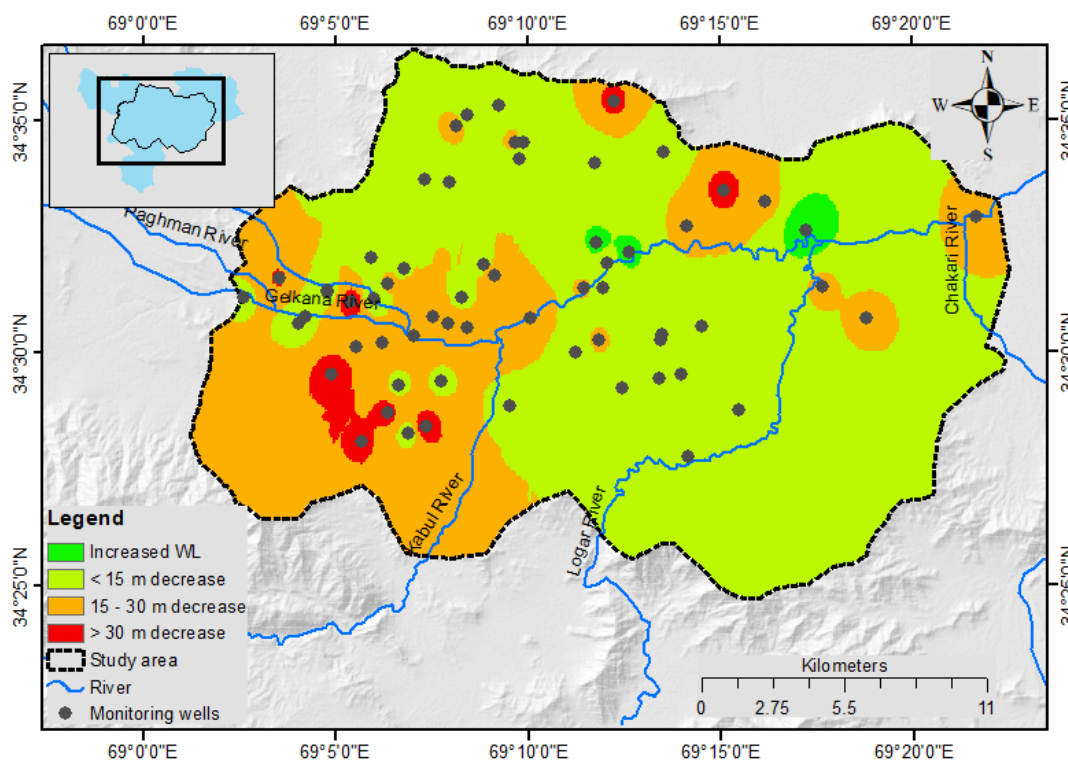


**Figure 4. 30 Spatial distribution of variance in groundwater level from 2007 to 2019**

As can be seen from the spatial map of variance in groundwater level from 2007 to 2019 (Figure 4.30), in the western, southwestern, and northern areas of the study area, some monitoring wells show a very sharp decrease (the decrease in the level of underground water in these wells are more than 30 meters). In the same way, in the western, southwestern, northern, and some northeastern parts of the basin, a large number of observation wells have witnessed a significant decrease of about 15-30 meters. The remaining parts of the study area have witnessed a decrease in the water of fewer than 15 meters. Only some wells located on the bank of the Kabul and Logar rivers have witnessed an increase in the water level.

## 4.5 Groundwater potential zone

### 4.5.1 AHP Weights and Ranks

The rankings of each parameter and weight in AHP are illustrated in Table 4.21. Every sub-feature within a parameter is multiplied by its weight. For each parameter, the AHP weights are given per subclass influences applied to the ranks, and the ranks are numbered from 1 to 9. The weights were measured in such a manner that each parameter's effect was significant.

### 4.5.2 Geology

The porosity and penetrance of the rocks are clear indicators of groundwater occurrence and recharge in a given area. Whereas geological configurations have a detrimental effect on groundwater occurrence, the geological map is significant (Maheswaran et al., 2016). The thematic geological map was digitized and georeferenced from the "geologic map of quadrangle 3468, Chak Wardak-Syahgerd (509) and Kabul (510) quadrangles, Afghanistan" (R. G. Bohannon & Turner, 2005). The common geological forms in the study area are sandstone and siltstone, conglomerate and sandstone, loess, fan alluvium and colluvium, and ultramafic intrusions (Figure 4.31 a). The thematic map is ranked based on regulating geological formations' permeability and groundwater effects. Loess, conglomerate, and sandstones are good aquifer materials due to their high weathering and fractures. Maximum values were classified for loess and conglomerate, and minimum ratings were allocated to sandstone and dolomite. The geological characteristic is assigned to a corresponding AHP weight of 0.14.

### 4.5.3 Drainage density

Drainage carries precipitation water, glacial, or snowmelt to the plains. It is essential in a given area as the source of groundwater recharge. Hydrogeological faults, fractures, and joints are essential factors for groundwater recharge, and they are perceived as guiding criteria that can impact a basin's drainage systems. Therefore, drainage operates as a transmission tool for passing snowmelt and glacial melting. Drainage density is the ratio of total stream lengths and the area in a watershed. The small runoff will happen within the neighbourhoods with high density due to their higher conductivity (Abijith et al., 2020; Pinto et al., 2017). The extraction of drainage density has been done in the arc GIS environment by processing SRTM-DEM data (Figure 4.31 b). The importance of drainage density and the occurrence of groundwater are closely associated. The thematic map of drainage density developed into five subclasses. The extracted interval values of 1.8 - 2.6 km/km<sup>2</sup> were highlighted with high ranking and 0.0 - 0.22 km/km<sup>2</sup> with a minor value. The influential layer of drainage density is assigned a corresponding weight of 0.12.

**Table 4. 21 AHP ranking and weighting with classes of parameters**

<b>Parameter &amp; AHP Weights</b>	<b>Rank</b>	<b>Parameter &amp; AHP Weights</b>	<b>Rank</b>
<b>Geology (14)</b>		<b>Geomorphology (8)</b>	
Limestone and dolomite	2	Mountain relief	7
Sandstone and siltstone	4	Holocene river valleys	8
Gneiss	5	<b>Soil (7)</b>	
Fan alluvium and colluvium	5	None	2
Conglomerate and sandstone	9	Moderately well-drained	5
Ultramafic intrusion	4	Well-drained	8
Loess	9	<b>Lineament density (9)</b>	
<b>Drainage Density (12)</b>		0.00 - 0.042	1
0.00 - 0.22	1	0.43 - 0.11	3
0.23 - 0.61	3	0.12 - 0.2	4
0.62 - 1.10	4	0.21 - 0.3	7
1.20 - 1.70	4	0.31 - 0.46	8
1.80 - 2.60	5	<b>Rainfall (8)</b>	
<b>Land-use land-cover (11)</b>		299.4 - 313.8	6
Cropland	9	313.9 - 322.9	8
Marshland	8	323 - 332.9	9
Barren land	6	333 - 346.6	7
Barren rock	4	346.7 - 365.2	5
Settlement	4	<b>Elevation (12)</b>	
<b>Slope (9)</b>		1763 - 1843	9
0.00 - 4.46	5	1843.1 - 1945	8
4.461 - 11.54	4	1945.1 - 2089	7
11.55 - 20.46	3	2089.1 - 2290	6
20.47 - 30.17	1	2290.1 - 2823	3
30.18 - 66.90	1		
<b>Water Depth (10)</b>			
2.7 - 7.7	9		
7.8 - 13	7		
14 - 21	6		
22 - 32	2		
33 - 53	1		

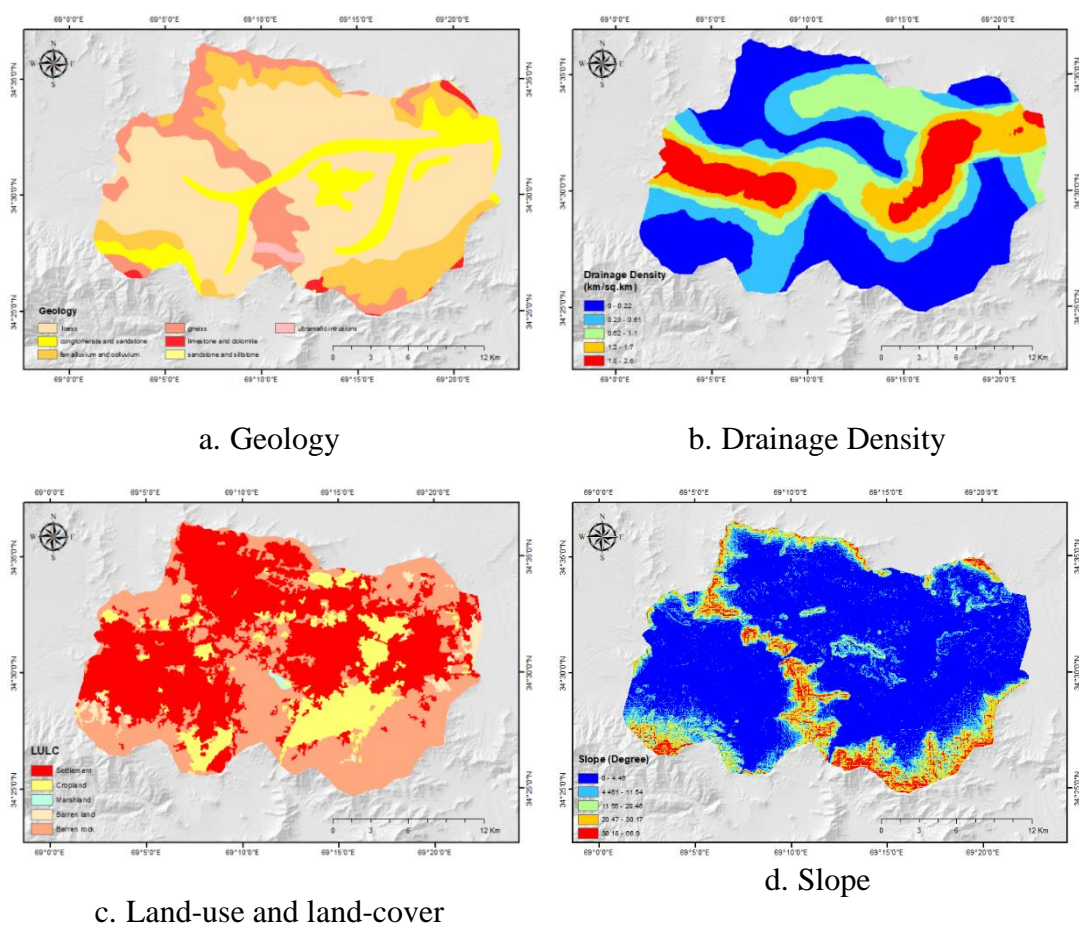


**Figure 4.31** Geology, Drainage Density, LULC, and Slope maps of the basin

#### 4.5.4 Land-use and land-cover

Land use and land cover are crucial aspects that significantly affect the recovery and occurrence of groundwater (MacHiwal et al., 2011; Martin et al., 2017). The development of cities and the impermeability of the land surface will reduce groundwater recharge. Remotely sensed Landsat-8 satellite data was interpreted to generate a LULC thematic map (Figure 4.31 c). A supervised classification technique was adopted. The study area has mountainous and plain bare land, a bare rock area, a cropland and vegetation area, settlements, and a permanently inundated marshland. Settlements diminish the effect on groundwater recharge, while vegetation-covered areas have more excellent groundwater recharge opportunities. Therefore, bare land and settlement areas are weak in terms of groundwater availability, but agricultural areas and vegetation are very appropriate. For assigning weights and ranks, the highest ranks are appointed on croplands, followed by marshland natural bar lands, and the slightest rank is given to settlements. The resultant AHP value of 0.11 is assigned to the LULC feature.



#### 4.5.5 Slope

The slope has a substantial impact on runoff and represents the elevation difference in a given area. Meanwhile, it has a graceful role in the occurrence and recharge of groundwater. Areas with steeper slopes are not considered valuable substrates for groundwater recharge, as steeper slopes cause rapid runoff, are associated with erosion, and reduce water infiltration into the soil. Nevertheless, on the contrary, lands with lower slopes and flat areas are a good bed for groundwater recharge because, in these areas, runoff moves at a slower speed, and there is enough time for the infiltration process to provide the situation for groundwater recharge (Martin et al., 2017; Pinto et al., 2017). SRTM-DEM data was interpreted in the Arc GIS environment to delineate the slope map. The study area is surrounded by mountains whose slope decreases towards the centre of the basin. The lateral parts and some central portions of the basin have a high slope, and the majority of the regions have a gentle slope with outstanding qualifications for groundwater. Five different slope categories are presented in the results of the classification of the slope map in the basin (Figure 4.31 d). The lower slope from  $0^{\circ}$  to  $4.46^{\circ}$  has been given a high rank, and the lowest rank is allocated to  $30.18^{\circ}$ - $66.9^{\circ}$ . The derived weight of 0.09 is assigned to the slope feature.

#### 4.5.6 Geomorphology

A geomorphological map illustrates notable geomorphic elements, landforms, and the underlying geological formations. The morphology and its characteristics exert a significant influence on the development, filtration, and replenishment of water into the subsurface layers of the Earth (Etikala et al., 2019; A. Kumar & Pandey, 2016). A thematic geomorphological layer has been digitized and extracted in Arc GIS 10.8 from the country geomorphological map prepared by AIMS (Figure 4.32 a). The basin has a Holocene River valley and mountain relief. Holocene river valley, having a gentle slope with medium vegetation, widely covers most parts of the basin. This geomorphologic point can be the appropriate infiltration bed for groundwater recharge potential. Mountain relief covers some parts of the area in the east and south. Both geomorphological typologies of the study area were assigned high rank. The derived weight of 0.08 is assigned to the geomorphological feature.

#### 4.5.7 Soil

Soil forms as a consequence of the erosion process from fragments of rocks. It is the only medium in which groundwater is recharged, so its attributes are essential for discovering groundwater potential. Soils cause groundwater recharge and storage in terms of their storage capacity and absorption rates, depending on the soil type (Abijith et al., 2020). The required data were extracted from the Afghanistan Soil Catalogue (Ahmadzai & Omuto, 2019) to delineate the soil map. Soil is labelled as per the drainage ranges, showing wetness period, well-drained, moderately well-drained, and none is observed in the basin (Figure 4.32 b). High and least ranks were assigned to well-drained and class of none accordingly. The derived weight of 0.07 is given to the soil feature.

#### 4.5.8 Lineament density

In the crystalline terrain, curved or linear geological formations are called lineaments and are massively crucial in groundwater potential recharge and flow. Primary lineaments and their convergence regions will serve as potential high-yield groundwater areas. Its role in the recharging of groundwater is also undeniable (Siddi Raju et al., 2019; Thapa et al., 2017). The lineament density map (Figure 4.32 c) is prepared from Landsat-8 OLI data (Landsat Scene Identifier: LC08\_L1TP\_153036\_20200704\_20200708\_01\_T1; Date of acquisition: 02-08-2020) using PCI Geomatica Banff and Arc GIS 10.8. The high to low-density scale is usually associated with the groundwater capacity. The alignments of lineament in the current study are SW-NE, N-S, and E-W. The intersection areas of lineaments have a high groundwater potential. The north, north-central, and south parts of the study area represent wider concentrations of lineament. The areas possessing larger lineament density (0.31–0.46 km.km<sup>-2</sup>) were assigned as high rank, and accordingly, areas with minor values of lineament density (0–0.042 km.km<sup>-2</sup>) were assigned low scale values. The derived weight of 0.09 is given to the lineament feature.

#### 4.5.9 Rainfall

Rainfall seems to be the only main groundwater recharge source and the water cycle's primary water source. It counts as the critical explanation for recharging groundwater where water from cracks and soil penetrates the earth's subsurface. Other attributes of precipitation, such as duration and frequency, also affect runoff and recharge (Abijith et al., 2020). Ten years (2008-2018) of daily precipitation data were obtained from NWARA Afghanistan, and its spatial distribution was interpolated in the Arc GIS environment using the IDW technique (Figure 4.32 d). The mean annual precipitation is obtained at 330 mm in the Kabul basin. According to average annual precipitation, the research area is subdivided into five distinct regions. As the whole basin is in a moderate state, the records show somewhat higher precipitation in the basin's northwestern parts. A high rainfall area (347-365) mm is ranked with a higher value, but the lower rank is assigned to 299-313 mm. The resulting derived weight of 0.08 is allocated to the precipitation feature.

#### 4.5.10 Elevation

The altitude variable is one of the primary factors in the differentiation of GWRPZ. There is an indirect correlation between elevation and infiltration rates (Thapa et al., 2017). The 30 m resolution SRTM-DEM data has been utilized to delineate the elevational map of the research area. The highest elevation is differentiated mainly in the south and southwestern sections of the study region. A linear algorithm of elevation from south to north east has appeared in the study area, which has relatively higher elevation.

Meanwhile, northern parts of the basin also encountered a higher elevation area (Figure 4.32 e). According to elevation from mean sea level, the basin is grouped into five subclasses, including 1363-1843, 1843.1-1945, 1945.1-2089, 2089.1-2290, and 2290.1-2823 m in the Arc GIS environment. Strong preference is assigned to lowlands, followed by moderate and high-elevation areas. The resulting weight of 0.12 is allocated to the elevation feature.

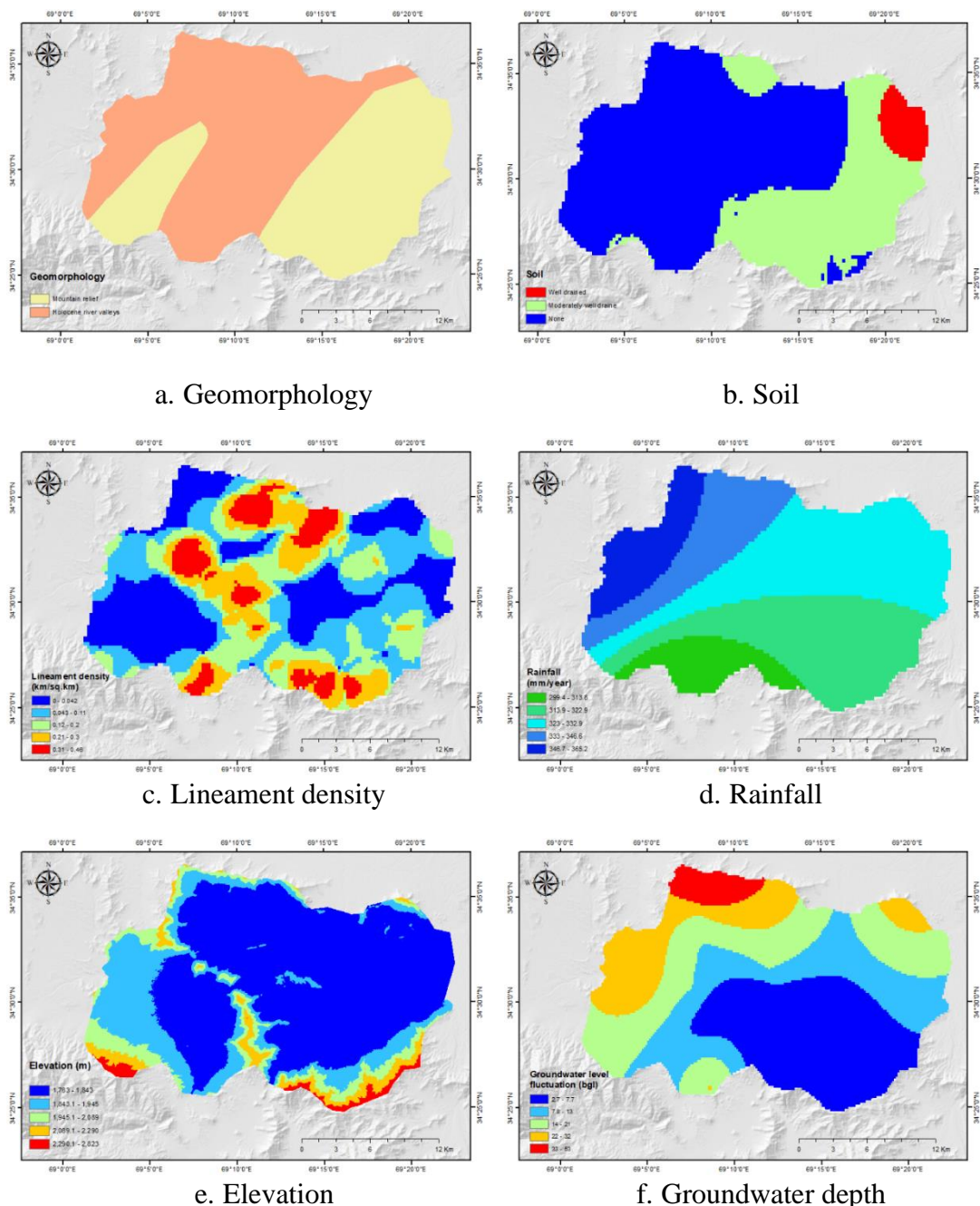


**Figure 4. 32 Geomorphology, Soil, Lineament density, Rainfall, Elevation and Groundwater depth maps of the study area**

#### 4.5.11 Groundwater levels

Long-term statistics on the variance of groundwater tables give insights into the prospects for groundwater. It is also regarded as one of the crucial variables for the discovery of possible groundwater recharge areas. The AGS, supported by USGS, recorded nine-year monthly monitoring (2004-2013) of groundwater levels in the Kabul basin. The total number of monitoring wells is 71, out of which forty wells' data were randomly selected to create a groundwater level thematic raster.

The water level data of 38 observation well stations located within the study area were utilized to validate the final produced GWPZ map. The data's interpretation revealed that, during observation, the minimum and maximum water depth ranged from 2.7 to 7.7 m and 33 to 53 m below ground level, respectively (Figure 4.32 f). The areas with shallow groundwater levels ranked higher weights, and conversely, less weight was given to the more in-depth groundwater classes. The resulting weight of 0.10 is allocated to the groundwater level feature.

#### 4.5.12 Groundwater potential zone mapping

Finally, weights were allocated to the input variables utilized by the AHP method for GWPZ delineation. All influential layers have been converted to a raster format and multiplied by using Arc GIS 10.8 with derived weights and ranks. Ultimately, the final output of processed thematic layers was obtained in five different categories. Finally, the findings were summarized and identified as very good, good, poor, and very poor (Figure 4.33). The following equation was considered for the development of the ultimate GWPZ map:

$$GWRPZ = \sum_i^n (GM_w * GM_r) + (LD_w * LD_r) + (LU\&LC_w * LU\&LC_r) + (G_w * G_r) + (S_w * S_r) + (So_w * So_r) + (SD_w * SD_r) + (R_w * R_r) + (E_w * E_r) + (GWL_w * GWL_r) + \dots \dots \dots (4. 6)$$

Where GWPZ = Groundwater Potential Zone, w = weighting, and r = ranking of the variables.

GM = Geomorphology, LD = Lineament Density, LU&LC = Land-use and Land-cover, G = Geology, S = Slope, So = Soil, SD = Stream Density, R = Rainfall, E = Elevation, GWL = Groundwater level.

A region with a weak and fragile potential is located in the basin's periphery, dominated by hills, slopes, and mountainous areas. The centre portion of the basin has a moderate to high groundwater potential. Geology has received a high priority, and lower priorities have been assigned to soil and geomorphology. The most significant groundwater potential zones identified are loess, conglomerate, and sandstone in geology, cropland in land-use, and land cover well-drained soil in soil types throughout the basin. The centre parts of the basin illustrate groundwater's intense potential, with a gentle slope and high drainage density. Rainfall has an essential function in the recharging of groundwater. The obtained outcomes from the AHP indicate that the percentage of the basin under very poor is about 16%, poor

(18%), good (35%), and very good (31%). High and very high GWPZs have been discovered in most parts of the basin, which are located along the river courses.

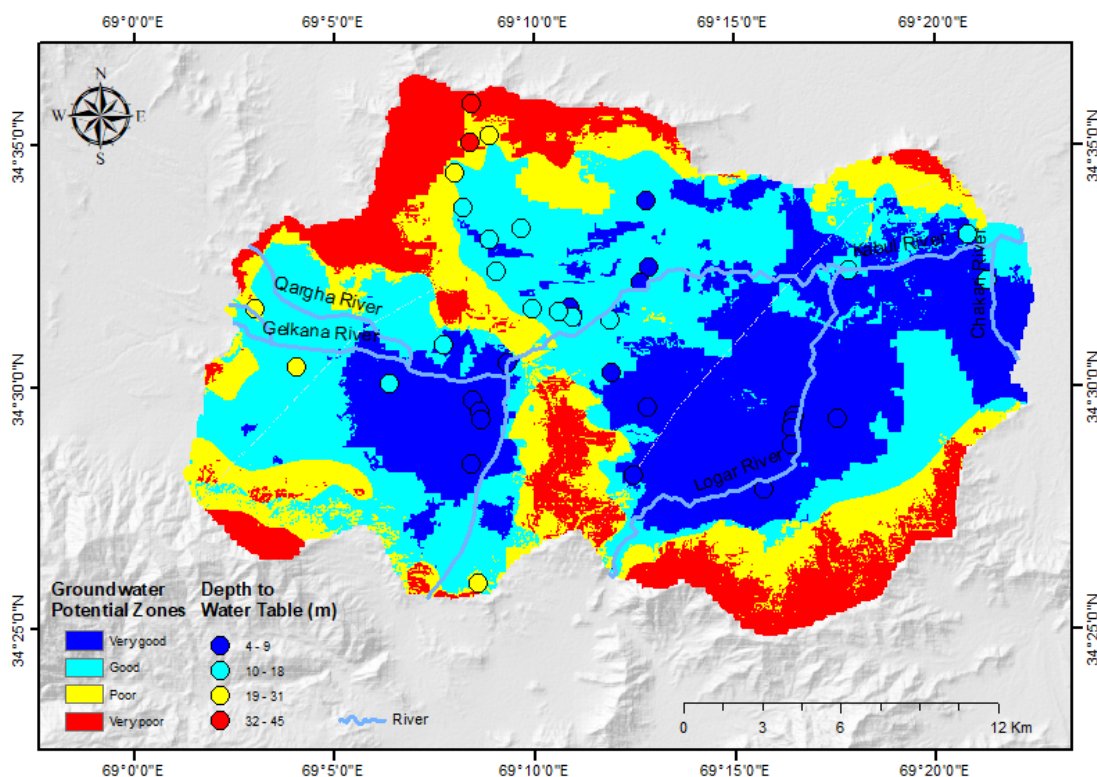


**Figure 4.33 Groundwater recharge potential zones map using AHP**

#### 4.5.13 Validation of results

The result has been validated using nine years (2004-2013) recorded data of the static water level for 38 monitoring wells through the AGS department supported by USGS. The monthly collected data has been classified with the minimum, average, and maximum values. Mean values of each monitoring well have been used to validate the results. All 71 monitoring wells that are available for the Kabul basin were added to ArcGIS, and the required monitoring wells for validation of the result were clipped through ArcGIS with the study area boundary. Out of 71 monitoring wells, only 38 wells were located within the study area (Figure 4.34). The average value of water depth in the observed monitoring wells ranged between 4 to 45 m. According to the observation of static water level in the well, the mentioned monitoring wells were classified into four classes viz. 4 - 9 m, 10 - 18 m, 10 - 31 m, and 32 - 45 m, which was attributed to as very good, good, poor, and very poor (Figure 4.34). Accuracy assessment is determining the relationship between the resulting groundwater potential zone map and field observations. An uncertainty matrix is used to determine reliability (Table 4.22). The following formula is applied to determine the overall accuracy (Siddi Raju et al., 2019).

$$\text{Overall accuracy} = \frac{\text{No. of correct MWL}}{\text{Total No. of MWL}} = \frac{32}{38} = 86.84\% \dots\dots\dots (4.7)$$

Where MWL = Monitoring Well Location.

The agreement's kappa coefficient has been used since 1980 in remote sensing as an index to remark the accuracy of classified images for thematic layers. The Kappa coefficient of the agreement is calculated using the following formula (Foody, 2020).

$$k = \frac{p_o - p_e}{1 - p_e} \dots\dots\dots (4. 8)$$

Where  $p_o$  is the percentage of the overall precision and  $p_e$  is the percentage of appropriate agreement with the values measured. The overall accuracy and kappa coefficient values are obtained at 86.84 per cent and 0.79, respectively. The accuracy assessment in both overall and kappa assessment methods indicates a very good association between potential groundwater zones and well record values.

**Table 4. 22 Uncertainty matrix of groundwater recharge potential zones**

No.	GWPZ	Very good	Good	Poor	Very poor	Total	Correct Samples
1	Very good	16	2	0	0	18	16
2	Good	2	11	0	0	13	11
3	Poor	0	1	4	0	5	4
4	Very poor	0	0	0	2	2	2
	Total	18	14	4	2	38	33
<b>Overall accuracy = 32/38 = 86.84%</b>							
<b>Kappa coefficient = 0.79</b>							

## 4.6 Artificial recharge potential of groundwater in urban area

### 4.6.1 Rainfall conditions

The rainfall in Kabul varies over the months, as seen in Figure 4.35. The last six months of the year are the wettest according to the coefficient of variation, and the coefficient of variation for the rainfall during these months reached as high as 127% (October). In contrast, it decreases during the first six months of the year, and the coefficient of variation has a minimum value of 46% (February).

According to many indexes, Kabul has inconsistent, seasonal, and intense precipitation (Figure 4.35). The most rainfall occurred during February, March, and April. In 2019, the first five months of the year (January through May) had more than 83 per cent of the year's total rainfall. In 2019, the two wettest months (February and April) alone saw up to 45 per cent of the yearly precipitation.

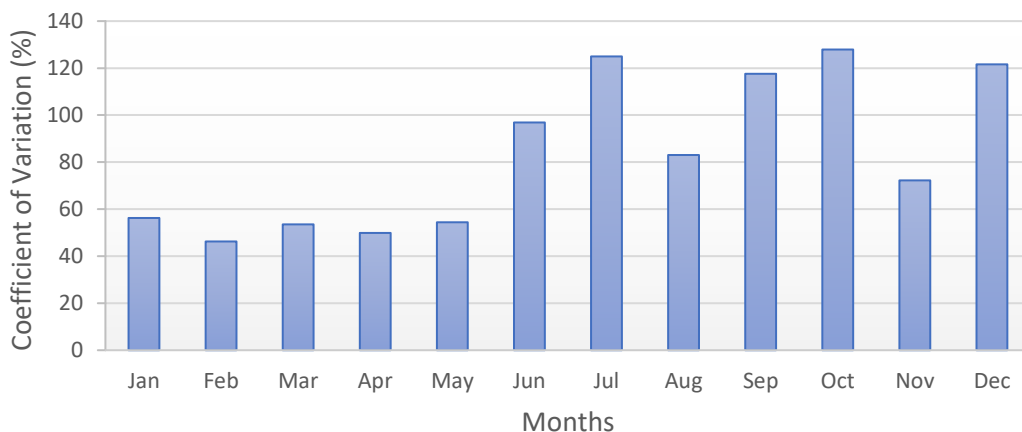


**Figure 4. 34 Variability of precipitation during regular times as determined by the coefficient of variation**

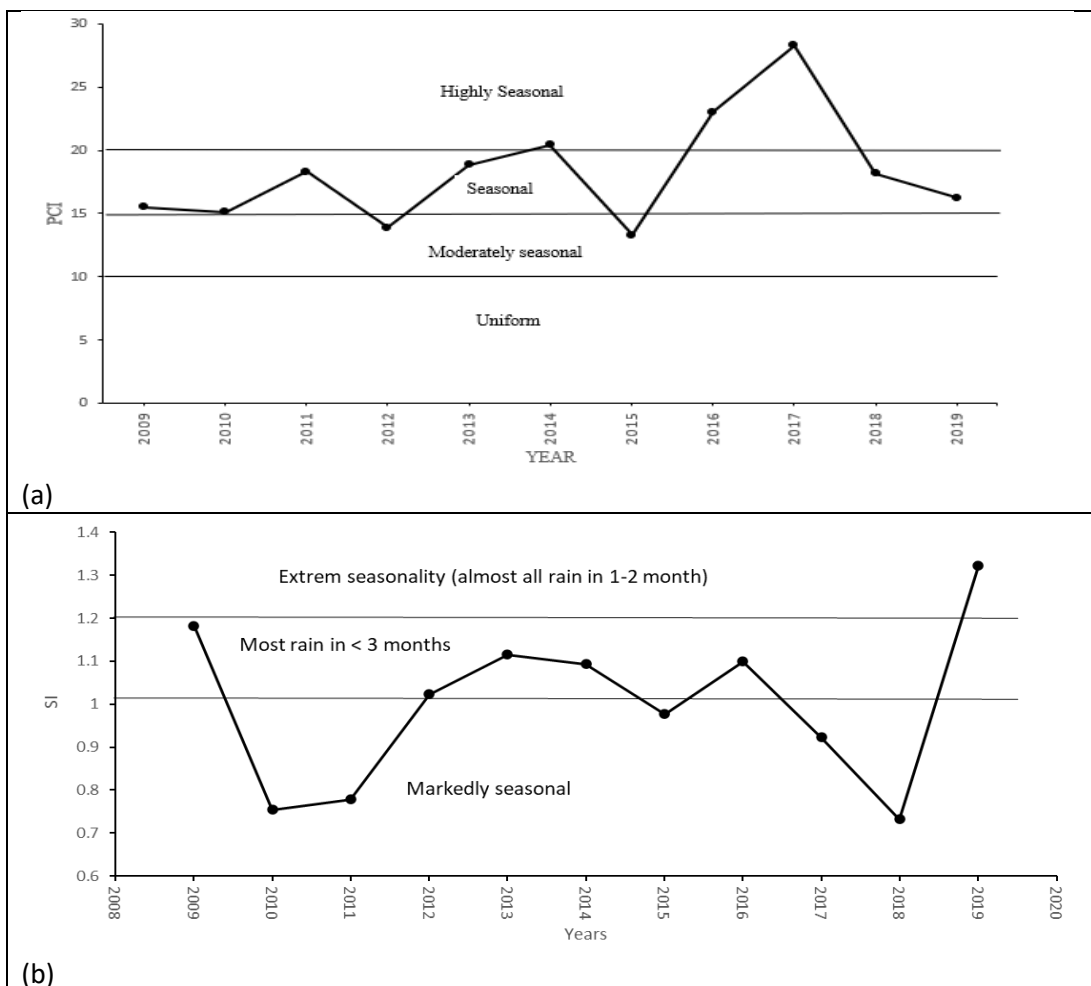


**Figure 4. 35 The seasonality and concentration of precipitation (a) precipitation concentration index, (b) seasonality index, and (c) average per cent contribution to annual rainfall.**

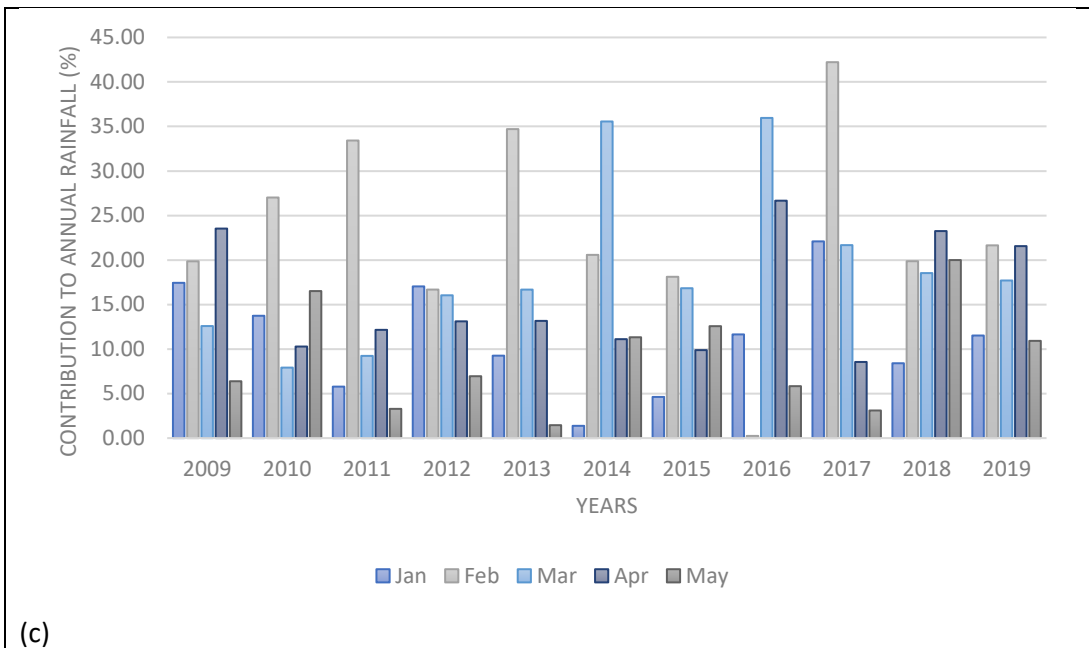


**Figure 4. 36 (Continued)**

Given the region's yearly rainy days, concentration feature, and low overall quantity of precipitation, understanding how much rain falls over a day is crucial. For the time series depicted in Figure 4.36, the mean annual rainfall is 368 mm, with an average rainy day of about 80 days each year.

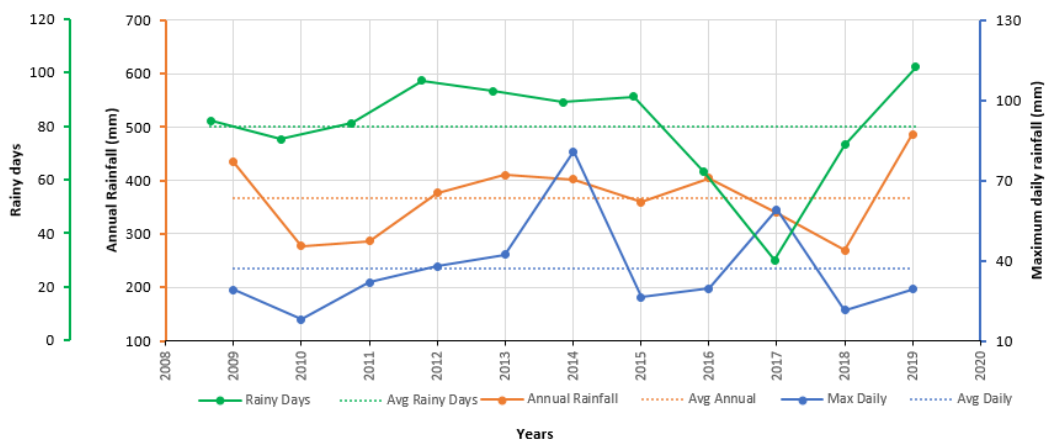


**Figure 4. 37 Time series of annual precipitation, daily maximum precipitation, and yearly rainy days.**

According to Figure 4.36, the year 2019 had the most precipitation, with a total of 486.21 mm. The minimum amount of precipitation happened in 2017, with a total record of 269.4 mm. The maximum daily precipitation was recorded on 17 March 2014 with a rainfall amount of 80.77 mm, which caused floods with an inundation



level of 60 to 80 cm (Manawi et al., 2020). According to the maximum rainfall record of the meteorological station, the minimum (from the daily maximum precipitation record) precipitation was observed on 28 January 2010 with a precipitation amount of 18.04 mm. According to observations of rainy days, the research region experienced a minimum of 30 rainy days in 2017 and a maximum of 102 rainy days in 2019.

The probability analysis using the Weibull approach for the years 2009 to 2019 (Figure 4.37) shows a return period of 3 to 4 years for daily rainfall of less than 30 mm. Therefore, the previously described urban issues, such as street floods, would definitely happen every 3-4 years. The quantity of 80.77 mm, which has a return cycle of ten years, was the largest amount of rainfall recorded in 2014 thus far.

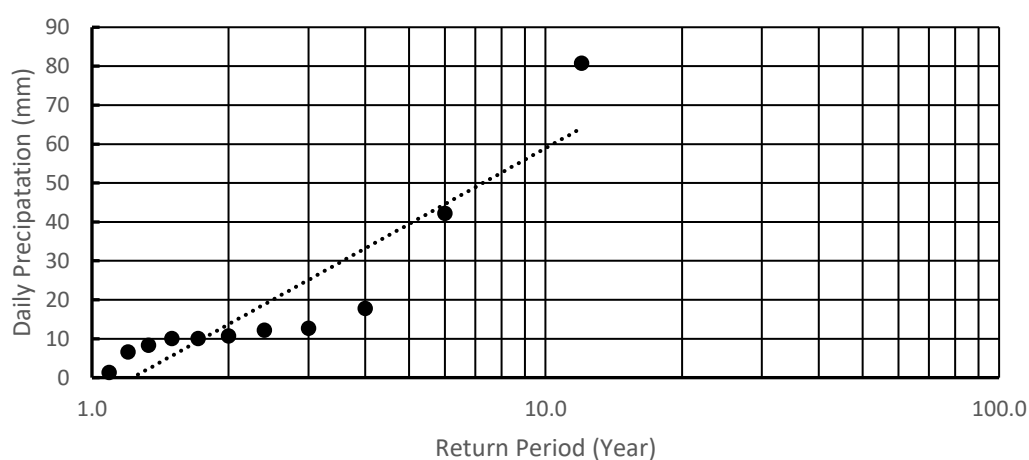


**Figure 4. 38 daily precipitation probability curve from Jan 2009 to Dec 2019**

The statistical analysis, which used the Gumbel technique for rainfall extremes, produced mean and standard deviation values of 36.87 mm and 18.23 mm, respectively. As a consequence, the constants  $y_n$  and  $S_n$  Eq. (7) had respective values of 0.4996 and 0.9676, respectively. Figure 4.37 depicts the probability curve for the highest daily precipitation.

Using Eq. (6), a return period of 1 to 5 years is calculated for the threshold rainfall depth of 55 mm, which is expected to enhance the danger of flooding in the city. For the 122 mm record, a return time of about 150 years has also been discovered. The findings above demonstrate that there is a very high likelihood that the problematic runoff from the 55 mm precipitation will reoccur. As a result, there is a very high likelihood that RWH will occur in the urban region of the Kabul basin.

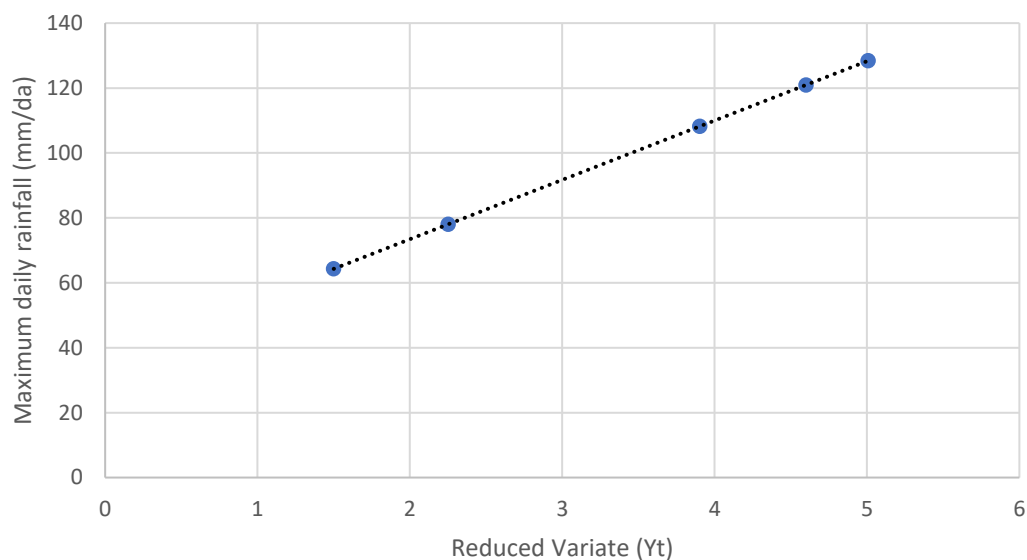


**Figure 4. 39 Maximum daily rainfall probability curve (2009–2019)**

#### 4.6.2 RWHRs vs non-RWHRs conditions

Based on a developed LULC map, the  $I_{c(eff)}$  was estimated for the research region under the circumstances with and without RWHRs. As stated previously, it is expected that the primary land covers of the urban environment are built up having  $I_c$  of 5% without RWHRs and 80% with RWHRs, arable land with  $I_c$  of 40%, and barren soil with  $I_c$  of 50% has been applied. After segregation of LULC of the study area, built-up, bare land, and arable land, as well as their  $I_c$ , it was possible to compute the total  $I_{c(eff)}$  of the entire region employing (Eq.9)

The spatial proportion of each LULC is illustrated in Table 4.23, including the computed  $I_{c(eff)}$  and groundwater infiltration rates for RWHRs and non-RWHRs situations with  $R = 368$  mm (average yearly rainfall at the region from 2009 to 2019 data from Payin-i- Qargha meteorological station). The significance of groundwater recharge by RWHRs for the regional and municipal water cycles is illustrated in Table 4.23. According to Table 4.23, compared to non-RWHRs circumstances, RWHRs will increase  $I_{c(eff)}$  by factors of 2.33 for the studied area.

**Table 4. 23 Calculated spatial proportion of LULC and their influence on  $I_c(eff)$  and groundwater recharge in the Kabul basin.**

LULC	Total area	Spatial fraction (%)	Calculated $I_{c(eff)}$		Calculated groundwater recharge (cu.m)	
			Without RWHRs	With RWHRs	Without RWHRs	With RWHRs
<b>Built up</b>	234.2079	48.06	27.13%	63.18%	4864510.227	11328409.74
<b>Arable land</b>	60.381	12.39				
<b>Bare Soil</b>	192.6495	39.53				

Implementing RWHRs across the entire built-up area of the city may increase average annual infiltration from 4.86 MCM (million cubic meters) to 11.33 MCM for  $I_{c(eff)}$  values of 27.13 per cent and 63.18 per cent, which are calculated for study area for non-RWHRs and RWHRs conditions, respectively. These factors, along with the total surface area of the Kabul basin, which is equal to 487.24 km<sup>2</sup>, and annual precipitation of 368 mm. This straightforward calculation indicates how the Kabul Basin's groundwater recharge might rise by 6.5 MCM as a result of the deployment of RWHRs, which is more than 200 per cent greater than groundwater recharge under non-RWHRs conditions. The computed  $I_{c(eff)}$  of 63.18 per cent has a limited potential to create severe flood events with regard to surface runoff. Based on Eqs. (3) and (4), it is predicted that the implementation of RWHRs in the study region will result in a 36% reduction in surface runoff volumes for an average land cover of 48% built-up, 12% arable land, and 40% barren land. Based on Eqs. (11) and (12), it is predicted that the implementation of RWHRs in the study region will result in a 36% reduction in surface runoff volumes for an average land cover of 48% built-up, 12% arable land, and 40% barren land.

#### 4.6.3 Surface runoff estimation

The land-use map of the Kabul Basin is depicted in Figure 4.31 c. The correlation between rainfall and runoff is determined by the land cover, which equates to the soil's ability to retain water. The region is discovered to be divided into five different types: settlements, cropland, marshland, barren land, and barren rocks. According to soil characteristics studied by (Ahmadzai & Omuto, 2019) the soil is deep and varies in texture from sandy loam to loam and clay. Therefore, based on soil classification by (USDA, 2009), the hydrological soil group of the area is assigned to group B. Soils in this group have moderately low runoff potential when thoroughly wet.

**Table 4. 24 Curve Number values based on LULC.**

No.	LULC	Area (sq.km)	Land cover area (%)	CN (%)	CN <sub>wi</sub> (%)
1	settlement (impervious area)	234.21	48.07	98	4710.707
2	cropland	60.38	12.39	76	941.8297
3	barren land	9.63	1.98	86	170.0537
4	barren rock	183.01	37.56	86	3230.306
<b>Total</b>		<b>487.2384</b>	<b>100</b>		<b>9052.896</b>

The CN<sub>wi</sub> values for each land use class are displayed in Table 4.24 in relation to the associated region. The area's domination of impervious surfaces is confirmed by the CN<sub>w</sub> value, which is determined to be 90.5% (Eq.13). The initial abstraction and maximum soil retention are equal to 26.6 mm and 5.3 mm, respectively when the CN<sub>w</sub> value is substituted in Eq. (12). This allows for the determination of the probable runoff depth for the daily precipitation. The amount of rainfall required to generate runoff is discovered to be 5.3 mm.

The highest daily precipitation for the year 2014 was 80.77 mm (Figure 4.36), and the accompanying runoff depth (potential) is calculated to be about 74.7 mm, resulting in a surface runoff volume of roughly 37 MCM (Figure 4.39). Since many rainfall-runoff models employ a rainfall threshold of 5 mm/event for runoff production, the US-NRCS technique provides a fair approximation of the rainfall-runoff relationship in the research region (Mahmoud et al., 2014). A projected runoff volume of 18.06 MCM would result from the 42 mm rainfall that occurred in 2013 as an intense rainstorm event. This volume is far more than the capacity of the urban drainage system and has a return period of 5 years (Figures 4.37 and 4.39). Consequently, it can be said that water harvesting in the research region has a great deal of potential to manage water deficits and mitigate drought.

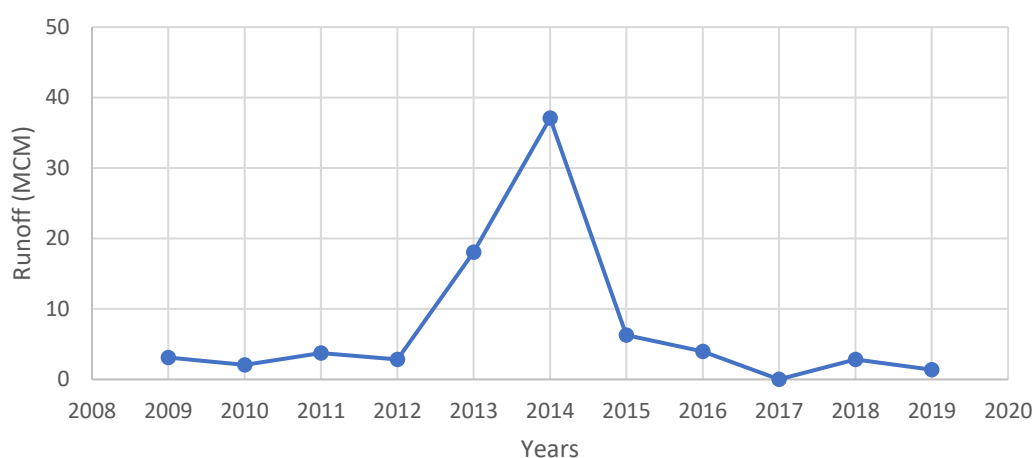


**Figure 4. 40 Potential runoff time series.**

#### **4.6.4 Rooftop and street surface rainwater harvesting for groundwater recharge.**

Residential houses in Kabul city typically have an area of 200-400 m<sup>2</sup> and 2-4 stories. In this study, a residential house with a total area of 300 m<sup>2</sup> was analyzed, 60% of which is considered for building, and the rest is considered as a yard. The groundwater recharge well with its accessories, which is fed by roof and yard rainwater, is considered inside the yard (Figure 4.40).

Considering the rainfall amount of 368 mm/year and taking into account the area of 300 m<sup>2</sup>, the total area of the residential house, including its yard, and taking into account 80% of the ability to collect rainwater, the total volume of rainwater that can be collected for groundwater recharge is about 88 cubic meters. To prevent oil and silt from entering the absorption well, rainwater, after collection, enters the grease and oil trap basin, whose dimensions have been taken 150 × 150 × 100 cm, with an overflow height of 120 cm (Figure 4.41). The oil trap basin has a capacity of 1.8 m<sup>3</sup>. The sand filter basin, which was installed after the oil trap basin, has a dimension of 150 x 300 x 100 cm. Its lower part contains filter material with a depth of 45 cm, and the upper part contains a freeboard with a depth of 30cm. The top layer (fine sand) has

a thickness of 24 cm, and the bottom layer, which consists of gravel, has a thickness of 20 cm.

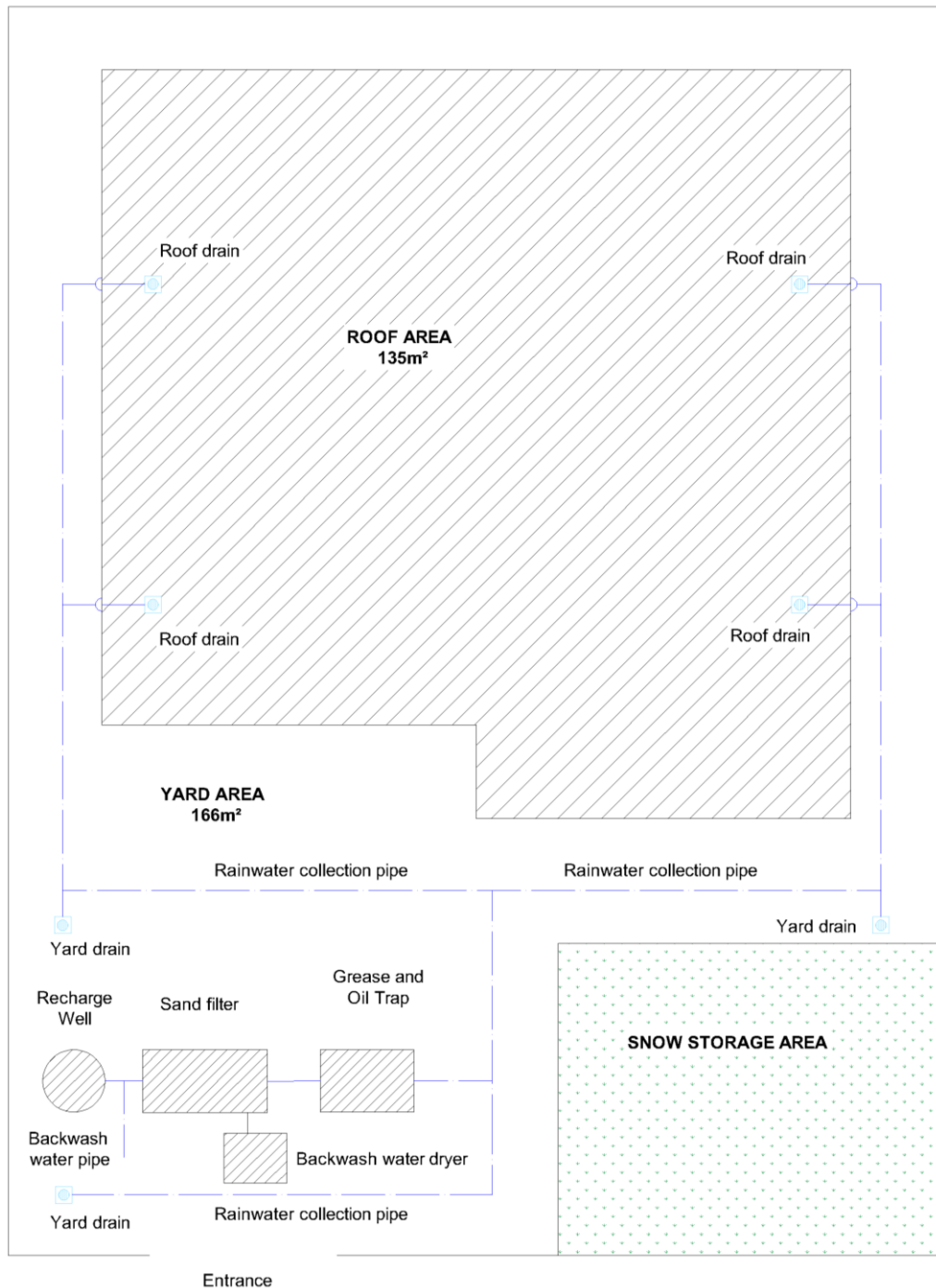


**Figure 4. 41 The proposed RWHR structure for residential houses.**

The maximum daily precipitation is about 81mm/day with a return period of 12 years (Figure 4.37). Since the soil characteristic in the Kabul basin has excellent hydraulic conductivity, the recharge wells have a total diameter of 1m, and their casing

is about 0.8 m in diameter. The depth of recharge will be typically considered 20 m based on the maximum daily rainfall and the total catchment area (total area of residential house).

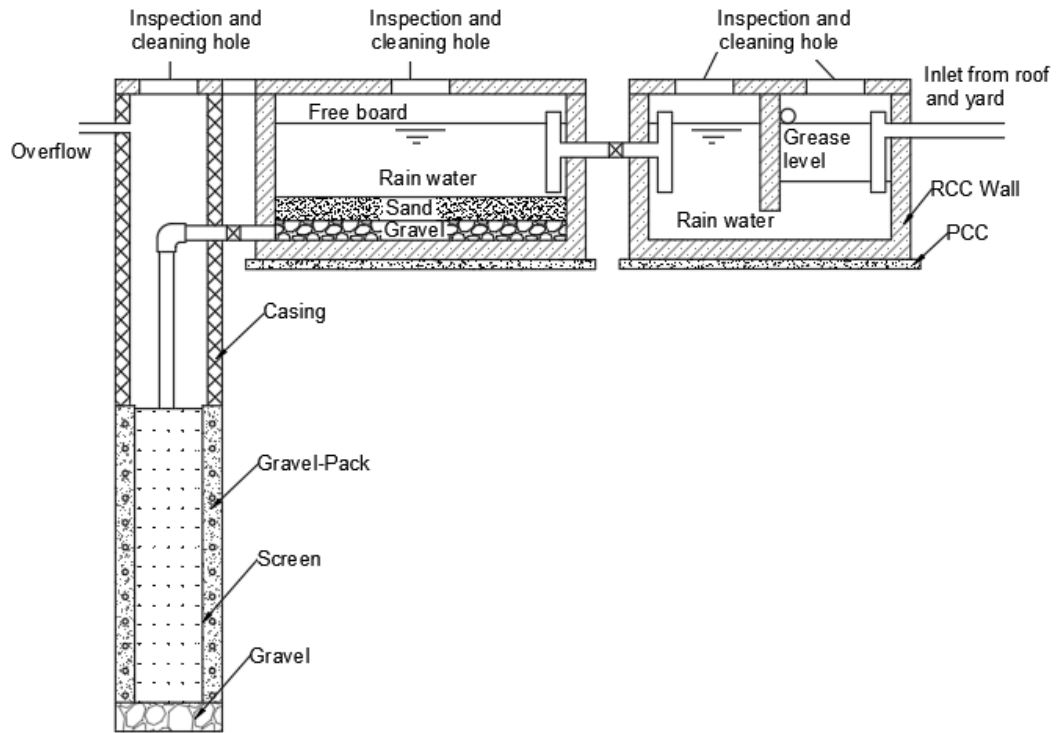


**Figure 4. 42 Cross-section of the recharge system**

In order to collect rainwater from roads, streets, and their sidewalk areas, the system of groundwater recharge wells with its accessories can be constructed at a distance of 100-150 meters on the sides of the road (pedestrian area) (Figure 4.42). The distance between the wells depends on the wide of the roads and the hydraulic conductivity of the soil. A settling tank has been considered before adding water to absorption wells in order to prevent the entry of silt and clay. The settling tank is separated into two separate parts by a buffer wall (Figure 4.43). The first part acts as the grease and oil separator, and the second part is for the settlement of solid particles. The tank is sized 350 x 150 x 100 cm with a 20 cm freeboard. The settling tank is connected to a recharge well, which is similar to recharge wells of residential houses based on construction.

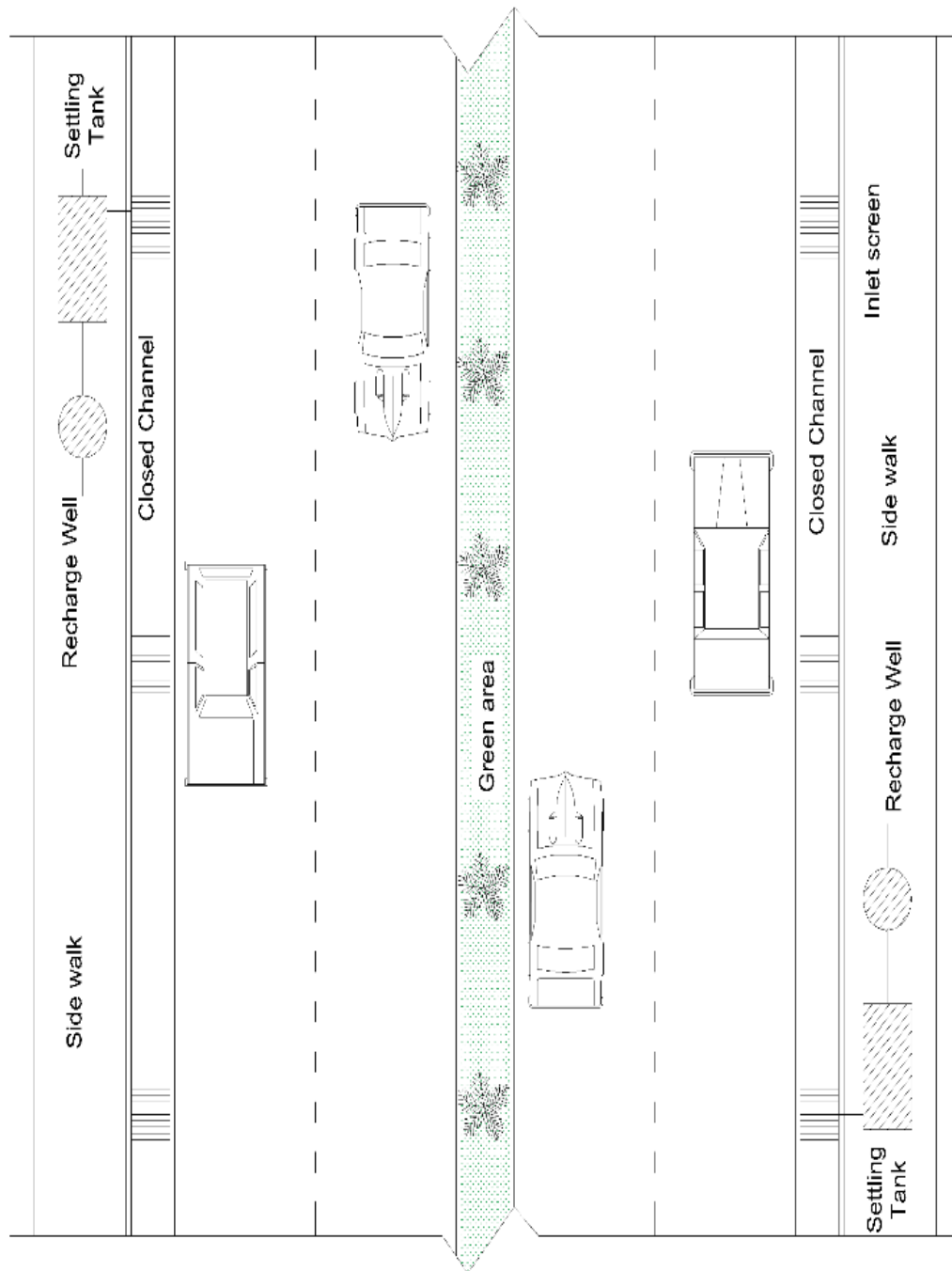


**Figure 4. 43 The proposed RWHR structure for roads and streets (plan)**

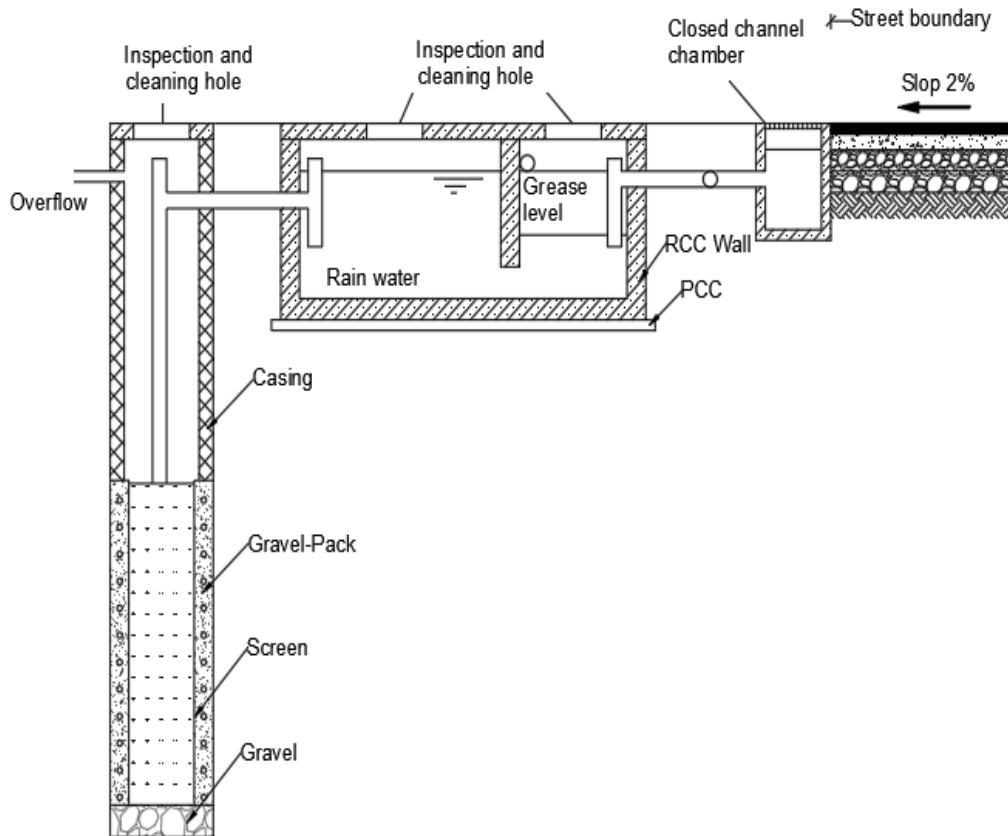


**Figure 4. 44** The proposed RWHR structure for roads and streets.

## 4.7 Delineation of groundwater recharge potential zones

### 4.7.1 Influential factors

Groundwater recharge, the process by which water infiltrates into the ground and replenishes underground aquifers, is significantly influenced by various factors. Geology plays a crucial role as different types of rocks and formations have varying permeability, affecting the rate at which water can infiltrate into the subsurface. Geomorphology, or the study of landforms, also influences recharge rates by determining surface runoff and infiltration patterns. Land use and land cover alter the natural hydrological cycle, with urbanization and deforestation often reducing recharge through increased surface runoff and impervious surfaces. Soil type is another critical factor, as soil permeability directly impacts the rate at which water can infiltrate into the ground. Lineament density, which refers to the presence of linear features such as faults or fractures, can enhance recharge by providing pathways for water movement. Drainage density affects groundwater recharge by influencing the concentration and velocity of surface water flow. Rainfall patterns dictate the availability of water for recharge, with higher precipitation rates generally leading to more significant recharge. Lastly, slope gradient influences the speed and direction of water flow, impacting infiltration rates and groundwater recharge accordingly.



Understanding the interplay of these factors is essential for managing groundwater resources sustainably.

#### **4.7.1.1 Geology**

Groundwater occurrence and recharge are affected by a region's geological makeup. Therefore, the basin's geological configuration is one of the critical determinants of groundwater occurrence and recharge (Maheswaran et al., 2016). This influential factor was digitized and mapped using a "geologic map of quadrangle 3468, Chak Wardak-Syahgerd (509) and Kabul (510) quadrangles, Afghanistan" (R. G. Bohannon & Turner, 2005). The following are some of the most prevalent geological features discovered in the research region: "Fan alluvium and colluvium, gneiss, loess, conglomerate and sandstone, limestone and dolomite, sandstone and siltstone, gabbro and monzonite, marble and quartzite, ultramafic intrusions, metamorphic rocks, basalt lava, and granodiorite" (Figure 4.44a). When rating theme layers, groundwater effects and permeability regulation of geological formations are taken into consideration. Conglomerate sandstones, loess, fan alluvium, and colluvium are attractive substrates for aquifers because of their high degradation and fracturing rates. The highest-ranking values were assigned to these geological features. Minimum ratings were allocated to basalt lava and granodiorite. A proposed weight of 20 was determined and assigned to the geological character of the basin.

#### **4.7.1.2 Geomorphology**

The landscapes, underlying geology, and main physiographic units of an area are depicted on a geomorphological map. Morphological qualities and features impact groundwater's creation, replenishment, and penetration. The geomorphological thematic layer of the Kabul basin has been georeferenced, digitized, and retrieved from a geomorphological map of the country (Scale 1: 6,000,000) in Arc GIS 10.7 environment (Figure 4.44b). According to geomorphological characteristics, the basin is split into four different types of relief: "mountain, Holocene River valleys, intermountain basin, and piedmont diluvial reliefs." The capacity for groundwater recharge may be lower, and the amount of runoff may be higher in mountain reliefs. Most of the basin is covered by a moderately sloped intermountain basin and a Holocene River valley. These geomorphologic features might serve as suitable infiltration platforms for groundwater replenishment. Some areas of the territory in the basin's southern-east have mountain relief. The Holocene River valley is assigned the highest rank, followed by the intermountain basin. The geomorphic characteristic is allotted the deduced weight of 18.

#### **4.7.1.3 land use and land cover**

Land use and land cover are important factors influencing groundwater conservation and occurrence. Groundwater recharging would be hampered by the increase of impermeable zones on the land surface, such as asphalt and concrete roads, streets, and waterproof roof materials. To create a LULC thematic map, remote sensing-based data (Landsat-8 satellite data) was processed using a supervised classification methodology (Figure 4.44c). The study area has bare land and rock,

cropland, vegetation area, settlements, water bodies, and marshland. Settlements lessen the impact of groundwater recharge, whereas areas covered in vegetation provide higher opportunities for groundwater recharge. The highest weights and rankings are assigned to farmland and barren land, whereas settlements receive the lowest weights and ranks. The LULC characteristic is given a weight of 12 as a consequence.

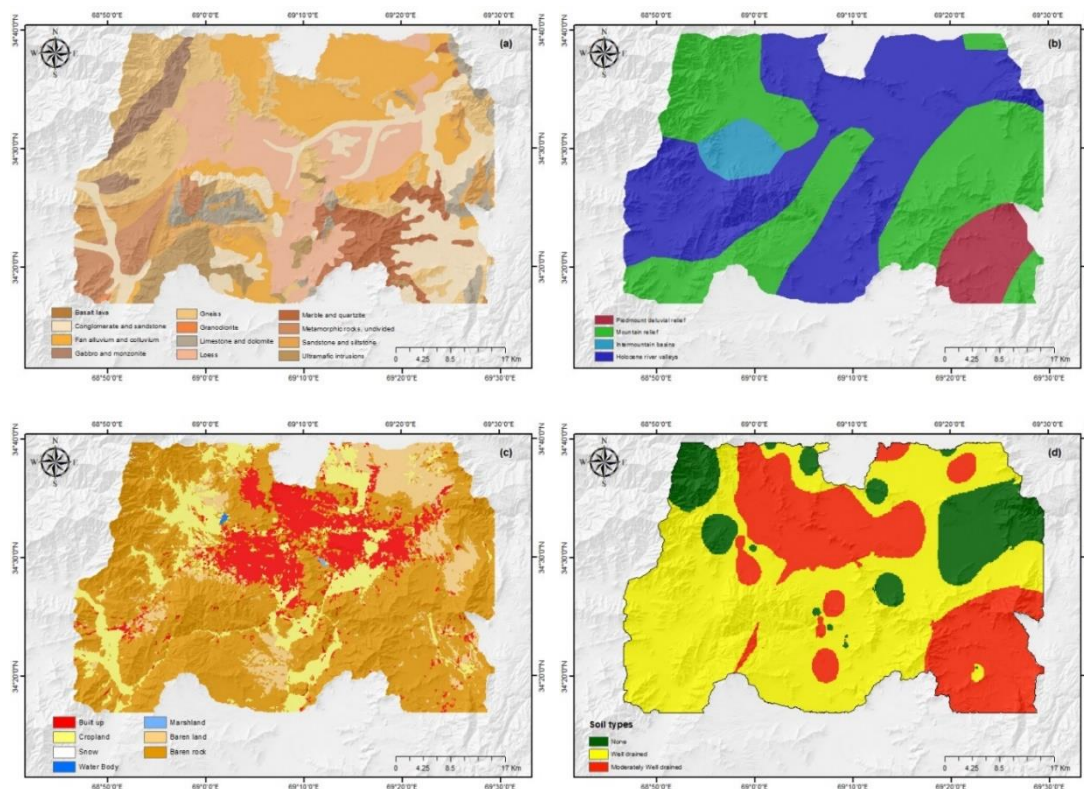


**Figure 4.45 a Geology, b Geomorphology, c Land use and Land cover types, and d Soil types of the basin**

#### 4.7.1.4 Soil,

Soil is formed from rock fractures as a result of the deposition process. Since it is the principal medium for groundwater to be recharged through it, its characteristics are critical for determining groundwater recharge potential. Depending on the soil types, they affect groundwater recharge and storage due to their storage capacity and absorption rates. To outline the soil map, the needed data for an influential layer of soil was acquired from the "Afghanistan Soil Catalogue". The soil in the basin is classified as well-drained, moderately well-drained, and none types of soil, with the permeability variations representing the soil's dampness frequency. A well-drained soil class covers the majority of the research region (Figure 4.44d). Well-drained and type of none were given high and low ratings, respectively. A calculated grade of 7 is attributed to the soil feature.

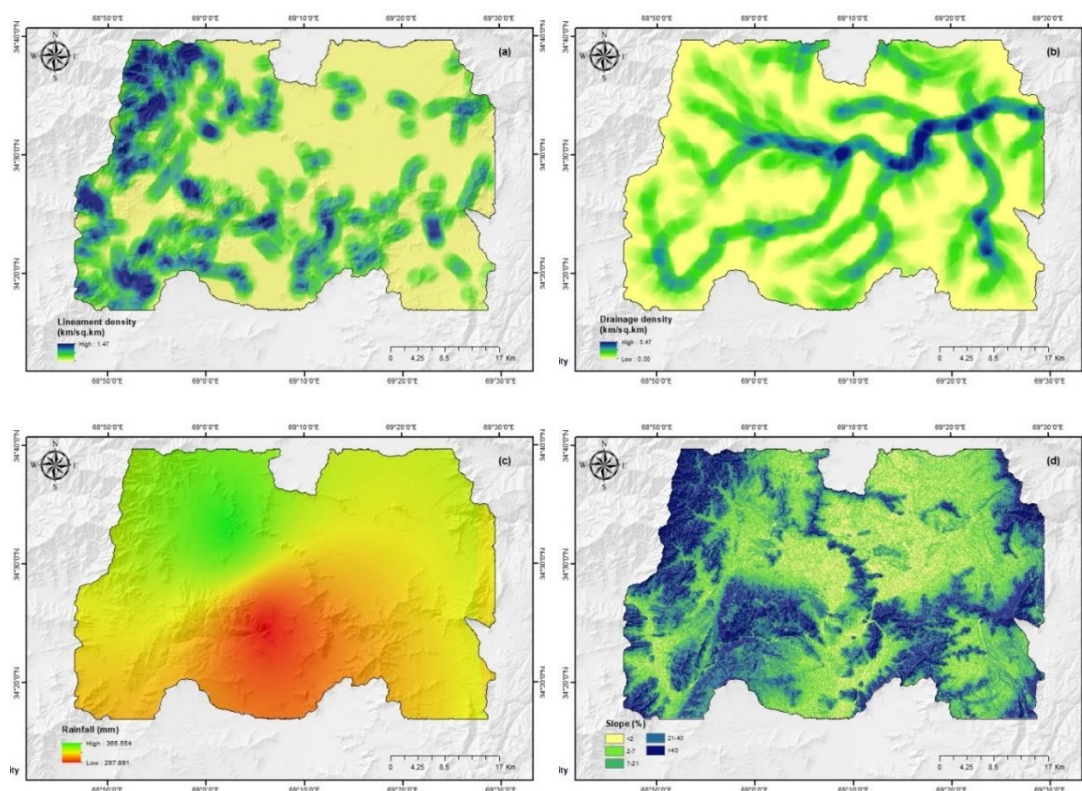


**Figure 4. 46 a Lineament density, b Drainage density, c Rainfall, and d Slope of the basin**

#### 4.7.1.5 Lineament density

Lineaments and curved or linear geological formations significantly influence groundwater recharge and transport. The primary lineaments and their intersection regions will contain potential high-yield groundwater areas. Its role in recharging groundwater is also undeniable. Utilizing PCI Geomatica Banff, Arc GIS 10.7, and visual interpretations, a lineament density conceptual layer (Figure 4.45a) is developed from "Landsat-8 OLI data (Landsat Scene Identifier: LC08 L1TP 153036 20200704 20200708 01 T1; Date of acquisition: 02-08-2020)". The density of lineament is correlated to groundwater potential and capacity. In the current research, the bulk of the lineament alignments are in the north-south direction, while there are also a few in the northwest-to-southeast, northeast-to-southwest, and east-to-west orientations. Substantial proportions of lineament are found in the basin's north, west, south, and southwest regions. Regions with higher lineament densities ( $0.52\text{--}1.48\text{ km}^2/\text{km}^2$ ) were given a higher ranking, and as a result, areas with lower densities ( $0\text{--}0.185\text{ km}^2/\text{km}^2$ ) were given a ranking with lower scale values. The influential factor weight of 12 was assigned to lineament density.

#### 4.7.1.6 Drainage density,

Surface runoff from rain, snow, and glacier melt generates drainage on a plain, which serves as a significant groundwater replenishment source in a particular location. Cracks, fissures, and gaps in a basin play a substantial role in groundwater recharge because they are viewed as a guiding element that may influence the drainage system of the basin. Thereby, the drainage systems in a specific region act as a transmission medium for surface runoff. The ratio of all stream segments to the surface area of a watershed is known as drainage density. Because of their increased conductivity, a modest runoff will occur in densely populated areas. The appropriate conceptual layer of drainage density for this investigation was created by interpreting SRTM-DEM in the arc GIS program (Figure 4.45b). The existence of groundwater and the relevance of drainage density are intimately connected. There are five subcategories in the drainage density thematic map. High rankings were provided for the obtained interval values of (2.9-5.5 km/km<sup>2</sup>) and low rankings for (0.0-0.4 km/km<sup>2</sup>). A weight of 11 has been applied to the drainage density influencing layer.

**Table 4. 25 Weightage of numerous thematic layers utilizing the MIF approach (Achu, Reghunath, et al., 2020; Kolanuvada, 2019; Magesh et al., 2012; Thapa et al., 2017c; Zghibi et al., 2020).**

Factors	Major effects (A) (1 for each)	Minor effects (B) (0.5 for each)	Proposed relative rates (A+B)	A proposed score for each factor
<b>Geology</b>	Geomorphology, Drainage Density, Slope, Lineament	Soil	5.5	20.4
<b>Geomorphology</b>	Lineament, Geology, Drainage Density, Soil	LULC, Soil	5	18.5
<b>Lineament Density</b>	Geomorphology, Drainage Density, Geology	Slope	3.5	13.0
<b>Slope</b>	Rainfall	LULC, Rainfall, Drainage Density, Lineament Density, Soil	3.5	13.0
<b>LULC</b>	Soil, Rainfall	Lineament Density, Slope	3	11.1
<b>Drainage Density</b>	Geology, Geomorphology	Rainfall, Lineament Density	3	11.1
<b>Soil</b>	LULC	Rainfall, Geomorphology	2	7.4
<b>Rainfall</b>	Slop	Geology	1.5	5.6
			$\Sigma 27$	$\Sigma 100$

#### **4.7.1.7 Rainfall,**

Precipitation is the principal water source in the water cycle and the primary source of groundwater recharge. Surface runoff and rainfall-derived water penetrate the earth's subsurface via fractures and soil texture. The severity and intensity of rainfall impact both runoff and groundwater recharge capacity in a basin. NWARA Afghanistan provided daily precipitation data for ten years (2008–2018), and the geographical distribution was assembled in the Arc GIS platform using the IDW approach (Figure 4.45c). In the Kabul basin, the average annual precipitation is found to be around 330 mm. The study area is divided into three sections based on mean yearly precipitation. Data show more precipitation in the north and lower precipitation in the south, indicating an intermediate condition across the basin. The high rainfall area (342-365) mm is given a higher rank, whereas the low rainfall area (298-320) mm is given a lower rank. As a consequence, the precipitation characteristic gets a derived weight of 7.

#### **4.7.1.8 Slope**

Runoff is significantly impacted by slope, which measures the difference in elevation in a specific location. However, it does contribute significantly to groundwater availability and recharge. Sharper slopes are not regarded as suitable media for groundwater recharge since they hasten runoff, eroding, and water penetration into the soil. On the other hand, lower slopes and flat areas provide an ideal habitat for groundwater recharge because the water flows at a moderate speed in these areas, giving ample time for penetration and creating ideal circumstances for groundwater recharge. The slope map was created using the Arc GIS system after processing the SRTM-DEM input. Mountains encircled the basin's west, south, and east sides, with a decreasing slope towards the basin's centre. The basin's northern, central, and smaller portions in the south, east, southeast, and southwestern parts comprise a moderate slope with excellent potential for groundwater recharge. The categorization of the slope map in the basin's data shows five distinct slope subclasses (Figure 4.45d). Areas with slopes between 0 and 2% have been ranked highly, whereas those with slopes more than 40% have received the lowest rankings. A derived weight of 13 is applied to the slope characteristic.

Table 4. 26 Weights of themes and their influences

Theme	Rank	Weight	Percentage of influence (%)	Theme	Rank	Weight	Percentage of influence (%)
Geology	20		25.51	LULC	12.7		12.76
Conglomerate and sandstone		9		Barren land		9	
Fan alluvium and colluvium		8		Barren rock		6	
Loess		8		Cropland		5	
Gneiss		6		Snow		3	
Metamorphic rocks, undivided		4		Settlement		2	
Limestone and dolomite		3		Water body		Restricted	
Sandstone and siltstone		3		Marshland		Restricted	
Gabbro and monzonite		3		Drainage density	10.9		12.76
Marble and quartzite		2		< 0.43		1	
Ultramafic intrusions		2		0.43 - 1.09		3	
Basalt lava		1		1.09 - 1.87		5	
Granodiorite		1		1.87 - 2.92		7	
Geomorphology	18.2		12.24	> 2.92		9	
Holocene river valleys		9		Soil	7.3		7.14
Mountain relief		6		Well drained		9	
Piedmont diluvial relief		5		Moderately well drained		4	
Intermountain basins		4		None		1	
Lineament Density (km/sq.km)	12.7		8.16	Rainfall	7.3		8.67
< 0.18		2		< 320		3	
0.18 - 0.52		5		320-340		5	
> 0.52		9		>340		9	
Slope (%)	12.7		12.76			∑ 196	∑ 100.00
< 2		9					
2 --- 7		7					
7--21		5					
21 -- 40		3					
> 40		1					

#### 4.7.2 Relative Importance of the Factors

The MIF approach was utilized to calculate the suggested scores since diverse geo-environmental variables impact groundwater recharge at different scales (Table 4.25). Out of the eight influential factors, geology has the highest factor (20.4), followed by geomorphology (18.5), slope and lineament density (13 each), LULC, and drainage density (11.1 each). The lowest score is recorded for soil type (7.4) and precipitation (5.6). Thematic layers were ranked using the suggested scores for each variable (Table 4.25), with each subclass of the thematic layer receiving distinct weights (Table 4.26).

The recommended scores were then used to calculate each component's influence proportion. Geology has the greatest effect on groundwater recharge potential in the current research region with 25.51 per cent, followed by LULC, slope, and drainage density (12.76 per cent each) and geomorphology (12.24 per cent). Other parameters, like rainfall, lineament density, and soil types, have far less impact on the basin's recharge potential (Table 4.26).

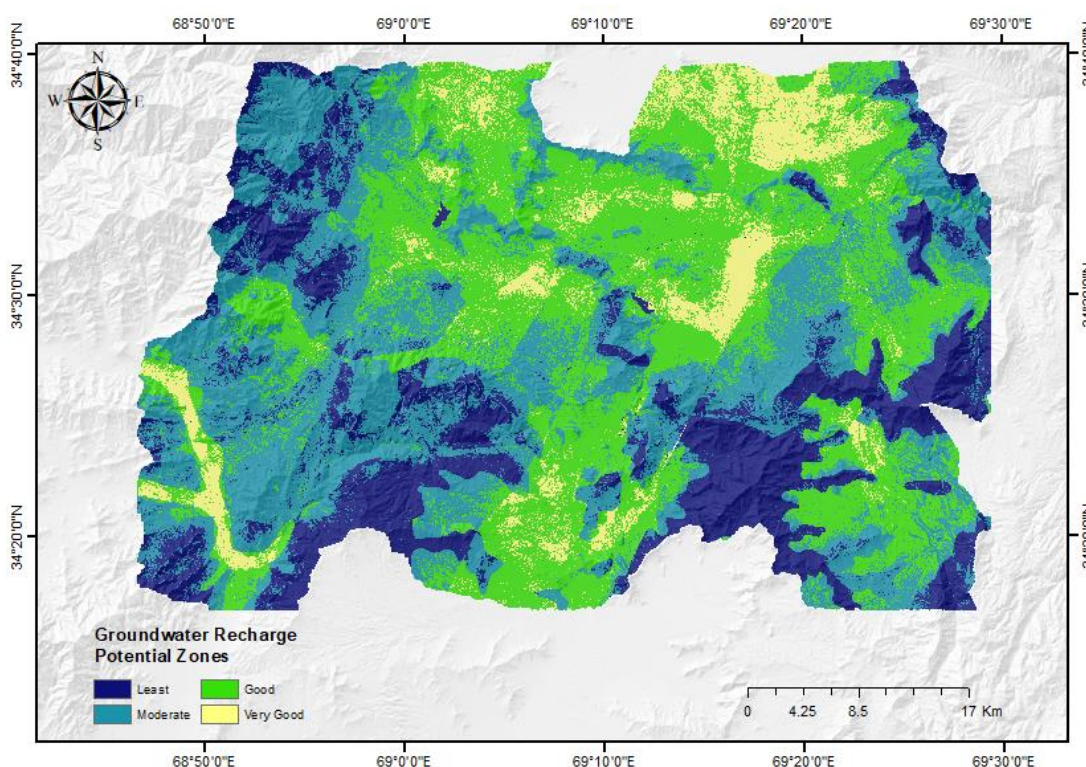


**Figure 4. 47 Potential groundwater recharge zones**

#### 4.7.3 Delineation of groundwater recharge potential zones

The geo-environmental characteristics were added to ArcGIS using weights generated by the MIF technique to determine the possible groundwater recharge areas in the Kabul basin. The resulting map was then divided into four

categories: places with the least, moderate, good, and very good potential for recharging (Figure 4.46). Around 20% of the basin's total area (462 km<sup>2</sup>) is covered by the least recharge potential zones, whereas the moderate recharge potential zones represent 831 km<sup>2</sup>. Roughly 36% of the study area was classified as good, and only 9% as very good recharge potential zones. Artificial recharge areas are commonly found in the centre and northern regions of the basin, which have gentle slopes. The presence of hills and hilly terrain in the upper parts of the basin causes the lowest recharge potential areas (Figure 4.45). Comparing the findings of the study with similar studies (Achu, Reghunath, et al., 2020; Kolanuvada, 2019; Thapa et al., 2017; Zghibi et al., 2020) showed that factors such as geology, geomorphology, and slope play an important role in identifying groundwater recharge potential zones.

In this study, the quantity of precipitation recharging groundwater is estimated using an empirical equation (Eq.3) from (UN, 1967), which is widely used in the literature (Achu, Reghunath, et al., 2020; Gosh et al., 2016; Souissi et al., 2018). Based on the (UN, 1967), the rechargeability of the various zones was estimated as follows: "Very good: 45–50% of precipitated water recharges the subsurface layers. Good = 30–35 % of precipitated water is recharged to the subsurface strata. Moderate = 10–20 % of precipitated water is recharged to the subsurface strata. Least = 5–10 % of precipitated water is recharged to the subsurface strata".

$$W = P \times R \times A \dots\dots\dots (4.9)$$

Where W indicates the recharge water quantity (m<sup>3</sup>/year), P is the amount of rainfall, R is the recharge ratio, and A is the percentage of the area. As the average rainfall in the basin is estimated at 330 mm/year (A. R. Noori & Singh, 2021b), the basin's volume of precipitated water might be around 778.8 × 10<sup>6</sup> m<sup>3</sup> /year. It was utilized to determine the total quantity of recharge water (W) for all four zones based on (Equation 4.9):

$$W = 778.8 \times 10^6 [(0.475 \times 0.0846) + (0.325 \times 0.3641) + (0.15 \times 0.3543) + (0.075 \times 0.197)] = 176.35 \times 10^6 \text{ m}^3/\text{year}$$

According to the observations above, only 22.64 per cent of precipitation in the Kabul basin infiltrates below to replenish groundwater reservoirs, while the rest evaporates or flows out as surface runoff. However, the volume of recharge water may be enhanced using artificial recharging technologies, which will aid in developing the basin's groundwater resources.

**Table 4. 27 Quantitative assessment of rechargeable categories**

Recharge potentiality	Very good	Good	Moderate	Least
Proposed recharge rates	45-50	30-35	10-20	5-10
Average (%)	47.5	32.5	15	7.5
Occupying study area (km <sup>2</sup> )	198.32	853.82	831	462.1
Area (%)	8.46	36.41	35.43	19.70



#### 4.7.4 Discovering Appropriate Recharge Approaches for Groundwater

Since groundwater recharge methods are highly site-specific, not all groundwater recharge measures are suitable for use in all basin locations. Therefore, a "rule-based" technique (Achu, Reghunath, et al., 2020; Aju et al., 2021) was employed to identify the areas appropriate for implementing different recharge measures (i.e., check dams, contour trench, recharge wells, rooftop rainwater harvesting, added recharge wells) in the moderate, good, and very good recharge potential areas of the Kabul basin.

Check dams are the most common structures found in (1-4) order streams with a slope of less than 15%. The appropriate sites of check dams throughout the basin region are highlighted in (Figure 4.46 a) to augment the surface water supply and improve subsurface infiltration. Check dams are well adapted to alluvial deposits and hard rock terrains. The weathering layer's depth and the substrate's conductivity affect groundwater recharge at check dam locations.

Contour trenches can be used in places with complicated terrain. The regions covered by barren lands and haven streams in the sequence of (1-2) are counted as contour trench-worthy (Figure 4.46 b). For the contour trench site selection, a slope constraint of (10-20%) was used, along with a low drainage density. The density and order of the streams determine the locations of recharge wells (Figure 4.46c). The recharge wells are positioned in areas with high stream density and higher stream orders (3-5).

Rooftop rainwater harvesting (Figure 4.47d) attached by recharge wells is suited for areas covered by built-up areas. The study area's LULC was used to identify ideal locations for rooftop rainwater harvesting added recharge wells. Figure 4.47 depicts the basin's ideal locations for adopting various artificial recharge technologies. As a result, the current research might be useful in building basin-wide groundwater management plans. Furthermore, the current work highlights the effectiveness of employing the MIF approach to distinguish groundwater recharge potential regions by integrating remotely sensed data and geoinformation data in a GIS platform.

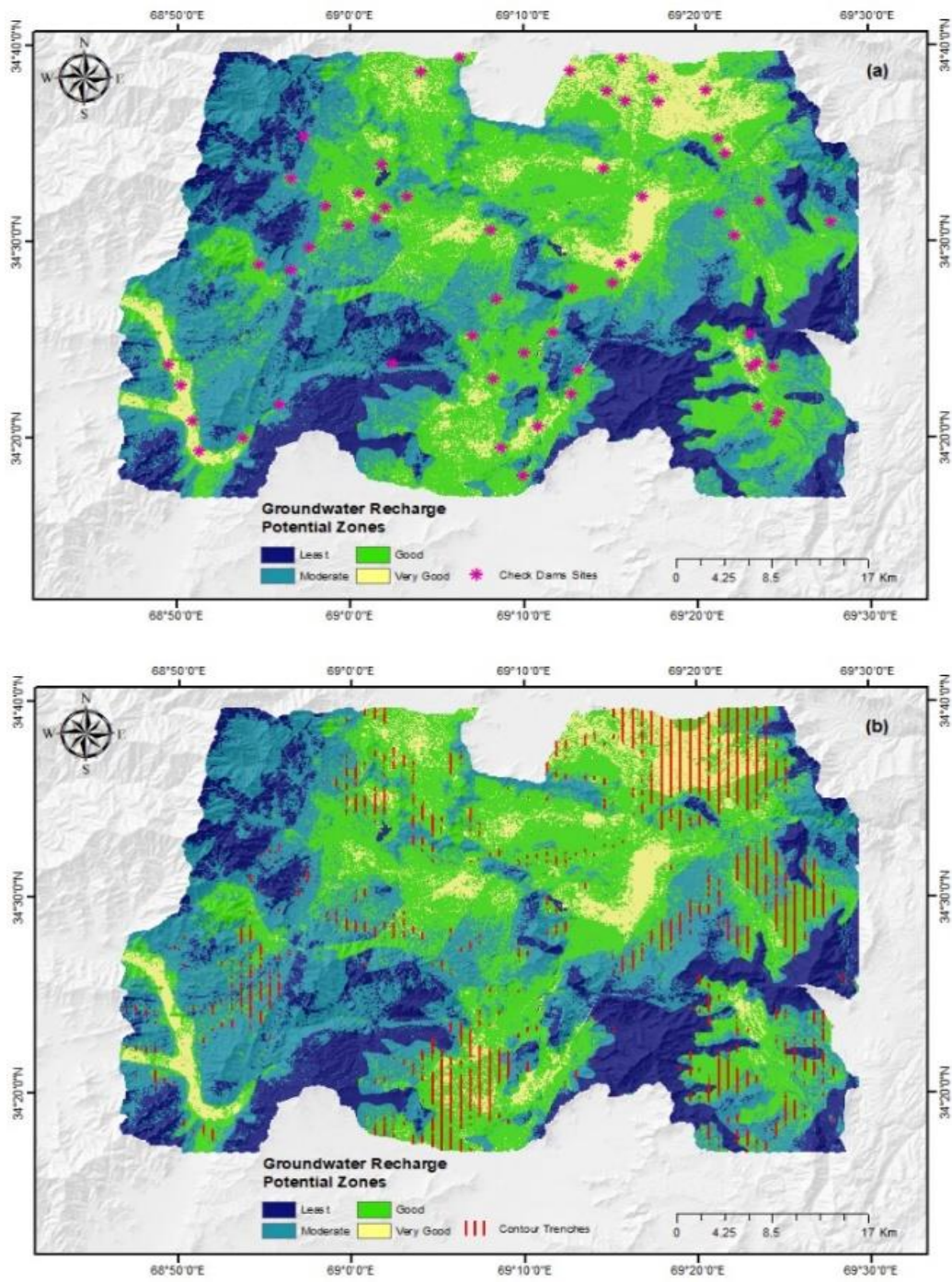


**Figure 4. 48 Proposed locations for implementing different groundwater recharging structures in the basin**

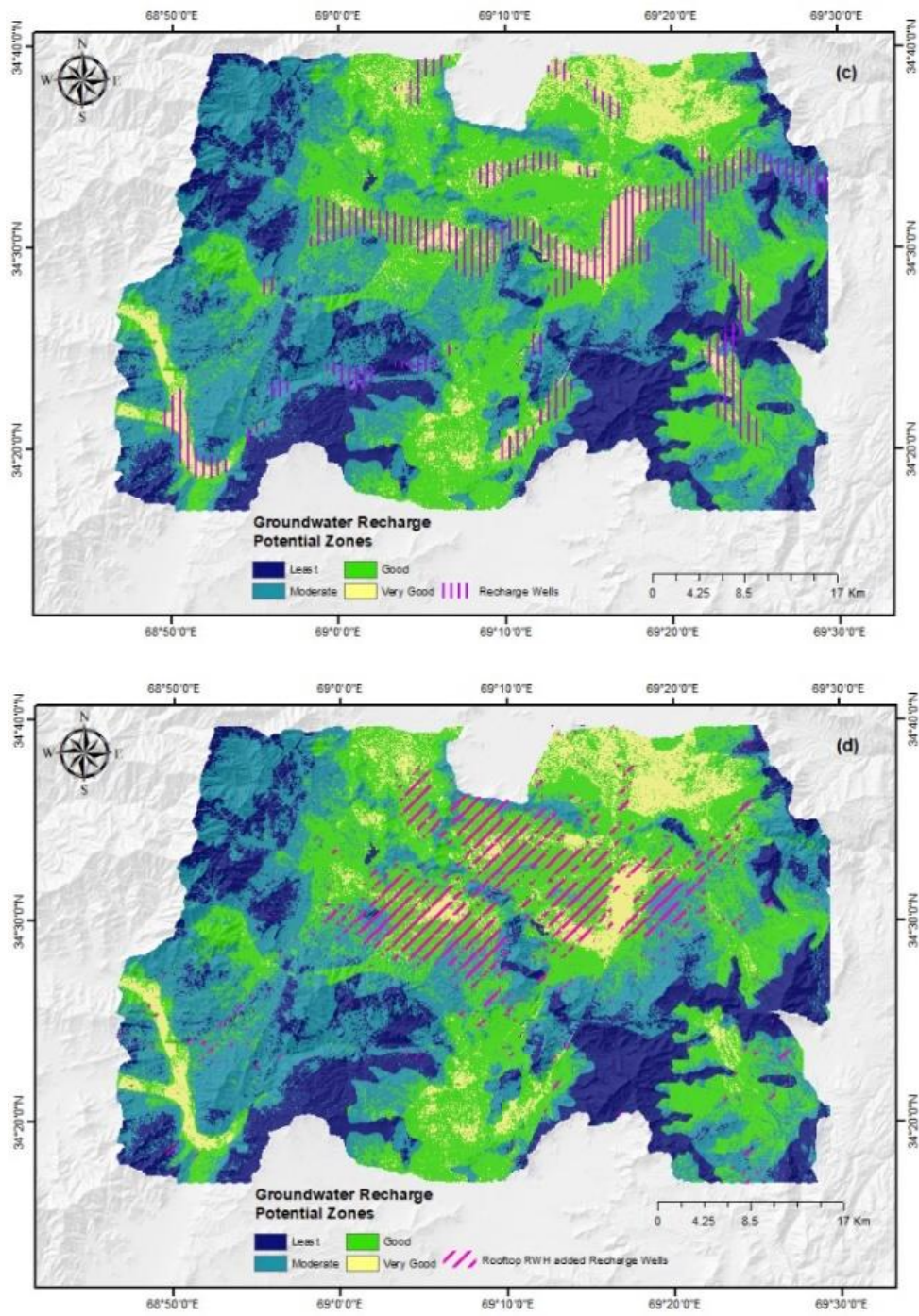


Figure 4. 49 Continued

## CHAPTER 5

### CONCLUSION, FUTURE SCOPE AND SOCIAL IMPACT

#### 5.1 Conclusion

##### 5.1.1 Water quality analysis

The research in Kabul comprises utilizing hydrogeochemical characterization, WQI, and GIS techniques to assess water quality in large parts of the city and most of its districts. According to WHO and ANSA guidelines, physicochemical characteristics such as EC, TDS, and TH are above acceptable levels in some samples. The number of anions in groundwater samples is in ascending order of  $F < NO_3 < SO_4 < Cl < HCO_3$  with percentages of  $0.03\% < 0.70\% < 9.20\% < 25.48\% < 64.59\%$ , respectively. And the quantity of cations is shown in ascending order of  $K^+ < Mg^{+2} < Ca^{+2} < Na^+$  contributing  $3.28\% < 20\% < 22\% < 55\%$  respectively. In observed samples of the basin, the primary ions are  $HCO_3$ ,  $Cl$  for anions, and  $Ca^{+2}$ ,  $Na^+$  for cations. In particular samples, major anions  $Cl$ ,  $SO_4$ ,  $NO_3$ , and cations  $Na$ ,  $Ca$ ,  $K$  in some samples and  $Mg$  in most samples have exceeded the permitted limit. As per the Piper diagram, the groundwater type is about 77%  $Mg-HCO_3$  type, 11%  $Na-Cl$  type, and about 7% each of Mixed  $Ca- Na-HCO_3$  and mixed  $Ca-Mg-Cl$  type. Bicarbonate leads the proportion in the anion's triangle with 83%, followed by chloride with 11%, and 6% of samples had no dominance. For cations, no dominance is the most prominent ion with 48.5% dominance, magnesium with 34%, and 17% of samples with sodium type. As per Gibbs plot conclusions, the bulk of the samples belonged to the rock dominance and evaporation dominance clusters. The poor water quality might be associated with lowering groundwater levels and reaching various geological formations, notably in the north of the research region. Furthermore, deterioration in groundwater quality might be ascribed to anthropogenic factors in the center sections of the basin due to higher groundwater levels. As per the water quality index (WQI), excellent to good water is found in 88.57% of the basin, whereas poor to very poor water is found in 11.4%, indicating pollution concentrations.

##### 5.1.2 ANN Model

The results of the ANN model for simulating sodium concentration in groundwater based on input data (EC, TDS, Salinity) have an average variance of 11.53%. The average variance for chloride and sulphate is 3.83% and -3.41%, respectively. However, the average variance for potassium and total hardness is 259.6% and 45.25%, respectively. These differences in mean percentage of variances show the accuracy of the models and their suitability. Based on these percentages one can conclude that the model is very suitable for simulating the concentrations of sodium, chloride and sulphate in groundwater with the suggested inputs (EC, TDS, and Salinity). Therefore, the model is not very suitable for the prediction of potassium and total hardness in groundwater with the same inputs.

### 5.1.3 Seasonal water quality analysis

The statistical analysis indicates that most of the water quality parameters in the study area were not statistically significant; however, the concentrations of calcium, sodium, iron, manganese, chloride, and fluoride increased significantly from the dry to the wet period of the observation. Other parameters such as electrical conductivity, pH, total hardness, total dissolved solids, bicarbonate, sulfate, phosphate, potassium, copper, aluminium, cyanide, and nitrate are the parameters that are not significantly changed from the dry to the wet period of the study time, according to the statistical test.

Variations in water quality parameters are correlated to recharge volume, hydraulic conductivity, and the geological formation of the region. The level of qualitative parameters, such as calcium, sodium, iron, manganese, chloride, and fluoride, has increased in the wet season, mainly in the wells close to river paths or in agricultural areas. The groundwater level in the study area's north and west has decreased in the last two decades. Also, groundwater recharge in these areas is much less due to changes in land use/land cover pattern. The recharge water is probably unable to reach the groundwater in a single season due to its tiny volume and weak hydraulic conductivity. As a result, there is less of a concentration of quality factors in the groundwater in these areas.

### 5.1.4 Groundwater level analysis

An extended period of seasonal and annual groundwater level trends has been assessed at 66 observational wells in Kabul City. Groundwater drought index (SGI) values were also calculated to measure the severity of drought in groundwater. Cluster classification was used to label the wells based on correlations with groundwater table variations. Evidence from the elbow approach indicated that 3 clusters are necessary to classify the water level variability into distinct groups. Cluster 1 consists of 32 wells with an average annual rate of groundwater decline of 1.38 meters. Clusters 2 and 3 contain 15 and 8 monitoring wells, respectively, with significant negative average groundwater level trends of 0.31 m and 2.84 m per annum. A substantial increase in annual groundwater level was found in four observational wells, with an overall gain of 0.7 m/year.

Based on the trend analysis of wells in the various clusters, the water levels in 89 per cent of cluster 1 wells and 82 per cent of all study area wells consistently declined. The calculation of SGI values has indicated that most wells in the research region have been experiencing severe and ongoing drought since 2014. The drought conditions in most wells started in 2014 and have generally intensified to 2020. Most of the wells experienced extreme drought conditions during 2019-2020. Additionally, some wells in different clusters have shown the effects of groundwater drought. For instance, well 50 has experienced several months of drought conditions during its operation. The SGI values for this well indicated that drought conditions appeared in this well alternatively from 2006 to 2011 and 2014 to 2020. The extreme drought in this well was recorded in 2008 with a magnitude of greater than 3 SGI.

Wells with positive water level trends show different behaviour. For instance, in well 14, drought conditions started in 2006 and ended in 2014. They reappeared in 2018 and continued to 2020, but the SGI values were generally low compared to many other wells. However, this well-experienced extreme drought condition was in 2014 when the SGI value was greater than 2. Only a few wells in the study area exhibited this type of water level behaviour.

Land use and land cover (LULC) patterns for the Kabul area were investigated in 2005, 2010, 2015, and 2020. The built-up area, which has a significant negative impact on groundwater recharge, increased from about 15% in 2005 to 32% in 2020 in the study area. From 2005 to 2020, the area of agricultural land use decreased from about 17% to 15%. The area covered by bare land in the study area has decreased from 67 % in 2005 to 52% in 2020. Precipitation records, especially in the southern region of the study area, show a decline in the annual rainfall amount. Changes in LULC and a decrease in precipitation are the two influential factors in reducing groundwater levels.

Overexploitation of groundwater due to population increase, the dryness of the riverbeds, the extent of urban development, the reduction of rainfall, and the mismanagement of groundwater resources are likely to be the leading causes of groundwater level declines in the area. To avoid further deterioration of valuable groundwater resources, this report suggests artificial groundwater recharge and advanced groundwater resource management, as well as the parallel utilization of surface and groundwater. This study would help implement regional groundwater policies for long-term water supply development in the Kabul Basin.

### **5.1.5 GWPZs**

This analysis examines the reconnaissance of groundwater potential zonation in the Kabul basin, Afghanistan. This research strongly indicates that the hybrid application of both GIS and remotely sensed data, in addition to the analytical hierarchy process, provides a powerful tool to assess the zones of groundwater potential and recharge. Ten different thematic variables were analyzed in the Arc GIS environment with various numerical weightage values in the basin. These variables included geology, geomorphology, land-use land cover, lineament density, drainage density, soil, slope, rainfall, elevation, and water depth. Static groundwater level records have been utilized to acquire precision and reliability for discovering groundwater potential zones. According to the final output of the results, most parts of the study area are covered by a reasonable and very good capacity of groundwater potential zones. Based on the results, four categories of the GWPZs were eventually recognized. According to the statistics, the area is divided into a zone with a very poor potential (16%), poor (18%), good (35%), and very good (31%).

### **5.1.6 Artificial recharge of groundwater in an urban area**

Kabul has inconsistent, seasonal, and intense precipitation. The average annual rainfall is 368 mm, and there are typically 80 wet days. Considering the LULC typology,  $I_{c(\text{eff})}$  was calculated for the study area for both conditions of employing

RWHRS and without RWHRS. By using RWHRS, the average yearly infiltration might rise from 4.86 MCM to 11.33 MCM. Using the "US-NRCS" approach, a weighted CN value of 90.5 per cent is discovered, attributing to the supremacy of imperviousness. Additionally, it is revealed that the threshold for runoff formation is 5.3 mm of rainfall. A return period of 3–4 years is predicted by the probability analysis using the Weibull approach for daily rainfall of less than 30 mm.

Two techniques for collecting rainwater to replenish groundwater were described: (1) RWHRS for a residential house with an area of 300 m<sup>2</sup>, which will yield about 88 m<sup>3</sup> of water for groundwater recharge, and (2) the RWHRS for a street sidewalk where the harvested water is being used to recharge the local aquifer.

### 5.1.7 GWRPZs

By integrating remotely sensed data and geoinformation inputs in a GIS environment and utilizing the MIF method, the potential recharge zones for artificial groundwater recharge mechanisms in a semi-arid area (the Kabul basin, Afghanistan) were determined. Eight different variables as thematic maps, viz., geology, geomorphology, slope, lineament density, land use and land cover, soil, rainfall, and drainage density, were integrated into the ArcGIS environment. Geology, lineament density, and slope are determined to considerably impact the basin's recharge potential among the eight relevant elements.

The anticipated potential zones for groundwater recharge in the basin are split into four categories based on their propensity for groundwater recharge, viz., very good (areal extent 8.45%), good (36.4%), moderate (35.4%), and least (19.7%) recharge potential zones. Based on the estimated calculation, only around 23% of the total amount of precipitation infiltrates into the groundwater reservoirs in the research region. Conglomerate and sandstone, loess, fan alluvium, and colluvium with a moderate slope are connected with very good and good groundwater recharge potential zones. In contrast, crystalline rocks with steep slopes and lacking secondary porosity are correlated with the least recharge potential zones. To discover the best locations for various site-specific recharging processes (check dams, counter trenches, recharge wells, and rooftop rainwater harvesting added recharge wells), a rule-based approach has been employed. It was proposed in this study that check dams be built at various points and above streams in a variety of configurations. It has been recommended that check dams be built with locally accessible construction materials. Contour trenches are suggested in places with complicated terrain with low drainage density. The regions covered by barren lands and haven streams (1-2) sequence are counted as contour trench-worthy. The recharge wells are positioned in locations with high stream density and higher stream orders (3-5). The areas occupied by built-up areas are suitable for rooftop rainwater harvesting attached to recharge wells. The outputs of this investigation would be helpful for regional authorities to develop sustainable water resources management.

## **5.2 Recommendations**

1. Since groundwater is the most prevalent source of water supply, a continuous monitoring system will ascertain the drinking water quality for the residents' accessing to safe water, resulting improved management with sustainable groundwater development.
2. A National water quality database must be developed in the ministry of Energy and Water of Afghanistan.
3. Models developed by ANN should be well-trained, tested, and used in laboratories.
4. The application of RWHRs for areas which have a regular sewage collection system must be compulsory.
5. Application of GIS and RS with the approaches of MCDA (MIF, AHP) is beneficial for developing GWPZ and GWRPZ. Stakeholder can employ it.
6. The developed maps can be utilized for sustainable water resources management.
7. A regular system of wastewater collection and treatment (of any type) is an urgent need for the city and must be developed as soon as possible.

## **5.3 Scope of future work**

1. Studying the quality of water in the whole country, especially the level of arsenic and heavy metals, and finding out their correlations with cancers. Since different types of cancer are increasing in the country for the groundwater supply.
2. Isotope analysis of GW is used to determine the age of water that is currently used.
3. Study and suggest appropriate recharge mechanisms (contour trench, check dams, recharge wells) from a structural point of view.
4. Modelling groundwater quality and quantity for both scenarios (current condition and application of artificial recharge)
5. Wastewater recycling should be considered and studied as an option for groundwater recharge.



## REFERENCES

- Abdeslam, I., Fehdi, C., & Djabri, L. (2017). Application of drastic method for determining the vulnerability of an alluvial aquifer: Morsott - El Aouinet north east of Algeria: Using arcgis environment. *Energy Procedia*, *119*, 308–317. <https://doi.org/10.1016/j.egypro.2017.07.114>
- Abijith, D., Saravanan, S., Singh, L., Jennifer, J. J., Saranya, T., & Parthasarathy, K. S. S. (2020). GIS-based multi-criteria analysis for identification of potential groundwater recharge zones - a case study from Ponnaniyar watershed, Tamil Nadu, India. *HydroResearch*, *3*, 1–14. <https://doi.org/10.1016/j.hydres.2020.02.002>
- Abuzied, S. M., & Alrefae, H. A. (2017). Mapping of groundwater prospective zones integrating remote sensing , geographic information systems and geophysical techniques in El-Qaà Plain area , Egypt. *Hydrogeology Journal*. <https://doi.org/10.1007/s10040-017-1603-3>
- Achu, A. L., Reghunath, R., & Thomas, J. (2020). Mapping of Groundwater Recharge Potential Zones and Identification of Suitable Site-Specific Recharge Mechanisms in a Tropical River Basin. *Earth Systems and Environment*, *4*(1), 131–145. <https://doi.org/10.1007/s41748-019-00138-5>
- Achu, A. L., Thomas, J., & Reghunath, R. (2020). Multi-criteria decision analysis for delineation of groundwater potential zones in a tropical river basin using remote sensing, GIS and analytical hierarchy process (AHP). *Groundwater for Sustainable Development*, *10*(January 2018), 100365. <https://doi.org/10.1016/j.gsd.2020.100365>
- Adhikari, R. K., Mohanasundaram, S., & Shrestha, S. (2020). Impacts of land-use changes on the groundwater recharge in the Ho Chi Minh city, Vietnam. *Environmental Research*, *185*(March), 109440. <https://doi.org/10.1016/j.envres.2020.109440>
- Adimalla, N. (2021). Application of the Entropy Weighted Water Quality Index (EWQI) and the Pollution Index of Groundwater (PIG) to Assess Groundwater Quality for Drinking Purposes: A Case Study in a Rural Area of Telangana State, India. *Archives of Environmental Contamination and Toxicology*, *80*(1), 31–40. <https://doi.org/10.1007/s00244-020-00800-4>
- Aenab, A. M., Singh, S. K., & Al-Rubaye, A. A. M. (2012). Evaluation of Tigris River by Water Quality Index Analysis Using C++ Program. *Journal of Water Resource and Protection*, *04*(07), 523–527. <https://doi.org/10.4236/jwarp.2012.47061>
- Ahmad, A., Cornelissen, E., van de Wetering, S., van Dijk, T., van Genuchten, C., Bundschuh, J., van der Wal, A., & Bhattacharya, P. (2018). Arsenite removal in groundwater treatment plants by sequential Permanganate—Ferric treatment. *Journal of Water Process Engineering*, *26*(October), 221–229. <https://doi.org/10.1016/j.jwpe.2018.10.014>
- Ahmadzai, H., & Omuto, C. (2019). Afghanistan soil catalogue. In *FAO*. <https://doi.org/10.1017/CBO9781107415324.004>

- Aju, C. . D., Achu, A. . L., Raicy, M. . C., & Reghunath, R. (2021). HydroResearch Identifi cation of suitable sites and structures for arti fi cial groundwater recharge for sustainable water resources management in Vamanapuram River Basin , South India. *HydroResearch*, 4, 24–37. <https://doi.org/10.1016/j.hydres.2021.04.001>
- Akinlalu, A. A., Adegbuyiro, A., Adiat, K. A. N., Akeredolu, B. E., & Lateef, W. Y. (2017). Application of multi-criteria decision analysis in prediction of groundwater resources potential : A case of Oke-Ana , Ilesa Area Southwestern , Nigeria. *NRIAG Journal of Astronomy and Geophysics*, 6(1), 184–200. <https://doi.org/10.1016/j.nrjag.2017.03.001>
- Akter, T., Jhohura, F. T., Akter, F., Chowdhury, T. R., Mistry, S. K., Dey, D., Barua, M. K., Islam, M. A., & Rahman, M. (2016). Water Quality Index for measuring drinking water quality in rural Bangladesh: A crosssectional study. *Journal of Health, Population and Nutrition*, 35(1), 1–12. <https://doi.org/10.1186/s41043-016-0041-5>
- Al-Abadi, A. M., Pourghasemi, H. R., Shahid, S., & Ghalib, H. B. (2016). Spatial Mapping of Groundwater Potential Using Entropy Weighted Linear Aggregate Novel Approach and GIS. *Arab J Sci Eng, December*. <https://doi.org/10.1007/s13369-016-2374-1>
- Alataway, A., & El Alfy, M. (2019). Rainwater Harvesting and Artificial Groundwater Recharge in Arid Areas: Case Study in Wadi Al-Alb, Saudi Arabia. *Journal of Water Resources Planning and Management*, 145(1). [https://doi.org/10.1061/\(ASCE\)WR.1943-5452.0001009](https://doi.org/10.1061/(ASCE)WR.1943-5452.0001009)
- Alum, O. L., Okoye, C. O. B., & Abugu, H. O. (2021). Quality assessment of groundwater in an agricultural belt in eastern Nigeria using a Water Quality Index. *African Journal of Aquatic Science*. <https://doi.org/10.2989/16085914.2021.1882375>
- Anbarasu, S., Brindha, K., & Elango, L. (2020). Multi-influencing factor method for delineation of groundwater potential zones using remote sensing and GIS techniques in the western part of Perambalur district, southern India. *Earth Science Informatics*, 13(2), 317–332. <https://doi.org/10.1007/s12145-019-00426-8>
- ANSA. (2013). *National Drinking Water Quality Standard*. ANSA.
- APHA. (2005). *Standard methods for the examination of water and wastewater, 20th*. American Public Health Association.
- Arefin, R. (2020). Groundwater potential zone identification at Plio-Pleistocene elevated tract, Bangladesh: AHP-GIS and remote sensing approach. *Groundwater for Sustainable Development*, 10(March 2019), 100340. <https://doi.org/10.1016/j.gsd.2020.100340>
- Arezo TV. (2020). *Interview with Engineer Hamidullah Yalani, President of Afghanistan Urban Water Supply and Sewerage Corporation (AUWSSC)*. Arezo Telvesion. <https://www.youtube.com/watch?v=jSJT8rCdTSE>
- Arnous, M. O. (2016). Groundwater potentiality mapping of hard-rock terrain in arid

- regions using geospatial modelling : example from Wadi Feiran. *Hydrogeology Journal*. <https://doi.org/10.1007/s10040-016-1417-8>
- Awawdeh, M., Obeidat, M., & Zaiter, G. (2015). Groundwater vulnerability assessment in the vicinity of Ramtha wastewater treatment plant, North Jordan. *Applied Water Science*, 5(4), 321–334. <https://doi.org/10.1007/s13201-014-0194-6>
- Banks, D. (2002). *Guidelines for Sustainable Use of Groundwater in Afghanistan*.
- Bloomfield, J. P., & Marchant, B. P. (2013). Analysis of groundwater drought building on the standardised precipitation index approach. *Hydrology and Earth System Sciences*, 17(12), 4769–4787. <https://doi.org/10.5194/hess-17-4769-2013>
- Bohannon, R. (2010). Geologic and Topographic Maps of the Kabul South 30' × 60' Quadrangle, Afghanistan: U.S. Geological Survey Scientific Investigations Map 3137. In *U.S. Geological Survey Scientific Investigations Map* (Vol. 3137).
- Bohannon, R. G., & Turner, K. J. (2005). *Department of the Interior (U.S.)*. USGS. <https://doi.org/10.4135/9781412953924.n288>
- Boyacioglu, H. (2007). Development of a water quality index based on a European classification scheme. *Water SA*, 33(1), 101–106. <https://doi.org/10.4314/wsa.v33i1.47882>
- Brati, M. Q., Ishihara, M. I., & Higashi, O. (2019). Groundwater level reduction and pollution in relation to household water management in Kabul, Afghanistan. *Sustainable Water Resources Management*, 5(3), 1315–1325. <https://doi.org/10.1007/s40899-019-00312-7>
- Broshears, R. E., Akbari, M. A., Chornack, M. P., Mueller, D. K., & Ruddy, B. C. (2005). *Inventory of ground-water resources in the Kabul Basin, Afghanistan* (Issue 001). USGS. <http://libproxy.lib.unc.edu/login?url=http://search.proquest.com/docview/904478814?accountid=14244%5Cnhttp://pubs.water.usgs.gov/sir2005-5090/>
- Chakraborty, B., Roy, S., Bera, A., Adhikary, P. P., Bera, B., Sengupta, D., Bhunia, G. S., & Shit, P. K. (2021). *Geospatial Assessment of Groundwater Quality for Drinking through Water Quality Index and Human Health Risk Index in an Upland Area of Chota Nagpur Plateau of West Bengal, India* (Issue February). [https://doi.org/10.1007/978-3-030-63422-3\\_19](https://doi.org/10.1007/978-3-030-63422-3_19)
- Chidambaram, S., Sarathidasan, J., Srinivasamoorthy, K., Thivya, C., Thilagavathi, R., Prasanna, M. V., Singaraja, C., & Napolian, M. (2018). Assessment of hydrogeochemical status of groundwater in a coastal region of Southeast coast of India. *Applied Water Science*, 8(1), 1–14. <https://doi.org/10.1007/s13201-018-0649-2>
- Chowdhury, A., Jha, M. K., & Chowdary, V. M. (2010). Delineation of groundwater recharge zones and identification of artificial recharge sites in West Medinipur district, West Bengal, using RS, GIS and MCDM techniques. *Environmental Earth Sciences*, 1209–1222. <https://doi.org/10.1007/s12665-009-0110-9>
- CIA. (2020). *The World Fact Book*. <https://www.cia.gov/library/publications/the->

world-factbook/geos/af.html

- DACAAR. (2011). *National Groundwater Monitoring Wells Network in Afghanistan*. DACAAR. <https://doi.org/10.16194/j.cnki.31-1059/g4.2011.07.016>
- DACAAR. (2019). *Hydro-geological Booklet Kabul Province*. DACAAR.
- Dadgar, M. A., Zeaieanfiroozabadi, P., Dashti, M., & Porhemmat, R. (2017). Extracting of prospective groundwater potential zones using remote sensing data , GIS , and a probabilistic approach in Bojnourd basin , NE of Iran. *Arab J Geosci*. <https://doi.org/10.1007/s12517-017-2910-7>
- Dadhich, A. P., Goyal, R., & Dadhich, P. N. (2021). Assessment and Prediction of Groundwater using Geospatial and ANN Modeling. *Water Resources Management*, 35(9), 2879–2893. <https://doi.org/10.1007/s11269-021-02874-8>
- Dey, M., Akter, A., Islam, S., Chandra Dey, S., Choudhury, T. R., Fatema, K. J., & Begum, B. A. (2021). Assessment of contamination level, pollution risk and source apportionment of heavy metals in the Halda River water, Bangladesh. *Heliyon*, 7(12), e08625. <https://doi.org/10.1016/j.heliyon.2021.e08625>
- Dinh, M., Hakimabadi, S. G., & Pham, A. L. T. (2020). Treatment of sulfolane in groundwater: A critical review. *Journal of Environmental Management*, 263(March), 110385. <https://doi.org/10.1016/j.jenvman.2020.110385>
- Domenico, P., & Schwartz, F. (1998). *Physical and chemical hydrogeology*. Wiley.
- Efron, B. (1994). Missing data, imputation, and the bootstrap. *Journal of the American Statistical Association*, 89(426), 463–475. <https://doi.org/10.1080/01621459.1994.10476768>
- El-Hames, A. S., Hannachi, A., Al-Ahmadi, M., & Al-Amri, N. (2013). Groundwater Quality Zonation Assessment using GIS, EOFs and Hierarchical Clustering. *Water Resources Management*, 27(7), 2465–2481. <https://doi.org/10.1007/s11269-013-0297-0>
- Elçi, A., & Polat, R. (2011). Assessment of the statistical significance of seasonal groundwater quality change in a karstic aquifer system near Izmir-Turkey. *Environmental Monitoring and Assessment*, 172(1–4), 445–462. <https://doi.org/10.1007/s10661-010-1346-2>
- Etikala, B., Golla, V., Li, P., & Renati, S. (2019). Deciphering groundwater potential zones using MIF technique and GIS: A study from Tirupati area, Chittoor District, Andhra Pradesh, India. *HydroResearch*, 1, 1–7. <https://doi.org/10.1016/j.hydres.2019.04.001>
- Evans, S. W., Jones, N. L., Williams, G. P., Ames, D. P., & Nelson, E. J. (2020). Groundwater Level Mapping Tool: An open source web application for assessing groundwater sustainability. *Environmental Modelling & Software*, 131(July), 104782. <https://doi.org/10.1016/j.envsoft.2020.104782>
- Fagbohun, B. J. (2018). Integrating GIS and multi-influencing factor technique for delineation of potential groundwater recharge zones in parts of Ilesha schist belt, southwestern Nigeria. *Environmental Earth Sciences*, 77(3), 69.

<https://doi.org/10.1007/s12665-018-7229-5>

- Foody, G. M. (2020). Explaining the unsuitability of the kappa coefficient in the assessment and comparison of the accuracy of thematic maps obtained by image classification. *Remote Sensing of Environment*, 239(December 2019), 111630. <https://doi.org/10.1016/j.rse.2019.111630>
- Frahmand, A. S. (2011). GIS based Ground Water Quality Analysis in Kabul City Region. *Geospatial World Forum*, 1–13. [https://www.researchgate.net/publication/284352960\\_GIS\\_based\\_Ground\\_Water\\_Quality\\_Analysis\\_in\\_Kabul\\_City\\_Region](https://www.researchgate.net/publication/284352960_GIS_based_Ground_Water_Quality_Analysis_in_Kabul_City_Region)
- Freeze, R. A., & Cherry, J. A. (1979). *Groundwater*. Englewood Cliffs.
- Gado, T. A., & El-Agha, D. E. (2020). Feasibility of rainwater harvesting for sustainable water management in urban areas of Egypt. *Environmental Science and Pollution Research*, 27(26), 32304–32317. <https://doi.org/10.1007/s11356-019-06529-5>
- Gesim, N. A., & Okazaki, T. (2018). Groundwater Quality Mapping Using Water Quality Index in the Kabul City , Afghanistan. *Proceedings of ISER 149th International Conference, Kyoto, Japan, 9th-10th August 2018, August*, 29–34.
- Ghazavi, R., Babaei, S., & Erfanian, M. (2018). Recharge Wells Site Selection for Artificial Groundwater Recharge in an Urban Area Using Fuzzy Logic Technique. *Water Resources Management*, 32(12), 3821–3834. <https://doi.org/10.1007/s11269-018-2020-7>
- Ghobadi, A., Cheraghi, M., Sobhanardakani, S., Lorestani, B., & Merrikhpour, H. (2022). Groundwater quality modeling using a novel hybrid data-intelligence model based on gray wolf optimization algorithm and multi-layer perceptron artificial neural network: a case study in Asadabad Plain, Hamedan, Iran. *Environmental Science and Pollution Research*, 29(6), 8716–8730. <https://doi.org/10.1007/s11356-021-16300-4>
- Gholami, V., Khaleghi, M. R., Pirasteh, S., & Booi, M. J. (2022). Comparison of Self-Organizing Map, Artificial Neural Network, and Co-Active Neuro-Fuzzy Inference System Methods in Simulating Groundwater Quality: Geospatial Artificial Intelligence. *Water Resources Management*, 36(2), 451–469. <https://doi.org/10.1007/s11269-021-02969-2>
- Gosh, P. K., Bandyopadhyay, S., & Jana, N. C. (2016). Mapping of groundwater potential zones in hard rock terrain using geoinformatics : a case of Kumari watershed in western part of West Bengal. *Modeling Earth Systems and Environment*, 2(1), 1–12. <https://doi.org/10.1007/s40808-015-0044-z>
- Halder, S., Roy, M. B., & Roy, P. K. (2020). Analysis of groundwater level trend and groundwater drought using Standard Groundwater Level Index: a case study of an eastern river basin of West Bengal, India. *SN Applied Sciences*, 2(3), 1–24. <https://doi.org/10.1007/s42452-020-2302-6>
- Hall, B., Currell, M., & Webb, J. (2020). Using multiple lines of evidence to map groundwater recharge in a rapidly urbanising catchment: Implications for future land and water management. *Journal of Hydrology*, 580(August 2019), 124265.

<https://doi.org/10.1016/j.jhydrol.2019.124265>

- Handa, B. K. (1975). Geochemistry and genesis of fluoride-containing ground waters in India. *Groundwater*.
- Hao, A., Zhang, Y., Zhang, E., Li, Z., Yu, J., Wang, H., Yang, J., & Wang, Y. (2018). Review: Groundwater resources and related environmental issues in China. *Hydrogeology Journal*, 26(5), 1325–1337. <https://doi.org/10.1007/s10040-018-1787-1>
- Haritash, A. K., Mathur, K., Singh, P., & Singh, S. K. (2017). Hydrochemical characterization and suitability assessment of groundwater in Baga–Calangute stretch of Goa, India. *Environmental Earth Sciences*, 76(9), 1–10. <https://doi.org/10.1007/s12665-017-6679-5>
- Hayat, E., & Baba, A. (2017). Quality of groundwater resources in Afghanistan. *Environmental Monitoring and Assessment*, 189(7). <https://doi.org/10.1007/s10661-017-6032-1>
- Hou, Q., Zhang, Q., Huang, G., Liu, C., & Zhang, Y. (2020). Elevated manganese concentrations in shallow groundwater of various aquifers in a rapidly urbanized delta, south China. *Science of the Total Environment*, 701, 134777. <https://doi.org/10.1016/j.scitotenv.2019.134777>
- Houben, G., Niard, N., Tünnermeier, T., & Himmelsbach, T. (2009). Hydrogeology of the Kabul Basin (Afghanistan), part I: Aquifers and hydrology. *Hydrogeology Journal*, 17(3), 665–677. <https://doi.org/10.1007/s10040-008-0377-z>
- Houben, G., & Tünnermeier, T. (2005). *Hydrogeology of the Kabul Basin Part II : Groundwater geochemistry and microbiology*. BGR. [https://www.bgr.bund.de/EN/Themen/Wasser/Projekte/abgeschlossen/TZ/Afghanistan/hydrogeology\\_kabul\\_basin\\_2.pdf?\\_\\_blob=publicationFile&v=3](https://www.bgr.bund.de/EN/Themen/Wasser/Projekte/abgeschlossen/TZ/Afghanistan/hydrogeology_kabul_basin_2.pdf?__blob=publicationFile&v=3)
- Houben, G., Tünnermeier, T., Eqrar, N., & Himmelsbach, T. (2009). Hydrogeology of the Kabul Basin (Afghanistan), part II: Groundwater geochemistry. *Hydrogeology Journal*, 17(4), 935–948. <https://doi.org/10.1007/s10040-008-0375-1>
- Hsin-Fu Yeh, H. F., & Chang, C. F. (2019). Using Standardized Groundwater Index and Standardized Precipitation Index to Assess Drought Characteristics of the Kaoping River Basin, Taiwan. *Water Resources*, 46(5), 670–678. <https://doi.org/10.1134/S0097807819050105>
- Huang, G., Liu, C., Li, L., Zhang, F., & Chen, Z. (2020). Spatial distribution and origin of shallow groundwater iodide in a rapidly urbanized delta: A case study of the Pearl River Delta. *Journal of Hydrology*, 585(March), 124860. <https://doi.org/10.1016/j.jhydrol.2020.124860>
- Huang, Z., Nya, E. L., Rahman, M. A., Mwamila, T. B., Cao, V., Gwenzi, W., & Noubactep, C. (2021). Integrated water resource management: Rethinking the contribution of rainwater harvesting. *Sustainability (Switzerland)*, 13(15), 1–9. <https://doi.org/10.3390/su13158338>
- Hussain, F., Hussain, R., Wu, R. S., & Abbas, T. (2019). Rainwater harvesting

- potential and utilization for artificial recharge of groundwater using recharge wells. *Processes*, 7(9). <https://doi.org/10.3390/pr7090623>
- Jeongju, L., Shinuk, K., Jihye, J., & Gunil, C. (2018). 가뭄 분석을 위한 지하수위 모니터링 및 예측기법 개발(I) - 표준지하수지수(SGI)를 이용한 지하수 가뭄 모니터링. *Journal of Korea Water Resources Association*, 51(11), 1011–1020. <https://doi.org/10.3741/JKWRA.2018.51.11.1011>
- JHARIYA, D. C., KUMAR, T., GOBINATH, M., DIWAN, P., & KISHORE, N. (2016). Assessment of Groundwater Potential Zone Using Remote Sensing , GIS and Multi Criteria Decision Analysis Techniques. *JOURNAL GEOLOGICAL SOCIETY OF INDIA*, 88, 481–492.
- JICA. (2011). *The study on groundwater resources potential in Kabul basin in the Islamic republic of Afghanistan final report*. JICA.
- Kalhor, K., & Emaminejad, N. (2019). Sustainable development in cities: Studying the relationship between groundwater level and urbanization using remote sensing data. *Groundwater for Sustainable Development*, 9(March), 100243. <https://doi.org/10.1016/j.gsd.2019.100243>
- Kalhor, K., Ghasemizadeh, R., Rajic, L., & Alshawabkeh, A. (2019). Assessment of groundwater quality and remediation in karst aquifers: A review. *Groundwater for Sustainable Development*, 8(July 2018), 104–121. <https://doi.org/10.1016/j.gsd.2018.10.004>
- Karami, S., Madani, H., Katibeh, H., & Fatehi Marj, A. (2018). Assessment and modeling of the groundwater hydrogeochemical quality parameters via geostatistical approaches. *Applied Water Science*, 8(1), 1–13. <https://doi.org/10.1007/s13201-018-0641-x>
- Karant, K. (1987). *Ground water assessment: development and management*. Tata McGraw-Hill Education.
- Karunanidhi, D., Aravinthasamy, P., Subramani, T., & Muthusankar, G. (2021). Revealing drinking water quality issues and possible health risks based on water quality index (WQI) method in the Shanmuganadhi River basin of South India. *Environmental Geochemistry and Health*, 43(2), 931–948. <https://doi.org/10.1007/s10653-020-00613-3>
- Khan, M. F., Yu, L., & Achari, G. (2020). Field evaluation of a pressurized ozone treatment system to degrade sulfolane in contaminated groundwaters. *Journal of Environmental Chemical Engineering, In Press*(May), 104037. <https://doi.org/10.1016/j.jece.2020.104037>
- KMARP. (2017). *Kabul Managed Aquifer Recharge Project Preparation*. KMARP. <https://kmarp.com/home>
- Kolandhavel, P., & Ramamoorthy, S. (2019). Investigation of groundwater potential zones in NandiAru Sub Basin , Tamilnadu , India — an integrated geophysical and geoinformatics approach. *Arabian Journal of Geosciences*.
- Kolanuvada, S. R. (2019). *Multi-criteria-based approach for optimal siting of*

*artificial recharge structures through hydrological modeling.*

- Krishna kumar, S., Logeshkumaran, A., Magesh, N. S., Godson, P. S., & Chandrasekar, N. (2015). Hydro-geochemistry and application of water quality index (WQI) for groundwater quality assessment, Anna Nagar, part of Chennai City, Tamil Nadu, India. *Applied Water Science*, 5(4), 335–343. <https://doi.org/10.1007/s13201-014-0196-4>
- Kumar, A., & Pandey, A. C. (2016). Geoinformatics based groundwater potential assessment in hard rock terrain of Ranchi urban environment, Jharkhand state (India) using MCDM-AHP techniques. *Groundwater for Sustainable Development*, 2–3(2016), 27–41. <https://doi.org/10.1016/j.gsd.2016.05.001>
- Kumar, P., Chandniha, S. K., Lohani, A. K., Nema, A. K., & Krishan, G. (2018). Trend Analysis of Groundwater Level Using Non-Parametric Tests in Alluvial Aquifers of Uttar Pradesh, India. *Current World Environment*, 13(1), 44–54. <https://doi.org/10.12944/cwe.13.1.05>
- Kuo, Y.-M., Liu, C.-W., & Lin, K.-H. (2004). Evaluation of the ability of an artificial neural network model to assess the variation of groundwater quality in an area of blackfoot disease in Taiwan. *Water Research*, 38(1), 148–158. <https://doi.org/10.1016/j.watres.2003.09.026>
- Lentswe, G. B., & Molwalefhe, L. (2020). Delineation of potential groundwater recharge zones using analytic hierarchy process-guided GIS in the semi-arid Motloutse watershed, eastern Botswana. *Journal of Hydrology: Regional Studies*, 28(January), 100674. <https://doi.org/10.1016/j.ejrh.2020.100674>
- Liou, S. M., Lo, S. L., & Wang, S. H. (2004). A generalized water quality index for Taiwan. *Environmental Monitoring and Assessment*, 96(1–3), 35–52. <https://doi.org/10.1023/B:EMAS.0000031715.83752.a1>
- Luo, D., Wen, X., Zhang, H., Xu, J., & Zhang, R. (2020). An improved FAHP based methodology for groundwater potential zones in Longchuan River basin, Yunnan Province, China. *Earth Science Informatics*, 13(3), 847–857. <https://doi.org/10.1007/s12145-020-00469-2>
- Machiwal, D., Jha, M. K., & Mal, B. C. (2011). Assessment of Groundwater Potential in a Semi-Arid Region of India Using Remote Sensing, GIS and MCDM Techniques. *Water Resources Management*, 25(5), 1359–1386. <https://doi.org/10.1007/s11269-010-9749-y>
- MacHiwal, D., Jha, M. K., & Mal, B. C. (2011). GIS-based assessment and characterization of groundwater quality in a hard-rock hilly terrain of Western India. *Environmental Monitoring and Assessment*, 174(1–4), 645–663. <https://doi.org/10.1007/s10661-010-1485-5>
- Mack, T. J., Akbari, M. A., Ashoor, M. H., Chornack, M. P., Coplen, T. B., Emerson, D. G., Hubbard, B. E., Litke, D. W., Michel, R. L., Plummer, L. N., Rezai, M. T., Senay, G. B., Verdin, J. P., & Verstraeten, I. M. (2009). Conceptual Model of Water Resources in the Kabul Basin , Afghanistan. In *USGS* (Issue 168). USGS. [http://pubs.usgs.gov/sir/2009/5262/pdf/sir2009-5262\\_front\\_text\\_508\\_Pt1\\_i-32\\_rev111312.pdf](http://pubs.usgs.gov/sir/2009/5262/pdf/sir2009-5262_front_text_508_Pt1_i-32_rev111312.pdf)



- Mack, T. J., Chornack, M. P., Coplen, T. B., Plummer, L. N., Rezai, M. T., & Verstraeten, I. M. (2010). *Availability of Water in the Kabul Basin, Afghanistan* (Issue May). USGS. <http://pubs.usgs.gov/sir/2009/5262>
- Mack, T. J., Chornack, M. P., & Taher, M. R. (2013). Groundwater-level trends and implications for sustainable water use in the Kabul Basin, Afghanistan. *Environment Systems and Decisions*, 33(3), 457–467. <https://doi.org/10.1007/s10669-013-9455-4>
- Magesh, N. S., Chandrasekar, N., & Soundranayagam, J. P. (2012). Delineation of groundwater potential zones in Theni district, Tamil Nadu, using remote sensing, GIS and MIF techniques. *Geoscience Frontiers*, 3(2), 189–196. <https://doi.org/10.1016/j.gsf.2011.10.007>
- Magesh, N. S., Krishnakumar, S., Chandrasekar, N., & Soundranayagam, J. P. (2013). Groundwater quality assessment using WQI and GIS techniques, Dindigul district, Tamil Nadu, India. *Arabian Journal of Geosciences*, 6(11), 4179–4189. <https://doi.org/10.1007/s12517-012-0673-8>
- Maheswaran, G., Geetha Selvarani, A., & Elangovan, K. (2016). Groundwater resource exploration in salem district, Tamil nadu using GIS and remote sensing. *Journal of Earth System Science*, 125(2), 311–328. <https://doi.org/10.1007/s12040-016-0659-0>
- Mahmoud, W. H., Elagib, N. A., Gaese, H., & Heinrich, J. (2014). Rainfall conditions and rainwater harvesting potential in the urban area of Khartoum. *Resources, Conservation and Recycling*, 91, 89–99. <https://doi.org/10.1016/j.resconrec.2014.07.014>
- Mahmud, A., Sikder, S., & Chandra, J. (2020). Assessment of groundwater quality in Khulna city of Bangladesh in terms of water quality index for drinking purpose. *Applied Water Science*, 10(11), 1–14. <https://doi.org/10.1007/s13201-020-01314-z>
- Malik, V. K., Singh, R. K., & Singh, S. K. (2010). Impact of Urbanization on Groundwater of Gurgaon District, Haryana, India. *International Journal of Rural Development and Management Studies*, 5(1), 45–57.
- Manago, K. F., Hogue, T. S., Porter, A., & Hering, A. S. (2019). A Bayesian hierarchical model for multiple imputation of urban spatio-temporal groundwater levels. *Statistics and Probability Letters*, 144, 44–51. <https://doi.org/10.1016/j.spl.2018.07.023>
- Manap, M. A., Nampak, H., Pradhan, B., Lee, S., Sulaiman, W. N. A., & Ramli, M. F. (2014). Application of probabilistic-based frequency ratio model in groundwater potential mapping using remote sensing data and GIS. *Arab J Geosci*, 711–724. <https://doi.org/10.1007/s12517-012-0795-z>
- Manawi, S. M. A., Nasir, K. A. M., Shiru, M. S., Hotaki, S. F., & Sediqi, M. N. (2020). Urban Flooding in the Northern Part of Kabul City: Causes and Mitigation. *Earth Systems and Environment*, 4(3), 599–610. <https://doi.org/10.1007/s41748-020-00165-7>
- Mandal, K. K., Ranjan, A., & Dharanirajan, K. (2021). Delineation of Groundwater

- Potential Zones (GWPZ) of Port Blair, Andaman Islands, India, using Multi Influencing Factors (MIF) method and geospatial techniques. *Remote Sensing Applications: Society and Environment*, 24, 100631. <https://doi.org/10.1016/j.rsase.2021.100631>
- Mansell, M. G. (2003). *Rural and urban hydrology*. Thomas Telford.
- Martin, S. L., Hayes, D. B., Kendall, A. D., & Hyndman, D. W. (2017). The land-use legacy effect: Towards a mechanistic understanding of time-lagged water quality responses to land use/cover. *Science of the Total Environment*, 579, 1794–1803. <https://doi.org/10.1016/j.scitotenv.2016.11.158>
- Masoom, M. F. (2018). *Artificial Recharge of Groundwater as a Management Tool for the Kabul Basin , Afghanistan* [Louisiana state University]. [https://digitalcommons.lsu.edu/gradschool\\_theses/4653%0AThis](https://digitalcommons.lsu.edu/gradschool_theses/4653%0AThis)
- Mengistu, H. A., Demlie, M. B., & Abiye, T. A. (2019). Review: Groundwater resource potential and status of groundwater resource development in Ethiopia. *Hydrogeology Journal*, 27(3), 1051–1065. <https://doi.org/10.1007/s10040-019-01928-x>
- Moritz, M. S. (2021). *Package ‘imputeTS’* (Vol. 2). <https://doi.org/10.32614/RJ-2017-009>. Author
- Moritz, S., & Bartz-Beielstein, T. (2017). imputeTS: Time series missing value imputation in R. *R Journal*, 9(1), 207–218. <https://doi.org/10.32614/rj-2017-009>
- Moritz, S., Sardá, A., Bartz-Beielstein, T., Zaefferer, M., & Stork, J. (2015). Comparison of different Methods for Univariate Time Series Imputation in R. *Cologne University of Applied Sciences*. <http://arxiv.org/abs/1510.03924>
- Mpofu, M., Madi, K., & Gwavava, O. (2020). Groundwater for Sustainable Development Remote sensing , geological , and geophysical investigation in the area of Ndlambe Municipality , Eastern Cape Province , South Africa : Implications for groundwater potential. *Groundwater for Sustainable Development*, 11(January 2019), 100431. <https://doi.org/10.1016/j.gsd.2020.100431>
- Muniraj, K., Jesudhas, C. J., & Chinnasamy, A. (2020). Delineating the Groundwater Potential Zone in Tirunelveli Taluk, South Tamil Nadu, India, Using Remote Sensing, Geographical Information System (GIS) and Analytic Hierarchy Process (AHP) Techniques. *Proceedings of the National Academy of Sciences India Section A - Physical Sciences*, 90(4), 661–676. <https://doi.org/10.1007/s40010-019-00608-5>
- Muralitharan, J., & Palanivel, K. (2015). Groundwater targeting using remote sensing, geographical information system and analytical hierarchy process method in hard rock aquifer system, Karur district, Tamil Nadu, India. *Earth Science Informatics*, 8(4), 827–842. <https://doi.org/10.1007/s12145-015-0213-7>
- Nachshon, U., Netzer, L., & Livshitz, Y. (2016). Land cover properties and rain water harvesting in urban environments. *Sustainable Cities and Society*, 27, 398–406. <https://doi.org/10.1016/j.scs.2016.08.008>
- Nachson, U., Silva, C. M., Sousa, V., Ben-Hur, M., Kurtzman, D., Netzer, L., &

- Livshitz, Y. (2022). New modelling approach to optimize rainwater harvesting system for non-potable uses and groundwater recharge: A case study from Israel. *Sustainable Cities and Society*, 85, 104097. <https://doi.org/10.1016/j.scs.2022.104097>
- Naik, P. K., Tambe, J. A., Dehury, B. N., & Tiwari, A. N. (2008). Impact of urbanization on the groundwater regime in a fast growing city in central India. *Environmental Monitoring and Assessment*, 146(1–3), 339–373. <https://doi.org/10.1007/s10661-007-0084-6>
- Najwa Mohd Rizal, N., Hayder, G., Mnzool, M., Elnaim, B. M. E., Mohammed, A. O. Y., & Khayyat, M. M. (2022). Comparison between Regression Models, Support Vector Machine (SVM), and Artificial Neural Network (ANN) in River Water Quality Prediction. *Processes*, 10(8), 1652. <https://doi.org/10.3390/pr10081652>
- Nguyen, D. Van, Ho, N. M., Hoang, K. D., Le, T. V., & Le, V. H. (2020). An investigation on treatment of groundwater with cold plasma for domestic water supply. *Groundwater for Sustainable Development*, 10(July 2019), 100309. <https://doi.org/10.1016/j.gsd.2019.100309>
- Niard, N. (2005). *Hydrogeology of the kabul basin part III: Modelling approach conceptual and numerical groundwater models*. BGR.
- Niu, B., Loáiciga, H. A., Wang, Z., Zhan, F. B., & Hong, S. (2014). Twenty years of global groundwater research: A Science Citation Index Expanded-based bibliometric survey (1993-2012). *Journal of Hydrology*, 519(PA), 966–975. <https://doi.org/10.1016/j.jhydrol.2014.07.064>
- Noori, A. R., & Singh, S. K. (2021a). Spatial and temporal trend analysis of groundwater levels and regional groundwater drought assessment of Kabul, Afghanistan. *Environmental Earth Sciences*, 80(20). <https://doi.org/10.1007/s12665-021-10005-0>
- Noori, A. R., & Singh, S. K. (2021b). Status of groundwater resource potential and its quality at Kabul , Afghanistan : a review. *Environmental Earth Sciences*, 80(18), 1–13. <https://doi.org/10.1007/s12665-021-09954-3>
- Noori, A. R., & Singh, S. K. (2023a). Assessment of seasonal groundwater quality variation employing GIS and statistical approaches in Kabul basin, Afghanistan. *Environment, Development and Sustainability*, 0123456789. <https://doi.org/10.1007/s10668-022-02876-5>
- Noori, A. R., & Singh, S. K. (2023b). Rainfall Assessment and Water Harvesting Potential in an Urban area for Artificial Groundwater Recharge with Land. *Water Resources Management*. <https://doi.org/https://doi.org/10.1007/s11269-023-03602-0> Rainfall
- Noori, A. R., & Singh, S. K. (2024). Delineation of optimal locations for artificial groundwater recharge utilizing MIF and GIS in a semi-arid area. *Environmental Earth Sciences*, 83(1), 33. <https://doi.org/10.1007/s12665-023-11338-8>
- Noori, K. M. A., & Nasimi, M. N. (2019). Kabul City Groundwater and Need for Artificial Recharge. *Proceedings of the 4th International Conference on Civil*,

- Structural and Transportation Engineering (ICCSTE'19)*, 1–7.  
<https://doi.org/10.11159/iccste19.215>
- NSIA. (2020). *Estimated Population of Afghanistan 2020-21*.
- Oliver, J. E. (1980). Monthly precipitation distribution: A comparative index. *Professional Geographer*, 32(3), 300–309. <https://doi.org/10.1111/j.0033-0124.1980.00300.x>
- Oroji, B. (2019). Groundwater vulnerability assessment with using GIS in Hamadan–Bahar plain, Iran. *Applied Water Science*, 9(8), 1–13.  
<https://doi.org/10.1007/s13201-019-1082-x>
- Oukil, A., Soltani, A. A., Boutaghane, H., Abdalla, O., Bermad, A., Hasbaia, M., & Boulassel, M. R. (2021). A Surrogate Water Quality Index to assess groundwater using a unified DEA-OWA framework. *Environmental Science and Pollution Research*. <https://doi.org/10.1007/s11356-021-13758-0>
- Paiman, Z., & Noori, A. R. (2019). Evaluation of Wastewater Collection and Disposal in Kabul City and Its Environmental Impacts. *Modern Environmental Science and Engineering*, 5(5), 451–458. [https://doi.org/10.15341/mese\(2333-2581\)/05.05.2019/012](https://doi.org/10.15341/mese(2333-2581)/05.05.2019/012)
- Palani, S., Liong, S.-Y., & Tkalich, P. (2008). An ANN application for water quality forecasting. *Marine Pollution Bulletin*, 56(9), 1586–1597.  
<https://doi.org/10.1016/j.marpolbul.2008.05.021>
- Patel, P. M., Saha, D., & Shah, T. (2020). Sustainability of groundwater through community-driven distributed recharge: An analysis of arguments for water scarce regions of semi-arid India. *Journal of Hydrology: Regional Studies*, 29(March), 100680. <https://doi.org/10.1016/j.ejrh.2020.100680>
- Pathak, A. A., & Dodamani, B. M. (2019). Trend Analysis of Groundwater Levels and Assessment of Regional Groundwater Drought: Ghataprabha River Basin, India. *Natural Resources Research*, 28(3), 631–643.  
<https://doi.org/10.1007/s11053-018-9417-0>
- Pauleit, S., & Duhme, F. (2000a). Assessing the environmental performance of land cover types for urban planning. *Landscape and Urban Planning*, 52(1), 1–20.  
[https://doi.org/10.1016/S0169-2046\(00\)00109-2](https://doi.org/10.1016/S0169-2046(00)00109-2)
- Pauleit, S., & Duhme, F. (2000b). Assessing the environmental performance of land cover types for urban planning. *Landscape and Urban Planning*.  
[https://doi.org/http://dx.doi.org/10.1016/s0169-2046\(00\)00109-2](https://doi.org/http://dx.doi.org/10.1016/s0169-2046(00)00109-2)
- Pell Frischmann. (2012). *Afghanistan Resource Corridor Development: Water Strategy Final Kabul River Basin Report Version 4.0*.
- Pinto, D., Shrestha, S., Babel, M. S., & Ninsawat, S. (2017). Delineation of groundwater potential zones in the Comoro watershed, Timor Leste using GIS, remote sensing and analytic hierarchy process (AHP) technique. *Applied Water Science*, 7(1), 503–519. <https://doi.org/10.1007/s13201-015-0270-6>
- Piper, A. M. (1944). A graphic procedure in the geochemical interpretation of water analyses. *American Geophysical Union*, 914–928.

- Prabhu, M. V., & Venkateswaran, S. (2015). Delineation of Artificial Recharge Zones Using Geospatial Techniques in Sarabanga Sub Basin Cauvery River, Tamil Nadu. *Aquatic Procedia*, 4(Icwrcoe), 1265–1274. <https://doi.org/10.1016/j.aqpro.2015.02.165>
- Qi, Q., Marwa, J., Mwamila, T. B., Gwenzi, W., & Noubactep, C. (2019). Making rainwater harvesting a key solution for water management: The universality of the Kilimanjaro Concept. *Sustainability (Switzerland)*, 11(20), 1–15. <https://doi.org/10.3390/su11205606>
- Qureshi, A. S. (2002). Water resources management in Afghanistan. In *International Water Management Institute* (Issue 14). International Water Management Institute. [http://www.afghaneic.net/library/hydrological\\_surveys/wor49.pdf](http://www.afghaneic.net/library/hydrological_surveys/wor49.pdf)
- Rabeiy, R. E. S. (2018). Assessment and modeling of groundwater quality using WQI and GIS in Upper Egypt area. *Environmental Science and Pollution Research*, 25(31), 30808–30817. <https://doi.org/10.1007/s11356-017-8617-1>
- Radouane, E. M., Chahlaoui, A., & Maliki, A. (2021). Assessment and modeling of groundwater quality by using water quality index ( WQI ) and GIS technique in meknes aquifer ( Morocco ). *Geology, Ecology, and Landscapes*, 00(00), 1–13. <https://doi.org/10.1080/24749508.2021.1944797>
- Rahbar, A., Vadiati, M., Talkhabi, M., Nadiri, A. A., Nakhaei, M., & Rahimian, M. (2020). A hydrogeochemical analysis of groundwater using hierarchical clustering analysis and fuzzy C-mean clustering methods in Arak plain, Iran. *Environmental Earth Sciences*, 79(13), 1–17. <https://doi.org/10.1007/s12665-020-09064-6>
- Rahman, A. T. M. S., Jahan, C. S., Mazumder, Q. H., Kamruzzaman, M., & Hosono, T. (2017). Drought analysis and its implication in sustainable water resource management in Barind area, Bangladesh. *Journal of the Geological Society of India*, 89(1), 47–56. <https://doi.org/10.1007/s12594-017-0557-3>
- Rajasekhar, M., Gadhiraaju, S. R., Kadam, A., & Bhagat, V. (2020). Identification of groundwater recharge-based potential rainwater harvesting sites for sustainable development of a semiarid region of southern India using geospatial, AHP, and SCS-CN approach. *Arabian Journal of Geosciences*, 13(1), 24. <https://doi.org/10.1007/s12517-019-4996-6>
- Ram, A., Tiwari, S. K., Pandey, H. K., Chaurasia, A. K., Singh, S., & Singh, Y. V. (2021). Groundwater quality assessment using water quality index (WQI) under GIS framework. *Applied Water Science*, 11(2), 1–20. <https://doi.org/10.1007/s13201-021-01376-7>
- Ramakrishnaiah, C. R., Sadashivaiah, C., & Ranganna, G. (2009). Assessment of water quality index for the groundwater in Tumkur taluk, Karnataka state, India. *E-Journal of Chemistry*, 6(2), 523–530. <https://doi.org/10.1155/2009/757424>
- Ranaee, E., Abbasi, A. A., Yazdi, J. T., & Ziyae, M. (2021). Feasibility of rainwater harvesting and consumption in a middle eastern Semiarid urban area. *Water (Switzerland)*, 13(15), 1–23. <https://doi.org/10.3390/w13152130>
- Reddy, A. G. S., Reddy, D. V., Rao, P. N., & Prasad, K. M. (2010).

- Hydrogeochemical characterization of fluoride rich groundwater of Wailpalli watershed, Nalgonda District, Andhra Pradesh, India. *Environmental Monitoring and Assessment*, 171(1–4), 561–577.  
<https://doi.org/10.1007/s10661-009-1300-3>
- Ribeiro, L., Kretschmer, N., Nascimento, J., Buxo, A., Rötting, T., Soto, G., Señoret, M., Oyarzún, J., Maturana, H., & Oyarzún, R. (2015). Utilisation du test de Mann-Kendall à l'évaluation des tendances piézométriques des aquifères alluviaux du bassin de l'Elqui, Chili. *Hydrological Sciences Journal*, 60(10), 1840–1852. <https://doi.org/10.1080/02626667.2014.945936>
- River, B., Fathi, E., Zamani, R., Rafat, A., & Bidaki, Z. (2018). Water quality evaluation using water quality index and multivariate. *Applied Water Science*, 8(7), 1–6. <https://doi.org/10.1007/s13201-018-0859-7>
- Sadat-Noori, S. M., Ebrahimi, K., & Liaghat, A. M. (2014). Groundwater quality assessment using the Water Quality Index and GIS in Saveh-Nobaran aquifer, Iran. *Environmental Earth Sciences*, 71(9), 3827–3843.  
<https://doi.org/10.1007/s12665-013-2770-8>
- Saffi, M. H. (2007). *Ground water resources at risk in Afghanistan* (Issue June 2007). DACAAR. <https://doi.org/10.13140/RG.2.1.4465.7128>
- Saffi, M. H. (2011). *Groundwater natural resources and quality concern in Kabul Basin , Afghanistan Scientific Investigation Report in Afghanistan* (Issue 1). DACAAR. [www.dacaar.org](http://www.dacaar.org)
- Saffi, M. H., & Jawid, A. (2013). *UNHCR public drinking water points analysed water quality data evaluation in* (Issue January). DACAAR.
- Saffi, M. H., & Kohistani, A. J. (2013). *Water Resources Potential, Quality Problems, Challenges and Solutions in Afghanistan*. DACAAR.
- Samson S. (2010). Groundwater quality characterization using GIS and artificial neural network, in Namakkal district, Tamilnadu (PhD thesis). In ANNA UNIVERSITY. ANNA UNIVERSITY.
- Saraswat, C., Kumar, P., Dasgupta, R., Avtar, R., & Bhalani, P. (2019). Sustainability assessment of the groundwater quality in the Western India to achieve urban water security. *Applied Water Science*, 9(4), 1–17.  
<https://doi.org/10.1007/s13201-019-0956-2>
- Selvakumar, S., Chandrasekar, N., & Kumar, G. (2017). Hydrogeochemical characteristics and groundwater contamination in the rapid urban development areas of Coimbatore, India. *Water Resources and Industry*, 17(February), 26–33. <https://doi.org/10.1016/j.wri.2017.02.002>
- Selvakumar, S., Ramkumar, K., Chandrasekar, N., Magesh, N. S., & Kaliraj, S. (2017). Groundwater quality and its suitability for drinking and irrigational use in the Southern Tiruchirappalli district, Tamil Nadu, India. *Applied Water Science*, 7(1), 411–420. <https://doi.org/10.1007/s13201-014-0256-9>
- Selvam, S., Dar, F. A., Magesh, N. S., Singaraja, C., Venkatramanan, S., & Chung, S. Y. (2016). Application of remote sensing and GIS for delineating groundwater recharge potential zones of Kovilpatti Municipality, Tamil Nadu

- using IF technique. *Earth Science Informatics*, 9(2), 137–150.  
<https://doi.org/10.1007/s12145-015-0242-2>
- Sen, P. K. (1968). Estimates of the Regression Coefficient Based on Kendall's Tau. *Journal of the American Statistical Association*, 63(324), 1379–1389.  
<https://doi.org/10.1080/01621459.1968.10480934>
- Senanayake, I. P., Dissanayake, D. M. D. O. K., Mayadunna, B. B., & Weerasekera, W. L. (2016). An approach to delineate groundwater recharge potential sites in Ambalantota, Sri Lanka using GIS techniques. *Geoscience Frontiers*, 7(1), 115–124. <https://doi.org/10.1016/j.gsf.2015.03.002>
- Shan, V., Singh, S. K., & Haritash, A. K. (2021). Evaluation of water quality and potential metal contamination in ecologically important Bhindawas bird sanctuary, India. *Applied Water Science*, 11(1), 1–9.  
<https://doi.org/10.1007/s13201-020-01334-9>
- Siddi Raju, R., Sudarsana Raju, G., & Rajasekhar, M. (2019). Identification of groundwater potential zones in Mandavi River basin, Andhra Pradesh, India using remote sensing, GIS and MIF techniques. *HydroResearch*, 2, 1–11.  
<https://doi.org/10.1016/j.hydres.2019.09.001>
- Sidiqi, M., & Shrestha, S. (2021). Assessment of Climate Change Impact on the Hydrology of the Kabul River Basin, Afghanistan. *Journal of Water Engineering and Management*, 2(1). <https://doi.org/10.47884/jweam.v2i1pp01-21>
- Singaraja, C. (2017). Relevance of water quality index for groundwater quality evaluation: Thoothukudi District, Tamil Nadu, India. *Applied Water Science*, 7(5), 2157–2173. <https://doi.org/10.1007/s13201-017-0594-5>
- Singh, S. K., & Noori, A. R. (2022a). Delineation of groundwater recharge potential zones for its sustainable development utilizing GIS approach in Kabul basin, Afghanistan. *Arabian Journal of Geosciences*, 15(2).  
<https://doi.org/10.1007/s12517-021-09410-3>
- Singh, S. K., & Noori, A. R. (2022b). Groundwater quality assessment and modeling utilizing water quality index and GIS in Kabul Basin, Afghanistan. *Environmental Monitoring and Assessment*, 194(10).  
<https://doi.org/10.1007/s10661-022-10340-0>
- Sinharay S. (2010). An Overview of Statistics in Education. In *International Encyclopedia Of Education* (pp. 1–11).
- Sishodia, R. P., Shukla, S., Graham, W. D., Wani, S. P., & Garg, K. K. (2016). Bi-decadal groundwater level trends in a semi-arid south indian region: Declines, causes and management. *Journal of Hydrology: Regional Studies*, 8, 43–58.  
<https://doi.org/10.1016/j.ejrh.2016.09.005>
- Souissi, D., Msaddek, M. H., Zouhri, L., May, M. El, & Dlala, M. (2018). Mapping groundwater recharge potential zones in arid region using GIS and Landsat approaches , southeast Tunisia. *Hydrological Sciences Journal*, 63(2), 251–268.  
<https://doi.org/10.1080/02626667.2017.1414383>
- Srinivas, Y., Aghil, T. B., Hudson Oliver, D., Nithya Nair, C., & Chandrasekar, N.

- (2017). Hydrochemical characteristics and quality assessment of groundwater along the Manavalakurichi coast, Tamil Nadu, India. *Applied Water Science*, 7(3), 1429–1438. <https://doi.org/10.1007/s13201-015-0325-8>
- Stiefel, J. M., Melesse, A. M., McClain, M. E., Price, R. M., Anderson, E. P., & Chauhan, N. K. (2009). Effects of rainwater-harvesting-induced artificial recharge on the groundwater of wells in Rajasthan, India. *Hydrogeology Journal*, 17(8), 2061–2073. <https://doi.org/10.1007/s10040-009-0491-6>
- Su, K., Wang, Q., Li, L., Cao, R., & Xi, Y. (2022). Water quality assessment of Lugu Lake based on Nemerow pollution index method. *Scientific Reports*, 12(1), 13613. <https://doi.org/10.1038/s41598-022-17874-w>
- Sunayana, Kalawapudi, K., Dube, O., & Sharma, R. (2020). Use of neural networks and spatial interpolation to predict groundwater quality. *Environment, Development and Sustainability*, 22(4), 2801–2816. <https://doi.org/10.1007/s10668-019-00319-2>
- Suresh, S., Raju, C., Krishma, R., Ravi kiran, N., & Chaitanya, G. S. S. R. (2020). An Empirical Analysis of Leaky Integrate and Fire Neuron Model. *International Journal of Engineering Research & Technology (IJERT)*, 9(5), 1043–1046. [www.ijert.org](http://www.ijert.org)
- Taher, M. R., Chornack, M. P., & Mack, T. J. (2013). *Groundwater Levels in the Kabul Basin , Afghanistan, 2004-2013* (Issue 182). USGS.
- Thapa, R., Gupta, S., Guin, S., & Kaur, H. (2017). Assessment of groundwater potential zones using multi-influencing factor (MIF) and GIS: a case study from Birbhum district, West Bengal. *Applied Water Science*, 7(7), 4117–4131. <https://doi.org/10.1007/s13201-017-0571-z>
- Tiwari, K., Goyal, R., & Sarkar, A. (2018). GIS-based Methodology for Identification of Suitable Locations for Rainwater Harvesting Structures. *Water Resources Management*, 32(5), 1811–1825. <https://doi.org/10.1007/s11269-018-1905-9>
- Todd, D. K. (1980). *Groundwater Hydrology*. Wiley.
- Tunc Dede, O., Telci, I. T., & Aral, M. M. (2013). The Use of Water Quality Index Models for the Evaluation of Surface Water Quality: A Case Study for Kirmir Basin, Ankara, Turkey. *Water Quality, Exposure and Health*, 5(1), 41–56. <https://doi.org/10.1007/s12403-013-0085-3>
- Tünnermeier, T., & Houben, D. G. (2005). *Hydrogeology of the Kabul Basin Part I : Geology , aquifer characteristics , climate and hydrography*. BGR.
- Uddin, M. G., Nash, S., & Olbert, A. I. (2021). A review of water quality index models and their use for assessing surface water quality. *Ecological Indicators*, 122, 107218. <https://doi.org/10.1016/j.ecolind.2020.107218>
- Uhl, W. V., & Tahiri, M. Q. (2003). *An overview of groundwater resources and challenges*. Vincent W. Uhl Uhl, Baron, Rana Associates, Inc. Washington Crossing, PA, USA.
- UN. (1967). *Hydrogeologic map of Lebanon. hydrog´eologique du Liban au*



*1/100000me, United Nations.*

- USDA. (2009). Chapet 7 Hydrologic Soil Groups. In *National Engineering Handbook*.
- Vaiphei, S. P., Kurakalva, R. M., & Sahadevan, D. K. (2020). Water quality index and GIS-based technique for assessment of groundwater quality in Wanaparthy watershed, Telangana, India. *Environmental Science and Pollution Research*, 27(36), 45041–45062. <https://doi.org/10.1007/s11356-020-10345-7>
- Varol, S., & Davraz, A. (2015). Evaluation of the groundwater quality with WQI (Water Quality Index) and multivariate analysis: a case study of the Tefenni plain (Burdur/Turkey). *Environmental Earth Sciences*, 73(4), 1725–1744. <https://doi.org/10.1007/s12665-014-3531-z>
- Vasanthavigar, M., Srinivasamoorthy, K., Vijayaragavan, K., Rajiv Ganthi, R., Chidambaram, S., Anandhan, P., Manivannan, R., & Vasudevan, S. (2010). Application of water quality index for groundwater quality assessment: Thirumanimuttar sub-basin, Tamilnadu, India. *Environmental Monitoring and Assessment*, 171(1–4), 595–609. <https://doi.org/10.1007/s10661-009-1302-1>
- Venegas-Quiñones, H. L., Thomasson, M., & Garcia-Chevesich, P. A. (2019). Trend Analysis of Precipitation, Groundwater Level and Flow Rate Data by using Mann-Kendall and Sen's Slope Estimator Statistical Tests in the Petorca Communer. *American Journal of Environmental Sciences*, 15(6), 180–187. <https://doi.org/10.3844/ajessp.2019.180.187>
- Venugopal, T., Giridharan, L., Jayaprakash, M., & Periakali, P. (2009). Environmental impact assessment and seasonal variation study of the groundwater in the vicinity of River Adyar, Chennai, India. *Environmental Monitoring and Assessment*, 149(1–4), 81–97. <https://doi.org/10.1007/s10661-008-0185-x>
- Verma, P., Singh, P. K., Sinha, R. R., & Tiwari, A. K. (2020). Assessment of groundwater quality status by using water quality index (WQI) and geographic information system (GIS) approaches: a case study of the Bokaro district, India. *Applied Water Science*, 10(1), 1–16. <https://doi.org/10.1007/s13201-019-1088-4>
- Vijaya, V., Sharma, S., & Batra, N. (2019). Comparative Study of Single Linkage, Complete Linkage, and Ward Method of Agglomerative Clustering. *Proceedings of the International Conference on Machine Learning, Big Data, Cloud and Parallel Computing: Trends, Perspectives and Prospects, COMITCon 2019*, 568–573. <https://doi.org/10.1109/COMITCon.2019.8862232>
- Walsh, R. P. D., & Lawler, D. M. (1981). Rainfall Seasonality: Description, Spatial Patterns and Change Through Time. *Weather*, 36(7), 201–208. <https://doi.org/10.1002/j.1477-8696.1981.tb05400.x>
- WHO. (2011). *Guidelines for Drinking-water Quality* (FOURTH EDI).
- WHO. (2017). *Guidelines for Drinking water Quality fourth edition incorporating the first addendum*. licence: CC BY-NC-SA 3.0 IGO
- Yadav, K. K., Gupta, N., Kumar, V., Arya, S., & Singh, D. (2012). Physico-chemical analysis of selected ground water samples of Agra city, India. *Recent Research*

*in Science and Technology*, 4(11), 51–54.

- Yeh, H. F., Cheng, Y. S., Lin, H. I., & Lee, C. H. (2016). Mapping groundwater recharge potential zone using a GIS approach in Hualien River, Taiwan. *Sustainable Environment Research*, 26(1), 33–43.  
<https://doi.org/10.1016/j.serj.2015.09.005>
- Yidana, S. M., Banoeng-Yakubo, B., & Akabzaa, T. M. (2010). Analysis of groundwater quality using multivariate and spatial analyses in the Keta basin, Ghana. *Journal of African Earth Sciences*, 58(2), 220–234.  
<https://doi.org/10.1016/j.jafrearsci.2010.03.003>
- Yisa, J., & Jimoh, T. (2010). Analytical studies on water quality index of river Landzu. *American Journal of Applied Sciences*, 7(4), 453–458.  
<https://doi.org/10.3844/ajassp.2010.453.458>
- Zabidi, H. A., Goh, H. W., Chang, C. K., Chan, N. W., & Zakaria, N. A. (2020). A review of roof and pond rainwater harvesting systems for water security: The design, performance and way forward. *Water (Switzerland)*, 12(11), 1–22.  
<https://doi.org/10.3390/w12113163>
- Zaryab, A., Noori, A. R., Wegerich, K., & Kløve, B. (2017). Assessment of water quality and quantity trends in Kabul aquifers with an outline for future drinking water supplies. *Central Asian Journal of Water Research*, 3(2), 3–11.  
<http://www.water-ca.org/article/1925-assessment-of-water-quality-and-quantity-trends-in-kabul-aquifers-with-an-outline-for-future-water-supplies>
- Zghibi, A., Mirchi, A., Msaddek, M. H., Merzougui, A., Zouhri, L., Taupin, J. D., Chekirbane, A., Chenini, I., & Tarhouni, J. (2020). and Multi-Influencing Factors to Map Groundwater Recharge Zones in a Semi-Arid Mediterranean. *Water*, 12(9), 2525.
- Zhang, D., Martinez, N., Lindholm, G., & Ratnaweera, H. (2018). Manage Sewer In-Line Storage Control Using Hydraulic Model and Recurrent Neural Network. *Water Resources Management*, 32(6), 2079–2098.  
<https://doi.org/10.1007/s11269-018-1919-3>
- Zhang, H., Xu, Y., & Kanyerere, T. (2019). Site assessment for MAR through GIS and modeling in West Coast, South Africa. *Water (Switzerland)*, 11(8).  
<https://doi.org/10.3390/w11081646>
- Zhang, Z., Yang, X., Li, H., Li, W., Yan, H., & Shi, F. (2017). Application of a novel hybrid method for spatiotemporal data imputation: A case study of the Minqin County groundwater level. *Journal of Hydrology*, 553, 384–397.  
<https://doi.org/10.1016/j.jhydrol.2017.07.053>

## Appendix-I

### List of Publications

#### A. Published Research Papers

Noori AR, Singh SK (2024) **Delineation of optimal locations for artificial groundwater recharge utilizing MIF and GIS in a semi-arid area.** Environ Earth Sci 83:33. <https://doi.org/10.1007/s12665-023-11338-8>

Noori AR, Singh SK (2023b) **Assessment of seasonal groundwater quality variation employing GIS and statistical approaches in Kabul basin, Afghanistan.** Environ Dev Sustain. <https://doi.org/10.1007/s10668-022-02876-5>

Noori AR, Singh SK (2023c) **Rainfall Assessment and Water Harvesting Potential in an Urban area for Artificial Groundwater Recharge with Land.** Water Resource Manag. <https://doi.org/https://doi.org/10.1007/s11269-023-03602-0>

Singh SK, Noori AR (2022a) **Groundwater quality assessment and modeling utilizing water quality index and GIS in Kabul Basin, Afghanistan.** Environ Monit Assess 194:. <https://doi.org/10.1007/s10661-022-10340-0>

Singh SK, Noori AR (2022b) **Delineation of groundwater recharge potential zones for its sustainable development utilizing GIS approach in Kabul basin, Afghanistan.** Arab J Geosci 15:. <https://doi.org/10.1007/s12517-021-09410-3>

Noori AR, Singh SK (2021a) **Assessment and modeling of sewer network development utilizing Arc GIS and SewerGEMS in Kabul city of Afghanistan.** J Eng Res 22–31. <https://doi.org/https://doi.org/10.36909/jer.ICARI.15287>

Noori AR, Singh SK (2021b) **Spatial and temporal trend analysis of groundwater levels and regional groundwater drought assessment of Kabul, Afghanistan.** Environ Earth Sci 80: <https://doi.org/10.1007/s12665-021-10005-0>

Noori AR, Singh SK (2021c) **Status of groundwater resource potential and its quality at Kabul, Afghanistan: a review.** Environ Earth Sci 80:1–13. <https://doi.org/10.1007/s12665-021-09954-3>

#### B. Conference Proceeding

Noori AR, Singh SK (2023a) **Drinking Water Quality Evaluation and Its Hydrochemical Aspects in the Kabul Basin, Afghanistan.** In: Al Khaddar, R., Singh, S.K., Kaushika, N.D., Tomar, R.K., Jain, S.K. (eds) Recent Developments in Energy and Environmental Engineering. TRACE 2022. Lecture Notes in Civil Engineering, vol 333. Springer, Singapore. pp 61–73, [https://doi.org/10.1007/978-981-99-1388-6\\_5](https://doi.org/10.1007/978-981-99-1388-6_5)

### **C. International Conferences**

**Noori A.R., Singh, S.K, (2021), Modeling of wastewater collection network using ArcGIS and Sewer GEMS in Kabul, Afghanistan,** in the International Conference of Advance Research and Innovation (ICARI-2021), Organized by Meerut Institute of Engineering and Technology, Meerut (Affiliated to Dr. Abdul Kalam Technical University, Lucknow) with International Journal of Advance Research and Innovation, January 30th 2021

**Noori A.R., Singh, S.K, (2022), Drinking Water Quality Evaluation and its Hydrochemical Aspects in the Kabul Basin, Afghanistan,** in the 4th International Conference on Trends and Recent Advances in Civil Engineering (TRACE - 2022), Organized by AMITY UNIVERSITY UTTAR PRADESH, NOIDA, INIDA during 18th - 19th October, 2022

**Noori A.R., Singh, S.K, (2024), Development and Application of an Artificial Neural Network Model for Assessing Groundwater Quality: A Study in the Kabul Basin, Afghanistan,** in the 5th International Conference on Trends and Recent Advances in Civil Engineering (TRACE - 2024), Organized by AMITY UNIVERSITY UTTAR PRADESH, NOIDA, INIDA during 15th - 16th October, 2024



## DELHI TECHNOLOGICAL UNIVERSITY

(Formerly Delhi College of Engineering)

Shahbad Daultpur, Main Bawana Road, Delhi-42

### Plagiarism Verification

Title of the thesis **Assessment of groundwater quality and recharge potential in Kabul, Afghanistan**

Total Pages **197** Name of the scholar **Ali Reza Noori**

Supervisor

**Prof. S.K. Singh**

Department **Environmental Engineering**

This is to report that the above thesis was scanned for similarity detection. Process and outcome are given below:

Software Used: **Turnitin** Similarity Index: **7%** Total Word Count: **54217**

Date:

A handwritten signature in blue ink, consisting of a large loop at the top and several horizontal strokes below, representing the candidate's name.

Candidate's Signature.

Signature of supervisor

## CURRICULUM VITA

### Ali Reza Noori

Research Area: Water Resources and Environmental Engineering

<https://orcid.org/0000-0003-2437-2119>

---

### EDUCATION

28/08/2019 – CURRENT, Delhi India

**Department of Environmental Engineering**

**Thesis: Assessment of groundwater quality and recharge potential in Kabul, Afghanistan**

01/09/2014 – 01/07/2016 Almaty, Kazakhstan

**MASTER OF TECHNICAL SCIENCE** at Kazakh National Research and Technical University after K.I. Satpaiv (КазННТУ)

**Field of study Water Resources Engineering**

23/07/2005 – 30/07/2009 Kabul, Afghanistan

**B.SC.** Kabul Polytechnic University

**Field of study: Water Supply and Environmental Engineering**

---

### WORK EXPERIENCE

01/12/2010 – CURRENT Kabul, Afghanistan

**UNIVERSITY LECTURER IN ENGINEERING AT KABUL POLYTECHNIC UNIVERSITY**

28/09/2022 – CURRENT

**PEER REVIEWER** VARIOUS SCIENTIFIC JOURNAL

20/03/2024 – CURRENT, KABUL, Afghanistan

**EDITORIAL BOARD MEMBER** KPU SCIENCE AND TECHNOLOGY JOURNAL

10/01/2015 – CURRENT Kabul, Afghanistan

**WATER SYSTEMS ENGINEER AND DESIGN CONSULTANT (FREELANCE)** BENA E SHARQ ARCHITECTURAL AND ENGINEERING SERVICES CO.

13/02/2023 – 01/03/2024 Kabul, Afghanistan

**MONITORING BOARD MEMBER OF KPU WATER SUPPLY PROJECT** KABUL POLYTECHNIC UNIVERSITY

20/11/2011 – 14/08/2013 Kabul and Potsdam, Afghanistan

**PROJECT COORDINATOR (VOLUNTEER)** KPU AND GFZ

---

---

**Volunteer Coordinator between GFZ and KPU (Freelance)**

---

**CONFERENCES AND SEMINARS**

---

04/03/2019 – 06/03/2019 Kabul

Afghanistan state of environmental workshop

The workshop was coordinated and sponsored by: UN Environment, National Environmental Protection Agency (NEPA)

09/10/2018 – 11/10/2018 Almaty

International Symposium on Water and Land Resources in Central Asia

The conference was coordinated and sponsored by GFZ, the German Federal Foreign Office, University of Wurzburg, Germany and the German Kazakh University, in Almaty, Kazakhstan

27/01/2018 – 31/01/2018 Ministry of Energy and Water, Kabul, Afghanistan, Application of Remote Sensing and Geographic Information Systems for Mapping and Monitoring of Glaciers in Afghanistan

The seminar was coordinated and sponsored by ICIMOD, USAID, NASA, SERVIR-HKH

03/10/2016 – 07/10/2016 Dushanbe, Tajikistan

Capacity Building of Researchers from Central Asia and Afghanistan

The workshop was coordinated and sponsored by OSCE Office in Tajikistan and German – Kazakh University, Almaty, Kazakhstan

22/04/2015 – 23/04/2015 German Kazakh University, Almaty, Kazakhstan

Global Water Partnership Universities ToolBox Workshop for Central Asia

The programme was coordinated and sponsored by German Kazakh University, Global Water Partnership and Central Asian Regional Water Network CAR@WAN

09/12/2013 – 13/12/2013 Central-Asian Institute for Applied Geosciences (CAIAG), Bishkek, Kyrgyzstan

Statistical analysis in hydrology, Introduction to R

The workshop was organized and sponsored by the German Research Centre for Geo Sciences (GFZ) and the Central-Asian Institute for Applied Geosciences (CAIAG)

The program included lectures and practical work applying R and RStudio in Statistical Approaches.

22/04/2013 – 26/04/2013 German Research Centre for Geo sciences (GFZ), Potsdam, Germany

Technical equipment for river runoff monitoring, sensors, handling and application GFZ organized the workshop

The program included lectures and practical works in the application of hydrological measurement instruments and software.

---

---

10/12/2012 – 14/12/2012 German Research Centre for Geo sciences (GFZ),  
Potsdam, Germany  
Use of GIS techniques in natural resource management  
GFZ organized the workshop  
The program included lectures and practical works on the use of GIS in natural  
resources management.

16/07/2012 – 22/07/2012 German Research Centre for Geo sciences (GFZ),  
Potsdam, Germany  
Use of remote sensing techniques in hydrometeorology  
GFZ organized the workshop  
The program included lectures and practical works for the use of remote sensing  
techniques and GIS in hydrometeorology.

05/12/2011 – 09/12/2011 German Research Centre for Geo sciences (GFZ),  
Potsdam, Germany  
Installation, operation and maintenance of CAWa meteorological monitoring  
stations  
GFZ organized the workshop  
The program included lectures, practical works, and fieldwork for the installation  
and commissioning of Hydro meteorological complex station.

---

## **COMPUTER SKILLS**

The application of the following computer programs in the planning and design of  
the comparative projects I have worked on and in the research articles, Master's  
and PhD theses, has been reflected. In addition to using the above programs, I have  
taught some of them for some time.

ArcGIS and QGIS  
R and RStudio  
SPSS  
Auto CAD 2D  
SewerGEMS and SewerCAD  
WaterGEMS and WaterCAD  
EPANET

---

## **SOFT SKILLS**

Content development  
Drawing and drafting  
Data analysis  
Project Management  
Problem-solving and critical thinking  
Communication  
Teamwork  
Attention to Detail

---



---

Responsibility

---

### **Laboratory Skills for Water Quality Analysis**

Skilled in conducting laboratory experiments related to water quality assessment and analysis.

Ability to calibrate and troubleshoot laboratory equipment used for water quality testing.

Familiarity with standard laboratory protocols for sample collection, preservation, and analysis.

Competence in interpreting and analyzing data obtained from laboratory experiments and field studies.

Knowledge of statistical methods for data analysis and interpretation in water quality research.

Familiarity with laboratory safety protocols and procedures for handling hazardous materials and chemicals.

---

### **HONOURS AND AWARDS**

06/04/2022

Commendable Research Award – Delhi Technological University, Delhi, India

The following papers received a research excellence award from DTU in 2022:

Singh, S. K., & Noori, A. R. (2022). Groundwater quality assessment and modelling utilizing water quality index and GIS in Kabul Basin, Afghanistan. *Environmental Monitoring and Assessment*, 194(10).

<https://doi.org/10.1007/s10661-022-10340-0>

The award includes a certificate of acknowledgement for authors and a prize of 50,000 INR.

06/04/2021

Excellence Research Award – Delhi Technological University

The following papers received a research excellence award from DTU in 2021:

Noori, AR, Singh, SK (2021) Spatial and temporal trend analysis of groundwater levels and regional groundwater drought assessment of Kabul, Afghanistan. *Environ Earth Sci* 80, 698. <https://doi.org/10.1007/s12665-021-10005-0>

<https://doi.org/10.1007/s12665-021-10005-0>

Noori, AR, Singh, SK (2021) Status of groundwater resource potential and its quality at Kabul, Afghanistan: a review. *Environ Earth Sci* 80, 654.

<https://doi.org/10.1007/s12665-021-09954-3>

The award includes a certificate of acknowledgement for authors and a prize of 100,000 INR.

---

### **PUBLICATIONS**

#### **Published papers**

1. Noori AR, Singh SK\* (2024): Delineation of optimal locations for artificial groundwater recharge utilizing MIF and GIS in a semi-arid area. *Environ Earth Sci* 83:33. <https://doi.org/10.1007/s12665-023-11338-8>
-

- 
2. Noori AR\*, Singh SK (2023): Rainfall Assessment and Water Harvesting Potential in an Urban area for Artificial Groundwater Recharge with Land. *Water Resour Manag.* <https://doi.org/https://doi.org/10.1007/s11269-023-03602-0>
  3. Noori AR\*, Singh SK (2023): Drinking Water Quality Evaluation and Its Hydrochemical Aspects in the Kabul Basin, Afghanistan. In: In: Al Khaddar, R., Singh, S.K., Kaushika, N.D., Tomar, R.K., Jain, S.K. (eds) *Recent Developments in Energy and Environmental Engineering. TRACE 2022. Lecture Notes in Civil Engineering*, vol 333. Springer, Singapore. pp 61–73
  4. Noori AR, Singh SK\* (2023): Assessment of seasonal groundwater quality variation employing GIS and statistical approaches in Kabul basin, Afghanistan. *Environ Dev Sustain.* <https://doi.org/10.1007/s10668-022-02876-5>
  5. Singh SK, Noori AR\* (2022): Groundwater quality assessment and modeling utilizing water quality index and GIS in Kabul Basin, Afghanistan. *Environ Monit Assess* 194:.. <https://doi.org/10.1007/s10661-022-10340-0>
  6. Singh SK, Noori AR\* (2022): Delineation of groundwater recharge potential zones for its sustainable development utilizing GIS approach in Kabul basin, Afghanistan. *Arab J Geosci* 15:.. <https://doi.org/10.1007/s12517-021-09410-3>
  7. Noori AR, Singh SK\* (2021): Assessment and modeling of sewer network development utilizing Arc GIS and SewerGEMS in Kabul city of Afghanistan. *J Eng Res* 22–31. <https://doi.org/https://doi.org/10.36909/jer.ICARI.15287>
  8. Noori AR, Singh SK\* (2021): Spatial and temporal trend analysis of groundwater levels and regional groundwater drought assessment of Kabul, Afghanistan. *Environ Earth Sci* 80:.. <https://doi.org/10.1007/s12665-021-10005-0>
  9. Noori AR\*, Singh SK (2021): Status of groundwater resource potential and its quality at Kabul, Afghanistan : a review. *Environ Earth Sci* 80:1–13. <https://doi.org/10.1007/s12665-021-09954-3>

\*= Corresponding author

### Submitted publications with peer review process

1. Noori, A.R, Singh, S.K. Development and Application of an Artificial Neural Network Model for Evaluating Groundwater Quality: A Study in the Kabul Basin, Afghanistan
2. Noori, A.R., Singh, S.K., Rezai, A. Evaluation of Arsenic Contamination in Groundwater and its Consequences on Human Health in Rural Areas

---

## REFERENCES

### Prof. S.K. Singh

PhD supervisor.

Previously Head of the Department of Environmental Engineering

Delhi Technological University, Delhi, India

Currently Vice Chancellor of Rajasthan Technical University, Rajasthan, India.

Email: [sksinghdce@gmail.com](mailto:sksinghdce@gmail.com)

### Prof. Assadullah Rezaie

---

---

Head Department of Water Supply and Environmental Engineering  
Kabul Polytechnic University, Kabul, Afghanistan  
Email: [a.rezai@kpu.edu.af](mailto:a.rezai@kpu.edu.af)

**Mohammad Musa Paiman**

CEO of Bena-e-Sharq Architectural and Engineering Services Co.  
Kabul, Afghanistan  
Email: [mmusa.paiman@gmail.com](mailto:mmusa.paiman@gmail.com)

---

